Universitat Autònoma de Barcelona

TESIS DOCTORAL

Contribution of perforant path synaptic markers and GSK-3 to cognitive impairment and Alzheimer´s Disease.

Autora:

Laura Molina Porcel

Directores:

Dra. Virginia M-Y Lee
Dra. Teresa Gómez Isla
Dr. Antonio Escartin Siquier

PROGRAMA DE DOCTORADO EN MEDICINA INTERNA

UNIVERSIDAD AUTÓNOMA DE BARCELONA

2015

Contribution of perforant path synaptic markers and GSK-3 to cognitive impairment and Alzheimer´s Disease.

Tesis presentada por Laura Molina Porcel para optar al grado de Doctor por la Universitat Autònoma de Barcelona.

Trabajo realizado en el Center for Neurodegenerative Disease Research, bajo la dirección de los Doctores Virginia M-Y Lee, Teresa Gomez Isla y Antonio Escartin.

Barcelona, 17 de noviembre de 2015

Doctoranda:

Laura Molina Porcel

Directores de tesis:

Dra. Virginia M-Y Lee **Dra. Teresa Gómez Isla** **Dr. Antonio Escartin Siquier**

UAB
Universitat Autònoma
de Barcelona

Virginia M-Y Lee, John H. Ware 3rd Endowed Professor in Alzheimer's Research, and Director of the Center for Neurodegenerative Disease Research of the department of Pathology and Laboratory Medicine of the Perelman School of Medicine at the University of Pennsylvania.

CERTIFY

The present doctoral thesis entitled "Contribution of perforant path synaptic markers and GSK-3 to cognitive impairment and Alzheimer´s Disease" presented by Laura Molina Porcel, has been made under my direction and is worthy of examination. I authorize its submission for the degree of Doctor from the Autonomous University of Barcelona in Spain.

Philadelphia, November 3rd, 2015

Virginia M-Y Lee

UAB
Universitat Autònoma
de Barcelona

Dra. Teresa Gómez Isla, profesora asociada de la Escuela de Medicina de Harvard y Neuróloga del Hospital General de Massachusetts.

CERTIFICA:

Que la presente tesis doctoral titulada: " Contribution of perforant path synaptic markers and GSK-3 to cognitive impairment and Alzheimer´s Disease", presentada por Laura Molina Porcel, ha sido realizada bajo mi dirección y reúne todos los requisitos necesarios para ser juzgada, autorizando su presentación para optar al grado de Doctora por la Universidad Autónoma de Barcelona

Para que así conste, firmo el presente certificado en Barcelona a 5 de noviembre de 2015

Teresa Gómez Isla

Universitat Autònoma de Barcelona

Dr. Antonio Escartín Siquier, profesor titular del Departamento de Medicina, de la Universidad Autónoma de Barcelona y Neurólogo del Hospital de la Santa Creu i Sant Pau.

CERTIFICA:

Que la presente tesis doctoral titulada: " Contribution of perforant path synaptic markers and GSK-3 to cognitive impairment and Alzheimer´s Disease", presentada por Laura Molina Porcel, ha sido realizada bajo mi dirección y reúne todos los requisitos necesarios para ser juzgada, autorizando su presentación para optar al grado de Doctora por la Universidad Autónoma de Barcelona

Para que así conste, firmo el presente certificado en Barcelona a 5 de noviembre de 2015

Antonio Escartín Siquier

A mi familia

CONTENT

I. INTRODUCTION

I. INTRODUCTION

The frequency of Alzheimer´s disease (AD) and other dementias is increasing worldwide due to the progressive ageing of the population. In Spain reported rates vary, but the prevalence appears to be about 6% among those aged 75 years or older (1). Moreover, the annual incidence of new cases of AD per 1000 people-year in our country increases with age, from about 1.5 at ages 65-69 up to 50 at age of 90 or above (2).

Researchers estimate that the prevalence of dementia and AD in Western Europe will duplicate by 2050, and quadruplicate in some large countries such as China and India (3). This increase will have a tremendous impact in our societies. First, because of the devastating effects of this disease on the health of patients and also their caregivers, who experience increased rates of stress and depression (4), and secondly, on our economies. Although these numbers vary between countries, the estimated cost per patient per year in Western European countries is over 30,000 USD, amounting to over 1.2% of the gross domestic product (5).

AD and other neurodegenerative dementias show a great diversity of clinical phenotypes but in general are clinically characterized by progressive cognitive and behavioral impairment that gradually interferes with activities of daily living (ADL). In the early stages, one or more cognitive domains are affected, but without interfering with ADL. This period has received several names, such as cognitive impairment but not dementia (CIND) or mild cognitive impairment (MCI) (6,7). In this dissertation, we used CIND to define individuals with cognitive or functional loss that did not meet the criteria for dementia using the Diagnostic and Statistical Manual of Mental Disorders 4^{th} edition criteria (8).

From the pathological point of view, AD and other neurodegenerative diseases share a common pathological hallmark which is the accumulation of characteristic abnormal proteins into insoluble aggregates inside or among selectively vulnerable neurons or

glial cells (9). These aggregates associate with neuronal and synaptic loss, but the mechanisms involved are not fully understood.

1. Alzheimer´s disease

1.1. Neuropathological changes

Macroscopic findings in AD brains include brain atrophy, with loss of brain volume involving the temporal (including the hippocampus), parietal and frontal lobes and thinning and shortening of the cortical ribbon of the temporal, frontal and parietal gyri. There is also associated ex vacuo ventricular dilation (10).

Microscopic findings of AD are senile plaques (SP), neurofibrillary tangles, dystrophic neurites, neuronal and synaptic loss, granulovacuolar degeneration, Hirano bodies, inflammatory glial reaction with reactive astrocytes and amyloid angiopathy. However, only SP and neurofibrillary pathology are included in the diagnostic criteria for AD.

SP are extracellular and insoluble deposits mainly composed of β-amyloid peptides (Aβ) (11,12). Plaques can be classified as focal or diffuse Aβ deposits. Classic or neuritic plaques are focal Aβ deposits which are characteristic of AD. They have a spherical structure with central condensation, positive for amyloid stains, and is surrounded by a peripheral halo, which is often separated by a clear zone that contains glial cells and dystrophic neuronal processes (13). In contrast, diffuse plaques, also present in AD and common in non-demented elderly and in Down syndrome, are morphologically diverse, can be larger than neuritic plaques, have irregular contours, stain weakly or are negative for amyloid stains, and have a lack of dystrophic neurites (10).

Neurofibrillary tangles (NFT) are intracellular filamentous inclusions composed of misfolded hyperphosphorylated tau protein (14) forming paired helical filaments

(PHF) and straight filaments (15) that occupy the cytoplasm and extend into apical dendrites. Although NFT are a key diagnostic feature of AD, they are not specific to the disease and can be present in normal brains and in several other conditions (i.e. progressive supranuclear palsy (16), cortical basal degeneration (17), parkinsonism-dementia complex of Guam (18)).

1.2. Physiopathology

AD is a complex and heterogeneous disorder. Family history increases the risk for AD by four times compared with the general population (19,20); however, it is estimated that only in around 0.5% of the cases a monogenic cause is identified (21). The three identified genes are the amyloid precursor protein (APP) (22), presenilin-1 (PSEN1)(23), and presenilin-2 (PSEN2) (23,24) that when mutated, or in the case of the APP gene also when duplicated (25–28), can cause an early-onset form of AD (<65 years). The pattern of inheritance of these three genes is autosomal dominant. They are strongly tied to APP and Aβ metabolism, and as I will discuss below, they are one of the bases of the amyloid hypothesis of AD.

Nevertheless, the most common form of AD is the late-onset (> 65 years). In this complex subtype of AD, a combination of biological, genetic, environmental and lifestyle factors are involved. For example, the presence of the allele ε4 of the apolipoprotein E (APOE), the primary genetic risk factor for late-onset AD, increases the probability of developing AD over time, and reduces the age of onset in a dose-dependent manner (29), while the ε2 allele decreases the risk and increases the age at onset (30).

The exact mechanism and how all of these factors interact and contribute to both forms of AD is still unknown. However, the presence of SP and NFT in the neuropathology together with the genetic causes of the disease indicates that it is related to APP and tau metabolism.

1.2.1. Amyloid-β peptides and amyloid precursor protein

The *APP* gene is located on chromosome 21 and contains 18 exons (26–28). APP is a type I integral membrane protein, with a large extracellular domain, and a short cytoplasmic domain. The normal function of APP is not well known; it has been proposed as a cell surface receptor and sequential downstream signaling molecule (31), or to be involved in cell adhesion (32), cell movement (33), or synaptic formation (34–36).

Two major proteolytic pathways have been described for APP, the amyloidogenic and the non-amyloidogenic pathway (Figure 1):

In the non-amyloidogenic pathway, APP is first cleaved by α-secretase between the amino acids lysine-16 and leucine-17 of the Aβ sequence, generating a larger APP soluble fragment α (APPsα), and a smaller α-C-terminal fragment (αCTF) with ~83 amino acids. Subsequently, αCTF is cleaved by γ-secretase, generating an amyloid precursor protein intracellular domain fragment (AICD) and a 3KDa peptide (p3) (37). γ-Secretase is an intramembrane aspartyl protease complex composed of four subunits presenilin, nicrastin, anterior pharynx-defective 1 (Aph-1), and presenilin enhancer 2 (PEN-2) (38–40).

In the amyloidogenic pathway, APP is first cleaved in the extracellular domain by β-secretase 1 (BACE1), a transmembrane aspartyl protease identified in 1999 (41,42). This cleavage generates two fragments, the shedding of nearly the entire ectodomain, named APP soluble β (APPsβ) fragment, and a membrane-tethered C-terminal fragment consisting of the last 99 amino acid residues of APP, named β-C-terminal fragment (βCTF) or C99. Then, β-CTF is cleaved by γ-secretase in the transmembrane domain generating two fragments: an extracellular peptide, Aβ, with a weight of ~4KDa, and a cytoplasmic polypeptide named AICD. γ-Secretase cleaves APP at multiples sites within the transmembrane domain, generating Aβ peptides of several lengths ranging from 38 to 43 amino acids. The majority of the secreted Aβ

peptides secreted have a terminal residue 40 (Aβ40) (~90%), whereas fewer than 10% of them end at residue 42 (Aβ42). Aβ42 and Aβ40 are the major components of SP in AD.

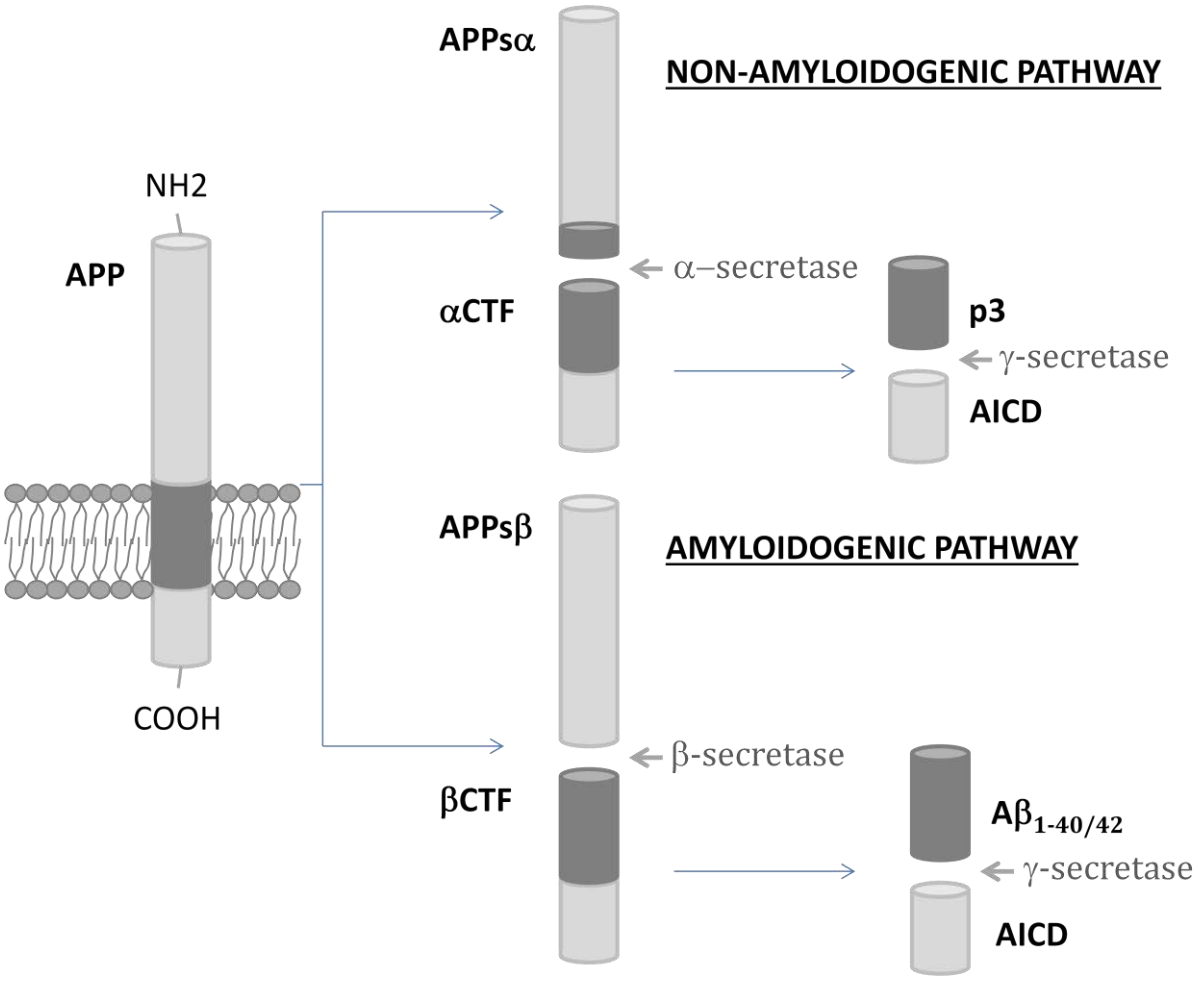

Figure 1: Proteolytic processing of the amyloid precursor protein.

Little is known about the physiological function of APP and its derivatives, such as Aβ. For example, Aβ1-42 is a conserved sequence within APP across species, suggesting that this peptide has a functional value (43). In fact, at low doses, Aβ can positively modulate synaptic plasticity and memory by increasing long-term potentiation in mice (44), induce angiogenesis in human endothelial cells and

zebrafish brain (43), and, at least *in vitro*, play a role in neurogenesis from neural stem cells (45).

However, the majority of studies have been focused on reproducing pathological conditions by using overexpression and mutation models. From these models we have learnt that an increase in Aβ leads to tau alterations (46–48), synaptic abnormalities (49–51), excitotoxicity (52), and neuronal loss (53).

1.2.2. Tau protein

Tau is a microtubule (MT)-associated protein discovered in 1975 (54). It is a very soluble protein and naturally unfolded. Tau is abundant in the central nervous system (CNS), in neurons and glia cells (55,56), and is also expressed in the peripheral nervous system (57). In neurons, tau is located predominantly in axons, in association with MT (54). Tau is encoded by a single gene (Microtubule-Associated Protein Tau gen (*MAPT*)) which is located on chromosome 17at position 21.1. *MAPT* consists of 16 exons: exons 2 and 3 encode N-terminal repeats, and exons 9, 10, 11 and 12 encode carboxy terminal tubulin/MT-binding domains. In the adult human CNS, alternative splicing of exons 2, 3 and 10 generate six isoforms (58,59). Each isoform differs from the next by the presence of zero, one or two N-terminal repeats (0N, 1N or 2N) and by the presence of three (3R) or four (4R) carboxy terminal tubulin/MT-binding domains. In the adult human brain, the ratio 3R and 4R is close to 1, and alterations in this ratio are related to pathology(60). The 6 isoforms are named 4R2N, 3R2N, 4R1N, 3R1N, 4R0N and 3R0N.

Tau has been implicated in binding, stabilizing and promoting the polymerization of MT (61). Isoforms with more MT binding domains (4R) are more efficient than 3R isoforms in this role (62). Other possible functions of tau are the regulation of motor-driven axonal transport (63), neurite outgrowth (64), cellular signaling, neuronal development, neuroprotection, apoptosis and scaffolding (65). Interestingly, Tau

knockout (KO) mice are viable. In these mice, MT stability and organization is altered in some small caliber axons, and an increase in MT-associated protein 1A was found suggesting a possible compensation mechanism (66).

Tau undergoes several posttranslational modifications such as phosphorylation, truncation, nitration, glycation, glycosylation, ubiquitination, polyamination and acetylation (for review see (67,68)). Their functions are not well known: some may be related to normal tau function, but others are thought to play a role in the pathogenesis of diseases such as AD. One post-translational modification that has been widely studied is phosphorylation. Tau phosphorylation seems to have a physiological role in development, and in axonal transport (69–71). However, in AD, hyperphosphorylated tau aggregates in PHF. PHF are abnormal twisted filaments and the major component of NFT. NFT are intracellular neuronal inclusions of tau that occupy the cytoplasm and extend into apical dendrites (14)

It is not fully understood how tau becomes hyperphosphorylated and aggregated, or what the consequences of this process are. It is possible than an increase in protein kinases and/or a decrease in phosphatase activity could increase tau phosphorylation (72). The largest isoform of tau has 79 potential serine and threonine phosphate acceptor sites, at least 39 of which have been reported to be phosphorylated in PHF and 9 in normal tau (73). These sites are clustered in regions flanking MT. MT are critical for axonal transportation, and an increase in tau phosphorylation may decrease MT binding, possibly compromising MT stability and axonal transport by loss of function (71,74–76). This increase of hyperphosphorylated, unbound and soluble tau may promote the aggregation of tau and other proteins, and produce axonal dysfunction, synaptic deficits and neuronal loss (for a review of tau in AD see (77–82)).

Multiple kinases are able to phosphorylate tau *in vitro,* such as mitogen-activated protein kinases (MAPK), cyclin-dependent kinase 5 (CDK-5), or Calcium/calmodulin-dependent protein kinase II α (CAMKIIα). However, there is evidence that glycogen synthase kinase 3 (GSK-3) plays an important role in regulating tau phosphorylation

in vivo under physiological and pathological conditions (67): therefore, GSK-3 has been identified as a possible therapeutic target in AD and other tauopathies.

Several findings implicate tau in the cascade of events leading to neuronal death in AD and other tauopathies. In AD, NFTs are necessary for diagnosis (83). They have a characteristic distribution and progression in AD brains (84,85), and correlate better with cognition than SP (86). Nonetheless, the way in which tau is involved in AD is not fully understood. Tau mutations are responsible for a hereditary neurodegenerative disease called frontotemporal dementia and parkinsonism linked to chromosome 17, but not for AD. Tau mutations induce tau pathology and neuronal loss, but no plaque formation (87). However, as stated previously, APP, PSEN1 and PSEN2 mutations generate SP but also NFT, suggesting that alterations in APP and Aβ formation can induce changes in tau processing. In addition, some studies suggest that Aβ-mediated neuronal cell death and memory deficits require tau (88,89). Altogether, these observations place tau pathology downstream of amyloid pathology. However, recent data suggest that in non-selected cases, tau deposition could start earlier than Aβ deposition (90). Nevertheless, the precise mechanistic link between Aβ and tau remains to be resolved. Several molecules, such as GSK-3, have been implicated in this role (for review, (91)).

1.3. Treatment

For the pharmacological treatment of AD, the United States Food and Drug Administration and the European Medicines Agency approved acetylcholinesterase inhibitors (Donepezile, Rivastigmine and Galantamine) for mild to moderate AD, and Memantine, an *N*-methyl-D-aspartate (NMDA) antagonist for moderate to severe AD.

The goal of these treatments is to modulate neurotransmitter imbalance observed in AD brains. On the one hand, several studies have suggested a deficiency in cholinergic neurotransmission in AD brains which may correlate with cognitive and

behavioral symptoms (92,93). Acetylcholinesterase inhibitors reduce degradation of acetylcholine by inhibition of a catabolic enzyme present in the synapses (acetylcholinesterase). This inhibition increases acetylcholine synaptic concentration and postsynaptic neurotransmission effects(94). On the other hand, memantine is a low-moderate affinity, uncompetitive NMDA receptor antagonist. Glutamate is an excitatory neurotransmitter involved in memory that interacts with NMDA receptors. An excess of stimulation on these receptors can produce an excitatory response by a massive entrance of calcium into the cell, leading to neuronal dysfunction and death. Pharmacological studies suggest that Memantine preferentially blocks activated NMDA receptors, but due to its low affinity and relatively fast off-rate it does not interfere with normal synaptic transmission (for review (95).

Unfortunately, current treatments provide some short symptomatic benefit but do not alter the underlying disease process. Further investigation is needed to identify new targets that potentially may be able to modify disease progression. In this dissertation, we first studied the correlations between synaptic markers and other pathological changes with cognitive status and global cognitive function in the oldest-old. In the second part, we sought to elucidate the contribution of GSK-3 in cognitive impairment and APP-related pathology in a mouse model of AD.

2. Contribution of synaptic markers in cognitive status and cognitive impairment in the oldest-old.

2.1. Relevance of studies in the oldest-old

Recently, researchers have been focusing in individuals 90 years old and older (90+), for several reasons. First, they are the segment of the population with the fastest growth of all. For example in Spain, there are currently approximately 339,000 people aged 90+, and this number is expected to increase to 1.5 million by 2050, which would account for 3.2 % of the Spanish population (Figure 2) (96). These numbers

are similar worldwide and in other developed countries such as the United States of America (see Table 1) (96).

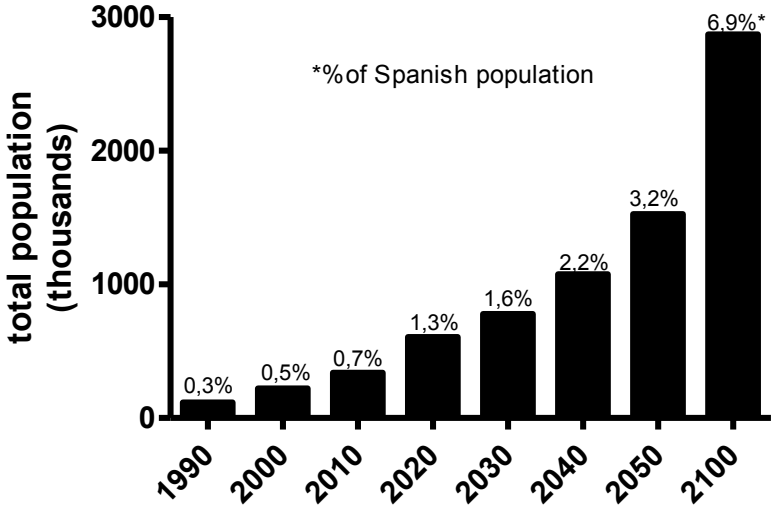

Figure 2: Oldest old population in Spain from 1990 to 2100. Source: United Nations, Department of Economic and Social Affairs, Population Division (2013). World Population Prospects: The 2012 Revision, DVD edition (medium fertility). (96).

	2010		2050	
AREA:	**total (thousands)**	**%**	**total (thousands)**	**%**
World	12,792	0,20	68,381	0,70
Spain	339	0,70	1,525	3,20
United States of America	1,918	0,60	7,895	2,00

Table 1: Oldest old total population and percentage estimation 2010 and 2050. Source: United Nations, Department of Economic and Social Affairs, Population Division (2013). World Population Prospects: The 2012 Revision, DVD edition (medium fertility) (96).

This progressing ageing of the population is alarming because the percentage of older people that are potentially care receivers is increasing overtime, while the percentage of people that are potential caregivers (people aged 20 to 64) is decreasing. For example in Spain, in 2000, for every person aged 90+ there were 113 people aged 20 to 64, but by the year 2050, it is estimated that there will only be 15 (96).

Second, although a high frequency of dementia and AD among the oldest old is anticipated, their prevalence and incidence are not well known. It is expected that the risk for AD and dementia would increase with age, but is unknown whether this increase will be doubling exponentially with every five years of life (97), such as in AD and people aged from 65 to 90 years (2,98); if this increase will slow down over time (99); or even whether it will decrease with age in the oldest old (100). Although the prevalence probably will keep increasing, the potential burden for public health systems is very different for each assumption, and several population studies are trying to address this issue.

Third, it is unknown whether factors that potentially confer protection in younger subjects such as antioxidants, physical and cognitive activities are operative for the oldest old (101). Similarly, it is unknown whether risk factors are the same. For example, the allele APOE ε4 is a well-known risk factor for AD in the younger elderly (102), but several studies have failed to find an association in older populations (97,103–105), suggesting that the association between APOE ε4 and dementia decreases with age or even disappears in the oldest old. A better understanding of risk and protective factors for AD and other dementias may help to delay the onset of these diseases.

Fourth, and more closely related to this dissertation, is the fact that the correlation between the pathological substrates of neurodegeneration and cognitive impairment are not well known in the oldest old. There is an extensive overlap in pathology among individuals with and without dementia (106). In our previous work, similarly to other studies, we found that a number of patients with dementia (22%) did not have

sufficient pathology to account for their cognitive loss (107,108). Conversely, about 1/3 of patients met the pathological criteria for AD but did no experience clinical dementia (109–111). This poor clinical and pathological correlation suggests that other factors may have an important role in cognition in the oldest old, and that further investigation is required.

In summary, studies in the oldest old are important for planning for the public health burden that this age group will produce in the future, and because it may reveal some disparities compared to the younger population that may allow us to better understand neurodegenerative diseases, and give us some clues to achieve a better and healthier ageing.

2.2. Common causes of dementia in the elderly.

The most common cause of dementia in the oldest-old is AD. In our previous paper, 86% of participants that met criteria for dementia before death were diagnosed with clinical AD (61% alone, 11% AD/dementia with Lewy bodies, 11% AD/Vascular dementia) (107).

However, the clinical-pathological correlation in the elderly is a little more complex than in younger patients. Dementia of unknown etiology increases with age (108). Although neocortical NFT and SP also correlates to dementia in this group of age (112–114,107), some studies suggest that the density of NFT and amyloid tends to stabilize with age in the oldest old with cognitive impairment (113,115–117). In fact, some patients display cognitive impairment besides of a lack of abundant AD or other pathology such as Lewy bodies, etc. (108). A possible explanation for this is that other age-related pathologies such as hippocampal sclerosis (HS), cerebrovascular diseases (CVD), or synaptic loss (118) may contribute to the cognitive impairment and to dementia (108,86).

2.2.1. Cerebrovascular disease (CVD)

CVD is a heterogeneous disease affecting the blood vessels that supply the brain. It includes among others, large vessel infarcts, microinfarcts, microhemorrhages, cerebral amyloid angiopathy, etc.

CVD is associated with dementia and cognitive impairment (108,119–122). CVD may have synergistic mechanisms with AD. For example, MCI patients with white matter hyperintensities have higher ratios of conversion to dementia than patients without them (123). In addition, patients with similar cognitive impairment and pathological changes of CVD display less AD pathology than those with AD pathology alone (124–126).

CVD frequency increases overtime. For example, in octogenarians (people 80 to 89 years old), white matter hyperintensities detected by magnetic resonance imaging (MRI) are present in over 75% (119), but in extreme old age it percentage increases up to 100% (127). On anatomopathological series, subtle CVD pathology has been observed in over 75% of 90+ individuals (124). Overall, this suggests that the contribution of CVD in cognitive impairment and dementia in the oldest old may play an important role.

2.2.2. Hippocampal sclerosis (HS)

HS is a neuropathological condition with severe neuronal loss and gliosis in both region 1 of the cornus ammonis (CA1) and the subiculum of the hippocampus. It was first described in 1880 by Wilhelm Sommer (128). HS is related to temporal lobe epilepsy, and vascular risk factors, but has recently been associated with the oldest old.

Recent studies suggest that there has been an important increase in the frequency of HS in extreme old age (129,130). For example, in a previous study our group

observed that 18% of participants of The 90+ study that underwent to autopsy displayed HS (107). Similar results have been found in other studies: for example 16% of the participants of the Bronx Longitudinal Aging Study who are 80 years old or older (80+) show HS (131). Most importantly, HS strongly correlates to cognitive impairment and dementia in this age group. For example, lower Mini-Mental State examination (MMSE) scores were observed in patients with unilateral or bilateral HS (up to 8 points) (112). Another example is that increased frequencies of HS have been reported in demented individuals compared to controls, and in some studies, HS was only observed in demented patients (107,131).

Clinically, HS individuals present prominent memory and language deficits and become progressively demented (132). They have similar initial symptoms to AD, except for subtle differences such as in apathy, trail-making test, or word list delay (129,133). Rates of dementia progression in HS are also similar to those individuals with AD, so HS is often misdiagnosed (133).

Isolated HS is a rare finding so it usually associated with other pathology such as SP, NFT, CVD and 43-kDa transactive response sequence DNA-binding protein (TDP-43) (132,112,107). TDP-43 is a multifunctional protein, able to bind both DNA and RNA, and involved in many cellular processes including RNA transcription, alternative splicing or mRNA stability (134). Hyper-phosphorylated TDP-43 is the major component of both amyotrophic lateral sclerosis and frontotemporal degeneration with ubiquitin-positive tau- and α-synuclein-negative inclusions (135), and it has been also associated to other pathologies such as AD (136). Interestingly, TDP-43 seems to be the only factor to increase the odds of HS (130). For example, in our previous 90+ study, aberrant TDP-43 immunoreactivity was seen in 79% of HS patients compared with 20% of HS negative patients wirth dementia (107). Other studies reported higher percentages of TDP-43 pathology in HS patients, up to 89.9% compared to 9.7% in patients without HS (129,130). Furthermore, HS with coexisting TDP-43 has been associated with lower function in multiple cognitive domains suggesting a synergistic effect (130). In addition, the sequence of events

that lead to HS in the oldest old is not well known, but the finding of TDP-43 immunoreactivity in the contralateral side of individuals with unilateral HS suggests that HS may be attributable to TDP-43 pathology and it can be a distinct entity related to aging (129).

2.3. Contribution of synaptic markers in dementia and cognitive impairment.

A common finding in degenerative disorders is the loss of synapses. Synaptic dysfunction is one of the earliest features in AD (137–140). Indeed, significant synapse loss has been documented in brain regions affected by AD pathology (141). Moreover, reductions in the number of synaptic proteins may be the most consistent progression marker of AD even in extreme old age (142,143).

However, it is unclear whether there is a loss of synapses related to normal aging. Some papers have reported reduced immunoreactivity of presynaptic markers in some regions such as the frontal or temporal cortex, while others do not (reviewed in (144)).

Nonetheless, the relationship between anatomy, synaptic proteins and AD pathology is complex. First, different synapse types change at different times and in specific brain regions. For example, cholinergic signaling in the cerebral cortex including entorhinal cortex and in the hippocampus are affected early due to the degeneration of the large cholinergic neurons of the ventral forebrain, while γ-aminobutyric acid (GABA) transmission is relatively preserved in late AD (reviewed in (145)). Second, the evolution of synaptic loss in a specific region does not always follow a linear decrease. Increased synaptic markers can be observed at early stages of the disease (146,147).

In addition, the mechanisms that relate AD pathology with synaptotoxicity remain uncertain. Several lines of evidence suggest that Aβ seems to regulate synaptic activities, and that Aβ production is regulated, at least in part, by neuronal activity

(148,149). Accumulation of Aβ may impair the inhibitory activity of interneurons and stimulate glutamate receptors which can result in excitotoxicity (150–152). Subsequently, aberrant neuronal activity may trigger a vicious cycle by augmenting Aβ production (reviewed (153)). In this line, oligomeric Aβ has been shown to induce synaptic dysfunction and neuritic degeneration (138,154). However, tau mouse models also show synaptic dysfunction and memory deficits, even before NFT formation (155,156). Altogether, this suggests than both Aβ and tau are involved in synaptic dysfunction during the early stages of disease.

In this dissertation, we aimed to understand the synaptic changes underlying cognitive impairment and dementia and therefore, synaptophysin, synaptic vesicle glycoprotein 2 isoform (SV2) and vesicular glutamate transporter 1 (VGLUT1) were measured in the outer molecular layer of the hippocampus, a region affected early in AD.

2.3.1. Synaptophysin

Synaptophysin is a presynaptic protein located in synaptic vesicles (157,158). It is the most abundant of the synaptic vesicle proteins, accounting for over 10% of them (159). Its function is not well known. Several roles have been proposed in synaptic function including exocytosis, synapse formation and endocytosis of synaptic vesicles (160–162). For example, synaptophysin is able to bind to synaptobrevin, a component of the SNARE complex (soluble N-ethylmaleimide sensitive factor attachment protein (SNAP) receptor) in the synaptic vesicle (163). The SNARE complex is a group of proteins It has been proposed that by this interaction, synaptophysin sequesters synaptovebrin and prevents its ability to interact with the two other components of the SNARE complex on the plasma membrane (syntaxin and SNAP-25), and therefore membrane fusion and exocytosis might be altered (164). Interestingly, it has been proposed that Aβ might regulate exocytosis by disrupting the ability of synaptophysin to interact with synaptobrevin and enhancing

synaptic vesicle release (165). But on the other hand, KO studies have shown that synaptophysin is not essential for neurotransmitter release, suggesting that it may play modulatory rather than fundamental roles at the nerve terminal (166).

Quantification of synaptophysin by western blot (WB), enzyme-linked immunosorbent assay (ELISA) or by other approaches is a method that is often used for measuring presynaptic integrity. Several papers have shown a reduction of synaptophysin in frontal (141,167–169), parietal (167,170), occipital (170) and temporal cortex (167,141) of AD individuals compared to controls. In some cases, this reduction can precede cell loss and AD pathology (170). In addition, synaptophysin levels correlate with cognition (170), although in other studies this correlation was not observed (141).

Reduction in synaptophysin levels have also been observed in other dementias such as vascular dementia, or mixed dementia (AD + vascular dementia) (168). Interestingly, some studies have found that a decrease, an increase or no changes at all of synaptophysin levels can be found in MCI patients compared to controls (147,171,172). For example, in a previous analysis of the 90+ cohort, synaptophysin levels in frontal cortex, measured by WB were significantly increased in MCI individuals compared to AD patients but not compared to controls (147). Overall this suggests that more data are necessary to better understand the role of synaptic integrity at early stages of the disease and in the oldest old.

2.3.2. Synaptic vesicle glycoprotein 2 (SV2)

Synaptic vesicle glycoprotein 2 (SV2) is an integral membrane presynaptic protein located in all synaptic vesicles (173). There are 3 isoforms: SV2A, SV2B and SV2C. SV2A is the most widely expressed in the CNS and in endocrine cells (173,174). SV2B is brain-specific, and SVC is a minor form in the brain. Interestingly, some neurons express SV2A and SV2B, and both isoforms may be present on the same synaptic vesicle (174).

The function of SV2 is not well known. SV2A KO mice seem normal at birth, but they fail to grow, developing severe seizures by 1.5 weeks of age, and dying within 3 weeks of birth, suggesting neural and metabolic alterations (175). It has been observed that neurotransmission is reduced in the absence of SV2A, without changes in synapse or synaptic vesicle density or morphology suggesting that it may have a modulatory role (175–177). SV2A binds synaptotagmin, a presynaptic protein localized to synaptic vesicles, which is considered to act as a calcium sensor for regulating calcium-dependent exocytosis of synaptic vesicles (178–180). Recent data suggest that SV2 may regulate the expression and trafficking of synaptotagmin, and consistent with this, a reduced calcium-mediated exocytosis is observed in neurons lacking SV2 (181).

SV2 is associated with several neurologic conditions. For example, it is the binding site for the antiepileptic drug levetiracetam (182). Another example is that SV2 has been indentified as a protein receptor for Botulinum neurotoxin A. Mice lacking SV2 isoforms display reduced sensitivity to this toxin (183).

In dementia, SV2 has been found to be decreased in the temporal cortex of AD patients (184); however, other studies failed to find this reduction in the hippocampus, entorhinal cortex, caudate nucleus, and occipital cortex (185). Reductions of SV2 levels have been also found in the dentate gyrus of the hippocampus of APP/PSEN1 mice at 12 months (186). However, although levetiracetam has been shown to reduce hippocampal hyperactivity and to improve cognition in CIND individuals (187), it is not well known what happens with SV2 protein levels during the early stages of disease or in the oldest old, and more studies are needed.

2.3.3. Vesicular glutamate transporeter (VGLUT1)

Glutamate is the major excitatory neurotransmitter in the CNS (188). Increased amounts of extracellular glutamate can lead to cell death (189). Glutamate is an

amino acid that is also involved in cell metabolism. It is unable to diffuse through the membranes, and is introduced into cells and different compartments by several glutamate transporters. Once glutamate is released into the synaptic cleft, it is rapidly taken up by astrocytes and converted into glutamine (190,191). Glutamine is discharged from glial cells and enters neurons (192). In neurons, glutamine is converted into glutamate and is stored in synaptic vesicles (193). VGLUT is a presynaptic protein responsible for the transportation of glutamate into synaptic vesicles (194,195). There are 3 isoforms in mammals (VGLUT1-3). VGLUT1 and VGLUT2 are more abundant, and are considered specific markers of glutamatergic neurons, but VGLUT3 is less abundant and often co-localizes with non-glutamatergic markers in neurons (for review (196,197)).

Glutamate transporters have been investigated and associated with several neurological diseases such as stroke, epilepsy or Huntington´s disease (198–200). Specifically, VGLUT1 has been involved in several diseases such as schizophrenia (201) or Parkinson disease (202).

In dementia and cognitive impairment, significant reduction in VGLUT1 in the frontal cortex (Brodmann area 9) has been found in patients with vascular dementia, mixed dementia and AD compared to patients with stroke but not dementia. In addition, VGLUT1 levels in frontal and temporal cortex (Brodmann area 20) correlated with cognitive tests, suggesting that the integrity of glutamatergic synapses might play an important role in maintaining cognition after stroke (168).

In AD, reduced protein levels of VGLUT1 were found in the parietal, occipital and frontal cortex of AD patients compared to controls, but not in the temporal cortex (170,203,204). Messenger ribonucleic acid (mRNA) levels were also reduced in the prefrontal cortex of AD patients (205). In the majority of studies, VGLUT1 correlated with cognitive symptoms (203,204). Interestingly, a paradoxical increase of VGLUT1 immunoreactive boutons has been found in the midfrontal gyrus of MCI patients (203). However is not well known what occurs in the oldest old.

3. Glycogen synthase kinase 3 (GSK-3) in Alzheimer´s disease pathology and cognitive impairment

3.1. Protein characteristics of GSK-3

GSK-3 is a serine/proline kinase initially identified for its ability to phosphorylate and inactivate glycogen synthase (206).

There are two mammalian GSK-3 isoforms (GSK-3α and GSK-3β) each encoded by distinct but closely related genes mapped to chromosomes 19q12.3 and 3q13.3, respectively (207–209). Both isoenzymes are highly conserved, GSK-3α and GSK-3β share an overall 84% sequence identity, with 98% homology in the kinase domain (207). The main difference between these two monomeric isoforms is in the N-terminal region. GSK-3α contains an extended Glycine-rich region, and therefore is bigger than GSK-3β (51KD and 46KD, respectively) (207). This high degree of homology suggests similar substrate specificities, but multiple data have shown that they also have different functions (210–212).

In addition to GSK-3α and GSK-3β, a splicing variant of GSK-3β with a 13 amino acid insert in an external loop near the catalytic domain was identified in 2002 and named GSK-3β_2 (213). Furthermore, both GSK-3β variants share substrates, but GSK-3β_2 shows some differences such as lower phosphorylation rate or different phosphorylation sites, at least *in vitro* (212,213).

It is important to note that GSK-3α and GSK-3β are ubiquitously expressed in many tissues, with particularly abundant levels in the CNS (207,213,214), while GSK-3β_2 expression is more restricted to the CNS (213).

Within cells, GSK-3 is predominantly a cytosolic protein (215,216), although it is also present in the nucleus (216) and mitochondria (217,218). In the CNS, GSK-3β is present in neurons and astrocytes. Within neurons, GSK-3β is present in the cytosol of the neuronal soma, dendrites, rough endoplasmic reticulum, free ribosomes and

mitochondria, while in astrocytes, GSK-3β is present in astrocytic processes and in rough endoplasmic reticulum, free ribosomes and mitochondria (219).

GSK-3 is a relatively stable protein (220), with a high activity in resting and unstimulated cells (206,221). Since GSK-3 can interact with numerous substrates (for a review of comprehensive list of over 100 suggested targets see (222)), it requires a complex control system to modulate its activity. Several regulatory mechanisms have been described including: protein complex association (223), priming/substrate specificity (224,225), subcellular localization (216,226), proteolytic cleavage (227,228), and the most well-known, phosphorylation (for review, see (229)). Phosphorylation of GSK-3α at serine-21 (p-S21-GSK-3α), or GSK-3β at serine-9 (p-S9-GSK-3β) significantly decreases the availability of the active site to interact with a substrate, and the activity of GSK-3 is reduced. Therefore, in some papers, p-S21-GSK-3α and p-S9-GSK-3β are considered the inactive forms. Conversely, when the phosphorylation is at tyrosine-279 of GSK-3α (p-Y279-GSK-3α) or at tyrosine-216 of GSK-3β (p-Y216-GSK-3β), their activity increases (230–232).

GSK-3 is involved in many physiological processes like glucose metabolism (233–236) and inflammation (237,238). In the central nervous system, GSK-3 has been implicated in basic functions such as in axonal growth (239–241), synaptogenesis (239,242), cell adhesion (243), cytoskeletal stability (244–247), plasticity (248–253), vesicular transport (254) or energy metabolism (217).

In fact, GSK-3 has been investigated due to its possible role in several diseases such as psychiatric disorders (255–257), neoplasms (258,259), hypoxic-ischemic disease (260,261), metabolic diseases (262), and neurodegenerative diseases such as AD (263–265).

3.2. Methods to reduce GSK-3 activity in mouse models

Over the years, different methods have been used to manipulate GSK-3 in animals such as drug inhibitors, overexpression models, conventional knockouts, conditional knockouts, etc. In this work, we wanted to study the role of GSK-3α and GSK-3β in amyloid pathology and cognitive impairment *in vivo*. To do this, we aimed to reduce GSK-3α, GSK-3β and GSK-3α+β activity in a mouse model of AD. Next, I will review different methods commonly used to reduce GSK-3 activity in mouse models.

3.2.1. GSK-3 inhibitors

The most common approach to reduce GSK-3 activity has been the use of inhibitory drugs such as lithium. This approach has several advantages since it is rapid; the investigator can decide when to initiate and the duration of treatment, and it is the closest method to human clinical trials. However, it has a number of disadvantages that can make it difficult to interpret results, with the main one being the lack of specificity.

In general, drugs have off-target effects that can interfere with results. Moreover, human kinases maintain a high degree of homology that can reduce the specificity of GSK-3 inhibitors (ATP competitors) (266). To date, there are no isoform-specific GSK-3 inhibitors. It is important to highlight this fact, because GSK-3 inhibitors are often called “GSK-3β" inhibitors in the literature (267), which is a term that is not accurate and is due to the historically higher interest on the isoform β over the α, rather than the real effect of the drug.

3.2.2. Conventional knockout

The classical method to study the effect of decreasing a protein *in vivo* is using the KO approach. Mice without GSK-3α are viable and appear morphologically normal (268). GSK-3α KO mice show some behavioral deficits such as decreased exploratory activity, decreased immobility time, anti-aggression behavior, decreased locomotion, increased sensitivity to environmental cues, decreased social motivation, impaired sensorimotor gating, associative memory, and coordination (210).

However, disruption of the murine GSK-3β gene results in embryonic lethality caused by severe liver degeneration during mid-gestation, around embryonic day 14 (211). Heterozygous KO mice are viable, appear morphologically normal, and have also shown some behavioral deficits (269,270).

Since GSK-3β KO mice are not viable, several methods have been used to selectively reduce GSK-3β, and to try to compare both isoforms. Our group generated two novel genetic approaches: short hairpin ribonucleic acid (shRNA), and two different lines of conditional knockout (CKO) mice.

3.2.3. Short hairpin Ribonucleic acid (shRNA)

ShRNA is an artificial RNA molecule that can be used to silence gene expression via the RNA interference pathway. ShRNA is delivered into mammalian cells through infection with viral vectors, which allow stable integration of shRNA and long-term knockdown (KD) of the targeted gene (271).

In several papers, this method has been used to successfully KD GSK-3 *in vitro* (272). To the best of our knowledge, our group was the first to utilize this approach in AD mouse models (273).

In parallel to the CKO work presented in this thesis, our group developed recombinant adeno-associated virus 2/1 (rAAV2/1) shRNA constructs which specifically reduced the expression and activity of GSK-3α (shRNA-α) or GSK-3β (shRNA-β). However, we failed to generate a construct that silenced both isoforms (α and β) equally. Constructs were injected intraventricularly in newborn mice. We observed a wide distribution of rAAV2/1. It was predominant in hippocampal regions CA1–CA3, the granular cell layer of the dentate gyrus, and with greater variability in deeper cortical layers four through six along with cortical amygdalar regions. Overall, cortical regions in close proximity to the lateral ventricles showed higher transduction. We observed a mosaic pattern, where cells expressing rAAV2/1 also showed a lack of Immunoreactivity to GSK-3α or GSK-3β if shRNA-α or shRNA-β was injected, respectively. The KD persisted over 11 months. Immunoblot analyses showed that GSK-3α protein levels were reduced by ~58–72% in shRNA-α-injected mice compared with shRNA-β-injected mice, and with controls (non-injected mice and scramble shRNA (shRNA-scr)-injected mice), whereas GSK-3β protein levels were reduced by ~40–54% in shRNA-β-injected mice (Figure 3) (273).

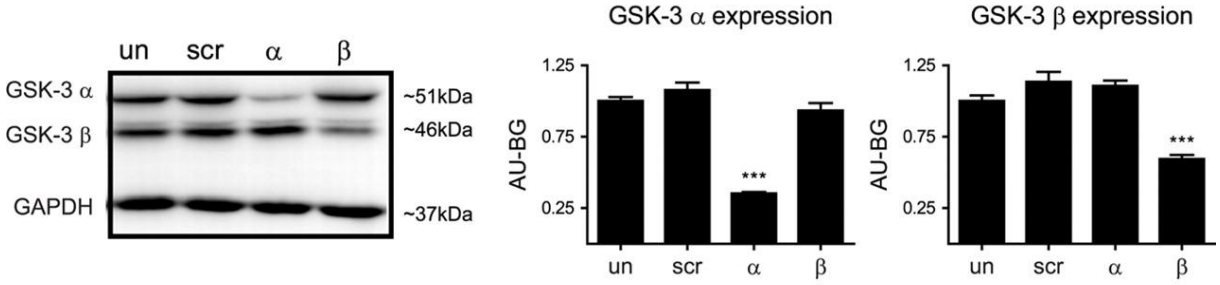

Figure 3: Immunoblot analyses of hippocampal lysates probed with GSK-3 antibodies. ShRNA-α treatment significantly reduced GSK-3α expression without altering GSK-3β expression ($F_{(3,12)}$=68.47, p<0.0001) and vice versa for shRNA-β treated mice ($F_{(3,12)}$=29.05, p<0.0001). un: un-injected; scr: shRNA-scr injected mice; α: shRNA-α injected mice, β: shRNA-β injected mice; GAPDH: glyceraldehyde 3-phosphate dehydrogenase (Source: Hurtado et al (273)).

The advantages of this method were that it was isoform-specific, the KD lasted through time, and it was relatively fast. However, shRNA also shows several

inconveniences. First, we observed variability, not only between mice, which we solved by increasing the number of mice injected, but also between different shRNA constructs injected. For example, rAAV2/1 with shRNA-α construct spread more widely than the shRNA-β, and therefore we cannot be certain whether the differences observed in our results were due to the specificity of targeted genes or it if was simply due to a different degree of KD. Furthermore, introduction of shRNA into cells and also *in vivo*, can generate several responses, such as activation of some components of the immune system that can interfere with the reliability of the results; therefore, confirmation using a different approach is recommended (for review several aspects of shRNA approach go to (274))

3.2.4. Conditional transgenic mice

The conditional transgenic technology allows us to generate complex animal models in which we can exert temporo-spatial control of the expression or deletion of a particular gene (275). This ability to switch gene expression ON/OFF in restricted tissues and at specific times allows us, among other things, to study certain genes whose deletion *in vivo* is not feasible as in the case of GSK-3β.

3.2.4.1. Dominant negative transgenic mice

When we started our project, dominant negative GSK-3 conditional transgenic mice were available. These mice expressed a mutated form of GSK-3β (K85R) that generated a catalytically inactive form of GSK-3β. K85R-GSK-3β inhibited GSK-3 function in a dominant-negative manner, possibly by non-productively sequestering *in vivo* substrates or regulators of GSK-3 (276). In these mice K85R-GSK-3β expression was controlled by the Tet-Off system. In this system, the gene expression was OFF in the presence of tetracycline, but in absence of treatment, a protein named tetracycline transactivator was able to recognize a specific Deoxyribonucleic

Acid (DNA) sequence (TetO) and the expression of the K85R GSK-3β transgene was ON. It is a very interesting model, since the process is reversible depending on the presence/absence of tetracycline treatment.

In order to avoid developmental effects due to GSK-3 lack of function during embryogenesis, tetracycline transactivator transgene was driven by the CAMKIIα promoter. This promoter, as we will see below, is only expressed postnatally and is restricted to the brain (277,278), which means that decreased activity of GSK-3 in these mice can only be induced in the CNS after birth.

Despite the complexity of this model, for our objectives, it showed a major drawback: the lack of isoform specificity. This dominant-negative GSK-3β mouse model showed increased levels of p-S21-GSK-3β, but more importantly it also showed increased levels of p-S9-GSK-3α, suggesting that the reduction of the activity affected both isoforms (278,279).

3.2.4.2. Conditional knockout transgenic mice

There are different techniques to generate CKO mice. We used the CRE-LoxP system derived from the P1 bacteriophage, which consists of two components: the CRE recombinase and a loxP recognition site.(280)

The CRE recombinase stands for "Causes REcombination". It is a protein that is able to recognize a specific sequence of DNA, the loxP (Locus Of X(cross)-over in P1), and catalyze a reciprocal crossover-event between two of these loxP regions. This recombination can generate deletions (Figure 4), inversions, etc., depending on the orientation of both loxP sites.

These components are part of the natural viral lifecycle of the bacteriophage, but researchers have adapted this system and used it widely as a site-specific recombinase technology in prokaryotic and eukaryotic cells.

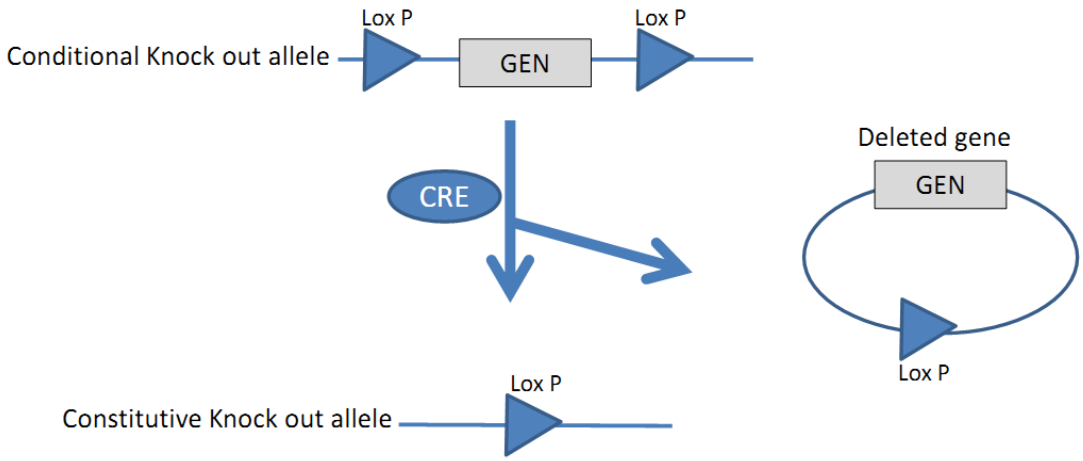

Figure 4: Deletion generated through the CRE-LoxP system

To obtain CKO mice, we usually need to generate double-transgenic mice. First, two loxP sequences with the proper orientation are inserted at specific sites of the DNA. For example, in our case, we inserted loxP at intron 1 and intron 4 of our targeted gene in a plasmid. Then, and usually after a laborious process of selection, a heterozygous flox mouse was generated. Next, we needed to add CRE protein to these mice. The most common way to do this is by crossing them with mice expressing CRE. There are several CRE lines, and it is important to select the best one to achieve our objectives. To do this, is important to look at the promoter driving CRE expression, because it defines in what tissues CRE is expressed and at what age. For example, Thy1-Cre mice express CRE specifically in neurons after birth, but Nestin-Cre mice express CRE in the central and peripheral nervous system, kidney and heart after embryonic day 11. Therefore, if the goal is to study the effects of the deletion in the CNS in adulthood, it would be better to choose the first model, but if the question is focused in the second half of pregnancy, the second model is better.

In addition, there are inducible CRE lines. Some lines express CRE-ERT2, a fusion protein of CRE recombinase combined to a mutant form of the human estrogen receptor. Under normal conditions the complex CRE-ERT2 remains attached and is

located in the cytoplasm. However, after exposure to 4-hydroxytamoxifen CRE is liberated; it is able to move into the nuclear compartment, and cause loxP recombination.

Inducible models are remarkable, because we can postpone a gene deletion until later periods of life in mice, such as when AD pathology is well established. However, on the other hand, some technical issues such as preparation, conservation and the need for administration of tamoxifen may cause more variability.

3.3. GSK-3 in Alzheimer´s disease

Since the role of GSK-3 in AD as a tau kinase was first observed in 1992 by Ishiguro et al. (281), several studies have suggested that GSK-3 activity is increased in AD brains. For example, it has been shown that in AD brains, GSK-3 localizes in pre-tangle neurons, NFT, and dystrophic neurites (282–287). Interestingly, similar results have been observed in double APP/tau transgenic mice (288). Furthermore, increased levels of GSK-3 expression measured either by microarrays in hippocampus (289), or by WB in post-synaptosomal fractions (286) also has been found.

A common approach to estimate GSK-3 activity in AD brains is by measuring GSK-3 phosphorylated forms. Increased levels of p-Y279-GSK-3α and p-Y216-GSK-3β, the "hyperactive" forms of GSK-3, but not of the inactive forms (p-S21-GSK-3α, p-S9-GSK-3β), have been found in hippocampus, entorrhinal, temporal and frontal cortex (282,283). However, other studies failed to find this increase in GSK-3 activity in AD brains (286), or even found data suggesting that it is reduced (287,290,291).

In peripheral blood, similar results have been found in white cells (292), and platelets (293,294) of patients with AD and MCI compared to controls, although the significance of these findings is still to be determined.

Furthermore, genetic associations between GSK-3 and AD have been recently found. Different polymorphisms in the promoter (295,296), or in an intronic region (297) of *GSK-3β* have been reported. In addition, synergistic effects of *GSK-3β* with other genes such as *MAPT* (296,298) or *cdk5* (299) have been related to late-onset and sporadic AD.

Furthermore, it has been proposed that PSEN1 indirectly inactivates GSK-3α and GSK-3β. Mutations or deletions in PSEN1 have shown to increase phosphorylation of tau by interfering with the inactivation of GSK-3 (300,301). Overall, this suggests that PSEN1 mutations, the most frequent known cause of familial AD, may have an additional mechanism by which they contribute to AD pathology through increased GSK-3 activity.

In summary, although there is no direct evidence of the increased activity of GSK-3 in AD, there is sufficient data suggesting GSK-3 involvement in several steps of the physiopathology of AD, such as tau phosphorylation and NFT formation, APP and Aβ, inflammation, and synaptic and neuronal dysfunction and loss (for review, see (264,265,302–304)).

Next, I will review the roles of GSK-3 in Tau phosphorylation and NFT formation, and in APP and PS formation, which is the aim of the second part of this dissertation.

3.3.1. GSK-3 and tau

In vitro studies have shown that both isoforms of GSK-3 (α and β) are able to phosphorylate tau in several primed and non-primed PHF phosphoepitopes (281,305–309). Conversely, treatment with GSK-3 inhibitors, such as lithium, reduces tau phosphorylation in cells (309). Overall, this suggests that GSK-3 may have an important role in NFT formation *in vivo.*

Consistent with this, different GSK-3β overexpression mouse models have shown hyperphosphorylation of tau (310–315). When GSK-3β overexpression was associated with human mutated tau overexpression, an exacerbation of NFT was found (312). Similar results have been found in the *Drosophila* model of co-expression of a constitutively active form of shaggy (the homologue form of GSK-3) and human wild type (WT) tau (316,317). Furthermore, although not all (310,312), the majority of these studies showed some degree of neuronal dysfunction or behavioral deficits. Importantly, these deficits could be reversed after the normalization of GSK-3β levels by silencing transgene expression (318), or by using GSK-3 inhibitors (317), suggesting that they may be a good therapeutic strategy in tauopathies. Interestingly, these deficits could be ameliorated by knocking out tau, which suggests that these deleterious effects due to an increased activity of GSK-3 are at least, in part, dependent on tau (319).

On the other hand, GSK-3 inhibitors have been shown to reduce tau pathology such as tau phosphorylation (267,320–323), insoluble tau levels (321,324) or intracellular inclusions (320) in tau mouse models of AD and other tauopathies. Furthermore, in these models, GSK-3 inhibitors were also shown to improve associated deficits such as cognitive and motor impairment (267,324), axonal degeneration (321) or neuronal loss (267). Similar results have been found after knocking down selectively GSK-3α or GSK-3β by different approaches *in vivo* (273,278,325,326). For example, as explained previously, in parallel to the work of this dissertation, our group developed AAV2/1 shRNA constructs which specifically reduced the expression and activity of GSK-3α or GSK-3β. These constructs were injected intraventricularly into newborn double APP/tau transgenic mice. We observed that both GSk-3α and GSK-3β KD reduced tau phosphorylation, conformational changes and NFT in this model (273) (Figure 5).

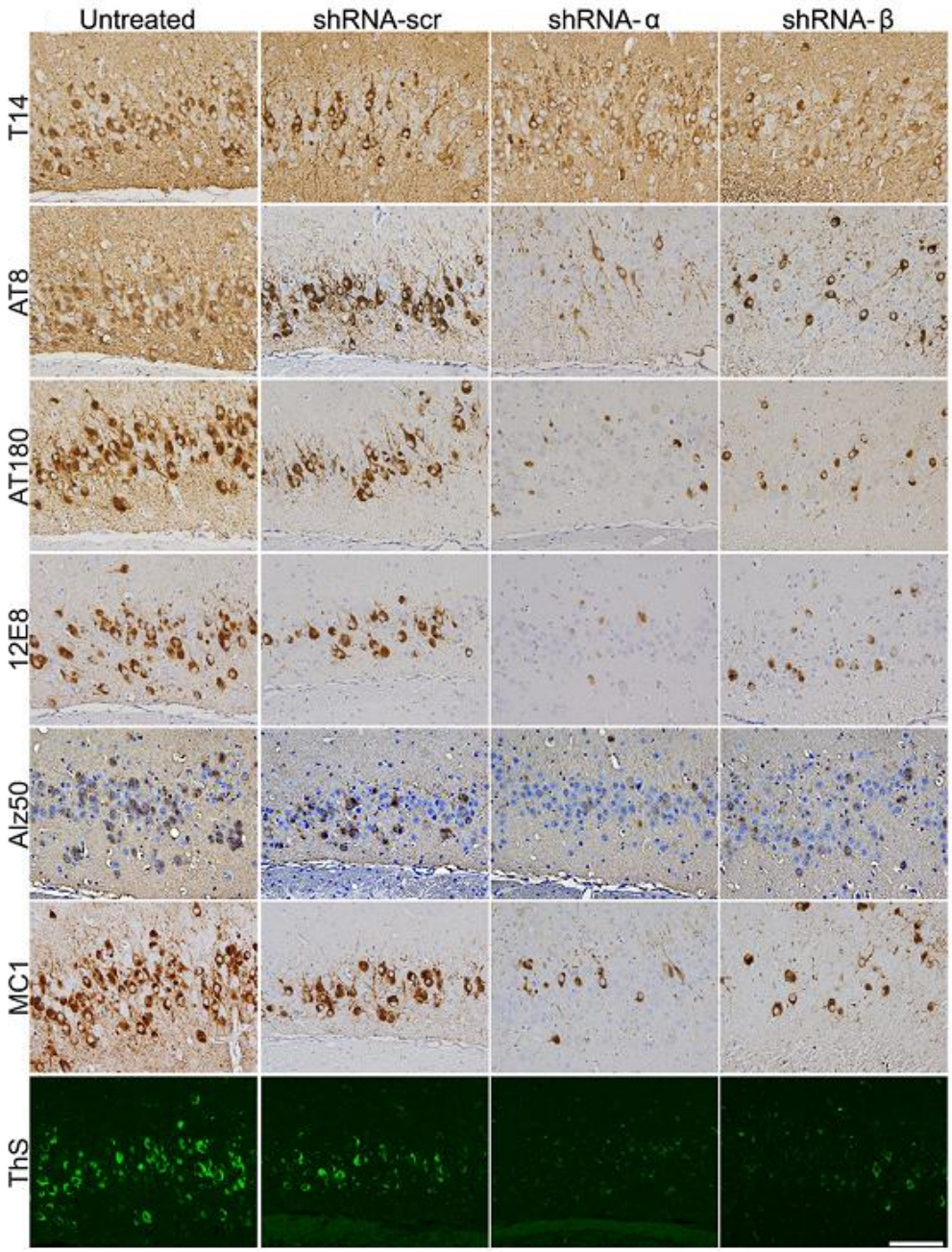

Figure 5: GSK-3α and GSK-3β KD reduces tau phosphorylation and conformational changes in APP/tau double transgenic mice. APP/tau double transgenic neonates were un-injected (un) or injected with shRNA-α, shRNA-β, or shRNA-scr (control) and evaluated at 11 months of age (n=15 per group). Representative immunohistochemistry images counterstained with hematoxylin show CA3 regions of posterior hippocampus stained with antibodies to total tau (T14), phospho-tau Ser202/Thr205 (AT8), phospho-tau Thr231 (AT180), phospho-tau Ser262 (12E8), or conformational specific antibodies Alz50, MC1, or thioflavin staining (ThS) as indicated. (Source: Hurtado et al (273)).

Unfortunately, despite all of these promising data, GSK-3 inhibitors have failed to show any efficacy in clinical trials of tauopathies. For example, a recent phase 2 trial with tideglusib (a GSK-3 inhibitor also known as NP12) failed to show any clinical efficacy after 52 weeks of treatment in patients with mild-to-moderate Progressive Supranuclear Palsy (n=146) (327); or after 26 weeks of treatment of AD patients (n=306) (328).

In summary, there are enough data to demonstrate the role of GSK-3 in tau phosphorylation and probably NFT formation. However, it is still unknown whether GSK-3 inhibitors could be an effective treatment in patients with different tauopathies. Additional studies are needed to further investigate this subject.

3.3.2. GSK-3 and APP.

As stated previously, GSK-3 has been proposed as a possible link between APP and tau. In this line, several studies have shown that Aβ may increase GSK-3 activity (53,217,312,329–331). For example, *in vitro*, the administration of Aβ oligomers to primary rat hippocampal cultures reduced p-S9-GSK-3β levels with normal levels of total GSK-3β suggesting an increase of GSK-3β activity (53). Similar results have been found *in vivo*, when Aβ oligomers were infused in mice (330). In both cases, increased levels of phospho-tau were also found (53,330) Likewise, double APP/tau transgenic mice have shown higher levels of p-Y279-GSK-3α and p-Y216-GSK-3β with normal levels of total GSK-3α and GSK-3β, suggesting increased GSK-3 activity, associated with an aggravation of NFT pathology when compared to parenteral single tau transgenic mice (312). These data suggest that Aβ oligomers could hyperphosphorylate tau and induce tauopathy through GSK-3 activation.

Importantly, Aβ can also induce other AD-related changes such as spine changes (331), neuronal dysfunction (332) or neuronal loss (329,331). Interestingly, removing tau has been shown to have a less protective effect than GSK-3 inhibition in some

studies (332), suggesting that GSK-3-mediated toxicity induced by Aβ was only in part dependent on tau, and that other downstream molecules might be involved.

On the other hand, several studies have suggested that GSK-3 is not only a downstream element of Aβ, but also upstream, and it may have some effect on Aβ production (267,272,325,332–337). For example, GSK-3 inhibitors are able to reduce Aβ levels in several cell cultures (COS7, CHO-APP^{695}, HEK293, NT2N, N2a and primary neurons from tg2576 mice) (272,334,336,337). Furthermore, *in vivo* studies have shown that acute treatment with lithium and valproic acid can reduce Aβ levels in PDAPP mice. Consistent with this, chronic treatment with different GSK-3 inhibitors can reduce Aβ levels after 3 weeks of treatment in 3 month-old Tg2576xPSEN1^{p264L} (272), after 1 month of treatment in 9 month-old tg2576 mice (337), or after 7 months of treatment in 8 month-old homozygous PDAPP mice (336). Furthermore, decreased levels of Aβ peptides have been found in double-transgenic mice overexpressing mutant APP and a dominant-negative form of GSK-3β (325). ilarly, inhibition of Shaggy either by expression of a dominant negative form in the adult nervous system or by treatment with lithium reduces Aβ42 levels in flies (332).

In addition, chronic treatment with GSK-3 inhibitors can also reduce the amyloid burden in 15 month-old tg2576 mice after 3 months of treatment (267), and in 8 month-old homozygous PDAPP mice after 7 months of treatment (336).

However, the effects of lithium and other GSK-3 inhibitors on Aβ production are controversial. Several studies have failed to show any effect on reducing Aβ levels, and even unexpected results have been found (323,338). For example, *in vitro,* treatment with lithium increased Aβ levels in rat cultured neurons (338). Furthermore, chronic treatment with lithium for 4 weeks did not significantly reduce Aβ levels, amyloid load, or working memory in 15 months-old APP/tau/PS1 triple transgenic mice, despite being able to reduce tau phosphorylation (323). There are several possible explanations which will be discussed later: and may also regulate unintended targets, which may confound experimental results.

Previously, and in this line, Phiel et al., in collaboration with our lab, observed that GSK-3α and GSK-3β may have different roles in APP processing and Aβ production *in vitro*. In CHO-APP_{695} cells, the transfection of short interfering RNAs directed against GSK-3α and GSK-3β reduced GSK-3 protein levels in an isoform-specific manner. A selective reduction of GSK-3α protein expression decreased Aβ-40 and Aβ-42 levels, while a selective reduction of GSK-3β protein expression resulted in a modest increase of Aβ-40 and Aβ-42 levels. Furthermore, overexpression of GSK-3α in CHO-APP_{695} cells increased Aβ-40 and Aβ-42 levels in a dose-dependent manner, suggesting that GSK-3α, but not GSK-3β, may be the key isoform that regulates the production of amyloid peptides (272).

However, other authors observed that GSK-3β inhibition by GSK-3β antisense oligonucleotides reduced Aβ levels in cells (335,336), suggesting that the GSK-3β isoform, and not only GSK-3α, may also have an important role in Aβ production.

In this context, a few groups have tried to explore the effect of GSk-3α and GSK-3β in Aβ *in vivo*. Our group decided to selectively reduce the expression of each isoform by two different genetic approaches: 1) by CRE/loxP system in triple CKO mice, which is described in this dissertation; and 2) as stated previously, by developing recombinant AAV2/1b shRNA constructs which specifically reduced the expression and activity of GSK-3α or GSK-3β. These constructs were injected intraventricularly in newborn single APP transgenic mice and in double APP/tau transgenic mice. Both systems were conducted in parallel, but shRNA was faster. Consistent with Phiel et al., we observed that GSk-3α KD, but not GSK-3β, reduced Aβ levels and amyloid load in both of ours 11 month-old AD mouse models (273) (Figure 6).

However, Jaworski et al. failed to show any evidence of GSK-3-mediated control of APP, not only for GSK-3β but also for GSK-3α, and concluded that the GSK-3 isozymes do not contribute significantly to the processing of APP in mice brain *in vivo*. (339).

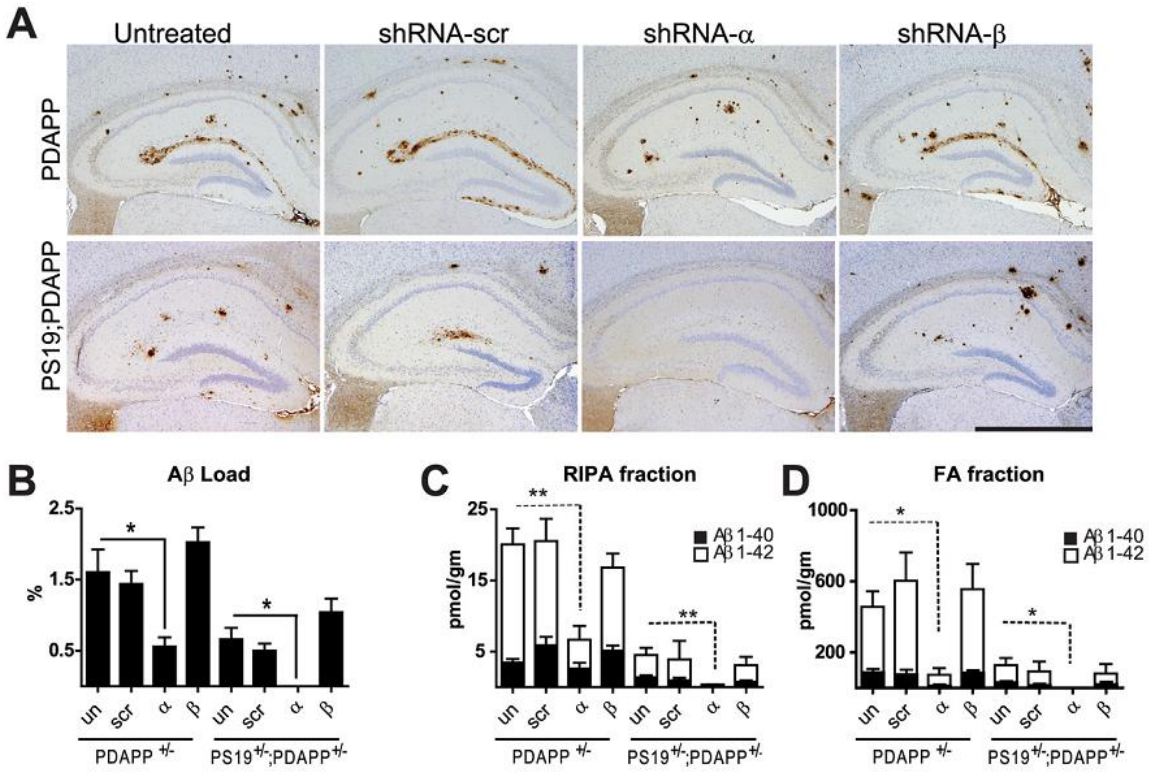

Figure 6: GSK-3α but not GSK-3β KD decreases Aβ levels and SP in APP and APP/tau transgenic mice. APP or APP/tau transgenic neonates were un-injected (un) or injected with shRNA-α (α), shRNA-β (β), or shRNA-scr (scr) and evaluated at 11 months of age (n=15 per group). A) Representative immunohistochemistry images immunostained for Aβ (Nab228) and counterstained with hematoxylin demonstrated a significant reduction in plaque load after GSK-3α KD in both APP and APP/tau transgenic mice (n=15 per group) Scale bar, 1mm. B) Hippocampal Aβ load was quantified using ImageJ software (n = 7–12 per group). In both APP and APP/tau transgenic mice shRNA-α treatment decreased Aβ burden compared with untreated mice. C, D) Hippocampal regions of APP and APP/tau mice were analyzed for soluble and insoluble Aβ using Aβ sandwich ELISA (n= 5–8/group). Aβ-40 and Aβ-42 levels were reduced in soluble (RIPA) and insoluble (FA) fractions in both APP and APP/tau transgenic mice. Data are shown as mean ± SEM. * p< 0.05, ** p< 0.01(Source: Hurtado et al (273)

Taken together, previous studies suggested that GSK-3 reduction may represent a potential therapeutic target for AD. However, the effect of each isoform on Aβ and APP *in vivo* is unknown. In this dissertation, we aimed to study whether GSK-3α and/or GSK-3β KO could ameliorate cognitive and behavioral deficits observed in AD mice, and to review the effect of each of the isoforms in amyloid pathology.

II. HYPOTHESIS

1. Synaptic loss in the dentate gyrus of the hippocampus is an independent and early event associated with cognitive impairment in the oldest old.

2. Reduction of GSK-3α but not GSK-3β levels may ameliorate amyloid-related pathology and cognitive impairment in AD mouse models.

III. OBJECTIVES

1. Contribution of synaptic markers to cognitive status and cognitive impairment in the oldest-old.

We aimed to:

a. study the correlation of synaptic markers with global cognitive scores and cognitive group in the oldest old

b. study the correlation of frequent pathological changes in the oldest old with global cognitive scores and cognitive group, and

c. estimate the independent contribution of both synaptic markers and pathological changes to global cognitive scores in the oldest old

2. Contribution of GSK3 to AD pathology and cognitive impairment in an APP mouse model.

We aimed to:

a. study the effect of the selective reduction of GSK-3α or GSK-3β isoforms in cognitive and behavioral deficits in an APP mouse model of AD, and

b. study the effect of the selective reduction of GSK-3α or GSK-3β isoforms in amyloid load in an APP mouse model of AD

To achieve these objectives we aimed to:

c. generate GSK-3α and GSK-3β double transgenic CKO mice,

d. generate GSK-3α+β triple transgenic CKO mice, and

e. generate GSK-3α/APP and GSK-3β/APP triple transgenic mice.

IV. METHODS AND RESULTS

STUDY 1: Contribution of synaptic markers to cognitive status and cognitive impairment in the oldest-old.

1.1. METHODS:

1. 1. 1. Study population:

Study participants were the first 157 individuals to come to autopsy from The 90+ Study, a longitudinal population-based study of ageing and dementia in people aged 90 and older who are survivors of the Leisure World Cohort Study (8). Briefly, individuals live at home as well as in institutions, and represent the full spectrum of health and cognitive abilities. All 90+ Study participants had evaluations every 6 months including a neurological examination by a trained physician or nurse practitioner and a full neuropsychological battery that included the MMSE. Relevant medical history, medication use, and demographic information were obtained from the participants or their informants. Medical records, including brain imaging evaluations were obtained from the participant's physicians. Information about cognitive (340) and functional abilities (341) were obtained from informants in frequent contact with the participants. To inquire about the onset of cognitive problems, the Dementia Questionnaire(342,343) interview was conducted over the phone with informants of participants with evidence of cognitive impairment. Shortly after death, the Dementia Questionnaire was done with the decedent's informant to inquire about the participant's condition since the last evaluation. The Institutional Review Board of the University of California, Irvine, approved all procedures and all participants or their surrogates gave written informed consent.

1. 1. 2. Determination of Cognitive Status:

After a participant's death, all available information was reviewed and discussed during a multidisciplinary consensus diagnostic conference led by 'The 90+ Study' principal investigator (C.K.). Participants were classified as normal, CIND, or as having dementia. Dementia diagnosis was established using Diagnostic and Statistical Manual of Mental Disorders 4th Edition criteria (344). CIND is defined by initial cognitive impairments such as deficits in episodic memory (345), executive dysfunction (346), naming difficulties or other aphasias (347). Participants were

classified as CIND if they showed cognitive or functional deficits that were not severe enough to meet criteria for dementia. All cognitive diagnoses were made blinded to pathological evaluations.

1. 1. 3. Neuropathology

All autopsies were performed at the University of California, Irvine. After weighing the whole brain and gross inspection, one hemisphere was dissected as previously described (348). Six-micrometre thick, coronal sections of mid-frontal cortex superior temporal cortex, anterior hippocampus, amygdala, substantia nigra and medulla oblongata were cut. All histological staining, immunohistochemistry and microscopic analyses were performed in the Centre for Neurodegenerative Disease Research at the University of Pennsylvania as described (107). Briefly, sections were subjected to immunohistochemistry using the avidin-biotin complex detection method (VECTASTAINABC kit; Vector Laboratories) with ImmPACTTM diaminobenzidine peroxidase substrate (VectorLaboratories) as the chromogen using monoclonal antibodies to phosphorylated tau (mouse PHF1; 1:1K, gift of Dr Peter Davies, Manhasset, NY), β-amyloid (mouse NAB228; 1:15K; generated in Centre for Neurodegenerative Disease Research), phosphorylated TDP-43 (rat 409/410; 1:500; gift of Dr Manuela Neumann, Zurich, Switzerland), SV2 (mouse SV2; 1:20K; DSH Iowa), synaptophysin (mouse MAB368; 1:1K; Millipore) and VGLUT1 (Guinea pig VGLUT1; 1:7.5K; SYSY).

Topographical Braak staging (stages I–VI) was assigned from PHF1 stained slides (n=157) (85). Thal phases were determined from NAB228 stained hippocampal slides: phase 0–1, 2, 3 and 4 (n=150) (349). TDP-43 inclusions and neurites were determined from 409/410 stained hippocampal slides: presence/absence.

The assessment of cerebrovascular disease pathology (n=108) and hippocampal sclerosis (n=155) was determined from Harris haematoxylin and eosin stained mid-

frontal cortex, superior temporal cortex, hippocampus, amygdala, substantia nigra and medulla sections. Hippocampal sclerosis was assessed as follows: 0 for no gliosis or neuronal loss; 1+ for mild gliosis or neuronal loss in the CA1 or subiculum; 2+ for moderate or severe gliosis and neuronal loss consistent with definite hippocampal sclerosis. Cerebrovascular lesions such as infarcts, micro-infarcts or micro-bleeds along with cerebral amyloid angiopathy and HS were used to generate CVD pathology scores following a simplified staging of Jellinger and Attems as follows: 0 for cases without major infarcts, hippocampal sclerosis, cerebral amyloid angiopathy or other lesions; 1+ for minimal vascular pathology cases with mild to moderate cerebral amyloid angiopathy and/or 1–2 small lacunes; 2+ for moderate vascular pathology cases with severe cerebral amyloid angiopathy and/or HS and/or major infarcts (350).

1. 1. 4. Synaptic protein measures

Synaptic relative immunointensity ratios (RIRs) were obtained by the following process. A preliminary study of synaptic and presynaptic proteins was done including antibodies to synaptophysin, SV2, VGLUT1, synataxin 1, vesicle-associated membrane protein 2 (VAMP2), synapsin 1, synaptotagmin 1, dynamin, vesicular GABA transporfter (VGAT), post synaptic density protein 95 (PSD95) and Glutamate receptor 1 (GLUR1); obvious outer molecular layer synaptic loss was observed on slides obtained from patients with AD when stained with antibodies to synaptophysin, SV2 and VGLUT1. For this study, hippocampal slides were stained for synaptophysin (n=149), SV2 (n=151) or VGLUT1 (n=152). Sections were scanned (Nikon DS-Fi2 camera, gain 1.2, exposure 15ms) at 10 on a Nikon Eclipse TE2000 microscope using NIS Elements software (Nikon Instruments, Inc.). ImageJ 1.47t (National Institutes of Health) was used for analysis.Mean pixel intensities of the inner- and outer molecular layer of the dentate gyrus just under CA1 were captured (Figure 7). Raw values on an 8-bit scale (range of 45–185) were normalized to a blank area for each slide (median value 41). Synaptic RIRs of the outer/inner molecular layer were

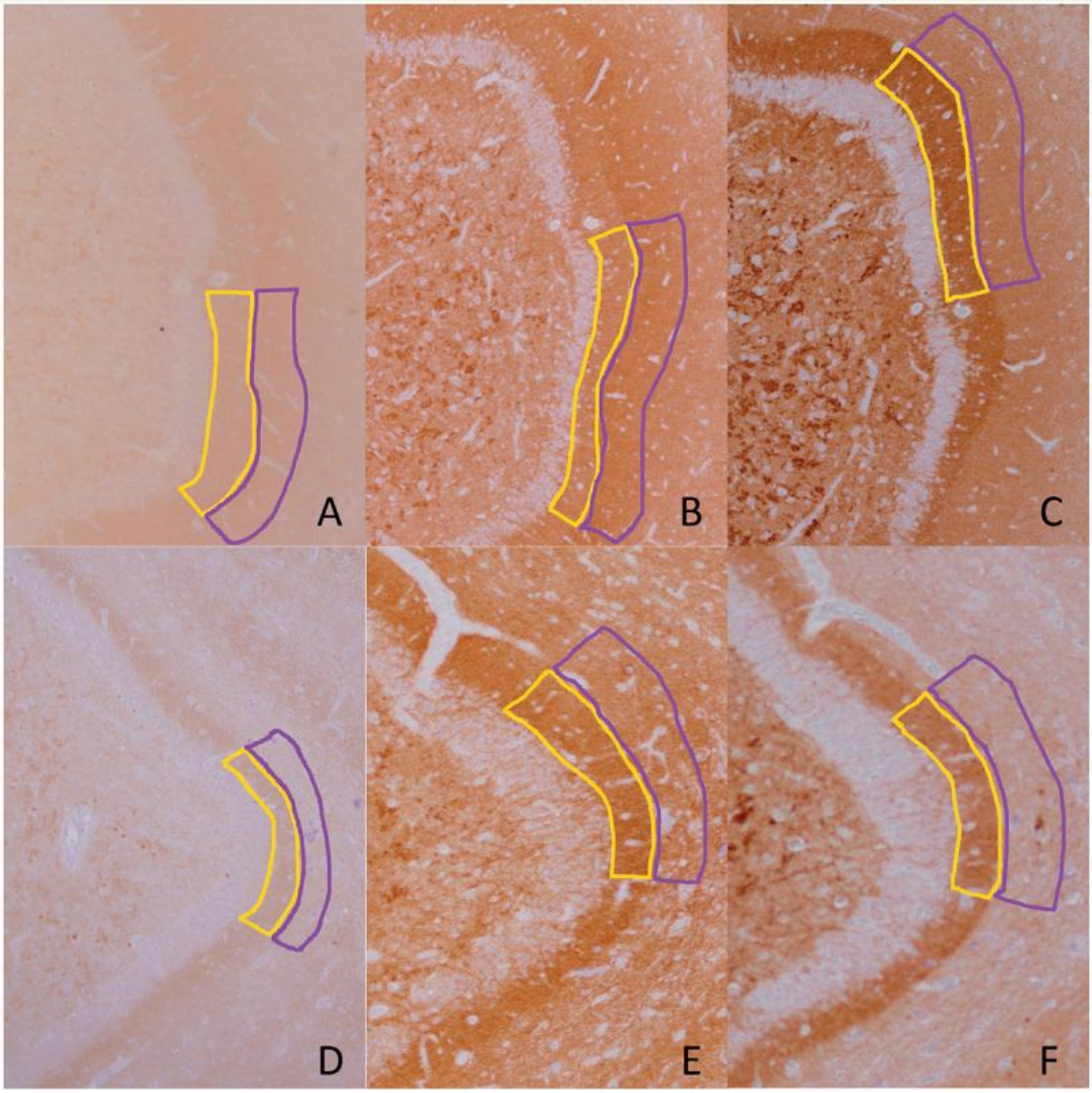

Figure 7: Representative images of synaptic protein immunoreactivity. Synaptic marker immunohistochemistry from two cases shows distinct staining of the inner molecular layer (highlighted in yellow) and the outer molecular (highlighted in purple) of the hippocampus. (A–C) The relatively healthy outer molecular layer: (A) synaptophysin, (B) SV2 and (C) VGLUT1 with synaptic ratios 1.19, 1.13 and 0.78, respectively (note that VGLUT1 is consistently lower than the other two). In contrast, (D–F) represents an individual with severely reduced outer molecular layer, whose inner molecular layer is preserved: (D) synaptophysin, (E) SV2 and (F) VGLUT1 with synaptic ratios 0.53, 0.74 and 0.56, respectively.

calculated from (outer molecular layer - blank) / (inner molecular layer - blank) for each case. To verify the repeatability of our measurements, 10 random cases were stained twice by the synaptic antibodies and synaptic RIRs were obtained independently by two researchers (L.M.P., J.L.R.). A K of 0.987 was obtained (Type C intraclass correlation coefficient).

All pathological diagnoses were done blinded to clinical diagnosis.

1. 1. 5. Statistical analysis

We compared characteristics of the three cognitive groups: normal, CIND and dementia using Chi-squared test for categorical variables and ANOVA for continuous variables. We used multinomial logistic regression models to determine the association between each individual neuropathological or synaptic protein measure and cognitive diagnosis. We report the odds of being in the CIND group compared to the normal group, the odds of being in the dementia group compared to the CIND group, and the odds of being in the dementia group compared to the normal group. Neuropathological and synaptic protein measures were analysed as continuous variables in the logistic regression analyses. Separate regression models were used for each neuropathological and synaptic protein measure.We also explored the association between the individual neuropathological or synaptic measures and the MMSE, a measure of global cognition, using multiple linear regression analyses. Finally, we analysed the relative contribution of the different pathological measures to global cognitive scores, by including all synaptic and pathological measures in a multiple regression model. All regression models were adjusted for age at death and gender and all analyses were performed using SAS version 9.3 (SAS Institute Inc.).

1.2. RESULTS:

1. 2. 1. Subject characteristics

Of the 157 participants of this study, 36 had normal cognition, 37 were diagnosed with CIND and the majority (n=84) had dementia (Table 2). The most frequent clinical diagnosis of the participants with dementia was AD alone (65%) or in combination with other dementias (21%) followed by vascular dementia (7%) and dementia with Lewy bodies (6%). Participants had an average age at death of 98 years (range: 94–101 years), were mostly female (71%), and highly educated (71% had at least a college education). MMSE scores were available for the majority of individuals within 1 year before death (Table 2). The overall frequency of the APOE alleles was 14% for the ε2 allele and 22% for the ε4 allele. While there was an increase in the frequency of the ε4 allele in the dementia group (27%) compared to the normal group (21%), this non-significant increase is consistent with previous work where we found that the ε4 allele no longer plays a role in dementia and mortality at very old ages (351). Brain weight was non-significantly lower in the dementia group.

1. 2. 2. Alzheimer's disease pathology

AD pathology was measured using Braak and Braak staging (85) and Thal phases (349). In the normal group, Braak stage (median III; mean 3.3) and Thal phase (median 1; mean 1.9) scores indicate that AD pathology was present in at least mild to moderate amounts (Figure 8). The CIND group presented with similar Braak stage (median III; mean 3.4) and Thal phase (median 3; mean 2.3) scores, while Braak stage (median V; mean 4.3) and Thal phase (median 3; mean 2.6) were more moderate to severe in the dementia group. Higher Braak stages were significantly associated with higher odds of being in the dementia ve rsus normal group [odds ratio (OR) =1.68, P=0.001] and of being in the dementia versus CIND group (OR = 1.52, P=0.02) (Table 3). Higher Thal phases were associated with higher odds of

being in the dementia versus the normal group (OR =1.64, P=0.011) but did not distinguish between the dementia and CIND groups (P>0.15).

Characteristic	All subjects (*n* = 157)	Normal (*n* = 36)	CIND (*n* = 37)	Dementia (*n* = 84)
	Mean (SD)			
Age at death	98.0 (3.6)	97.8 (2.5)	98.4 (4.0)	97.7 (3.7)
Last MMSE score[a]	18.1 (10.1)	27.8 (1.6)	23.7 (5.4)	11.2 (8.6)
MMSE interval to death (months)	7.5 (7.7)	5.9 (3.3)	6.5 (4.5)	8.6 (9.8)
Brain weight (g)	1127 (121)	1179 (104)	1123 (125)	1104 (121)
	n (%)			
APOE E4[b]				
0 alleles	119 (78)	27 (79)	33 (89)	59 (73)
⩾ 1 alleles	33 (22)	7 (21)	4 (11)	22 (27)
APOE E2				
0 alleles	131 (86)	29 (85)	31 (84)	71 (88)
⩾ 1 alleles	21 (14)	5 (15)	6 (16)	10 (12)
Gender				
Male	45 (29)	15 (42)	10 (27)	20 (24)
Female	112 (71)	21 (58)	27 (73)	64 (76)
Education[c]				
⩽ High school	45 (29)	7 (19)	8 (22)	30 (36)
Any college	73 (47)	16 (44)	20 (54)	37 (45)
Any graduate school	38 (24)	13 (36)	9 (24)	16 (19)
Normal cognition	36 (23)	36 (100)		
CIND	37 (24)			
Memory impairment			13 (35)	
Executive impairment			12 (32)	
Other impairment[d]			12 (32)	
Dementia	84 (54)			
Alzheimer's disease only				55 (65)
Alzheimer's disease plus[e]				18 (21)
Vascular dementia				6 (7)
Other dementia				5 (6)

Table 2: Characteristics of The 90+ Study participants. [a] Excludes four participants with missing MMSE score. [b] Excludes five participants with unknown ApoE allele status. [c] Excludes one participant with unknown degree of education. [d] Includes impairment in domains other than memory or executive function. [e] Includes mixed Alzheimer's disease/vascular dementia, Alzheimer's disease/other and Alzheimer's disease with dementia with Lewy bodies.

Neither AD marker distinguished between the normal and CIND groups. Higher levels of AD plaque and tangle burdens were significantly associated with lower MMSE scores (Thal phase, P=0.02; Braak stage, P<0.001). The greatest decreases on the cognitive tests occurred with the highest plaque and tangle burdens. The mean MMSE score was significantly lower in Thal phase 4 compared to Thal phases 2 and

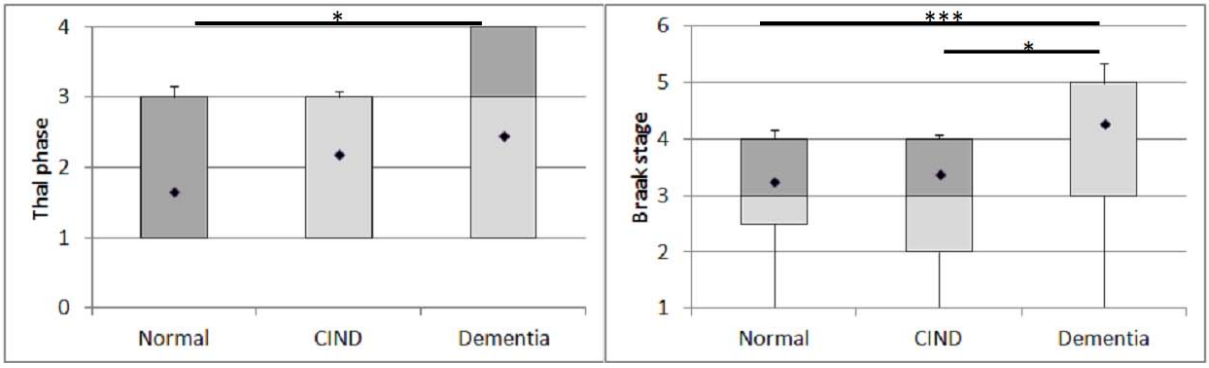

Figure 8: Thal phase and Braak stage measures by cognitive group in the oldest-old. Thal phase stage scores were increased in Demented compared to normal, Braak stage score was significantly different in demented compared to CIND and Normal (* <0.05; *** <0.001 p-values from multinomial logistic regression after adjusting for age at death and gender).

earlier (P<0.01) and even to Thal phase 3 (P<0.05). For Braak stage, the mean MMSE score was significantly lower in stage VI compared to all the other Braak stages (P<0.001), and in stage V compared to stages III and IV (P<0.05).

1. 2 .3. Hippocampal sclerosis

As the prevalence of HS increases with age, we investigated what proportion of individuals had these lesions in our cohort. HS was found in 15% of all individuals, but in only one individual without dementia. The presence of HS in 28% of those with dementia (23/82) allowed the measure to significantly distinguish the dementia group from both the normal (P=0.003) and CIND (P=0.002) groups (Table 3).

1. 2. 4. Cerebrovascular disease

As the prevalence of CVD pathology increases with age, we investigated what proportion of individuals had these lesions in our cohort. Cerebrovascular lesions and cerebral amyloid angiopathy were present in modest amounts in The 90+ Study.

Cerebral amyloid angiopathy was found in 52% (56/108) of the cases whereas CVD lesions such as infarcts, micro-infarcts or micro-bleeds were rarer (10%; 11/108). Althogether, 63% of all individuals had some level of CVD pathology, including 45% of both the normal and CIND groups and 74% of the dementia group. Although the prevalence of CVD was not different between the normal and CIND groups (Figure 9), people with higher levels were more likely to be in the dementia group compared to both the normal and CIND groups (both P=0.009) (Table 3).

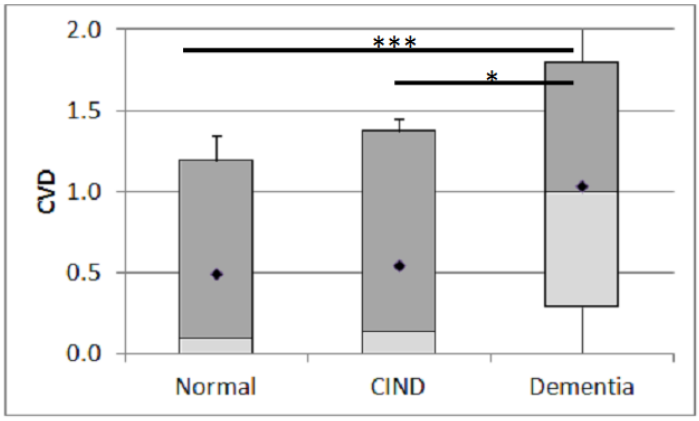

Figure 9. Cerebrovascular pathology scores by cognitive group in the oldest old. CVD scores were increased in Demented compared to normal and CIND. (*<0.05; *** <0.001 p-values from multinomial logistic regression after adjustin for age at death and gender)

1. 2. 5. TDP-43

TDP-43 is a common co-morbidity and may associate with a more rapid cognitive decline in the ageing brain (352). In our cohort, TDP-43 pathology was present in the hippocampus of 24% (35/146) of the cases. While a small number of both normal 11%, 4/35) and CIND (12%, 4/33) individuals had pathology, TDP-43 inclusions affected a more substantial portion of the dementia group (35%, 27/78). As in our earlier study (107), TDP-43 was almost exclusively in individuals with HS. 77% (17/22) of the cases with HS also had TDP-43 inclusions. While 15% (18/124) of

individuals without HS also had TDP-43 pathology, the numbers were too low to analyse the significance of the TDP-43 pathology after controlling for HS (data not shown).

1. 2. 6. Synaptic markers

As described above, to measure the synaptic levels of the perforant pathway, synaptic RIRs were generated by measuring the intensity of synaptophysin, SV2, and VGLUT1 by immunohistochemistry in the outer molecular layer of the hippocampus relative to the inner molecular layer. Higher RIRs represent a relatively healthy outer layer in relation to the inner layer, whereas lower RIRs correspond to synaptic loss in the outer layer (Figure 10). In the normal group, synaptophysin (mean 0.94) and SV2 (mean 0.94) had RIRs close to 1.00, whereas the glutamate-specific VGLUT1 RIR was lower (mean 0.67). Similar values were obtained in the CIND group: synaptophysin (mean 0.98), SV2 (mean 0.96) and VGLUT1 (mean 0.64). In the dementia group, these values were mildly lower: synaptophysin (mean 0.87), SV2 (mean 0.89) and VGLUT1 (mean 0.63).

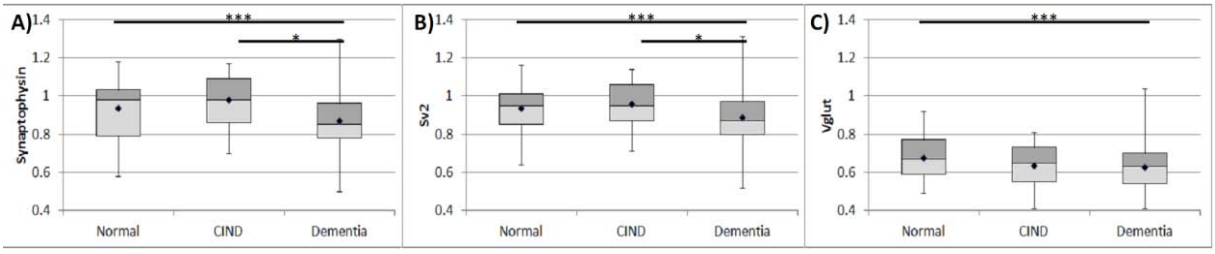

Figure 10: Synaptic ratios measures by cognitive group in the oldest old. All three synaptic RIRs were reduced in dementia compared to normal with (A) synaptophysin and (B) SV2 were significantly different between the three cognitive groups; however, (C) VGLUT1 did not distinguish between CIND and dementia. No synaptic RIR distinguished normal from CIND. (*<0.05; *** <0.001 p-values from multinomial logistic regression after adjustin for age at death and gender)

All three synaptic RIRs distinguished between the dementia and normal groups with higher RIRs associated with lower odds of being in the dementia group (P<0.05) (Table 3). The synaptophysin and SV2 RIRs also distinguished between the dementia and CIND groups (synaptophysin, P<0.001; SV2, P=0.008), whereas the VGLUT1 RIR did not (P=0.747). No RIR distinguished between the CIND and normal groups (all P>0.12). We also examined the association between synaptic RIRs and global cognitive scores and found that for all three synaptic markers, higher RIR values were significantly associated with higher MMSE scores (synaptophysin, P<0.001; SV2, P<0.001, VGLUT1, P<0.05).

Measure	Wald test *P*-value	CIND versus Normal OR (95% CI) *P*-value	Dementia versus CIND OR (95% CI) *P*-value	Dementia versus Normal OR (95% CI) *P*-value
Synaptophysin	0.002	5.59 (0.20–159.45) 0.314	0.01 (<0.01–0.11) **0.001**	0.03 (<0.01–0.59) **0.021**
SV2	0.017	2.85 (0.10–84.75) 0.546	0.02 (<0.01–0.35) **0.008**	0.05 (<0.01–0.93) **0.045**
VGLUT1	0.099	0.04 (<0.01–2.41) 0.124	0.56 (0.02–18.84) 0.747	0.02 (<0.01–0.76) **0.034**
Braak stage	0.001	1.06 (0.75–1.50) 0.740	1.52 (1.07–2.16) **0.020**	1.68 (1.24–2.30) **0.001**
Thal phase	0.037	1.37 (0.89–2.11) 0.158	1.20 (0.84–1.71) 0.318	1.64 (1.12–2.38) **0.011**
Hippocampal sclerosis	<0.001	0.94 (0.36–2.49) 0.906	3.32 (1.56–7.05) **0.002**	3.13 (1.48–6.64) **0.003**
Cerebrovascular disease	0.004	0.94 (0.35–2.55) 0.900	2.99 (1.31–6.83) **0.009**	2.81 (1.29–6.13) **0.009**
TDP-43	0.008	0.90 (0.20–4.05) 0.893	4.32 (1.34–13.95) **0.014**	3.89 (1.23–12.36) **0.021**

Table 3: Association between markers and cognitive groups in the oldest old.
Odds ratios and 95% CIs were generated from multinomial logistic regression models where the dependent (outcome) variable was cognitive group (normal, CIND, or dementia) and the independent variables were the neuropathological markers as continuous variables, except TDP-43 which was a binary variable. P-values 50.05 are in bold. Age at death and gender were included as covariates and each neuropathological measure was analysed in a separate model. The overall P-value corresponds to the type 3 analyses and tests whether the neuropathological marker (independent variable) is significantly associated with the cognitive group (outcome variable). Odds ratios are per unit. *n* for each group =149 (synaptophysin), 151 (SV2), 152 (VGLUT1), 157 (Braak stage), 150 (Thal phase), 155 (HS), 108 (cerebrovascular disease) and 146 (TDP-43).

1. 2. 7. Multiple pathologies

Pearson correlation coefficients showed significant correlations between the three synaptic RIRs (VGLUT1 and SV2, corr =0.37, P<0.001; VGLUT1 and synaptophysin, corr =0.45, P<0.001; SV2 and synaptophysin, corr =0.50, P<0.001). Given the correlation between synaptic markers, we wanted to explore the independent contribution of each with respect to global cognitive scores. In a multiple regression

model that included all three synaptic markers, we found that higher RIRs for both synaptophysin (beta =20.3, P=0.002) and SV2 (beta =13.4, P=0.03) remained significantly associated with better MMSE scores.

Post hoc analysis revealed that the SV2 RIR was significantly lower at Braak stage VI (P<0.001) and the VGLUT1 RIR was significantly lower in individuals with HS (P=0.024). To estimate the independent contribution of all the different measures to global cognitive scores, we included all three synaptic RIRs, the AD pathology scores, and HS in a multiple regression analysis. In this model, the synaptophysin ratio, Braak stage, TDP-43 and HS all remained significantly associated with MMSE scores (P-values:<0.05, 0.001, <0.01 and 0.001, respectively).

1. 2. 8. Memory impairment only subjects

The primary impairment in 13 of the CIND individuals was memory (Table 2). As those with executive impairment may have dysfunction related more to a frontotemporal lobar degeneration rather than Alzheimer's disease and those with 'other' impairment cannot be well defined, it's possible that the 13 with memory impairment are more likely to be on the continuum between normal cognition and Alzheimer's disease. To test this hypothesis, we compared the RIRs and our pathological markers in the 'memory impairment only' CIND subjects to the normal and dementia subjects to see if our results had more significance. No new associations were found (data not shown), except for VGLUT1 RIR that almost

distinguished between memory impairment only CINDR subjects and normal groups (p=0.05), suggesting that a reduction of the Vglut1 may be an early event in memory impairment only CIND group. Similar subgroup analysis with the executive impairment and ‘other’ impairment CIND individuals also did not reveal any new associations that the comparisons with the group as a whole hadn’t already shown (data not shown).

STUDY 2: Contribution of GSK-3 in Alzheimer´s disease pathology and cognitive impairment in an APP mouse model.

2. 1. METHODS:

2. 1. 1. Generation of conditional knockout transgenic mice

Because GSK-3β KO in mice is lethal, GSK-3α CKO and GSK-3β CKO mice were generated using the CRE-loxP system.

2. 1. 1. 1. Generation of heterozygous GSK-3 floxed mice by Taconic.

Heterozygous GSK-3 floxed mice (the GSK-$3\alpha^{flox/-}$ line, and the GSK-$3\beta^{flox/-}$ line) were generated through a contract with Taconic.

For the GSK-$3\alpha^{flox/-}$ line, the targeting vector based on a 9.9 kb genomic fragment of the GSK-3 gene encompassing exons 1–11 and surrounding sequences was obtained from the C57BL/6J RP23 Bacterial Artificial Chromosomes Library and was modified by inserting a loxP site and an FRT-flanked neomycin resistance gene in intron 1 and a loxP site in intron 4, as well as a ZsGreen cassette at its 3´ end (Figure 11).

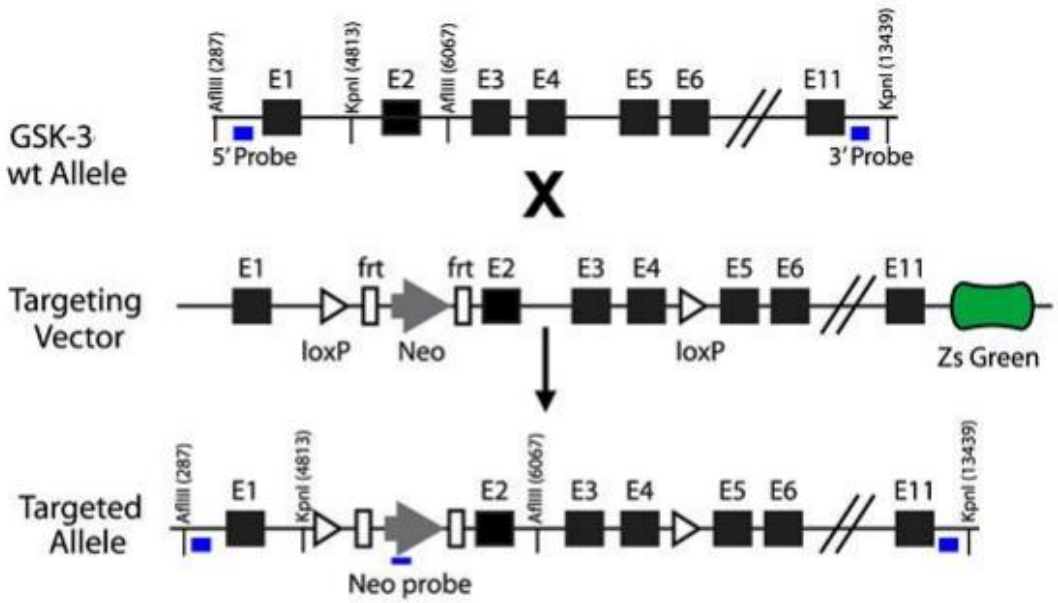

Figure 11: GSK-3 targeted gene after homologous recombination of GSK-3 wt allelele and the targeting vector.

Thirty micrograms of linearized DNA vector were electroporated using a Bio-RadGene Pulser at 240 V and 500 μF into 1 x 10^7 cells of the C57BL/6N embryonic stem cell lines. Only nonfluorescent clones suggesting the absence of the ZsGreen region were selected on day eight. After expansion and freezing clones in nitrogen, 176 clones were analyzed by using 5´,3´, and neomycin probes after digestion by KpnI, EcoRI, AflIII, PflFI, and BglII restriction enzymes in standard Southern blotting techniques. Proper homologous recombination was identified in four of the clones (B-A6, B-C3, B-C9 and B-G11) (Figure 12), and clone B-C9 was used for blastocyst injection.

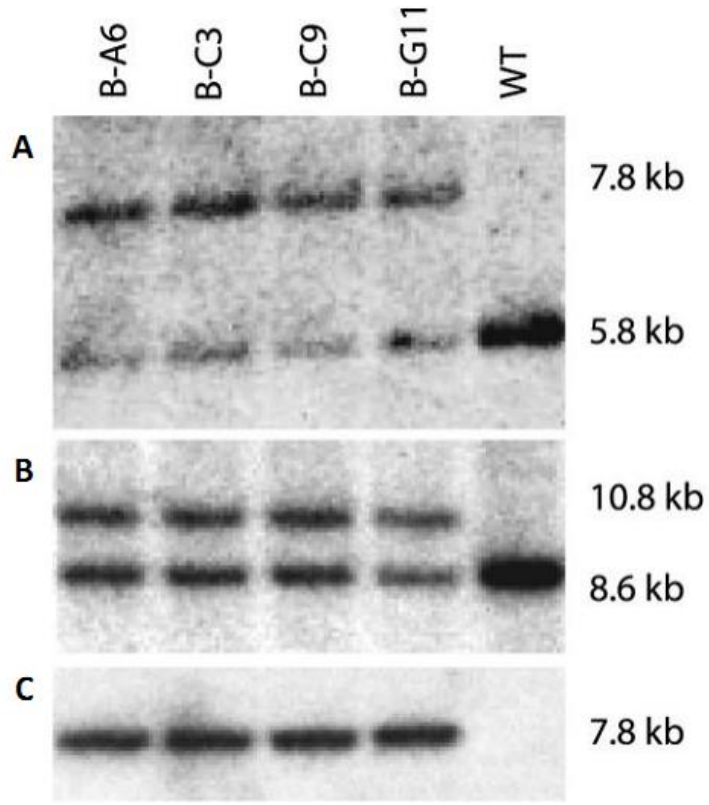

Figure 12: Identification of proper homologous recombination by Southern blotting. *176 clones were analyzed by using 5´ end **(A)**, 3´ end **(B)**, and neomycin probes **(C)** after digestion by AflIII **(A, C)**, KpnI **(B)**, PflFI, and BglII restriction enzymes in standard Southern blotting techniques.*

Ten to fifteen targeted C57BL/6N.tac embryonic stem cells were microinjected into each blastocyst obtained after superovulation of BALB/c females and eight injected blastocysts were transferred to each uterine horn of a 2.5 days postcoitum, pseudopregnant Naval Medical Research Institute female mouse. Highly chimeric mice were bred to female C57BL/6 mice with Flp-Deleter recombinase gene to remove the Neo selection marker (Figure 13). Germline transmission was identified by the presence of black C57BL/6 offspring.

The same protocol was used to generate the GSK-3β flox/- line.

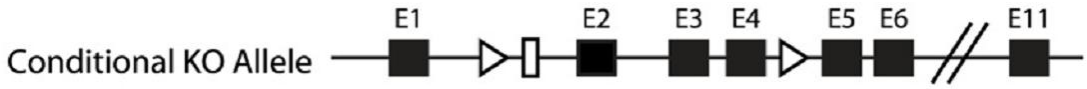

Figure 13: Gene structure of the GSK-3 CKO allele after FLP mediated deletion

2. 1. 1. 2. CRE lines

To introduce the CRE protein in the system, GSK-3 floxed mice were mated with two different lines of mice that expressed CRE: CAMKIIα-CRE and UBC-CRE-ERT2 lines.

CAMKIIα-CRE lines

CAMKIIα-CRE mice were described by Tsien et al. (353) In these mice, CRE expression is driven by the calcium/calmodulin-dependent protein kinase II (CAMKIIα) promoter, which is restricted to the brain and has been shown to be silent until several days after birth when the nervous system is still developing (277). Consistently, CRE-LoxP recombination is restricted to cells in the forebrain and

occurs during the third postnatal week (353). The CAMKIIα-CRE line is very interesting in the study of AD for two reasons: first, because its expression is specifically in the brain, especially in the cortex and hippocampus, which are targeted regions in AD; and second, since the KO occurs at the third postnatal week, we can avoid most of the developmental effects of the gene deletion, and are thus able to have a more accurate analysis of its effect in adulthood.

UBC-CRE-ERT2 lines

These mice were described by Ruzankina et al. (354) The CRE-ERT2 is a fusion protein of Cre recombinase fused to a triple mutant form of the human estrogen receptor. Its expression is driven by the Human Ubiquitin C (UBC) promoter and therefore present in all tissues (355). At physiological concentration, this mutant form of the estrogen receptor is unable to bind to its natural ligand, so under normal conditions, CRE-ERT2 remains in the cytoplasm and there is no any effect of CRE. However, after exposure to 4-hydroxytamoxifen, CRE is liberated and is able to go into the nuclear compartment. If this line is bred with a line of mice containing a loxP flanking sequence, such as our GSK-3 floxed lines, tamoxifen induction will result in deletion of the flanking sequences in widespread tissues generating KO mice. With this system, we can decide at what age we want to induce the KO, but once the established, it is irreversible.

2. 1. 1. 3. PDAPP mice:

PDAPP mice were described by Games et al. (356) These mice overexpress the human **APP** minigene harboring the Indiana mutation (V717F) driven by the **P**latelet-**D**erived Growth Factor promoter, and are therefore labeled PDAPP. PDAPP mice recapitulate several of the features of AD such as increased Aβ levels in the brain, neuritic plaques surrounded by astrocytes and glia, dystrophic neurites (356),

hyperphosphorylated tau (357), synaptic loss (356), and age-dependent behavioral deficits such as spatial memory in the water maze (358) and hyperactivity in the open field test (359). In general, these findings seem to be dependent on the dosage of the mutant APP allele, as they appear earlier or are more severe in homozygous mice than in heterozygous mice (360). Other not age related deficits present in these mice (such as significant size reduction in the hippocampus or deficits in working memory) are thought to be related to aberrant neurodevelopment due to the mutant APP (360).

The aim of this dissertation is to analyze the effect of knocking out GSK-3α and GSK-3β in heterozygous PDAPP mice.

2. 1. 1. 4. Breeding schemes:

GENERATION OF TRIPLE TRANSGENIC GSK-3α CKO;PDAPP AND GSK-3β CKO;PDAPP MICE

Triple transgenic mice were generated by crossing GSK-3$\alpha^{flox/-}$ mice with heterozygous CAMKIIα-CRE mice (353) and homozygous PDAPP mice.(356) Four crosses resulted in the targeted triple transgenic mouse: GSK-3$\alpha^{flox/flox}$;CAMKIIα-CRE$^{+/-}$;PDAPP$^{+/-}$ (GSK-3α cko;PDAPP). Line expansion was accomplished by mating GSK-3α cko;PDAPP mice with GSK-3$\alpha^{flox/flox}$ mice. This cross generated four genotypes of mice: GSK-3$\alpha^{flox/flox}$;CaMKIIα-cre$^{-/-}$;PDAPP$^{-/-}$ (GSK-3α wt), GSK-3$\alpha^{flox/flox}$;CaMKIIα-cre$^{+/-}$ PDAPP$^{-/-}$ (GSK-3α cko), GSK-3$\alpha^{flox/flox}$; CaMKIIα-cre$^{-/-}$;PDAPP$^{+/-}$ (GSK-3α wt;PDAPP), and GSK-3$\alpha^{flox/flox}$; CaMKIIα-cre$^{+/-}$;PDAPP$^{+/-}$ (GSK-3α cko;PDAPP). Each of the four groups consisted of n=10-15 mice that were analyzed at 17 months of age (Figure 14).

We used the same scheme to breed GSK-3β cko;PDAPP mice, but after the first generation of GSK-3β cko;PDAPP mice, they were unable to breed and we were not able to expand and maintain the line.

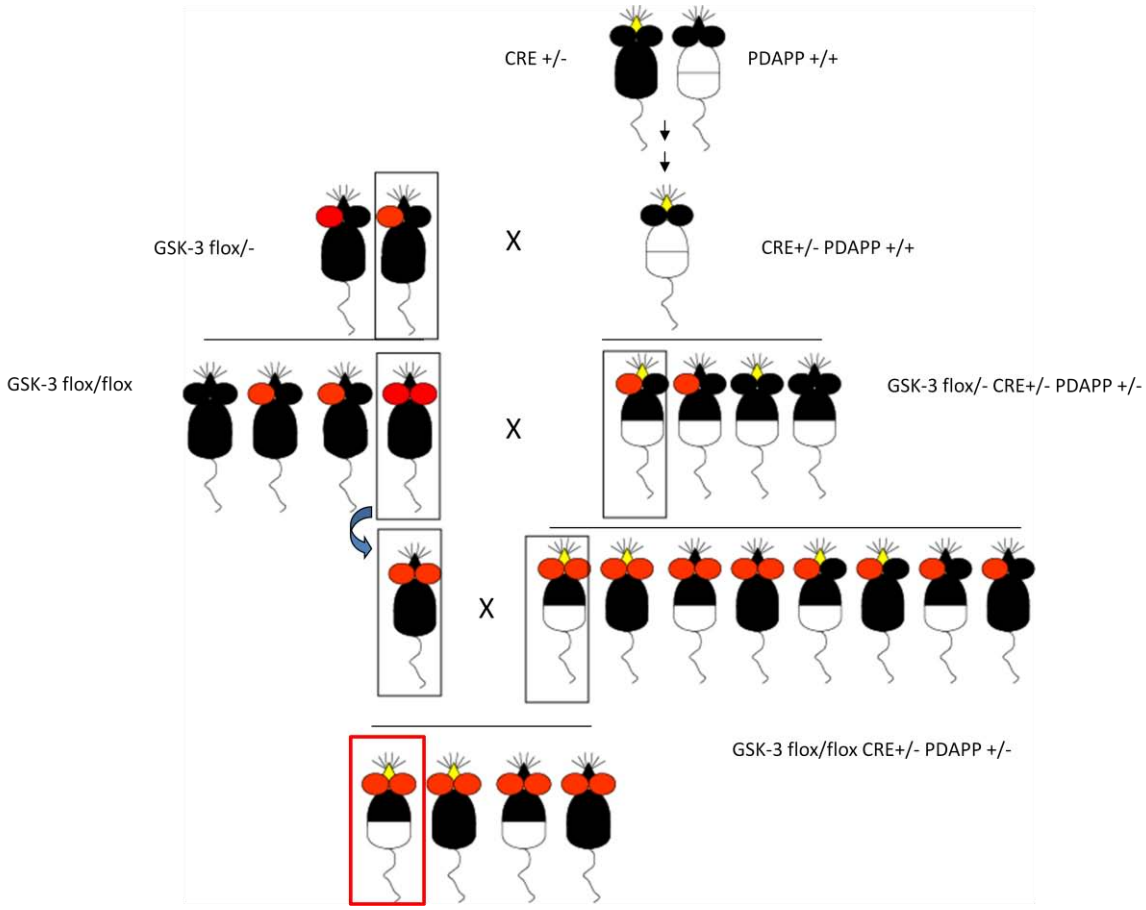

Figure 14: Triple transgenic breeding scheme. Our founders were a heterozygous GSK-3$\alpha^{flox/-}$ floxed mouse (one read ear), a homozygous PDAPP$^{+/+}$ mouse (white body) and the heterozygous CAMKIIα-CRE$^{+/-}$ line (yellow nose). Before GSK.3α flox animals arrived, CAMKIIα-CRE$^{+/-}$;PDAPP$^{+/+}$ mice were generated. Then, breedings were done in parallel. Homozygous GSK-3$\alpha^{flox/flox}$ mice (two read ears) were generated and used to mantain the line. Simultaneosly, GSK-3$\alpha^{flox/-}$;CAMKIIα-cre$^{+/-}$;PDAPP$^{+/-}$ was generated by crossing CAMKIIα-cre$^{+/-}$;PDAPP$^{+/+}$ with GSK-3$\alpha^{flox/-}$. Next, GSK-3$\alpha^{flox/-}$;CAMKIIα-cre$^{+/-}$;PDAPP$^{+/-}$ was crossed with GSK-3$\alpha^{flox/flox}$, and the desired genotype, GSK-3$\alpha^{flox/flox}$;CAMKIIα-cre$^{+/-}$;PDAPP$^{+/-}$ was obtained. Finally, we expanded the line by crossing it with GSK-3$\alpha^{flox/flox.}$ The last breeding generated the target mouse and all of the controls nedeed. Black rectangles highlight the targeted genotype used as a breeder at the next breeding. Red rectangle: target mouse. Half white body: heterozygous PDAPP$^{+/-}$ mouse

GENERATION OF TRIPLE TRANSGENIC GSK3α+β CKO MICE

Triple transgenic mice were generated by crossing the GSK-3$\alpha^{flox/flox}$ mice with GSK-3$\beta^{flox/flox}$ and UBC-CRE-ERT2 lines.(354) Eight crosses resulted in triple transgenic GSK-3$\alpha^{flox/flox}$; GSK-3$\beta^{flox/flox}$;UBC-CRE-ert2 $^{+/-}$ mice.

Concurrently, double transgenic mice were generated by crossing the GSK-3$\alpha^{flox/flox}$ mice with GSK-3$\beta^{flox/flox}$. Two crosses resulted in double transgenic GSK-3$\alpha^{flox/flox}$; GSK-3$\beta^{flox/flox}$ mice.

Subsequently, GSK-3$\alpha^{flox/flox}$; GSK-3$\beta^{flox/flox}$;UBC-CRE-ERT2 $^{+/-}$ were mated with GSK-3$\alpha^{flox/flox}$;GSK-3$\beta^{flox/flox}$ mice, generating two genotypes: GSK-3$\alpha^{flox/flox}$;GSK-3$\beta^{flox/flox}$;UBC-CRE.ert2$^{+/-}$ (UBC-GSK-3α+β CKO) and their control littermates GSK-3$\alpha^{flox/flox}$; GSK-3$\beta^{flox/flox}$ (UBC-GSK-3α+β wt).

GENERATION OF DOUBLE TRANSGENIC GSK-3α CKO AND GSK-3β CKO MICE

During the development of our triple transgenic mice, we generated several cohorts of mice that we used to generate preliminary data to test the effectiveness, reproducibility and distribution of the KO.

We generated two UBC-CRE-ERT2 lines: the alpha line, GSK-3$\alpha^{flox/flox}$;UBC-CRE-ERT2$^{+/-}$ (UBC-GSK-3α CKO), with GSK-3$\alpha^{flox/flox}$;UBC-CRE-ERT2$^{-/-}$ (UBC-GSK-3α WT) mice as controls, and the beta line, GSK-3$\beta^{flox/flox}$;UBC-CRE-ERT2$^{+/-}$ (UBC-GSK-3β CKO), with GSK-3$\beta^{flox/flox}$;UBC-CRE-ERT2$^{-/-}$ (UBC-GSK-3β wt) mice as controls.

Similarly, we generated two CAMKIIα-CRE lines: the alpha line, GSK-3$\alpha^{flox/flox}$; CAMKIIα-CRE$^{+/-}$ (GSK-3α cko), and GSK-3$\alpha^{flox/flox}$;CAMKIIα-CRE$^{-/-}$ (GSK-3α wt) mice as controls. And the beta line: GSK-3$\beta^{flox/flox}$;CAMKIIα-CRE$^{+/-}$ (GSK-3β cko) and their littermates GSK-3$\beta^{flox/flox}$;CAMKIIα-CRE$^{-/-}$ (GSK-3β wt) mice as controls.

2. 1. 1. 5. Tamoxifen induction in CRE-ERT2 lines

To recombine the GSK-3 floxed alleles using the CRE-ERT2 system, we tried two different methods to deliver tamoxifen into the mice: by adding tamoxifen (500 mg/Kg) to a chow diet chow ad libitum for 7 to 30 days, or by oral gavage or intraperitoneal injection. As previously described, tamoxifen was solubilized at 20mg/ml in a mixture of 98% corn oil and 2% ethanol, and administered at 0.5mM/g body weight, once per day for 5 days (354).

Several cohorts of mice were generated and analyzed at seven days, one month and three months post-induction.

2. 1. 2. Histology and brain preparation

As previously described (361), mice were anesthetized and transcardially perfused with phosphate buffered saline, pH 7.0 in accordance with protocols approved by the Institutional Animal Care and Use Committee of the University of Pennsylvania. Brains were surgically removed and the right hemisphere was fixed in 4% neutral buffered formalin, while the left hemisphere was dissected into various brain regions and frozen at -80°C for biochemical analysis. To maintain consistency of dissection and to facilitate analysis, brains were coronally sliced starting with an initial cut parallel to the olfactory tract as it bends towards the medial eminence. Bisection at this point generated anterior and posterior cortical regions, which were fixed in neutral buffered formalin and paraffin embedded. Paraffin blocks were sectioned exhaustively to a thickness of 6 μm. Tissue sections were stained using a Polymer horseradish peroxidase detection system (Biogenex).

2. 1. 2. 1. Antibodies Used in Histology

GSK-3 expression was monitored using GSK-3α rabbit polyclonal antibody (9338)

and GSK-3β rabbit mouse monoclonal antibody (mAb) (27C10) (Cell Signaling Technology). To track the distribution of Aβ plaques, we used mouse mAb Nab228, which binds to amino acids 1-11 in Aβ peptides (362).

2. 1. 2. 2. Immunohistochemical quantification

Aβ deposits were quantified by a researcher blinded to experimental condition as previously described (363). Images from immunolabelled sections were captured and digitized using a video capture system (Nikon camera coupled to an Olympus DP71 upright microscope). Using NIH ImageJ software, the areas of interest were drawn freehand (i.e. CA1). Afterwards, digital grayscale images were converted into binary positive/negative data using a constant threshold limit. The percentage of positive pixels (i.e., immunoreactivity area) was quantified for each image to generate immunoreactivity "load" values (i.e., percentage area occupied by the immunoreactivity product). For Aβ deposit quantification, images of Nab228-stained sections of the hippocampus (Bregma -1.95) were measured.

2. 1. 3. Western blots

To measure soluble proteins, hippocampi and cortex were homogenized in radioimmunoprecipitation assay (RIPA) buffer in the presence of protease inhibitors and briefly sonicated. Samples were centrifuged at 100,000 g for 30 min at 4 °C, and protein concentration was measured by bicinchoninic acid assay. Samples were electrophoresed on 10% Tris-glycine acrylamide gels and transferred to a nitrocellulose or Polyvinylidene fluoride membrane. Immunoblots were probed with the following antibodies: GSK-3αβ mouse mAb (Calbiochem), and GAPDH mouse mAb (Advanced Immunochemical) as a loading control. Immunoblots were then exposed to species-specific horseradish peroxidase-conjugated anti-IgG antibodies (Santa Cruz Biotechnology) and visualized by enhanced chemiluminescence

(PerkinElmer) using a Fuji Imager. Images were quantified using Multi Gauge version 3.2 FujiFilm software.

2. 1. 4. Behavioral analysis

The effect of GSK-3α KO on age related deficits described in heterogyzous PDAPP mice were tested by the open field test (activity) and the Barnes maze (hippocampal-dependent spatial memory).

2. 1. 4. 1. Open field test:

To assess general activity, locomotion, and anxiety, mice were tested in the open field. This test is based on conflicting innate tendencies in mice to explore a novel environment and to avoid bright and open spaces that resemble dangerous situations, such as predator risk. The test was performed and adapted from previously described (364,365): the apparatus was a square arena (52 x 52 x 40 cm) with black Plexiglas walls and white floor that was evenly illuminated. Mice were individually placed in the center and allowed to explore freely for 13 min while the trial was videotaped (Figure 15A-B). Subsequent video scoring was completed by an observer blind to treatment groups using the SMARTv25 video tracking software (Panlab, SL). Total distance moved was automatically calculated by the tracking software as a direct measure of locomotion and activity (Figure 15C).

2. 1. 4. 2. Barnes maze:

Mice were tested for hippocampal-dependent spatial learning and memory in the Barnes maze (San Diego Instruments) The Barnes maze consists of a circular table with 20 circular holes around the circumference of the table. Under each hole is a slot

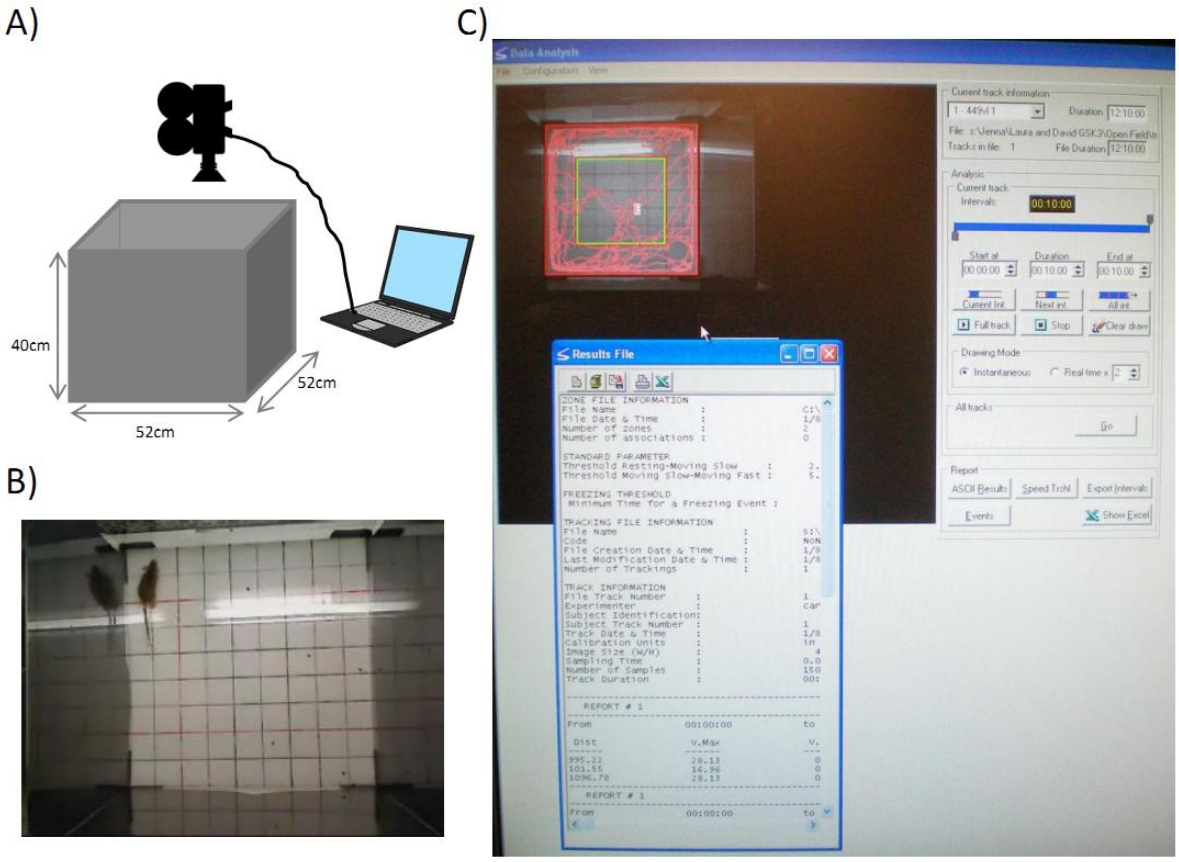

Figure 15: Open field test. (A). Open field apparatus scheme: square arena (52x 52 x 40 cm) with black Plexiglas walls and white floor. Web-camera connected to a computer registered all activity from the top. (B) Image from the top. (C) Data analysis using SMARTv25 (Panlab, SL)

for a box. There are 19 small boxes and a larger one (the goal box) in which to hide. Individually, mice are exposed on the surface of the table which is evenly illuminated. As mentioned before, mice try to avoid bright and open spaces, and the goal of the maze is to reach the goal box where they can escape. Fixed visual cues around the platform serve to orient mice to find the goal box. Mice that are unable to find it after 2.5 min of exposure are gently guided to the goal box (Figure 16).

As described previously in our laboratory (366), mice were tested over six days. On training days 1-3, mice were exposed to the Barnes maze for three 2.5 min trials, 15 min apart. On testing days 4-6, they were exposed to two 2.5 min trials. On all six days, only the last two trials were scored. Mice were tested on their ability to learn

and remember a fixed position of an escape compartment, and their performance was scored for strategy and latency in finding the escape compartment. Strategies were defined as follows: a) spatial (mouse navigates directly to the escape hole with both first intent deviation and total errors < or =3), b) serial (mouse systematically searches for consecutive holes with no center crosses), and c) random (no strategy at all) as previously described (367).

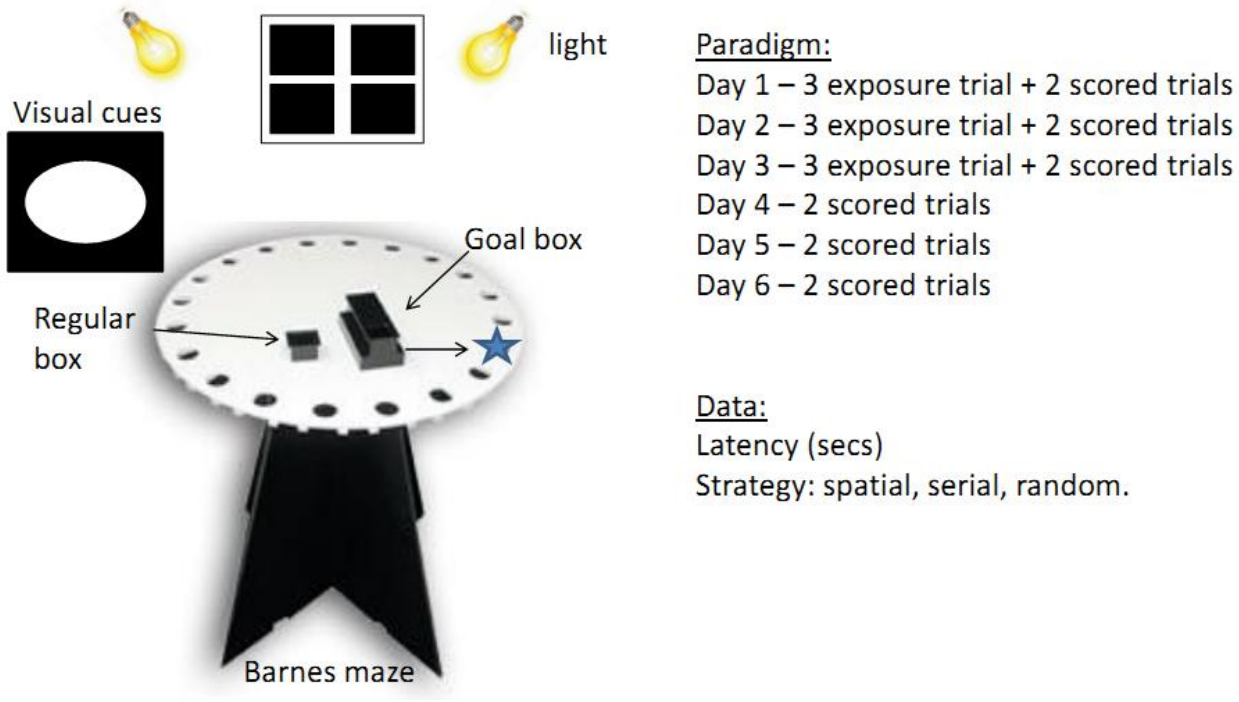

Figure 16: Barnes maze apparatus and paradigm.

2. 1. 5. Statistical analysis

The majority of data analysis was completed using one-way ANOVA followed by Bonferroni´s *post-hoc* test. Barnes maze search strategy was analyzed using a Chi-

Squared test, and latency with a two-way ANOVA. Life span studies were analyzed using the Kaplan-Meier survival curve.

2. 2. RESULTS:

2. 2. 1. GSK-3 expression in GSK-3α CKO mice and in GSK-3β CKO mice

CAMKIIα-CRE lines

Immunohistochemical studies showed a dramatic reduction in GSK-3α immunostaining in the brains of GSK-3α CKO mice without altering GSK-3β immunostaining (Figure 17). Although complete KO of GSK-3α was not achieved, only a small number of GSK-3α-positive neurons were detected in clearly defined regions.

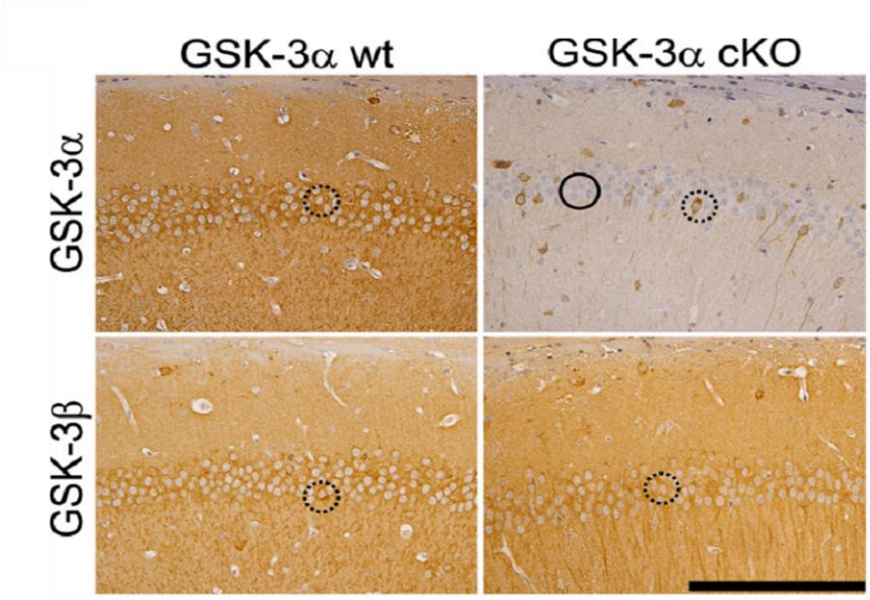

Figure 17: GSK-3α CKO produced a mosaic pattern of GSK-3α expression in the CA1 region of hippocampus, but no reduced GSK-3β immunoreactivity. *Scale bar, 100 μm. Neurons with reduced GSK-3 expression are highlighted by black circles and neurons expressing normal GSK-3 levels are highlighted by dashed black circles.*

Consistent with a previous report (353), the most robust reduction overall was observed in the forebrain, mainly in CA1 of the hippocampus and cortex. To a lesser extent we observed a reduction in lateral amygdale nuclei, CA3 of the hippocampus, layers four and five of the cortex, caudate, putamen, thalamus, and the reticular part of the substantia nigra. There were no changes in the hypothalamus, fornix, septal nuclei, brainstem, or cerebellum. These changes appeared consistently in all GSK-3α CKO mice (Figure 18).

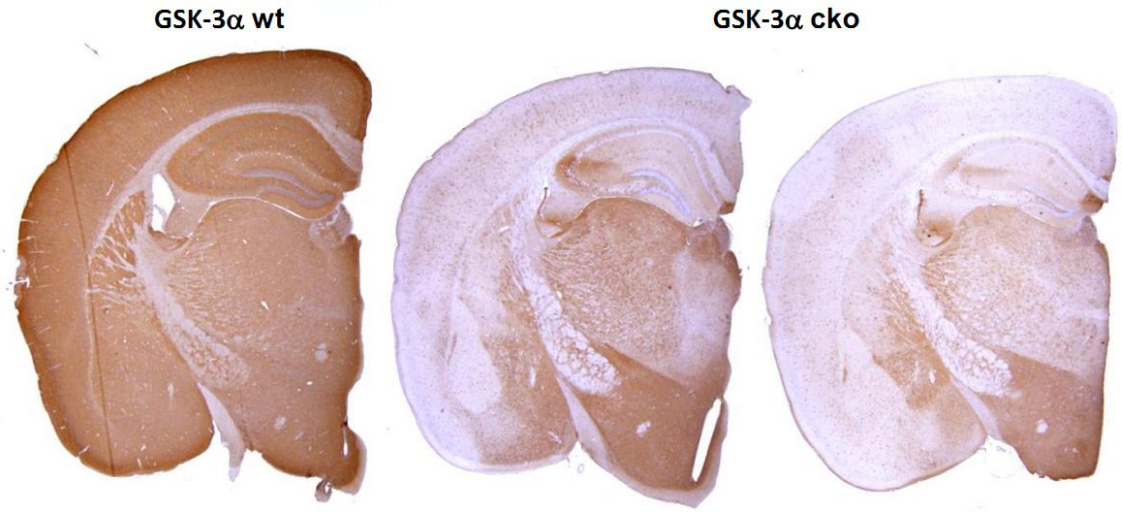

Figure 18: Distribution and consistency of GSK-3α immunoreactivity in GSK-3α CKO mice.

Moreover, ~70% reduction in hippocampal GSK-3α levels was detected by immunoblot analyses without any evident compensatory increase in GSK-3β expression (Figure 19).

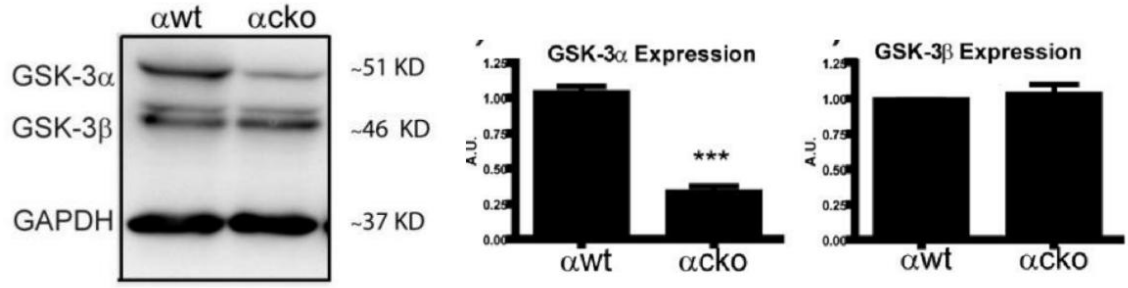

Figure 19: Confirmation of GSK-3α reduction in hippocampal lysates from GSK-3α CKO mice by WB. *Densitometric analysis showed a significant reduction in GSK-3α (67%, $t_{(5)}$=9, p=0.0003) but not in GSK-3β levels ($t_{(3)}$=0.4912, p=0.6570). Data show mean ± SEM. ***p<0.01 compared with αwt. GSK-3α WT (αwt) and GSK-3α CKO (αcko). n=4 mice per group.*

The same findings regarding specificity, distribution, consistency and intensity of the reduction in GSK-3β expression were observed in GSK-3β CKO mice (data not shown).

UBC-CRE-ERT2 lines

We explored two different methods for the delivering of tamoxifen into mice: directly by oral gavage or intraperitoneal injection once per day for 5 days, and by adding tamoxifen to chow diet and feeding ad libitum for 7 or 30 days. Both methods were equally successful in reducing GSK-3 proteins as shown by WB and immunohistochemical analysis. Complete KO was not achieved in this CRE line either. We observed a mosaic pattern of immunoreactivity with GSK-3α or GSK-3β specific antibodies in UBC-GSK-3α CKO or UBC-GSK-3β CKO mice lines respectively.

After tamoxifen induction UBC-GSK-3α CKO and UBC-GSK-3β CKO were sacrificed at different time points and analyzed by immunohistochemistry. At seven days, a reduction in the intensity of immunoreactivity was observed, and isolated cells showed no immunoreactivity at all. At one month, the number of unstained cells

increased and the number of immunoreactive cells was reduced. As expected, after four months of induction, the KO persisted.

As observed with CAMKIIα-CRE lines, the KO was isoform specific, and we did not observe any compensatory increase in the levels of the other GSK-3 isoform by WB.

The UBC-CRE line showed a wider distribution of the KO than the CAMKIIα-CRE line. We observed an intense reduction of GSK-3 levels in the hippocampus, spinal cord, cerebellum and other structures (basal ganglia and brain stem). The extent of GSK-3 reduction was less in the cortex (Figure 20). Other organs were analyzed (liver, muscle, heart), and a significant decrease in the intensity of GSK-3 immunoreactivity was also observed.

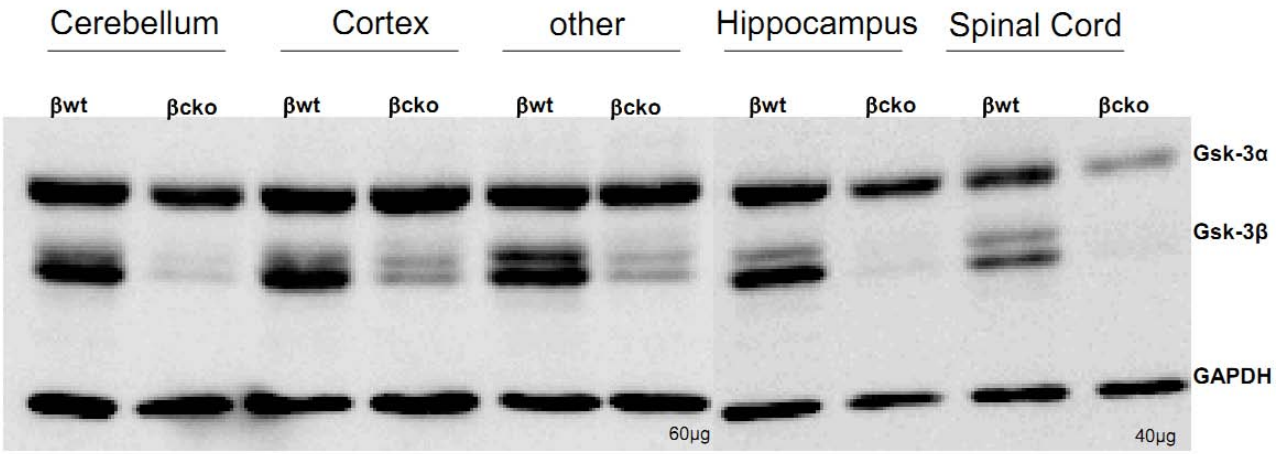

Figure 20: Reduced GSK-3β protein levels in GSK-3β CKO mice after five days of tamoxifen induction by oral gavage, and one month survival. *Representative WB "Other" includes subcortical white matter and basal ganglia. 60 µg or 40 µg of protein were loaded per well.*

2. 2. 2. GSK-3α+β CKO mice did not survive after tamoxifen induction

To better understand the contribution of GSK 3 in AD, we initially planned to KO both isoforms GSK-3 α and β in the same mouse, and compare the results with the

GSK.3α CKO line and the GSK-3β CKO line.

To this end, we used the inducible UBC-CRE-ERT2 system, and generated a cohort of UBC-GSK-3α+β CKO mice and their UBC-GSK-3α+β WT littermates as controls. We explored two different methods to deliver tamoxifen into the mice: directly by oral gavage/intraperitoneal injection once per day for 5 days, or by tamoxifen diet chow ad libitum for 7 or 30 days.

In our first experiment, five one-month-old UBC-GSK3α+β CKO mice received tamoxifen by oral gavage or intraperitoneal injection. All of them died on the sixth or seventh day after the initiation of induction with tamoxifen. Only one of the three control UBC-GSK3α+β WT mice died, and it was due to a complication during the oral gavage procedure.

We conducted a second experiment. One-month-old mice were feed a chow diet containing tamoxifen. All six UBC-GSK3α+β CKO died between the 6^{th} and 13^{th} days after the initiation of induction with tamoxifen, while none of the three UBC-GSK-3α+β WT controls died.

2. 2. 3. Double transgenic GSK-3α cko-PDAPP and GSK-3β cko-PDAPP mouse lines generation

To study the effects of GSK-3α and GSK-3β on Aβ deposits and cognitive impairment, we attempted to generate two lines of transgenic CKO mice overexpressing mutant APP (GSK-3α cko;PDAPP line and GSK-3β cko;PDAPP line).

After several crosses we were able to generate the first generation of GSK-3α cko;PDAPP mice. Lastly, we successfully expanded this line, and generated four genotypes: GSK-3α cko;PDAPP, and their littermates (GSK-3α wt, GSK-3α cko, GSK-3α wt;PDAPP) as controls. Each of the four groups consisted of n=10-15 mice that were analyzed at 17 months of age.

However, when we attempted to generate the GSK-3β cko;PDAPP line we had several difficulties. First, althought we were able to generate the first generation of GSK-3β CKO;PDAPP mice (11 mice), we observed that the real ratio for this genotype was 1:15, which was higher than the theoretical 1:8 expected ratio for this breeding. Second, when we tried to expand the line (nine different matings), we were unable to obtain any pregnant females. Third, GSK-3β cko;PDAPP mice showed a high mortality. Survival analyses were not planned between littermates in this generation of mice, but when compared with the survival of the first generation of GSK-3α cko;PDAPP mice, GSK-3β cko;PDAPP mice displayed a significantly higher mortality ($\chi^2_{(1)}$ =8.411, p<0.01, n=11-12 mice per group) (Figure 21). Finally, since 9 of 11 mice died before 6 months with a median age of 3.5 months, we could not do any analysis of the effect of GSK-3β KO on plaque load or behavior.

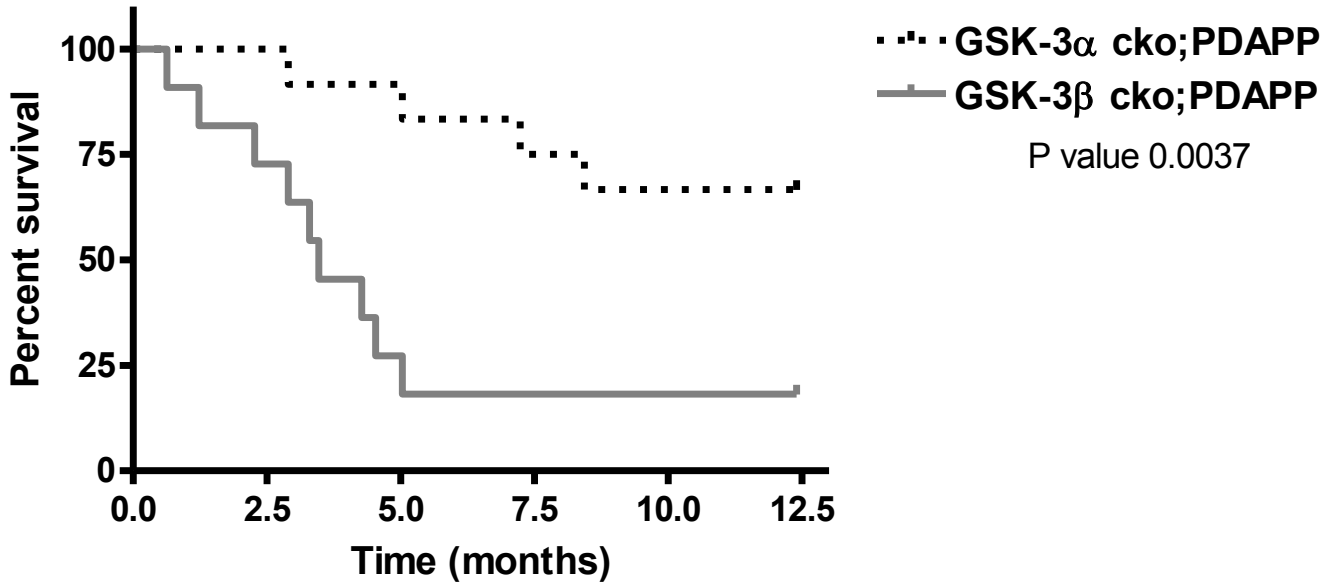

Figure 21: GSK-3β cko;PDAPP mice displayed higher mortality than GSK-3α cko;PDAPP mice.

2. 2. 4. GSK-3α KO decreases Aβ amyloid deposition in PDAPP mice

To evaluate the effect of GSK-3α KO on Aβ senile plaque burden in our mice, hippocampi from age-matched GSK-3α wt;PDAPP and GSK-3α cko;PDAPP mice were analyzed by immunohistochemistry with anti-Aβ mAb Nab228. Aβ immunoreactivity was quantified using ImageJ. In the CA1, we observed a significant reduction in Aβ load in GSK-3α cko;PDAPP compared to GSK-3α wt;PDAPP females ($t_{(12)}$=2.253, p=0.0438) (Figure 22).

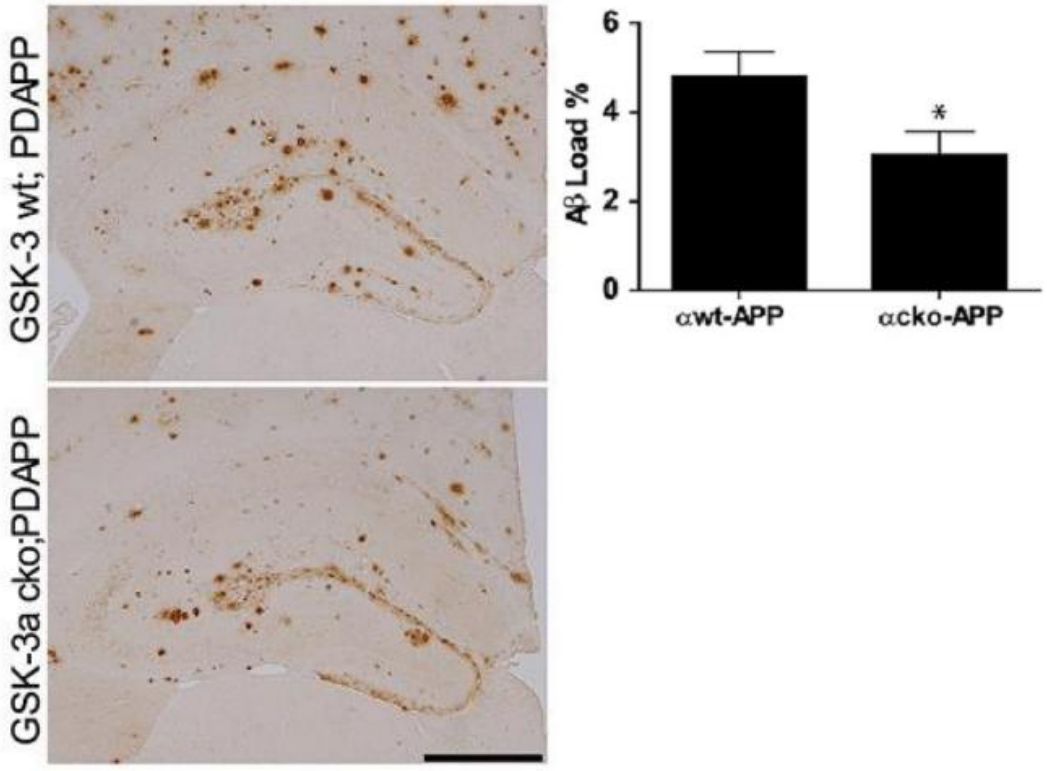

Figure 22: In CA1, GSK-3α CKO significantly decreases amyloid load in PDAPP females. *Scale bar 500 μm. R *p< 0.05. GSK-3α wt;PDAPP (αwt-APP) and GSK-3α cko;PDAPP (αcko-APP).*

2. 2. 5. GSK-3α CKO prevents age-dependent behavioral deficits in PDAPP mice.

Lastly, to determine whether the above-mentioned changes in Aβ load corresponded to alterations in motor activity or spatial learning, GSK-3α wt, GSK-3α cko, GSK-3α wt;PDAPP and GSK-3α cko;PDAPP mice were tested on the open field and Barnes maze.

GSK-3α wt;PDAPP mice manifested an increased level of locomotor activity in the open field compared with control groups, whereas GSK-3α cko;PDAPP performed at a level indistinguishable from GSK-3α wt and GSK-3α cko mice ($F_{(3,25)}$=5.234, p=0.0061) (Figure 23).

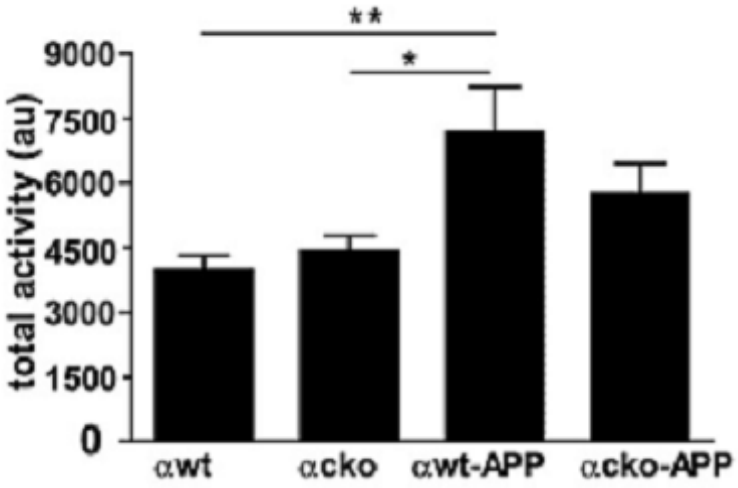

Figure 23: GSK-3α wt;PDAPP displayed hyperactivity on the open field test while GSK-3α cko;PDAPP did not. **p<0.05, **p<0.01. GSK-3α wt (αwt), GSK-3α cko (αcko), GSK-3α wt;PDAPP (αwt-APP) and GSK-3α cko;PDAPP (αcko-APP).*

In the Barnes maze, differences between groups were observed in latency ($F_{(3,43)}$=3.589, p=0.021). GSK-3α wt;PDAPP mice displayed significant deficits compared with GSK-3α wt mice, while GSK-3α cko;PDAPP mice were statistically

indistinguishable from control groups (Figure 24). Lastly, significant differences between groups were also observed in the strategies used by mice to find the target ($\chi^2_{(6)}$=26.198, p<0.0001). GSK-3α wt;PDAPP mice were more likely to utilize a poor search strategy (random) in the Barnes maze compared with the other three genotype groups, while GSK-3α cko;PDAPP were more likely to utilize beneficial search strategies (serial and spatial) (Figure 24).

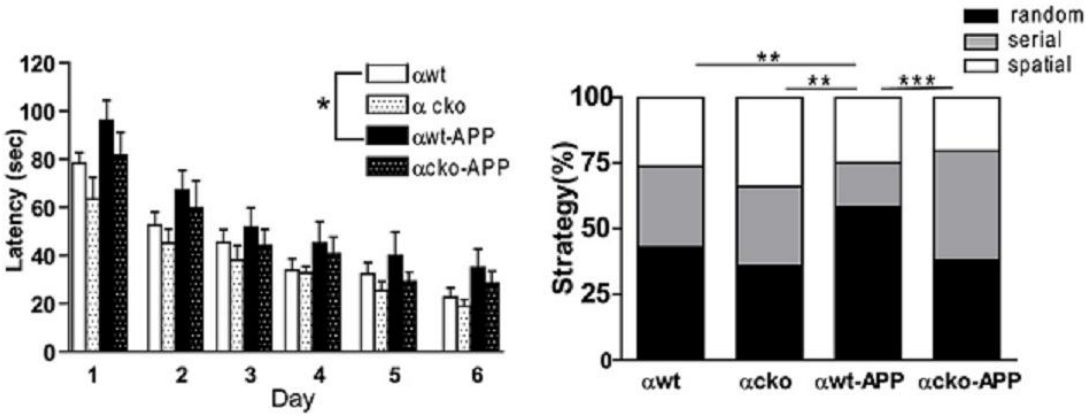

Figure 24: GSK-3α cko prevents spatial memory deficits in PDAPP mice in the Barnes maze. Search strategy data are shown as the percentage of mice utilizing each strategy per genotype column. *p< 0.05, **p<0.01, ***p< 0.001. GSK-3α wt (αwt), GSK-3α cko (αcko), GSK-3α wt;PDAPP (αwt-APP), and GSK-3α cko;PDAPP (αcko-APP).

Importantly, these results are not confounded by GSK-3α KO as we did not detect any differences between GSK-3α wt and GSK-3α cko mice in locomotor activity or spatial memory.

V. DISCUSSION

STUDY 1: Contribution of synaptic markers to cognitive status and cognitive impairment in the oldest-old.

In this autopsy study of a large cohort of very elderly individuals, we sought to elucidate which pathologies among those examined here associate with normal ageing, which associate with dementia and which, if any, associate with cognitive impairment. We review all of our findings below.

First, cognitively normal nonagenarians in The 90+ Study have pathological changes, a median Braak stage of III and a Thal phase of one, consistent with predictable, age-dependent deposition of AD pathology (90). Of course, many pathologies besides AD affect the ageing brain including other neurodegenerative diseases, CVD and HS among others. In this study, we did not examine the role of multiple neurodegenerative diseases, but we previously reported that synuclein and TDP-43 pathology affect <20% of cognitively normal individuals in this age category and then primarily as co-morbidities (107). CVD, on the other hand, was common, affecting 45% of the group while HS was almost non-existent (n=1).

Against this background level of multiple age-related pathologies in cognitively normal individuals, we can analyze the increases in AD burden, CVD and HS associated with dementia (Figure 25A). As 90+ individuals have a moderate burden of age-related tangles and plaques and a particularly high prevalence of dementia (368), it is not surprising that AD pathology is the most common underlying contributor to dementia in this group (369). For individuals with dementia, the median Braak stage is V and the Thal phase is three. Compared with the normal group, these are substantial increases consistent with an intermediate burden of AD neuropathological change (83). Along with AD, the prevalence of CVD—not including HS—increased to 74% of individuals in the dementia group. Additionally, dementia was associated with the appearance of HS in a substantial minority (28%). Similarly, and primarily comorbidly, TDP-43 also affected a large minority (35%). Both the CVD and HS percentages are consistent with reported frequencies of these pathologies in this age-group (370,371), adding further evidence of the association of both entities with dementia in the oldest-old.

The changes in all three of the synaptic markers studied here are consistent with the

interpretation that significant perforant pathway loss occurs with dementia in the 90+ subjects (Figure 25B). This is consistent with our previous work involving 32 individuals in The 90+ Study, where neocortical synaptophysin protein levels were significantly decreased with dementia (147). In our multiple logistic regression analysis, both the synaptophysin RIR and Braak stage were tightly associated with cognitive scores. Concurrently, post hoc analysis revealed that the SV2 RIR was significantly lower at Braak stage VI, raising the possibility that synaptic protein loss is tightly correlated with tau burden. This is supported by studies in tau transgenic mice (156), and in human cohorts where synaptic protein loss only occurs at the highest Braak stages (372).

On the other hand, as the synaptophysin RIR, Braak stage, HS and TDP-43 pathology measures all remained significantly associated with MMSE scores in our multiple logistic regression analysis, perhaps something more than pathological AD is taking place, and it could be that synaptic protein loss in the perforant pathway and HS are independent factors that contribute to dementia in the oldest-old.

If cognitively normal individuals have age-related tangles and plaques, and these pathologies increase along with synaptic loss in dementia, what changes occur during CIND? We observed that none of the pathological changes measured in this study distinguished the normal and CIND groups, that all of them distinguished normal and dementia groups, and that, except for Thal phase, all variables were able to differentiate CIND versus dementia (Table 3). These data suggest that plaque deposition could be an early event related to cognitive impairment in the oldest-old (Figure 25A). Cognitively normal nonagenarians have a median Thal phase of one, which means that Aβ pathology is absent in the medial temporal lobe or restricted to the temporal neocortex, in at least 50% of them. However, CIND individuals have a median Thal phase of three, which is consistent with a greater plaque burden, and it means that at least 50% of them have Aβ pathology in the white matter, parvopyramidal layer of the presubicular region, temporal cortex and in the perforant pathway (molecular layer of the dentate fascia and entorhinal cortex) (349).

Importantly, there is no concurrent increase in the Braak stage (median III) or HS (median 0): this may signify that plaques are having an earlier effect than tangles, which is consistent with numerous biomarker studies that show Aβ becomes abnormal before tau in cognitively normal individuals (373,374).

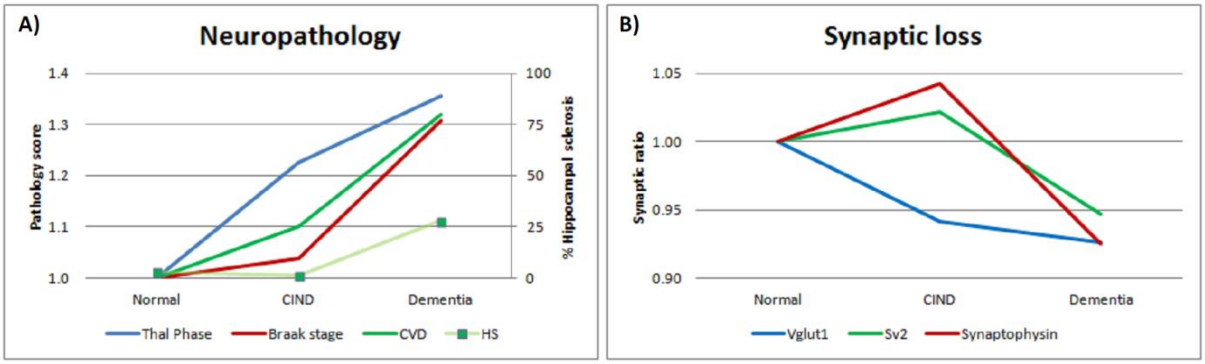

Figure 25: A model of changes associated with cognitive impairment and dementia in the oldest-old. Neuropathology and synaptic measures are associated with cognitive impairment in 'The 90+ Study'. (A) Mild to moderate Alzheimer's disease pathology already exists in the oldest-old for cognitively normal individuals and the Thal phase may increase with cognitive impairment.With dementia, all markers increase significantly, especially Braak stage, cerebrovascular disease (CVD) pathology and hippocampal sclerosis (HS). (B) Glutamatergic specific synaptic loss (VGLUT1) in the perforant pathway pathology may occur during cognitive impairment, while significant synaptic loss occurs with dementia. All values are relative to the normal group's means normalized to 1.0, except cerebrovascular disease which factors out the contribution of hippocampal sclerosis before normalizing; the hippocampal sclerosis percentages are graphed separately on the right axis.

We hypothesized that perforant pathway synaptic loss may be one of the early correlates of cognitive impairment in The 90+ Study, but this was not the case. We focused on the perforant pathway, because it is a very well known system. Neurons in layer II of the entorhinal cortex that are significantly affected in early AD (clinical dementia rating score of 0.5) (375) project into the OML of the hippocampal dentate gyrus. However, none of the synaptic markers measured in this study distinguished the normal and CIND groups; and, similar to pathological changes, all of them distinguished the normal and dementia groups, suggesting that synaptic loss is tightly

linked to pathology associated with dementia in the oldest old, and is consistent with an acceleration of the pathological cascade implied by other studies.

We focused on AD because it was the most prevalent disease in our cohort (107), and we selected VGLUT1, SV2 and synaptophysin because they showed an obvious OML synaptic loss on slides obtained from AD patients: therefore, we cannot rule out that other regions may have earlier synaptic changes in the oldest-old.

Importantly, a close review of the literature shows that the relationship between early cognitive impairment and synapses is more complicated than expected. Several factors such as localization, specificity of the synaptic marker, etiology, plasticity, and the different methods used to measure the synaptic markers need to be taken into account.

For example, we observed that although the VGLUT1 RIR can clearly distinguish the normal and dementia groups (P=0.034), this measure did not distinguish the CIND from the dementia group (P=0.747), whereas the synaptophysin (P<0.001) and SV2 RIRs (P=0.008) still do (Table 25B). These data suggest that CIND may be associated with a decrease in glutamatergic neurons, whereas non-glutamatergic neurons remain relatively unaffected. If true, this is consistent with previous work showing that observed pre-synaptic proteins, such as synaptophysin, remain constant or increase in earlier phases of illness before decreasing with dementia onset (147,376).

However, our data disagree with a previous published study in which VGLUT1 immunoreactive boutons were found increased in the frontal cortex of MCI patients (203). Several reasons may account for this incongruency. For example, the different brain regions analyzed (mid-frontal cortex vs. OML); and that, as it is well established that different non-prion proteins, such as Aβ, tau, TDP-43 or synuclein show a sequential topographical distribution (for review see (9)), synaptic changes may follow a similar pattern, and synaptic changes in one region may not necessarily correlate with another at the same time.

CIND is a heterogeneous group.We hypothesized that memory-CIND individuals are more likely to be on the continuum between normal cognition and Alzheimer's disease than those individuals with executive impairment or 'other'. Therefore, we compared the RIRs and our pathological markers in the memory-CIND subjects (n=13) to the normal and dementia subjects to see if our results had more significance. No new associations were found. However, VGLUT1 RIR almost distinguished between memory-CIND subjects and normal groups (p=0.05), suggesting that glutamatergic terminals may be more affected in early AD.

Interestingly, in our study the decrease in the VGLUT1 RIR is coincident with the increase in Thal phase. This finding is interesting, because a link between Aβ and glutamatergic synapses has been suggested. For example, Aβ appears to accumulate preferentially in VGLUT synaptosomes (377). Reduction of VGLUT1 staining has been found in human induced pluripotent stem cell derived neurons after application of Aβ (378) Furthermore, reduced VGLUT1 protein levels have been found in Aβ plaque rich regions of AD mice models that overexpress human APP (379). Moreover, in humans, reduced VGLUT1 RIR has also been found in non-demented cases with substantial neocortical plaque pathology in the absence of NFT compared to controls (379). Overall, these data suggest that Aβ and plaques may damage glutamatergic synapses. If true, this is interesting, because increased amounts of glutamate can lead to cell death (189), and VGLUT1 is a presynaptic protein responsible for the transportation of glutamate into synaptic vesicles (194,195). Then, reduced levels of VGLUT1 could alter the recycling/clearance of glutamate in synaptic terminals, increase the excitotoxic damage produced, and contribute to the acceleration of the deleterious events associated to AD.

In summary our study has several strengths: it is a poblational study, which correlates clinical and pathological data of a large cohort of individuals over 90 years old, with a large sample of CIND individuals. However, one potential caveat of this study is that we did not count neurons or synapses. It would be interesting to analyze whether these synaptic marker changes really correlate with the number of synapses,

and also to know whether neuronal loss can be detected before or after synaptic RIR deficits.

In this study we focused in three synaptic proteins: synaptophysin, SV2 and VGLUT1 and, in one region, OML. However, it would also be very interesting to expand the number of synaptic markers and regions analyzed here to have a better understanding of the physiopathological changes involved with cognitive impairment, and to identify possible plasticity and compensatory events.

Importantly, our study suggests that individuals with CIND are for the most part pathologically and synaptically indistinguishable from individuals with normal cognition. This being the case, pharmaceutical interventions that target tau and Aβ or protect synapses are all viable therapeutic strategies for a population at risk of dementia due to Alzheimer's disease. In addition, interventions designed to maintain a healthy synaptic system and a strict control of vascular risk factors may be good strategies to preserve cognitive function in nonagenarians and centenarians.

STUDY 2: Contribution of GSK3 to Alzheimer´s disease and cognitive impairment in an APP mouse model

To identify the respective roles of both GSK-3α and GSK-3β on SP formation and behavioral deficits *in vivo*, we utilized a novel genetic approach to manipulate the levels of these two GSK-3 isoforms. We successfully generated CKO of GSK-3α in GSK-3α cko and GSK-3α cko;PDAPP$^{+/-}$ mice, and CKO of GSK-3β in GSK-3β cko mice. However, we failed to generate GSK-3α+β CKO and GSK-3β cko;PDAPP$^{+/-}$ mice. Importantly, we report that GSK-3α CKO reduced the formation of SP and ameliorated the behavioral and cognitive deficits observed in AD transgenic mice.

Our study corroborates previous reports demonstrating that GSK-3 may regulate APP metabolism (267,272,325,332–337). The role of GSK-3α in AD has been underestimated over the years. In fact, very few studies have tried to elucidate the role of each isoform in APP metabolism. Previously, in our shRNA KD model, and in accordance with an earlier cell-based study (272), we observed that inhibition of GSK-3α but not GSK-3β, was sufficient to reduce Aβ levels and plaque load in aged AD mouse models (361). Unfortunately, our shRNA approach has a major drawback, which is the variability of KD efficiency between GSK-3 α and β isoforms. Specifically, GSK-3β protein levels were only reduced by ~50% compared to ~70% for GSK-3α. This variability limited the interpretation of our results, because it is unknown whether the different effects observed in Aβ levels and SP load were because both isoforms have different effects on Aβ, or simply because the level of KD was different. To overcome this technical aspect, we tried to generated triple GSK-3α cko;PDAPP$^{+/-}$ mice and GSK-3β cko;PDAPP$^{+/-}$ mice. Unfortunately, we could not further investigate the role of GSK-3β on APP, but we demonstrated that GSK-3α cko reduced amyloid load in PDAPP mice compared with GSK-3α wt littermates, providing further evidence of the possible role of GSK-3α in APP metabolism and SP formation.

To our knowledge, only one other group has studied the role of GSK-3α or GSk-3β on APP metabolism *in vivo*. However, they did not explore the effects on plaque load or behavior deficits. In disagreement with our results, they observed no differences in

mouse or human Aβ40 or Aβ42 levels in their GSK-3α CKO mice (339). Important to note are the differences between their approach and ours. First, they injected an adeno-associated viral vector expressing triple mutant APP into the hippocampus of GSK-3α. In addition, human amyloid peptides were analyzed only three weeks later. This difference is most likely due to technical issues such as the different levels of APP expression between these two different approaches (adenovirus-APP injection in hippocampus vs. PDAPP mice), or the drastically shorter treatment term of three weeks, compared with 11 or 17 months in our shRNA-α and GSK-3α cko PDAPP mice, respectively.

We were able to obtain a first generation of GSK-3β cko;PDAPP$^{+/-}$ mice with several difficulties. The real ratio for this genotype was higher than the theoretically expected ratio (1/15 and 1/8, respectively), while the GSK-3α cko;PDAPP$^{+/-}$ ratio was 1/10. Mice were unable to breed and displayed higher mortality, with a median age of 3.5 months of survival: therefore, we could not analyze the effect of GSK-3β CKO on plaque load or behavior. Interestingly, these results are similar to those of a previous report, in which they observed that the combination of GSK-3β cko with APP (V717I) did not yield viable offspring, in contrast to GSK-3α cko with APP (V717I) (339).We did not conduct survival studies on our GSK-3β CKO mice, but we did not observe any rough differences compared with their GSK-3β WT littermates. The most parsimonious explanation is that a lack of GSK-3β may generate toxic species, probably originating from APP or its derivatives that may compromise survival. It is possible that under normal conditions, a small amount of these toxic species may not have any consequences, but in mice overexpressing APP, large quantities are produced, which compromises survival.

Similar results were observed with our viral approach: shRNA-β APP/tau mice also displayed a significant increase in mortality, compared with uninjected APP/tau mice ($\chi^2_{(1)}$ =4.76, P<0.05). Conversely, shRNA-β did not alter the survival of APP mice when compared with APP controls (273). It is important to note, that the level of GSK-

3β KD achieved was lower with shRNA than with the CKO method, suggesting that in addition to the amount of APP (or derivatives), the degree of GSK-3β reduction may be important for toxicity in these mice. In summary, although we could not study the role of GSK-3β on APP metabolism, our results suggest that an excess of APP or derivatives is more deleterious in GSK-3β CKO mice than in GSK-3α CKO mice, and provide further evidence of the substantial functional difference of both isoforms *in vivo*; our study highlights the importance of further effort aimed at uncovering the mechanism behind GSK-3 regulation of APP and Aβ processing.

Furthermore, to our knowledge, this is the first study to analyze whether GSK-3α CKO have any beneficial effect on cognition in APP mice. This is especially relevant because GSK-3 has been involved in synaptic plasticity, learning, and memory, and both the excess and lack of GSK-3 activity may alter cognition. For example, behavioral deficits have been observed in GSK-3α KO mice (210), and in heterozygous GSK-3β KO mice (269,270). On the other hand, it has been proposed that memory failure in AD results from to LTP inhibition due to GSK-3 hyperactivity, and that GSK-3 inhibiton can be a good strategy to improve cognition (for a review see (253,380)). We observed that GSK-3α cko prevented spatial memory deficits and hyperactivity in PDAPP mice, highlighting the potential benefits of inhibiting the GSK-3α isoform as a therapeutic strategy in AD.

To be able to study the role of GSK-3α and GSK-3β on AD *in vivo*, we first needed to generate GSK-3α, GSK-3β and GSK-3α+β CKO mice. The generation of these lines was a secondary objective of this work, therefore, some aspects were not studied in depth. Nevertheless, the process helped us to better understand CKO models and some aspects of the GSK-3 protein.

First, neither of the CRE lines (UBC-CRE-ERT2 and CAMKIIα-CRE) generated an absolute GSK-3 KO. We observed a significant reduction in levels of the targeted GSK-3 isoform in both GSK-3α and GSK-3β lines. Nonetheless, even in regions

where the reduction was over 95%, neurons highly immunoreactive to the targeted GSK-3 isoform were observed by immunohistochemistry.

We observed that the inhibition of GSK-3 was isoform specific in both CKO lines and with the shRNA approach. No decreased immunoreactivity or decreased levels of the non-targeted GSK-3 form were observed by immunohistochemistry or by WB. As discussed in the introduction, all GSK-3 inhibitors inactivate GSK-3α and GSK-3β. The same goes for dominant negative GSK-3β conditional transgenic mice, where increased levels of p-S21-GSK-3α and p-S9-GSK-3β are observed. Overall, these results suggest that to date, shRNA and CKO are the best approaches to achieve selective isoform inhibition. However, in the near future, we may have isoform-selective inhibitors (381), since some experimental drugs have shown up to 27-fold selectivity for GSK-3α over GSK-3β (382).

As in other studies, we observed that the reduction of GSK-3α or GSK-3β with this approach did not have an obvious impact on the expression of the other isoform (339). We observed a similar lack of compensation of the protein levels or activity of the non-targeted isoform of GSK-3 with the shRNA approach. Overall, these results suggest that the two isoforms have different regulatory systems.

To generate triple transgenic GSK-3 cko;PDAPP$^{+/-}$ mice. We used the CAMKIIα-CRE line (353). This line presented several advantages, such as the great uniformity of the KO achieved. We observed that the severity and the distribution of the KO on both GSK-3α cko and GSK-3β cko mice were almost identical in all adult mice analyzed by immunohistochemistry. On the contrary, the UBC-CRE-ERT2 line displayed more variability, probably because it is an inducible and more complex model, in which additional variables related to the correct administration and preparation of the drug, among others, may interefere with the induction of the KO.

In addition, the CAMKIIα line only expresses CRE in the CNS (353). This is important because some proteins, such as GSK-3, have other important systemic roles (eg. glucose metabolism) that may interfere with the results. Tissue specific CKO

technology allows us to focus and better understand the role of a protein deletion in a specific tissue such as the CNS.

However, the CAMKIIα-CRE line also showed some disadvantages. The KO was less severe and its distribution narrower than in the UBC-CRE-ERT2 line. For example, in some regions such as CA2, no KO was observed inte the CAMKIIα-CRE line. This is important because it can dilute the results. For example, when we examined the plaque burden on the hippocampus in PDAPP mice, we observed that GSK-3α cko;PDAPP$^{+/-}$ mice tended to have lower plaque loads than their GSK-3α wt;PDAPP$^{+/-}$ littermates, but this difference was not significant. However, when we decided to exclude the CA2 region from the analysis and just focus on CA1, the difference observed in plaque burden between GSK-3α cko;PDAPP$^{+/-}$ and controls was significant.

Importantly, the expression of CRE with the CAMKIIα promoter occurs early, between two and three weeks after birth. Similarly, in our previous work, we injected our shRNA construct on the day the mice were born. With both systems, we achieved the KO/KD months before plaque deposition and age-related cognitive impairments were present. Therefore, our results show that GSK-3α reduction prevented AD pathology and cognitive impairment in AD mice, but it is unknown whether GSK-3 inhibition can be beneficial once AD pathology is already established.

Our results were similar to those obtained with GSK-3 inhibitors in AD mouse models and in humans. Prepathological AD mouse models treated for a period of one to seven months with GSK-3 inhibitors showed reduced Aβ levels, amyloid load, and behavioral deficits, compared with control groups (267,272,336,337). In humans, amnestic MCI participants treated with lithium for 12 months showed a better performance in cognitive tests that the placebo group (383). Similarly, low doses of tideglusib for 26 weeks also showed significant responses in several cognitive tests (ADAS-cog, MMSE and word fluency) in mild to moderate AD (328). Overall, these

data add further evidence that GSK-3 reduction may be beneficial in the early stages of AD.

Convesely, after short-term treatment with GSK-3 inhibitors in aged AD mouse models, such as 1 month of treatment with lithium in 14-months-old APP/tau/PSEN1 mice, no changes were observed in Aβ levels, amyloid load, or working memory, (323). In agreement with this result, phase II clinical trials in humans have shown that short-term treatment with GSK-3 inhibitors (lithium for 10 weeks (384), or tideglusib for 26 weeks (328)) did not show benefits with respect to biomarkers or any of the cognitive assessments performed.

In summary, all of these data suggest that GSK-3α CKO and GSK-3 inhibitors may prevent SP formatiom and other APP related disorders; however, they may not be able to reverse pathology after it has been well established. In this respect, more studies are necessary to determine whether APP-related changes can be reversed by inducible CKO of GSK-3α mice, or by treating both aged APP mouse models and mild AD patients with GSK-3 inhibitors for longer periods of time.

Finally, to better understand the role of GSK-3 on APP, we tried to generate inducible triple GSK-3α+β cko mice, but they died during the first week after the initiation of induction. We did not perform any further analysis, so it is unknown if the cause of death was CNS-related or systemic (heart, liver, etc). We did not repeat this experiment in the CAMKIIα-CRE line, so is unknown if they would survive, but it is very unlikely. Another group tried to generate triple GSK-3α+β CKO mice using the Thy1-CRE line, contanining a neuron specific promoter that expresses after birth. Interestingly, although not much information regarding breedings was provided, they yielded 354 offspring, none of which was the desired GSK-3$\alpha^{flox/flox}$;GSK-3$\beta^{flox/flox}$;Thy1-cre$^{+/-}$. These data indicate that GSK-3 is vital to the CNS, and provides further evidence that isoform-specific GSK-3 inhibitors can be safer and very likely could display fewer side effects that inhibiting both isoforms.

In summary, our study highlights the importance of GSK-3α in AD. Our observations demonstrate that reducing GSK-3α expression ameliorates SPs, and prevents AD-like cognitive impairment in our mouse models. We have also shown that reducing GSK-3β expression had deleterious effects in our APP mice. We indeed illustrated that the lack of both GSK-3 isoforms is incompatible with life in mice. Altogether, this study suggests that strategies selectively reducing one isoform of GSK-3 may be safer and better tolerated than GKS-3 inhibitors targeting both; although more studies are needed to better understand the molecular mechanisms involved, our study highlights GSK-3α as a potential therapeutic target in AD.

VI. CONCLUSIONS

1. Contribution of synaptic markers to cognitive status and cognitive impairment in the oldest-old.

a. Synaptophysin, SV2 and VGLUT1 correlated with global cognitive scores in the oldest old, and distinguished normal from demented patients, but not normal from CIND individuals. Synaptophysin and SV2 also distinguished CIND from demented individuals.

b. Braak stage, Thal phase, HS, CVD and TDP-43 correlated with global cognitive scores in the oldest old, and distinguished normal from demented patients, but not normal from CIND individuals. Except for the Thal phase, all these pathological changes also distinguished CIND from demented individuals.

c. Synaptophysin, Braak stage, HS and the TDP-43 pathology measures remained significantly associated with MMSE scores in our multiple logistic regression analysis.

2. Contribution of GSK3 to AD and cognitive impairment in AD mouse models.

a. GSK-3α CKO prevented cognitive and behavioral deficits in an APP mouse model of AD.

b. GSK-3α CKO partially prevented amyloid load in an APP mouse model of AD.

c. We successfully generated both, GSk-3α and GSK-3β CKO mice with two different CKO systems: a tissue specific (CAMKII-CRE line), and a ubiquitously expressed but inducible model (UBC-CRE-ERT2 line). However, we were unable to generate triple transgenic GSK-α+β CKO mice using the inducible system.

d. We successfully generated triple transgenic GSK-3α cko;PDAPP$^{+/-}$ mice and GSK-3β cko;PDAPP$^{+/-}$. However, GSK-3β cko;PDAPP$^{+/-}$ were unable to breed and displayed a high rate of mortatility.

VII. REFERENCES

REFERENCES

1. Virués-Ortega J, de Pedro-Cuesta J, Vega S, Seijo-Martínez M, Saz P, Rodríguez F, et al. Prevalence and European comparison of dementia in a ≥75-year-old composite population in Spain. Acta Neurol Scand. mayo de 2011;123(5):316-24.

2. Bermejo-Pareja F, Benito-León J, Vega S, Medrano MJ, Román GC. Incidence and subtypes of dementia in three elderly populations of central Spain. J Neurol Sci. 15 de enero de 2008;264(1-2):63-72.

3. WorldAlzheimerReport.pdf [Internet]. [citado 21 de marzo de 2014]. Recuperado a partir de: http://www.alz.co.uk/research/files/WorldAlzheimerReport.pdf

4. Cuijpers P. Depressive disorders in caregivers of dementia patients: a systematic review. Aging Ment Health. julio de 2005;9(4):325-30.

5. world_alzheimer_report_2010.pdf [Internet]. [citado 21 de marzo de 2014]. Recuperado a partir de: http://www.alz.org/documents/national/world_alzheimer_report_2010.pdf

6. Rubin EH, Morris JC, Grant EA, Vendegna T. Very mild senile dementia of the Alzheimer type. I. Clinical assessment. Arch Neurol. abril de 1989;46(4):379-82.

7. Petersen RC, Smith GE, Waring SC, Ivnik RJ, Tangalos EG, Kokmen E. Mild cognitive impairment: clinical characterization and outcome. Arch Neurol. marzo de 1999;56(3):303-8.

8. Corrada MM, Berlau DJ, Kawas CH. A population-based clinicopathological study in the oldest-old: the 90+ study. Curr Alzheimer Res. julio de 2012;9(6):709-17.

9. Brettschneider J, Del Tredici K, Lee VM-Y, Trojanowski JQ. Spreading of pathology in neurodegenerative diseases: a focus on human studies. Nat Rev Neurosci. febrero de 2015;16(2):109-20.

10. James Lowe, Suzanne S Mirro, Bradley T Hyman, Dennis W Dickson. Greenfield´s Neuropathology. 8.ª ed. Seth Love DWE, David Louis, editores. London: Hodder Arnold; 2008. 1040 - 1041 p.

11. Masters CL, Simms G, Weinman NA, Multhaup G, McDonald BL, Beyreuther K. Amyloid plaque core protein in Alzheimer disease and Down syndrome. Proc Natl Acad Sci USA. junio de 1985;82(12):4245-9.

12. Glenner GG, Wong CW. Alzheimer's disease: initial report of the purification and characterization of a novel cerebrovascular amyloid protein. Biochem Biophys Res Commun. 16 de mayo de 1984;120(3):885-90.

13. Selkoe DJ. Cell biology of the amyloid beta-protein precursor and the mechanism of Alzheimer's disease. Annu Rev Cell Biol. 1994;10:373-403.

14. Grundke-Iqbal I, Iqbal K, Tung YC, Quinlan M, Wisniewski HM, Binder LI. Abnormal phosphorylation of the microtubule-associated protein tau (tau) in Alzheimer cytoskeletal pathology. Proc Natl Acad Sci USA. julio de 1986;83(13):4913-7.

15. KIDD M. Paired helical filaments in electron microscopy of Alzheimer's disease. Nature. 12 de enero de 1963;197:192-3.

16. Ishino H, Otsuki S. Distribution of Alzheimer's neurofibrillary tangles in the basal ganglia and brain stem of progressive supranuclear palsy and Alzheimer's disease. Folia Psychiatr Neurol Jpn. 1975;29(2):179-87.

17. Komori T. Tau-positive glial inclusions in progressive supranuclear palsy, corticobasal degeneration and Pick's disease. Brain Pathol. octubre de 1999;9(4):663-79.

18. Umahara T, Hirano A, Kato S, Shibata N, Yen SH. Demonstration of neurofibrillary tangles and neuropil thread-like structures in spinal cord white matter in parkinsonism-dementia complex on Guam and in Guamanian amyotrophic lateral sclerosis. Acta Neuropathol. 1994;88(2):180-4.

19. Graves AB, White E, Koepsell TD, Reifler BV, van Belle G, Larson EB, et al. A case-control study of Alzheimer's disease. Ann Neurol. diciembre de 1990;28(6):766-74.

20. Mendez MF, Underwood KL, Zander BA, Mastri AR, Sung JH, Frey WH 2nd. Risk factors in Alzheimer's disease: a clinicopathologic study. Neurology. abril de 1992;42(4):770-5.

21. Cruts M, Theuns J, Van Broeckhoven C. Locus-specific mutation databases for neurodegenerative brain diseases. Hum Mutat. septiembre de 2012;33(9):1340-4.

22. Goate A, Chartier-Harlin MC, Mullan M, Brown J, Crawford F, Fidani L, et al. Segregation of a missense mutation in the amyloid precursor protein gene with familial Alzheimer's disease. Nature. 21 de febrero de 1991;349(6311):704-6.

23. Sherrington R, Rogaev EI, Liang Y, Rogaeva EA, Levesque G, Ikeda M, et al. Cloning of a gene bearing missense mutations in early-onset familial Alzheimer's disease. Nature. 29 de junio de 1995;375(6534):754-60.

24. Levy-Lahad E, Wasco W, Poorkaj P, Romano DM, Oshima J, Pettingell WH, et al. Candidate gene for the chromosome 1 familial Alzheimer's disease locus. Science. 18 de agosto de 1995;269(5226):973-7.

25. Rovelet-Lecrux A, Hannequin D, Raux G, Le Meur N, Laquerrière A, Vital A, et al. APP locus duplication causes autosomal dominant early-onset Alzheimer disease with cerebral amyloid angiopathy. Nat Genet. enero de 2006;38(1):24-6.

26. Goldgaber D, Lerman MI, McBride WO, Saffiotti U, Gajdusek DC. Isolation, characterization, and chromosomal localization of human brain cDNA clones coding for the precursor of the amyloid of brain in Alzheimer's disease, Down's syndrome and aging. J Neural Transm Suppl. 1987;24:23-8.

27. Robakis NK, Wisniewski HM, Jenkins EC, Devine-Gage EA, Houck GE, Yao XL, et al. Chromosome 21q21 sublocalisation of gene encoding beta-amyloid peptide in cerebral vessels and neuritic (senile) plaques of people with Alzheimer disease and Down syndrome. Lancet. 14 de febrero de 1987;1(8529):384-5.

28. Kang J, Lemaire HG, Unterbeck A, Salbaum JM, Masters CL, Grzeschik KH, et al. The precursor of Alzheimer's disease amyloid A4 protein resembles a cell-surface receptor. Nature. 19 de febrero de 1987;325(6106):733-6.

29. Corder EH, Saunders AM, Strittmatter WJ, Schmechel DE, Gaskell PC, Small GW, et al. Gene dose of apolipoprotein E type 4 allele and the risk of Alzheimer's disease in late onset families. Science. 13 de agosto de 1993;261(5123):921-3.

30. Corder EH, Saunders AM, Risch NJ, Strittmatter WJ, Schmechel DE, Gaskell PC, et al. Protective effect of apolipoprotein E type 2 allele for late onset Alzheimer disease. Nat Genet. junio de 1994;7(2):180-4.

31. Zheng H, Koo EH. Biology and pathophysiology of the amyloid precursor protein. Mol Neurodegener. 2011;6(1):27.

32. Breen KC, Bruce M, Anderton BH. Beta amyloid precursor protein mediates neuronal cell-cell and cell-surface adhesion. J Neurosci Res. enero de 1991;28(1):90-100.

33. Sabo SL, Ikin AF, Buxbaum JD, Greengard P. The Alzheimer amyloid precursor protein (APP) and FE65, an APP-binding protein, regulate cell movement. J Cell Biol. 25 de junio de 2001;153(7):1403-14.

34. Small DH, Clarris HL, Williamson TG, Reed G, Key B, Mok SS, et al. Neurite-outgrowth regulating functions of the amyloid protein precursor of Alzheimer's disease. J Alzheimers Dis. noviembre de 1999;1(4-5):275-85.

35. Wang Z, Wang B, Yang L, Guo Q, Aithmitti N, Songyang Z, et al. Presynaptic and postsynaptic interaction of the amyloid precursor protein promotes peripheral and central synaptogenesis. J Neurosci. 2 de septiembre de 2009;29(35):10788-801.

36. Young-Pearse TL, Bai J, Chang R, Zheng JB, LoTurco JJ, Selkoe DJ. A critical function for beta-amyloid precursor protein in neuronal migration revealed by in utero RNA interference. J Neurosci. 26 de diciembre de 2007;27(52):14459-69.

37. Haass C, Hung AY, Schlossmacher MG, Teplow DB, Selkoe DJ. beta-Amyloid peptide and a 3-kDa fragment are derived by distinct cellular mechanisms. J Biol Chem. 15 de febrero de 1993;268(5):3021-4.

38. Edbauer D, Winkler E, Regula JT, Pesold B, Steiner H, Haass C. Reconstitution of gamma-secretase activity. Nat Cell Biol. mayo de 2003;5(5):486-8.

39. Kimberly WT, LaVoie MJ, Ostaszewski BL, Ye W, Wolfe MS, Selkoe DJ. Gamma-secretase is a membrane protein complex comprised of presenilin, nicastrin, Aph-1, and Pen-2. Proc Natl Acad Sci USA. 27 de mayo de 2003;100(11):6382-7.

40. Takasugi N, Tomita T, Hayashi I, Tsuruoka M, Niimura M, Takahashi Y, et al. The role of presenilin cofactors in the gamma-secretase complex. Nature. 27 de marzo de 2003;422(6930):438-41.

41. Vassar R, Bennett BD, Babu-Khan S, Kahn S, Mendiaz EA, Denis P, et al. Beta-secretase cleavage of Alzheimer's amyloid precursor protein by the transmembrane aspartic protease BACE. Science. 22 de octubre de 1999;286(5440):735-41.

42. Sinha S, Anderson JP, Barbour R, Basi GS, Caccavello R, Davis D, et al. Purification and cloning of amyloid precursor protein beta-secretase from human brain. Nature. 2 de diciembre de 1999;402(6761):537-40.

43. Cameron DJ, Galvin C, Alkam T, Sidhu H, Ellison J, Luna S, et al. Alzheimer's-related peptide amyloid-β plays a conserved role in angiogenesis. PLoS ONE. 2012;7(7):e39598.

44. Morley JE, Farr SA, Banks WA, Johnson SN, Yamada KA, Xu L. A physiological role for amyloid-beta protein:enhancement of learning and memory. J Alzheimers Dis. 2010;19(2):441-9.

45. López-Toledano MA, Shelanski ML. Neurogenic effect of beta-amyloid peptide in the development of neural stem cells. J Neurosci. 9 de junio de 2004;24(23):5439-44.

46. Ferreira A, Lu Q, Orecchio L, Kosik KS. Selective phosphorylation of adult tau isoforms in mature hippocampal neurons exposed to fibrillar A beta. Mol Cell Neurosci. 1997;9(3):220-34.

47. Zheng W-H, Bastianetto S, Mennicken F, Ma W, Kar S. Amyloid beta peptide induces tau phosphorylation and loss of cholinergic neurons in rat primary septal cultures. Neuroscience. 2002;115(1):201-11.

48. Leschik J, Welzel A, Weissmann C, Eckert A, Brandt R. Inverse and distinct modulation of tau-dependent neurodegeneration by presenilin 1 and amyloid-beta in cultured cortical neurons: evidence that tau phosphorylation is the limiting factor in amyloid-beta-induced cell death. J Neurochem. junio de 2007;101(5):1303-15.

49. Busche MA, Eichhoff G, Adelsberger H, Abramowski D, Wiederhold K-H, Haass C, et al. Clusters of hyperactive neurons near amyloid plaques in a mouse model of Alzheimer's disease. Science. 19 de septiembre de 2008;321(5896):1686-9.

50. Fraser PE, Lévesque L, McLachlan DR. Alzheimer A beta amyloid forms an inhibitory neuronal substrate. J Neurochem. marzo de 1994;62(3):1227-30.

51. Pike CJ, Cotman CW. Calretinin-immunoreactive neurons are resistant to beta-amyloid toxicity in vitro. Brain Res. 13 de febrero de 1995;671(2):293-8.

52. Mattson MP. Cellular actions of beta-amyloid precursor protein and its soluble and fibrillogenic derivatives. Physiol Rev. octubre de 1997;77(4):1081-132.

53. Reifert J, Hartung-Cranston D, Feinstein SC. Amyloid beta-mediated cell death of cultured hippocampal neurons reveals extensive Tau fragmentation without increased full-length tau phosphorylation. J Biol Chem. 10 de junio de 2011;286(23):20797-811.

54. Weingarten MD, Lockwood AH, Hwo SY, Kirschner MW. A protein factor essential for microtubule assembly. Proc Natl Acad Sci USA. mayo de 1975;72(5):1858-62.

55. Binder LI, Frankfurter A, Rebhun LI. The distribution of tau in the mammalian central nervous system. J Cell Biol. octubre de 1985;101(4):1371-8.

56. Shin RW, Iwaki T, Kitamoto T, Tateishi J. Hydrated autoclave pretreatment enhances tau immunoreactivity in formalin-fixed normal and Alzheimer's disease brain tissues. Lab Invest. mayo de 1991;64(5):693-702.

57. Couchie D, Mavilia C, Georgieff IS, Liem RK, Shelanski ML, Nunez J. Primary structure of high molecular weight tau present in the peripheral nervous system. Proc Natl Acad Sci USA. 15 de mayo de 1992;89(10):4378-81.

58. Goedert M, Spillantini MG, Jakes R, Rutherford D, Crowther RA. Multiple isoforms of human microtubule-associated protein tau: sequences and localization in neurofibrillary tangles of Alzheimer's disease. Neuron. octubre de 1989;3(4):519-26.

59. Andreadis A, Brown WM, Kosik KS. Structure and novel exons of the human tau gene. Biochemistry. 3 de noviembre de 1992;31(43):10626-33.

60. Hong M, Zhukareva V, Vogelsberg-Ragaglia V, Wszolek Z, Reed L, Miller BI, et al. Mutation-specific functional impairments in distinct tau isoforms of hereditary FTDP-17. Science. 4 de diciembre de 1998;282(5395):1914-7.

61. Drechsel DN, Hyman AA, Cobb MH, Kirschner MW. Modulation of the dynamic instability of tubulin assembly by the microtubule-associated protein tau. Mol Biol Cell. octubre de 1992;3(10):1141-54.

62. Goedert M, Jakes R. Expression of separate isoforms of human tau protein: correlation with the tau pattern in brain and effects on tubulin polymerization. EMBO J. diciembre de 1990;9(13):4225-30.

63. Trinczek B, Ebneth A, Mandelkow EM, Mandelkow E. Tau regulates the attachment/detachment but not the speed of motors in microtubule-dependent transport of single vesicles and organelles. J Cell Sci. julio de 1999;112 (Pt 14):2355-67.

64. Caceres A, Kosik KS. Inhibition of neurite polarity by tau antisense oligonucleotides in primary cerebellar neurons. Nature. 1 de febrero de 1990;343(6257):461-3.

65. Ittner A, Ke YD, van Eersel J, Gladbach A, Götz J, Ittner LM. Brief update on different roles of tau in neurodegeneration. IUBMB Life. julio de 2011;63(7):495-502.

66. Harada A, Oguchi K, Okabe S, Kuno J, Terada S, Ohshima T, et al. Altered microtubule organization in small-calibre axons of mice lacking tau protein. Nature. 9 de junio de 1994;369(6480):488-91.

67. Avila J, Lucas JJ, Perez M, Hernandez F. Role of tau protein in both physiological and pathological conditions. Physiol Rev. abril de 2004;84(2):361-84.

68. Pevalova M, Filipcik P, Novak M, Avila J, Iqbal K. Post-translational modifications of tau protein. Bratisl Lek Listy. 2006;107(9-10):346-53.

69. Johnson GVW, Stoothoff WH. Tau phosphorylation in neuronal cell function and dysfunction. J Cell Sci. 15 de noviembre de 2004;117(Pt 24):5721-9.

70. Ebneth A, Godemann R, Stamer K, Illenberger S, Trinczek B, Mandelkow E. Overexpression of tau protein inhibits kinesin-dependent trafficking of vesicles, mitochondria, and endoplasmic reticulum: implications for Alzheimer's disease. J Cell Biol. 2 de noviembre de 1998;143(3):777-94.

71. Lindwall G, Cole RD. Phosphorylation affects the ability of tau protein to promote microtubule assembly. J Biol Chem. 25 de abril de 1984;259(8):5301-5.

72. Planel E, Miyasaka T, Launey T, Chui D-H, Tanemura K, Sato S, et al. Alterations in glucose metabolism induce hypothermia leading to tau hyperphosphorylation through differential inhibition of kinase and phosphatase activities: implications for Alzheimer's disease. J Neurosci. 10 de marzo de 2004;24(10):2401-11.

73. Hanger DP, Anderton BH, Noble W. Tau phosphorylation: the therapeutic challenge for neurodegenerative disease. Trends Mol Med. marzo de 2009;15(3):112-9.

74. Alonso AC, Grundke-Iqbal I, Iqbal K. Alzheimer's disease hyperphosphorylated tau sequesters normal tau into tangles of filaments and disassembles microtubules. Nat Med. julio de 1996;2(7):783-7.

75. Wagner U, Utton M, Gallo JM, Miller CC. Cellular phosphorylation of tau by GSK-3 beta influences tau binding to microtubules and microtubule organisation. J Cell Sci. junio de 1996;109 (Pt 6):1537-43.

76. Lu Q, Wood JG. Functional studies of Alzheimer's disease tau protein. J Neurosci. febrero de 1993;13(2):508-15.

77. Lee VM, Goedert M, Trojanowski JQ. Neurodegenerative tauopathies. Annu Rev Neurosci. 2001;24:1121-59.

78. Lee VM-Y, Brunden KR, Hutton M, Trojanowski JQ. Developing therapeutic approaches to tau, selected kinases, and related neuronal protein targets. Cold Spring Harb Perspect Med. septiembre de 2011;1(1):a006437.

79. Ballatore C, Brunden KR, Trojanowski JQ, Lee VM-Y, Smith AB 3rd, Huryn DM. Modulation of protein-protein interactions as a therapeutic strategy for the treatment of neurodegenerative tauopathies. Curr Top Med Chem. 2011;11(3):317-30.

80. Brunden KR, Trojanowski JQ, Lee VM-Y. Evidence that non-fibrillar tau causes pathology linked to neurodegeneration and behavioral impairments. J Alzheimers Dis. agosto de 2008;14(4):393-9.

81. Brunden KR, Trojanowski JQ, Lee VM-Y. Advances in tau-focused drug discovery for Alzheimer's disease and related tauopathies. Nat Rev Drug Discov. octubre de 2009;8(10):783-93.

82. Santacruz K, Lewis J, Spires T, Paulson J, Kotilinek L, Ingelsson M, et al. Tau suppression in a neurodegenerative mouse model improves memory function. Science. 15 de julio de 2005;309(5733):476-81.

83. Montine TJ, Phelps CH, Beach TG, Bigio EH, Cairns NJ, Dickson DW, et al. National Institute on Aging-Alzheimer's Association guidelines for the

neuropathologic assessment of Alzheimer's disease: a practical approach. Acta Neuropathol. enero de 2012;123(1):1-11.

84. Braak H, Braak E. Neuropathological stageing of Alzheimer-related changes. Acta Neuropathol. 1991;82(4):239-59.

85. Braak H, Alafuzoff I, Arzberger T, Kretzschmar H, Del Tredici K. Staging of Alzheimer disease-associated neurofibrillary pathology using paraffin sections and immunocytochemistry. Acta Neuropathol. octubre de 2006;112(4):389-404.

86. Nelson PT, Alafuzoff I, Bigio EH, Bouras C, Braak H, Cairns NJ, et al. Correlation of Alzheimer disease neuropathologic changes with cognitive status: a review of the literature. J Neuropathol Exp Neurol. mayo de 2012;71(5):362-81.

87. Reed LA, Grabowski TJ, Schmidt ML, Morris JC, Goate A, Solodkin A, et al. Autosomal dominant dementia with widespread neurofibrillary tangles. Ann Neurol. octubre de 1997;42(4):564-72.

88. Rapoport M, Dawson HN, Binder LI, Vitek MP, Ferreira A. Tau is essential to beta -amyloid-induced neurotoxicity. Proc Natl Acad Sci USA. 30 de abril de 2002;99(9):6364-9.

89. Roberson ED, Scearce-Levie K, Palop JJ, Yan F, Cheng IH, Wu T, et al. Reducing endogenous tau ameliorates amyloid beta-induced deficits in an Alzheimer's disease mouse model. Science. 4 de mayo de 2007;316(5825):750-4.

90. Braak H, Thal DR, Ghebremedhin E, Del Tredici K. Stages of the pathologic process in Alzheimer disease: age categories from 1 to 100 years. J Neuropathol Exp Neurol. noviembre de 2011;70(11):960-9.

91. Hernández F, Gómez de Barreda E, Fuster-Matanzo A, Lucas JJ, Avila J. GSK3: a possible link between beta amyloid peptide and tau protein. Exp Neurol. junio de 2010;223(2):322-5.

92. Bartus RT, Dean RL, Beer B, Lippa AS. The cholinergic hypothesis of geriatric memory dysfunction. Science. 30 de julio de 1982;217(4558):408-14.

93. Mufson EJ, Counts SE, Perez SE, Ginsberg SD. Cholinergic system during the progression of Alzheimer's disease: therapeutic implications. Expert Rev Neurother. noviembre de 2008;8(11):1703-18.

94. Nochi S, Asakawa N, Sato T. Kinetic study on the inhibition of acetylcholinesterase by 1-benzyl-4-[(5,6-dimethoxy-1-indanon)-2-yl]methylpiperidine hydrochloride (E2020). Biol Pharm Bull. agosto de 1995;18(8):1145-7.

95. Lipton SA. Failures and Successes of NMDA Receptor Antagonists: Molecular Basis for the Use of Open-Channel Blockers like Memantine in the Treatment of Acute and Chronic Neurologic Insults. NeuroRx. enero de 2004;1(1):101-10.

96. World Population Prospects, the 2012 Revision [Internet]. [citado 7 de abril de 2015]. Recuperado a partir de: http://esa.un.org/wpp/Excel-Data/population.htm

97. Corrada MM, Brookmeyer R, Paganini-Hill A, Berlau D, Kawas CH. Dementia incidence continues to increase with age in the oldest old: the 90+ study. Ann Neurol. enero de 2010;67(1):114-21.

98. Jorm AF, Jolley D. The incidence of dementia: a meta-analysis. Neurology. septiembre de 1998;51(3):728-33.

99. Gao S, Hendrie HC, Hall KS, Hui S. The relationships between age, sex, and the incidence of dementia and Alzheimer disease: a meta-analysis. Arch Gen Psychiatry. septiembre de 1998;55(9):809-15.

100. Miech RA, Breitner JCS, Zandi PP, Khachaturian AS, Anthony JC, Mayer L. Incidence of AD may decline in the early 90s for men, later for women: The Cache County study. Neurology. 22 de enero de 2002;58(2):209-18.

101. Kawas CH, Corrada MM. Alzheimer's and dementia in the oldest-old: a century of challenges. Curr Alzheimer Res. diciembre de 2006;3(5):411-9.

102. Strittmatter WJ, Saunders AM, Schmechel D, Pericak-Vance M, Enghild J, Salvesen GS, et al. Apolipoprotein E: high-avidity binding to beta-amyloid and increased frequency of type 4 allele in late-onset familial Alzheimer disease. Proc Natl Acad Sci USA. 1 de marzo de 1993;90(5):1977-81.

103. Juva K, Verkkoniemi A, Viramo P, Polvikoski T, Kainulainen K, Kontula K, et al. APOE epsilon4 does not predict mortality, cognitive decline, or dementia in the oldest old. Neurology. 25 de enero de 2000;54(2):412-5.

104. Sobel E, Louhija J, Sulkava R, Davanipour Z, Kontula K, Miettinen H, et al. Lack of association of apolipoprotein E allele epsilon 4 with late-onset Alzheimer's disease among Finnish centenarians. Neurology. mayo de 1995;45(5):903-7.

105. Ganguli M, Lee C-W, Snitz BE, Hughes TF, McDade E, Chang C-CH. Rates and risk factors for progression to incident dementia vary by age in a population cohort. Neurology. 1 de junio de 2015;84(1):72-80.

106. Neuropathology Group. Medical Research Council Cognitive Function and Aging Study. Pathological correlates of late-onset dementia in a multicentre, community-based population in England and Wales. Neuropathology Group of the Medical Research Council Cognitive Function and Ageing Study (MRC CFAS). Lancet. 20 de enero de 2001;357(9251):169-75.

107. Robinson JL, Geser F, Corrada MM, Berlau DJ, Arnold SE, Lee VM-Y, et al. Neocortical and hippocampal amyloid-β and tau measures associate with dementia in the oldest-old. Brain. diciembre de 2011;134(Pt 12):3708-15.

108. Crystal HA, Dickson D, Davies P, Masur D, Grober E, Lipton RB. The relative frequency of «dementia of unknown etiology» increases with age and is nearly 50% in nonagenarians. Arch Neurol. mayo de 2000;57(5):713-9.

109. Polvikoski T, Sulkava R, Myllykangas L, Notkola IL, Niinistö L, Verkkoniemi A, et al. Prevalence of Alzheimer's disease in very elderly people: a prospective neuropathological study. Neurology. 26 de junio de 2001;56(12):1690-6.

110. Katzman R, Terry R, DeTeresa R, Brown T, Davies P, Fuld P, et al. Clinical, pathological, and neurochemical changes in dementia: a subgroup with preserved mental status and numerous neocortical plaques. Ann Neurol. febrero de 1988;23(2):138-44.

111. Silver MH, Newell K, Brady C, Hedley-White ET, Perls TT. Distinguishing between neurodegenerative disease and disease-free aging: correlating neuropsychological evaluations and neuropathological studies in centenarians. Psychosom Med. junio de 2002;64(3):493-501.

112. Nelson PT, Abner EL, Schmitt FA, Kryscio RJ, Jicha GA, Smith CD, et al. Modeling the association between 43 different clinical and pathological variables and the severity of cognitive impairment in a large autopsy cohort of elderly persons. Brain Pathol. enero de 2010;20(1):66-79.

113. Dolan D, Troncoso J, Resnick SM, Crain BJ, Zonderman AB, O'Brien RJ. Age, Alzheimer's disease and dementia in the Baltimore Longitudinal Study of Ageing. Brain. agosto de 2010;133(Pt 8):2225-31.

114. Wilson RS, Leurgans SE, Boyle PA, Schneider JA, Bennett DA. Neurodegenerative basis of age-related cognitive decline. Neurology. 21 de septiembre de 2010;75(12):1070-8.

115. Savva GM, Wharton SB, Ince PG, Forster G, Matthews FE, Brayne C, et al. Age, neuropathology, and dementia. N Engl J Med. 28 de mayo de 2009;360(22):2302-9.

116. Haroutunian V, Schnaider-Beeri M, Schmeidler J, Wysocki M, Purohit DP, Perl DP, et al. Role of the neuropathology of Alzheimer disease in dementia in the oldest-old. Arch Neurol. septiembre de 2008;65(9):1211-7.

117. von Gunten A, Ebbing K, Imhof A, Giannakopoulos P, Kövari E. Brain aging in the oldest-old. Curr Gerontol Geriatr Res. 2010;

118. Masliah E, Mallory M, Hansen L, DeTeresa R, Terry RD. Quantitative synaptic alterations in the human neocortex during normal aging. Neurology. enero de 1993;43(1):192-7.

119. Garde E, Mortensen EL, Krabbe K, Rostrup E, Larsson HB. Relation between age-related decline in intelligence and cerebral white-matter hyperintensities in healthy octogenarians: a longitudinal study. Lancet. 19 de agosto de 2000;356(9230):628-34.

120. Snowdon DA, Greiner LH, Mortimer JA, Riley KP, Greiner PA, Markesbery WR. Brain infarction and the clinical expression of Alzheimer disease. The Nun Study. JAMA. 12 de marzo de 1997;277(10):813-7.

121. Gold G, Kövari E, Herrmann FR, Canuto A, Hof PR, Michel J-P, et al. Cognitive consequences of thalamic, basal ganglia, and deep white matter lacunes in brain aging and dementia. Stroke. junio de 2005;36(6):1184-8.

122. Schneider JA, Boyle PA, Arvanitakis Z, Bienias JL, Bennett DA. Subcortical infarcts, Alzheimer's disease pathology, and memory function in older persons. Ann Neurol. julio de 2007;62(1):59-66.

123. Prasad K, Wiryasaputra L, Ng A, Kandiah N. White matter disease independently predicts progression from mild cognitive impairment to Alzheimer's disease in a clinic cohort. Dement Geriatr Cogn Disord. 2011;31(6):431-4.

124. Nelson PT, Jicha GA, Schmitt FA, Liu H, Davis DG, Mendiondo MS, et al. Clinicopathologic correlations in a large Alzheimer disease center autopsy cohort: neuritic plaques and neurofibrillary tangles «do count» when staging disease severity. J Neuropathol Exp Neurol. diciembre de 2007;66(12):1136-46.

125. Zekry D, Duyckaerts C, Moulias R, Belmin J, Geoffre C, Herrmann F, et al. Degenerative and vascular lesions of the brain have synergistic effects in dementia of the elderly. Acta Neuropathol. mayo de 2002;103(5):481-7.

126. Petrovitch H, Ross GW, Steinhorn SC, Abbott RD, Markesbery W, Davis D, et al. AD lesions and infarcts in demented and non-demented Japanese-American men. Ann Neurol. enero de 2005;57(1):98-103.

127. Polvikoski TM, van Straaten ECW, Barkhof F, Sulkava R, Aronen HJ, Niinistö L, et al. Frontal lobe white matter hyperintensities and neurofibrillary pathology in the oldest old. Neurology. 7 de diciembre de 2010;75(23):2071-8.

128. Sommer W. Erkrankung des Ammonshorns als aetiologisches Moment der Epilepsie. Archiv f Psychiatrie. octubre de 1880;10(3):631-75.

129. Nelson PT, Schmitt FA, Lin Y, Abner EL, Jicha GA, Patel E, et al. Hippocampal sclerosis in advanced age: clinical and pathological features. Brain. mayo de 2011;134(Pt 5):1506-18.

130. Nag S, Yu L, Capuano AW, Wilson RS, Leurgans SE, Bennett DA, et al. Hippocampal sclerosis and TDP-43 pathology in aging and Alzheimer disease. Ann Neurol. junio de 2015;77(6):942-52.

131. Dickson DW, Davies P, Bevona C, Van Hoeven KH, Factor SM, Grober E, et al. Hippocampal sclerosis: a common pathological feature of dementia in very old (> or = 80 years of age) humans. Acta Neuropathol. 1994;88(3):212-21.

132. Corey-Bloom J, Sabbagh MN, Bondi MW, Hansen L, Alford MF, Masliah E, et al. Hippocampal sclerosis contributes to dementia in the elderly. Neurology. enero de 1997;48(1):154-60.

133. Leverenz JB, Agustin CM, Tsuang D, Peskind ER, Edland SD, Nochlin D, et al. Clinical and neuropathological characteristics of hippocampal sclerosis: a community-based study. Arch Neurol. julio de 2002;59(7):1099-106.

134. Cohen TJ, Lee VMY, Trojanowski JQ. TDP-43 functions and pathogenic mechanisms implicated in TDP-43 proteinopathies. Trends Mol Med. noviembre de 2011;17(11):659-67.

135. Neumann M, Sampathu DM, Kwong LK, Truax AC, Micsenyi MC, Chou TT, et al. Ubiquitinated TDP-43 in frontotemporal lobar degeneration and amyotrophic lateral sclerosis. Science. 6 de octubre de 2006;314(5796):130-3.

136. Uryu K, Nakashima-Yasuda H, Forman MS, Kwong LK, Clark CM, Grossman M, et al. Concomitant TAR-DNA-binding protein 43 pathology is present in Alzheimer disease and corticobasal degeneration but not in other tauopathies. J Neuropathol Exp Neurol. junio de 2008;67(6):555-64.

137. DeKosky ST, Scheff SW. Synapse loss in frontal cortex biopsies in Alzheimer's disease: correlation with cognitive severity. Ann Neurol. mayo de 1990;27(5):457-64.

138. Lambert MP, Barlow AK, Chromy BA, Edwards C, Freed R, Liosatos M, et al. Diffusible, nonfibrillar ligands derived from Abeta1-42 are potent central nervous system neurotoxins. Proc Natl Acad Sci USA. 26 de mayo de 1998;95(11):6448-53.

139. Scheff SW, Price DA. Alzheimer's disease-related alterations in synaptic density: neocortex and hippocampus. J Alzheimers Dis. 2006;9(3 Suppl):101-15.

140. Scheff SW, Price DA, Schmitt FA, DeKosky ST, Mufson EJ. Synaptic alterations in CA1 in mild Alzheimer disease and mild cognitive impairment. Neurology. 1 de mayo de 2007;68(18):1501-8.

141. DeKosky ST, Scheff SW, Styren SD. Structural correlates of cognition in dementia: quantification and assessment of synapse change. Neurodegeneration. diciembre de 1996;5(4):417-21.

142. Terry RD, Masliah E, Salmon DP, Butters N, DeTeresa R, Hill R, et al. Physical basis of cognitive alterations in Alzheimer's disease: synapse loss is the major correlate of cognitive impairment. Ann Neurol. octubre de 1991;30(4):572-80.

143. Beeri MS, Haroutunian V, Schmeidler J, Sano M, Fam P, Kavanaugh A, et al. Synaptic protein deficits are associated with dementia irrespective of extreme old age. Neurobiol Aging. junio de 2012;33(6):1125.e1-8.

144. Scheff SW, Price DA, Sparks DL. Quantitative assessment of possible age-related change in synaptic numbers in the human frontal cortex. Neurobiol Aging. junio de 2001;22(3):355-65.

145. Davies P, Anderton B, Kirsch J, Konnerth A, Nitsch R, Sheetz M. First one in, last one out: the role of gabaergic transmission in generation and degeneration. Prog Neurobiol. agosto de 1998;55(6):651-8.

146. Counts SE, Nadeem M, Lad SP, Wuu J, Mufson EJ. Differential expression of synaptic proteins in the frontal and temporal cortex of elderly subjects with mild cognitive impairment. J Neuropathol Exp Neurol. junio de 2006;65(6):592-601.

147. Head E, Corrada MM, Kahle-Wrobleski K, Kim RC, Sarsoza F, Goodus M, et al. Synaptic proteins, neuropathology and cognitive status in the oldest-old. Neurobiol Aging. julio de 2009;30(7):1125-34.

148. Kamenetz F, Tomita T, Hsieh H, Seabrook G, Borchelt D, Iwatsubo T, et al. APP processing and synaptic function. Neuron. 27 de marzo de 2003;37(6):925-37.

149. Cirrito JR, Yamada KA, Finn MB, Sloviter RS, Bales KR, May PC, et al. Synaptic activity regulates interstitial fluid amyloid-beta levels in vivo. Neuron. 22 de diciembre de 2005;48(6):913-22.

150. Meilandt WJ, Yu G-Q, Chin J, Roberson ED, Palop JJ, Wu T, et al. Enkephalin elevations contribute to neuronal and behavioral impairments in a transgenic mouse model of Alzheimer's disease. J Neurosci. 7 de mayo de 2008;28(19):5007-17.

151. Palop JJ, Mucke L. Amyloid-beta-induced neuronal dysfunction in Alzheimer's disease: from synapses toward neural networks. Nat Neurosci. julio de 2010;13(7):812-8.

152. Verret L, Mann EO, Hang GB, Barth AMI, Cobos I, Ho K, et al. Inhibitory interneuron deficit links altered network activity and cognitive dysfunction in Alzheimer model. Cell. 27 de abril de 2012;149(3):708-21.

153. Huang Y, Mucke L. Alzheimer mechanisms and therapeutic strategies. Cell. 16 de marzo de 2012;148(6):1204-22.

154. Walsh DM, Klyubin I, Fadeeva JV, Cullen WK, Anwyl R, Wolfe MS, et al. Naturally secreted oligomers of amyloid beta protein potently inhibit hippocampal long-term potentiation in vivo. Nature. 4 de abril de 2002;416(6880):535-9.

155. Polydoro M, Acker CM, Duff K, Castillo PE, Davies P. Age-dependent impairment of cognitive and synaptic function in the htau mouse model of tau pathology. J Neurosci. 26 de agosto de 2009;29(34):10741-9.

156. Yoshiyama Y, Higuchi M, Zhang B, Huang S-M, Iwata N, Saido TC, et al. Synapse loss and microglial activation precede tangles in a P301S tauopathy mouse model. Neuron. 1 de febrero de 2007;53(3):337-51.

157. Jahn R, Schiebler W, Ouimet C, Greengard P. A 38,000-dalton membrane protein (p38) present in synaptic vesicles. Proc Natl Acad Sci USA. junio de 1985;82(12):4137-41.

158. Navone F, Jahn R, Di Gioia G, Stukenbrok H, Greengard P, De Camilli P. Protein p38: an integral membrane protein specific for small vesicles of neurons and neuroendocrine cells. J Cell Biol. diciembre de 1986;103(6 Pt 1):2511-27.

159. Takamori S, Holt M, Stenius K, Lemke EA, Grønborg M, Riedel D, et al. Molecular anatomy of a trafficking organelle. Cell. 17 de noviembre de 2006;127(4):831-46.

160. Daly C, Ziff EB. Ca2+-dependent formation of a dynamin-synaptophysin complex: potential role in synaptic vesicle endocytosis. J Biol Chem. 15 de marzo de 2002;277(11):9010-5.

161. Gordon SL, Leube RE, Cousin MA. Synaptophysin is required for synaptobrevin retrieval during synaptic vesicle endocytosis. J Neurosci. 28 de septiembre de 2011;31(39):14032-6.

162. Kwon SE, Chapman ER. Synaptophysin regulates the kinetics of synaptic vesicle endocytosis in central neurons. Neuron. 9 de junio de 2011;70(5):847-54.

163. Calakos N, Scheller RH. Vesicle-associated membrane protein and synaptophysin are associated on the synaptic vesicle. J Biol Chem. 7 de octubre de 1994;269(40):24534-7.

164. Pennuto M, Dunlap D, Contestabile A, Benfenati F, Valtorta F. Fluorescence resonance energy transfer detection of synaptophysin I and vesicle-associated membrane protein 2 interactions during exocytosis from single live synapses. Mol Biol Cell. agosto de 2002;13(8):2706-17.

165. Russell CL, Semerdjieva S, Empson RM, Austen BM, Beesley PW, Alifragis P. Amyloid-β acts as a regulator of neurotransmitter release disrupting the interaction between synaptophysin and VAMP2. PLoS ONE. 2012;7(8):e43201.

166. McMahon HT, Bolshakov VY, Janz R, Hammer RE, Siegelbaum SA, Südhof TC. Synaptophysin, a major synaptic vesicle protein, is not essential for neurotransmitter release. Proc Natl Acad Sci USA. 14 de mayo de 1996;93(10):4760-4.

167. Masliah E, Terry RD, DeTeresa RM, Hansen LA. Immunohistochemical quantification of the synapse-related protein synaptophysin in Alzheimer disease. Neurosci Lett. 28 de agosto de 1989;103(2):234-9.

168. Kirvell SL, Elliott MS, Kalaria RN, Hortobágyi T, Ballard CG, Francis PT. Vesicular glutamate transporter and cognition in stroke: a case-control autopsy study. Neurology. 16 de noviembre de 2010;75(20):1803-9.

169. Masliah E, Terry RD, Mallory M, Alford M, Hansen LA. Diffuse plaques do not accentuate synapse loss in Alzheimer's disease. Am J Pathol. diciembre de 1990;137(6):1293-7.

170. Kirvell SL, Esiri M, Francis PT. Down-regulation of vesicular glutamate transporters precedes cell loss and pathology in Alzheimer's disease. J Neurochem. agosto de 2006;98(3):939-50.

171. Sze CI, Troncoso JC, Kawas C, Mouton P, Price DL, Martin LJ. Loss of the presynaptic vesicle protein synaptophysin in hippocampus correlates with cognitive decline in Alzheimer disease. J Neuropathol Exp Neurol. agosto de 1997;56(8):933-44.

172. Scheff SW, Price DA, Ansari MA, Roberts KN, Schmitt FA, Ikonomovic MD, et al. Synaptic change in the posterior cingulate gyrus in the progression of Alzheimer's disease. J Alzheimers Dis. 2015;43(3):1073-90.

173. Buckley K, Kelly RB. Identification of a transmembrane glycoprotein specific for secretory vesicles of neural and endocrine cells. J Cell Biol. abril de 1985;100(4):1284-94.

174. Bajjalieh SM, Frantz GD, Weimann JM, McConnell SK, Scheller RH. Differential expression of synaptic vesicle protein 2 (SV2) isoforms. J Neurosci. septiembre de 1994;14(9):5223-35.

175. Crowder KM, Gunther JM, Jones TA, Hale BD, Zhang HZ, Peterson MR, et al. Abnormal neurotransmission in mice lacking synaptic vesicle protein 2A (SV2A). Proc Natl Acad Sci USA. 21 de diciembre de 1999;96(26):15268-73.

176. Janz R, Goda Y, Geppert M, Missler M, Südhof TC. SV2A and SV2B function as redundant Ca2+ regulators in neurotransmitter release. Neuron. diciembre de 1999;24(4):1003-16.

177. Xu T, Bajjalieh SM. SV2 modulates the size of the readily releasable pool of secretory vesicles. Nat Cell Biol. agosto de 2001;3(8):691-8.

178. Schivell AE, Batchelor RH, Bajjalieh SM. Isoform-specific, calcium-regulated interaction of the synaptic vesicle proteins SV2 and synaptotagmin. J Biol Chem. 1 de noviembre de 1996;271(44):27770-5.

179. Pyle RA, Schivell AE, Hidaka H, Bajjalieh SM. Phosphorylation of synaptic vesicle protein 2 modulates binding to synaptotagmin. J Biol Chem. 2 de junio de 2000;275(22):17195-200.

180. Brose N, Petrenko AG, Südhof TC, Jahn R. Synaptotagmin: a calcium sensor on the synaptic vesicle surface. Science. 15 de mayo de 1992;256(5059):1021-5.

181. Yao J, Nowack A, Kensel-Hammes P, Gardner RG, Bajjalieh SM. Cotrafficking of SV2 and synaptotagmin at the synapse. J Neurosci. 21 de abril de 2010;30(16):5569-78.

182. Lynch BA, Lambeng N, Nocka K, Kensel-Hammes P, Bajjalieh SM, Matagne A, et al. The synaptic vesicle protein SV2A is the binding site for the antiepileptic drug levetiracetam. Proc Natl Acad Sci USA. 29 de junio de 2004;101(26):9861-6.

183. Dong M, Yeh F, Tepp WH, Dean C, Johnson EA, Janz R, et al. SV2 is the protein receptor for botulinum neurotoxin A. Science. 28 de abril de 2006;312(5773):592-6.

184. Lassmann H, Weiler R, Fischer P, Bancher C, Jellinger K, Floor E, et al. Synaptic pathology in Alzheimer's disease: immunological data for markers of synaptic and large dense-core vesicles. Neuroscience. 1992;46(1):1-8.

185. Sze CI, Bi H, Kleinschmidt-DeMasters BK, Filley CM, Martin LJ. Selective regional loss of exocytotic presynaptic vesicle proteins in Alzheimer's disease brains. J Neurol Sci. 15 de abril de 2000;175(2):81-90.

186. Kaufman AC, Salazar SV, Haas LT, Yang J, Kostylev MA, Jeng AT, et al. Fyn inhibition rescues established memory and synapse loss in Alzheimer mice. Ann Neurol. junio de 2015;77(6):953-71.

187. Bakker A, Krauss GL, Albert MS, Speck CL, Jones LR, Stark CE, et al. Reduction of hippocampal hyperactivity improves cognition in amnestic mild cognitive impairment. Neuron. 10 de mayo de 2012;74(3):467-74.

188. Fonnum F. Glutamate: a neurotransmitter in mammalian brain. J Neurochem. enero de 1984;42(1):1-11.

189. Choi DW, Maulucci-Gedde M, Kriegstein AR. Glutamate neurotoxicity in cortical cell culture. J Neurosci. febrero de 1987;7(2):357-68.

190. Martinez-Hernandez A, Bell KP, Norenberg MD. Glutamine synthetase: glial localization in brain. Science. 25 de marzo de 1977;195(4284):1356-8.

191. Rothstein JD, Tabakoff B. Alteration of striatal glutamate release after glutamine synthetase inhibition. J Neurochem. noviembre de 1984;43(5):1438-46.

192. Chaudhry FA, Reimer RJ, Edwards RH. The glutamine commute: take the N line and transfer to the A. J Cell Biol. 29 de abril de 2002;157(3):349-55.

193. Conti F, Minelli A. Glutamate immunoreactivity in rat cerebral cortex is reversibly abolished by 6-diazo-5-oxo-L-norleucine (DON), an inhibitor of phosphate-activated glutaminase. J Histochem Cytochem. junio de 1994;42(6):717-26.

194. Bellocchio EE, Reimer RJ, Fremeau RT, Edwards RH. Uptake of glutamate into synaptic vesicles by an inorganic phosphate transporter. Science. 11 de agosto de 2000;289(5481):957-60.

195. Takamori S, Rhee JS, Rosenmund C, Jahn R. Identification of a vesicular glutamate transporter that defines a glutamatergic phenotype in neurons. Nature. 14 de septiembre de 2000;407(6801):189-94.

196. Liguz-Lecznar M, Skangiel-Kramska J. Vesicular glutamate transporters (VGLUTs): the three musketeers of glutamatergic system. Acta Neurobiol Exp (Wars). 2007;67(3):207-18.

197. Shen J. Modeling the glutamate-glutamine neurotransmitter cycle. Front Neuroenergetics. 2013;5:1.

198. Behrens PF, Franz P, Woodman B, Lindenberg KS, Landwehrmeyer GB. Impaired glutamate transport and glutamate-glutamine cycling: downstream effects of the Huntington mutation. Brain. agosto de 2002;125(Pt 8):1908-22.

199. Maragakis NJ, Rothstein JD. Glutamate transporters: animal models to neurologic disease. Neurobiol Dis. abril de 2004;15(3):461-73.

200. Sepkuty JP, Cohen AS, Eccles C, Rafiq A, Behar K, Ganel R, et al. A neuronal glutamate transporter contributes to neurotransmitter GABA synthesis and epilepsy. J Neurosci. 1 de agosto de 2002;22(15):6372-9.

201. Eastwood SL, Harrison PJ. Decreased expression of vesicular glutamate transporter 1 and complexin II mRNAs in schizophrenia: further evidence for a

synaptic pathology affecting glutamate neurons. Schizophr Res. 1 de marzo de 2005;73(2-3):159-72.

202. Kashani A, Betancur C, Giros B, Hirsch E, El Mestikawy S. Altered expression of vesicular glutamate transporters VGLUT1 and VGLUT2 in Parkinson disease. Neurobiol Aging. abril de 2007;28(4):568-78.

203. Bell KFS, Bennett DA, Cuello AC. Paradoxical upregulation of glutamatergic presynaptic boutons during mild cognitive impairment. J Neurosci. 3 de octubre de 2007;27(40):10810-7.

204. Kashani A, Lepicard E, Poirel O, Videau C, David JP, Fallet-Bianco C, et al. Loss of VGLUT1 and VGLUT2 in the prefrontal cortex is correlated with cognitive decline in Alzheimer disease. Neurobiol Aging. noviembre de 2008;29(11):1619-30.

205. Chen KH, Reese EA, Kim H-W, Rapoport SI, Rao JS. Disturbed neurotransmitter transporter expression in Alzheimer's disease brain. J Alzheimers Dis. 2011;26(4):755-66.

206. Embi N, Rylatt DB, Cohen P. Glycogen synthase kinase-3 from rabbit skeletal muscle. Separation from cyclic-AMP-dependent protein kinase and phosphorylase kinase. Eur J Biochem. junio de 1980;107(2):519-27.

207. Woodgett JR. Molecular cloning and expression of glycogen synthase kinase-3/factor A. EMBO J. agosto de 1990;9(8):2431-8.

208. Shaw PC, Davies AF, Lau KF, Garcia-Barcelo M, Waye MM, Lovestone S, et al. Isolation and chromosomal mapping of human glycogen synthase kinase-3 alpha and -3 beta encoding genes. Genome. octubre de 1998;41(5):720-7.

209. Hansen L, Arden KC, Rasmussen SB, Viars CS, Vestergaard H, Hansen T, et al. Chromosomal mapping and mutational analysis of the coding region of the glycogen synthase kinase-3alpha and beta isoforms in patients with NIDDM. Diabetologia. agosto de 1997;40(8):940-6.

210. Kaidanovich-Beilin O, Lipina TV, Takao K, van Eede M, Hattori S, Laliberté C, et al. Abnormalities in brain structure and behavior in GSK-3alpha mutant mice. Mol Brain. 2009;2:35.

211. Hoeflich KP, Luo J, Rubie EA, Tsao MS, Jin O, Woodgett JR. Requirement for glycogen synthase kinase-3beta in cell survival and NF-kappaB activation. Nature. 6 de julio de 2000;406(6791):86-90.

212. Soutar MPM, Kim W-Y, Williamson R, Peggie M, Hastie CJ, McLauchlan H, et al. Evidence that glycogen synthase kinase-3 isoforms have distinct substrate preference in the brain. J Neurochem. noviembre de 2010;115(4):974-83.

213. Mukai F, Ishiguro K, Sano Y, Fujita SC. Alternative splicing isoform of tau protein kinase I/glycogen synthase kinase 3beta. J Neurochem. junio de 2002;81(5):1073-83.

214. Yao H-B, Shaw P-C, Wong C-C, Wan DC-C. Expression of glycogen synthase kinase-3 isoforms in mouse tissues and their transcription in the brain. J Chem Neuroanat. mayo de 2002;23(4):291-7.

215. Hemmings BA, Yellowlees D, Kernohan JC, Cohen P. Purification of glycogen synthase kinase 3 from rabbit skeletal muscle. Copurification with the activating factor (FA) of the (Mg-ATP) dependent protein phosphatase. Eur J Biochem. octubre de 1981;119(3):443-51.

216. Bijur GN, Jope RS. Proapoptotic stimuli induce nuclear accumulation of glycogen synthase kinase-3 beta. J Biol Chem. 5 de octubre de 2001;276(40):37436-42.

217. Hoshi M, Takashima A, Noguchi K, Murayama M, Sato M, Kondo S, et al. Regulation of mitochondrial pyruvate dehydrogenase activity by tau protein kinase I/glycogen synthase kinase 3beta in brain. Proc Natl Acad Sci USA. 2 de abril de 1996;93(7):2719-23.

218. Bijur GN, Jope RS. Rapid accumulation of Akt in mitochondria following phosphatidylinositol 3-kinase activation. J Neurochem. diciembre de 2003;87(6):1427-35.

219. Perez-Costas E, Gandy JC, Melendez-Ferro M, Roberts RC, Bijur GN. Light and electron microscopy study of glycogen synthase kinase-3beta in the mouse brain. PLoS ONE. 2010;5(1):e8911.

220. Hongisto V, Vainio JC, Thompson R, Courtney MJ, Coffey ET. The Wnt pool of glycogen synthase kinase 3beta is critical for trophic-deprivation-induced neuronal death. Mol Cell Biol. marzo de 2008;28(5):1515-27.

221. Cohen P, Yellowlees D, Aitken A, Donella-Deana A, Hemmings BA, Parker PJ. Separation and characterisation of glycogen synthase kinase 3, glycogen synthase kinase 4 and glycogen synthase kinase 5 from rabbit skeletal muscle. Eur J Biochem. mayo de 1982;124(1):21-35.

222. Kaidanovich-Beilin O, Woodgett JR. GSK-3: Functional Insights from Cell Biology and Animal Models. Front Mol Neurosci. 2011;4:40.

223. Aberle H, Bauer A, Stappert J, Kispert A, Kemler R. beta-catenin is a target for the ubiquitin-proteasome pathway. EMBO J. 1 de julio de 1997;16(13):3797-804.

224. Dajani R, Fraser E, Roe SM, Young N, Good V, Dale TC, et al. Crystal structure of glycogen synthase kinase 3 beta: structural basis for phosphate-primed substrate specificity and autoinhibition. Cell. 15 de junio de 2001;105(6):721-32.

225. ter Haar E, Coll JT, Austen DA, Hsiao HM, Swenson L, Jain J. Structure of GSK3beta reveals a primed phosphorylation mechanism. Nat Struct Biol. julio de 2001;8(7):593-6.

226. Taelman VF, Dobrowolski R, Plouhinec J-L, Fuentealba LC, Vorwald PP, Gumper I, et al. Wnt signaling requires sequestration of glycogen synthase kinase 3 inside multivesicular endosomes. Cell. 23 de diciembre de 2010;143(7):1136-48.

227. Ma S, Liu S, Huang Q, Xie B, Lai B, Wang C, et al. Site-specific phosphorylation protects glycogen synthase kinase-3β from calpain-mediated truncation of its N and C termini. J Biol Chem. 29 de junio de 2012;287(27):22521-32.

228. Jurado-Arjona J, Goñi-Oliver P, Rodríguez-Prada L, Engel T, Henshall DC, Ávila J, et al. Excitotoxicity induced by kainic acid provokes glycogen synthase kinase-3 truncation in the hippocampus. Brain Res. 22 de junio de 2015;1611:84-92.

229. Medina M, Wandosell F. Deconstructing GSK-3: The Fine Regulation of Its Activity. Int J Alzheimers Dis. 2011;2011:479249.

230. Doble BW, Woodgett JR. GSK-3: tricks of the trade for a multi-tasking kinase. J Cell Sci. 1 de abril de 2003;116(Pt 7):1175-86.

231. Hughes K, Nikolakaki E, Plyte SE, Totty NF, Woodgett JR. Modulation of the glycogen synthase kinase-3 family by tyrosine phosphorylation. EMBO J. febrero de 1993;12(2):803-8.

232. Cole A, Frame S, Cohen P. Further evidence that the tyrosine phosphorylation of glycogen synthase kinase-3 (GSK3) in mammalian cells is an autophosphorylation event. Biochem J. 1 de enero de 2004;377(Pt 1):249-55.

233. Park IK, Roach P, Bondor J, Fox SP, DePaoli-Roach AA. Molecular mechanism of the synergistic phosphorylation of phosphatase inhibitor-2. Cloning, expression, and site-directed mutagenesis of inhibitor-2. J Biol Chem. 14 de enero de 1994;269(2):944-54.

234. Dent P, Campbell DG, Hubbard MJ, Cohen P. Multisite phosphorylation of the glycogen-binding subunit of protein phosphatase-1G by cyclic AMP-dependent protein kinase and glycogen synthase kinase-3. FEBS Lett. 8 de mayo de 1989;248(1-2):67-72.

235. Dent P, Lavoinne A, Nakielny S, Caudwell FB, Watt P, Cohen P. The molecular mechanism by which insulin stimulates glycogen synthesis in mammalian skeletal muscle. Nature. 22 de noviembre de 1990;348(6299):302-8.

236. Fiol CJ, Haseman JH, Wang YH, Roach PJ, Roeske RW, Kowalczuk M, et al. Phosphoserine as a recognition determinant for glycogen synthase kinase-3: phosphorylation of a synthetic peptide based on the G-component of protein phosphatase-1. Arch Biochem Biophys. diciembre de 1988;267(2):797-802.

237. Martin M, Rehani K, Jope RS, Michalek SM. Toll-like receptor-mediated cytokine production is differentially regulated by glycogen synthase kinase 3. Nat Immunol. agosto de 2005;6(8):777-84.

238. Jope RS, Yuskaitis CJ, Beurel E. Glycogen synthase kinase-3 (GSK3): inflammation, diseases, and therapeutics. Neurochem Res. mayo de 2007;32(4-5):577-95.

239. Lucas FR, Salinas PC. WNT-7a induces axonal remodeling and increases synapsin I levels in cerebellar neurons. Dev Biol. 1 de diciembre de 1997;192(1):31-44.

240. Lucas FR, Goold RG, Gordon-Weeks PR, Salinas PC. Inhibition of GSK-3beta leading to the loss of phosphorylated MAP-1B is an early event in axonal remodelling induced by WNT-7a or lithium. J Cell Sci. mayo de 1998;111 (Pt 10):1351-61.

241. Eickholt BJ, Walsh FS, Doherty P. An inactive pool of GSK-3 at the leading edge of growth cones is implicated in Semaphorin 3A signaling. J Cell Biol. 15 de abril de 2002;157(2):211-7.

242. Hall AC, Lucas FR, Salinas PC. Axonal remodeling and synaptic differentiation in the cerebellum is regulated by WNT-7a signaling. Cell. 3 de marzo de 2000;100(5):525-35.

243. Mackie K, Sorkin BC, Nairn AC, Greengard P, Edelman GM, Cunningham BA. Identification of two protein kinases that phosphorylate the neural cell-adhesion molecule, N-CAM. J Neurosci. junio de 1989;9(6):1883-96.

244. Guan RJ, Khatra BS, Cohlberg JA. Phosphorylation of bovine neurofilament proteins by protein kinase FA (glycogen synthase kinase 3). J Biol Chem. 5 de mayo de 1991;266(13):8262-7.

245. Berling B, Wille H, Röll B, Mandelkow EM, Garner C, Mandelkow E. Phosphorylation of microtubule-associated proteins MAP2a,b and MAP2c at Ser136 by proline-directed kinases in vivo and in vitro. Eur J Cell Biol. junio de 1994;64(1):120-30.

246. Guidato S, Tsai LH, Woodgett J, Miller CC. Differential cellular phosphorylation of neurofilament heavy side-arms by glycogen synthase kinase-3 and cyclin-dependent kinase-5. J Neurochem. abril de 1996;66(4):1698-706.

247. García-Pérez J, Avila J, Díaz-Nido J. Implication of cyclin-dependent kinases and glycogen synthase kinase 3 in the phosphorylation of microtubule-associated protein 1B in developing neuronal cells. J Neurosci Res. 15 de mayo de 1998;52(4):445-52.

248. Peineau S, Taghibiglou C, Bradley C, Wong TP, Liu L, Lu J, et al. LTP inhibits LTD in the hippocampus via regulation of GSK3beta. Neuron. 1 de marzo de 2007;53(5):703-17.

249. Peineau S, Bradley C, Taghibiglou C, Doherty A, Bortolotto ZA, Wang YT, et al. The role of GSK-3 in synaptic plasticity. Br J Pharmacol. marzo de 2008;153 Suppl 1:S428-37.

250. Peineau S, Nicolas CS, Bortolotto ZA, Bhat RV, Ryves WJ, Harwood AJ, et al. A systematic investigation of the protein kinases involved in NMDA receptor-dependent LTD: evidence for a role of GSK-3 but not other serine/threonine kinases. Mol Brain. 2009;2:22.

251. Zhu L-Q, Wang S-H, Liu D, Yin Y-Y, Tian Q, Wang X-C, et al. Activation of glycogen synthase kinase-3 inhibits long-term potentiation with synapse-associated impairments. J Neurosci. 7 de noviembre de 2007;27(45):12211-20.

252. Hooper C, Markevich V, Plattner F, Killick R, Schofield E, Engel T, et al. Glycogen synthase kinase-3 inhibition is integral to long-term potentiation. Eur J Neurosci. enero de 2007;25(1):81-6.

253. Bradley CA, Peineau S, Taghibiglou C, Nicolas CS, Whitcomb DJ, Bortolotto ZA, et al. A pivotal role of GSK-3 in synaptic plasticity. Front Mol Neurosci. 2012;5:13.

254. Morfini G, Szebenyi G, Elluru R, Ratner N, Brady ST. Glycogen synthase kinase 3 phosphorylates kinesin light chains and negatively regulates kinesin-based motility. EMBO J. 1 de febrero de 2002;21(3):281-93.

255. Li X, Jope RS. Is glycogen synthase kinase-3 a central modulator in mood regulation? Neuropsychopharmacology. octubre de 2010;35(11):2143-54.

256. Kozlovsky N, Nadri C, Agam G. Low GSK-3beta in schizophrenia as a consequence of neurodevelopmental insult. Eur Neuropsychopharmacol. enero de 2005;15(1):1-11.

257. Polter A, Beurel E, Yang S, Garner R, Song L, Miller CA, et al. Deficiency in the inhibitory serine-phosphorylation of glycogen synthase kinase-3 increases sensitivity to mood disturbances. Neuropsychopharmacology. julio de 2010;35(8):1761-74.

258. Darrington RS, Campa VM, Walker MM, Bengoa-Vergniory N, Gorrono-Etxebarria I, Uysal-Onganer P, et al. Distinct expression and activity of GSK-3α and GSK-3β in prostate cancer. Int J Cancer. 15 de septiembre de 2012;131(6):E872-83.

259. Plyte SE, Hughes K, Nikolakaki E, Pulverer BJ, Woodgett JR. Glycogen synthase kinase-3: functions in oncogenesis and development. Biochim Biophys Acta. 16 de diciembre de 1992;1114(2-3):147-62.

260. Juhaszova M, Zorov DB, Yaniv Y, Nuss HB, Wang S, Sollott SJ. Role of glycogen synthase kinase-3beta in cardioprotection. Circ Res. 5 de junio de 2009;104(11):1240-52.

261. Das S, Wong R, Rajapakse N, Murphy E, Steenbergen C. Glycogen synthase kinase 3 inhibition slows mitochondrial adenine nucleotide transport and regulates voltage-dependent anion channel phosphorylation. Circ Res. 24 de octubre de 2008;103(9):983-91.

262. Wagman AS, Johnson KW, Bussiere DE. Discovery and development of GSK3 inhibitors for the treatment of type 2 diabetes. Curr Pharm Des. 2004;10(10):1105-37.

263. Cohen P, Goedert M. GSK3 inhibitors: development and therapeutic potential. Nat Rev Drug Discov. junio de 2004;3(6):479-87.

264. Hooper C, Killick R, Lovestone S. The GSK3 hypothesis of Alzheimer's disease. J Neurochem. marzo de 2008;104(6):1433-9.

265. Medina M, Avila J. Glycogen synthase kinase-3 (GSK-3) inhibitors for the treatment of Alzheimer's disease. Curr Pharm Des. 2010;16(25):2790-8.

266. Eldar-Finkelman H, Martinez A. GSK-3 Inhibitors: Preclinical and Clinical Focus on CNS. Front Mol Neurosci. 2011;4:32.

267. Serenó L, Coma M, Rodríguez M, Sánchez-Ferrer P, Sánchez MB, Gich I, et al. A novel GSK-3beta inhibitor reduces Alzheimer's pathology and rescues neuronal loss in vivo. Neurobiol Dis. septiembre de 2009;35(3):359-67.

268. MacAulay K, Doble BW, Patel S, Hansotia T, Sinclair EM, Drucker DJ, et al. Glycogen synthase kinase 3alpha-specific regulation of murine hepatic glycogen metabolism. Cell Metab. octubre de 2007;6(4):329-37.

269. O'Brien WT, Harper AD, Jové F, Woodgett JR, Maretto S, Piccolo S, et al. Glycogen synthase kinase-3beta haploinsufficiency mimics the behavioral and molecular effects of lithium. J Neurosci. 28 de julio de 2004;24(30):6791-8.

270. Kimura T, Yamashita S, Nakao S, Park J-M, Murayama M, Mizoroki T, et al. GSK-3beta is required for memory reconsolidation in adult brain. PLoS ONE. 2008;3(10):e3540.

271. Moore CB, Guthrie EH, Huang MT-H, Taxman DJ. Short Hairpin RNA (shRNA): Design, Delivery, and Assessment of Gene Knockdown. Methods Mol Biol. 2010;629:141-58.

272. Phiel CJ, Wilson CA, Lee VM-Y, Klein PS. GSK-3alpha regulates production of Alzheimer's disease amyloid-beta peptides. Nature. 22 de mayo de 2003;423(6938):435-9.

273. Hurtado DE, Molina-Porcel L, Carroll JC, Macdonald C, Aboagye AK, Trojanowski JQ, et al. Selectively silencing GSK-3 isoforms reduces plaques and tangles in mouse models of Alzheimer's disease. J Neurosci. 23 de mayo de 2012;32(21):7392-402.

274. Cejka D, Losert D, Wacheck V. Short interfering RNA (siRNA): tool or therapeutic? Clin Sci. enero de 2006;110(1):47-58.

275. Ryding AD, Sharp MG, Mullins JJ. Conditional transgenic technologies. J Endocrinol. octubre de 2001;171(1):1-14.

276. Dominguez I, Itoh K, Sokol SY. Role of glycogen synthase kinase 3 beta as a negative regulator of dorsoventral axis formation in Xenopus embryos. Proc Natl Acad Sci USA. 29 de agosto de 1995;92(18):8498-502.

277. Burgin KE, Waxham MN, Rickling S, Westgate SA, Mobley WC, Kelly PT. In situ hybridization histochemistry of Ca2+/calmodulin-dependent protein kinase in developing rat brain. J Neurosci. junio de 1990;10(6):1788-98.

278. Gómez-Sintes R, Hernández F, Bortolozzi A, Artigas F, Avila J, Zaratin P, et al. Neuronal apoptosis and reversible motor deficit in dominant-negative GSK-3 conditional transgenic mice. EMBO J. 6 de junio de 2007;26(11):2743-54.

279. Gómez-Sintes R, Hernández F, Lucas JJ, Avila J. GSK-3 Mouse Models to Study Neuronal Apoptosis and Neurodegeneration. Front Mol Neurosci. 2011;4:45.

280. Sternberg N, Hamilton D. Bacteriophage P1 site-specific recombination. I. Recombination between loxP sites. J Mol Biol. 25 de agosto de 1981;150(4):467-86.

281. Ishiguro K, Takamatsu M, Tomizawa K, Omori A, Takahashi M, Arioka M, et al. Tau protein kinase I converts normal tau protein into A68-like component of paired helical filaments. J Biol Chem. 25 de mayo de 1992;267(15):10897-901.

282. Pei JJ, Braak E, Braak H, Grundke-Iqbal I, Iqbal K, Winblad B, et al. Distribution of active glycogen synthase kinase 3beta (GSK-3beta) in brains staged for Alzheimer disease neurofibrillary changes. J Neuropathol Exp Neurol. septiembre de 1999;58(9):1010-9.

283. Leroy K, Yilmaz Z, Brion J-P. Increased level of active GSK-3beta in Alzheimer's disease and accumulation in argyrophilic grains and in neurones at different stages of neurofibrillary degeneration. Neuropathol Appl Neurobiol. febrero de 2007;33(1):43-55.

284. Yamaguchi H, Ishiguro K, Uchida T, Takashima A, Lemere CA, Imahori K. Preferential labeling of Alzheimer neurofibrillary tangles with antisera for tau protein kinase (TPK) I/glycogen synthase kinase-3 beta and cyclin-dependent kinase 5, a component of TPK II. Acta Neuropathol. septiembre de 1996;92(3):232-41.

285. Imahori K, Uchida T. Physiology and pathology of tau protein kinases in relation to Alzheimer's disease. J Biochem. febrero de 1997;121(2):179-88.

286. Pei JJ, Tanaka T, Tung YC, Braak E, Iqbal K, Grundke-Iqbal I. Distribution, levels, and activity of glycogen synthase kinase-3 in the Alzheimer disease brain. J Neuropathol Exp Neurol. enero de 1997;56(1):70-8.

287. Ferrer I, Barrachina M, Puig B. Glycogen synthase kinase-3 is associated with neuronal and glial hyperphosphorylated tau deposits in Alzheimer's disease, Pick's disease, progressive supranuclear palsy and corticobasal degeneration. Acta Neuropathol. diciembre de 2002;104(6):583-91.

288. Ishizawa T, Sahara N, Ishiguro K, Kersh J, McGowan E, Lewis J, et al. Co-localization of glycogen synthase kinase-3 with neurofibrillary tangles and granulovacuolar degeneration in transgenic mice. Am J Pathol. septiembre de 2003;163(3):1057-67.

289. Blalock EM, Geddes JW, Chen KC, Porter NM, Markesbery WR, Landfield PW. Incipient Alzheimer's disease: microarray correlation analyses reveal major transcriptional and tumor suppressor responses. Proc Natl Acad Sci USA. 17 de febrero de 2004;101(7):2173-8.

290. Swatton JE, Sellers LA, Faull RLM, Holland A, Iritani S, Bahn S. Increased MAP kinase activity in Alzheimer's and Down syndrome but not in schizophrenia human brain. Eur J Neurosci. mayo de 2004;19(10):2711-9.

291. Baum L, Hansen L, Masliah E, Saitoh T. Glycogen synthase kinase 3 alteration in Alzheimer disease is related to neurofibrillary tangle formation. Mol Chem Neuropathol. diciembre de 1996;29(2-3):253-61.

292. Hye A, Kerr F, Archer N, Foy C, Poppe M, Brown R, et al. Glycogen synthase kinase-3 is increased in white cells early in Alzheimer's disease. Neurosci Lett. 3 de enero de 2005;373(1):1-4.

293. Forlenza OV, Torres CA, Talib LL, de Paula VJ, Joaquim HPG, Diniz BS, et al. Increased platelet GSK3B activity in patients with mild cognitive impairment and Alzheimer's disease. J Psychiatr Res. febrero de 2011;45(2):220-4.

294. Pláteník J, Fišar Z, Buchal R, Jirák R, Kitzlerová E, Zvěřová M, et al. GSK3β, CREB, and BDNF in peripheral blood of patients with Alzheimer's disease and depression. Prog Neuropsychopharmacol Biol Psychiatry. 3 de abril de 2014;50:83-93.

295. Mateo I, Infante J, Llorca J, Rodríguez E, Berciano J, Combarros O. Association between glycogen synthase kinase-3beta genetic polymorphism and late-onset Alzheimer's disease. Dement Geriatr Cogn Disord. 2006;21(4):228-32.

296. Zhang N, Yu J-T, Yang Y, Yang J, Zhang W, Tan L. Association analysis of GSK3B and MAPT polymorphisms with Alzheimer's disease in Han Chinese. Brain Res. 19 de mayo de 2011;1391:147-53.

297. Schaffer BAJ, Bertram L, Miller BL, Mullin K, Weintraub S, Johnson N, et al. Association of GSK3B with Alzheimer disease and frontotemporal dementia. Arch Neurol. octubre de 2008;65(10):1368-74.

298. Kwok JBJ, Loy CT, Hamilton G, Lau E, Hallupp M, Williams J, et al. Glycogen synthase kinase-3beta and tau genes interact in Alzheimer's disease. Ann Neurol. octubre de 2008;64(4):446-54.

299. Mateo I, Vázquez-Higuera JL, Sánchez-Juan P, Rodríguez-Rodríguez E, Infante J, García-Gorostiaga I, et al. Epistasis between tau phosphorylation regulating genes (CDK5R1 and GSK-3beta) and Alzheimer's disease risk. Acta Neurol Scand. agosto de 2009;120(2):130-3.

300. Baki L, Shioi J, Wen P, Shao Z, Schwarzman A, Gama-Sosa M, et al. PS1 activates PI3K thus inhibiting GSK-3 activity and tau overphosphorylation: effects of FAD mutations. EMBO J. 7 de julio de 2004;23(13):2586-96.

301. Tanemura K, Chui D-H, Fukuda T, Murayama M, Park J-M, Akagi T, et al. Formation of tau inclusions in knock-in mice with familial Alzheimer disease (FAD) mutation of presenilin 1 (PS1). J Biol Chem. 24 de febrero de 2006;281(8):5037-41.

302. Kremer A, Louis JV, Jaworski T, Van Leuven F. GSK3 and Alzheimer's Disease: Facts and Fiction…. Front Mol Neurosci. 2011;4:17.

303. Jope RS, Johnson GVW. The glamour and gloom of glycogen synthase kinase-3. Trends Biochem Sci. febrero de 2004;29(2):95-102.

304. Giese KP. GSK-3: a key player in neurodegeneration and memory. IUBMB Life. mayo de 2009;61(5):516-21.

305. Hanger DP, Hughes K, Woodgett JR, Brion JP, Anderton BH. Glycogen synthase kinase-3 induces Alzheimer's disease-like phosphorylation of tau: generation of paired helical filament epitopes and neuronal localisation of the kinase. Neurosci Lett. 23 de noviembre de 1992;147(1):58-62.

306. Lovestone S, Reynolds CH, Latimer D, Davis DR, Anderton BH, Gallo JM, et al. Alzheimer's disease-like phosphorylation of the microtubule-associated protein tau by glycogen synthase kinase-3 in transfected mammalian cells. Curr Biol. 1 de diciembre de 1994;4(12):1077-86.

307. Cho J-H, Johnson GVW. Glycogen synthase kinase 3beta phosphorylates tau at both primed and unprimed sites. Differential impact on microtubule binding. J Biol Chem. 3 de enero de 2003;278(1):187-93.

308. Hanger DP, Byers HL, Wray S, Leung K-Y, Saxton MJ, Seereeram A, et al. Novel phosphorylation sites in tau from Alzheimer brain support a role for casein kinase 1 in disease pathogenesis. J Biol Chem. 10 de agosto de 2007;282(32):23645-54.

309. Hong M, Chen DC, Klein PS, Lee VM. Lithium reduces tau phosphorylation by inhibition of glycogen synthase kinase-3. J Biol Chem. 3 de octubre de 1997;272(40):25326-32.

310. Spittaels K, Van den Haute C, Van Dorpe J, Geerts H, Mercken M, Bruynseels K, et al. Glycogen synthase kinase-3beta phosphorylates protein tau and rescues the axonopathy in the central nervous system of human four-repeat tau transgenic mice. J Biol Chem. 29 de diciembre de 2000;275(52):41340-9.

311. Lucas JJ, Hernández F, Gómez-Ramos P, Morán MA, Hen R, Avila J. Decreased nuclear beta-catenin, tau hyperphosphorylation and neurodegeneration in GSK-3beta conditional transgenic mice. EMBO J. 15 de enero de 2001;20(1-2):27-39.

312. Terwel D, Muyllaert D, Dewachter I, Borghgraef P, Croes S, Devijver H, et al. Amyloid activates GSK-3beta to aggravate neuronal tauopathy in bigenic mice. Am J Pathol. marzo de 2008;172(3):786-98.

313. Brownlees J, Irving NG, Brion JP, Gibb BJ, Wagner U, Woodgett J, et al. Tau phosphorylation in transgenic mice expressing glycogen synthase kinase-3beta transgenes. Neuroreport. 20 de octubre de 1997;8(15):3251-5.

314. Li B, Ryder J, Su Y, Moore SA Jr, Liu F, Solenberg P, et al. Overexpression of GSK3betaS9A resulted in tau hyperphosphorylation and morphology reminiscent of pretangle-like neurons in the brain of PDGSK3beta transgenic mice. Transgenic Res. agosto de 2004;13(4):385-96.

315. Hernández F, Borrell J, Guaza C, Avila J, Lucas JJ. Spatial learning deficit in transgenic mice that conditionally over-express GSK-3beta in the brain but do not form tau filaments. J Neurochem. diciembre de 2002;83(6):1529-33.

316. Jackson GR, Wiedau-Pazos M, Sang T-K, Wagle N, Brown CA, Massachi S, et al. Human Wild-Type Tau Interacts with wingless Pathway Components and

Produces Neurofibrillary Pathology in Drosophila. Neuron. 16 de mayo de 2002;34(4):509-19.

317. Mudher A, Shepherd D, Newman TA, Mildren P, Jukes JP, Squire A, et al. GSK-3β inhibition reverses axonal transport defects and behavioural phenotypes in Drosophila. Mol Psychiatry. 2 de marzo de 2004;9(5):522-30.

318. Engel T, Hernández F, Avila J, Lucas JJ. Full reversal of Alzheimer's disease-like phenotype in a mouse model with conditional overexpression of glycogen synthase kinase-3. J Neurosci. 10 de mayo de 2006;26(19):5083-90.

319. Gómez de Barreda E, Pérez M, Gómez Ramos P, de Cristobal J, Martín-Maestro P, Morán A, et al. Tau-knockout mice show reduced GSK3-induced hippocampal degeneration and learning deficits. Neurobiol Dis. marzo de 2010;37(3):622-9.

320. Pérez M, Hernández F, Lim F, Díaz-Nido J, Avila J. Chronic lithium treatment decreases mutant tau protein aggregation in a transgenic mouse model. J Alzheimers Dis. agosto de 2003;5(4):301-8.

321. Noble W, Planel E, Zehr C, Olm V, Meyerson J, Suleman F, et al. Inhibition of glycogen synthase kinase-3 by lithium correlates with reduced tauopathy and degeneration in vivo. Proc Natl Acad Sci USA. 10 de mayo de 2005;102(19):6990-5.

322. Plattner F, Angelo M, Giese KP. The roles of cyclin-dependent kinase 5 and glycogen synthase kinase 3 in tau hyperphosphorylation. J Biol Chem. 1 de septiembre de 2006;281(35):25457-65.

323. Caccamo A, Oddo S, Tran LX, LaFerla FM. Lithium reduces tau phosphorylation but not A beta or working memory deficits in a transgenic model with both plaques and tangles. Am J Pathol. mayo de 2007;170(5):1669-75.

324. Nakashima H, Ishihara T, Suguimoto P, Yokota O, Oshima E, Kugo A, et al. Chronic lithium treatment decreases tau lesions by promoting ubiquitination in a mouse model of tauopathies. Acta Neuropathol. diciembre de 2005;110(6):547-56.

325. Rockenstein E, Torrance M, Adame A, Mante M, Bar-on P, Rose JB, et al. Neuroprotective effects of regulators of the glycogen synthase kinase-3beta signaling pathway in a transgenic model of Alzheimer's disease are associated with reduced amyloid precursor protein phosphorylation. J Neurosci. 21 de febrero de 2007;27(8):1981-91.

326. Alon LT, Pietrokovski S, Barkan S, Avrahami L, Kaidanovich-Beilin O, Woodgett JR, et al. Selective loss of glycogen synthase kinase-3α in birds reveals distinct roles for GSK-3 isozymes in tau phosphorylation. FEBS Lett. 20 de abril de 2011;585(8):1158-62.

327. Tolosa E, Litvan I, Höglinger GU, Burn D, Lees A, Andrés MV, et al. A phase 2 trial of the GSK-3 inhibitor tideglusib in progressive supranuclear palsy. Mov Disord. abril de 2014;29(4):470-8.

328. Lovestone S, Boada M, Dubois B, Hüll M, Rinne JO, Huppertz H-J, et al. A phase II trial of tideglusib in Alzheimer's disease. J Alzheimers Dis. 2015;45(1):75-88.

329. Takashima A, Noguchi K, Sato K, Hoshino T, Imahori K. Tau protein kinase I is essential for amyloid beta-protein-induced neurotoxicity. Proc Natl Acad Sci USA. 15 de agosto de 1993;90(16):7789-93.

330. Hu S, Begum AN, Jones MR, Oh MS, Beech WK, Beech BH, et al. GSK3 inhibitors show benefits in an Alzheimer's disease (AD) model of neurodegeneration but adverse effects in control animals. Neurobiol Dis. febrero de 2009;33(2):193-206.

331. Tackenberg C, Brandt R. Divergent pathways mediate spine alterations and cell death induced by amyloid-beta, wild-type tau, and R406W tau. J Neurosci. 18 de noviembre de 2009;29(46):14439-50.

332. Sofola O, Kerr F, Rogers I, Killick R, Augustin H, Gandy C, et al. Inhibition of GSK-3 ameliorates Abeta pathology in an adult-onset Drosophila model of Alzheimer's disease. PLoS Genet. septiembre de 2010;6(9).

333. Aplin AE, Jacobsen JS, Anderton BH, Gallo JM. Effect of increased glycogen synthase kinase-3 activity upon the maturation of the amyloid precursor protein in transfected cells. Neuroreport. 10 de febrero de 1997;8(3):639-43.

334. Sun X, Sato S, Murayama O, Murayama M, Park J-M, Yamaguchi H, et al. Lithium inhibits amyloid secretion in COS7 cells transfected with amyloid precursor protein C100. Neurosci Lett. 15 de marzo de 2002;321(1-2):61-4.

335. Ryder J, Su Y, Liu F, Li B, Zhou Y, Ni B. Divergent roles of GSK3 and CDK5 in APP processing. Biochem Biophys Res Commun. 26 de diciembre de 2003;312(4):922-9.

336. Su Y, Ryder J, Li B, Wu X, Fox N, Solenberg P, et al. Lithium, a common drug for bipolar disorder treatment, regulates amyloid-beta precursor protein processing. Biochemistry. 8 de junio de 2004;43(22):6899-908.

337. Rezai-Zadeh K, Douglas Shytle R, Bai Y, Tian J, Hou H, Mori T, et al. Flavonoid-mediated presenilin-1 phosphorylation reduces Alzheimer's disease beta-amyloid production. J Cell Mol Med. marzo de 2009;13(3):574-88.

338. Feyt C, Kienlen-Campard P, Leroy K, N'Kuli F, Courtoy PJ, Brion J-P, et al. Lithium chloride increases the production of amyloid-beta peptide independently from its inhibition of glycogen synthase kinase 3. J Biol Chem. 30 de septiembre de 2005;280(39):33220-7.

339. Jaworski T, Dewachter I, Lechat B, Gees M, Kremer A, Demedts D, et al. GSK-3α/β kinases and amyloid production in vivo. Nature. 8 de diciembre de 2011;480(7376):E4-5; discussion E6.

340. Clark CM, Ewbank DC. Performance of the dementia severity rating scale: a caregiver questionnaire for rating severity in Alzheimer disease. Alzheimer Dis Assoc Disord. 1996;10(1):31-9.

341. Pfeffer RI, Kurosaki TT, Harrah CH, Chance JM, Filos S. Measurement of functional activities in older adults in the community. J Gerontol. mayo de 1982;37(3):323-9.

342. Silverman JM, Breitner JC, Mohs RC, Davis KL. Reliability of the family history method in genetic studies of Alzheimer's disease and related dementias. Am J Psychiatry. octubre de 1986;143(10):1279-82.

343. Kawas C, Segal J, Stewart WF, Corrada M, Thal LJ. A validation study of the Dementia Questionnaire. Arch Neurol. septiembre de 1994;51(9):901-6.

344. American Psychiatric Association, American Psychiatric Association, and Task Force on DSM-IV (1994). Diagnostic and statistical manual of mental disorders: DSM-IV. (Washington, DC: American Psychiatric Association)

345. Albert MS, Moss MB, Tanzi R, Jones K. Preclinical prediction of AD using neuropsychological tests. J Int Neuropsychol Soc. julio de 2001;7(5):631-9.

346. Chen P, Ratcliff G, Belle SH, Cauley JA, DeKosky ST, Ganguli M. Patterns of cognitive decline in presymptomatic Alzheimer disease: a prospective community study. Arch Gen Psychiatry. septiembre de 2001;58(9):853-8.

347. Saxton J, Lopez OL, Ratcliff G, Dulberg C, Fried LP, Carlson MC, et al. Preclinical Alzheimer disease: neuropsychological test performance 1.5 to 8 years prior to onset. Neurology. 28 de diciembre de 2004;63(12):2341-7.

348. Berlau DJ, Corrada MM, Head E, Kawas CH. APOE epsilon2 is associated with intact cognition but increased Alzheimer pathology in the oldest old. Neurology. 3 de marzo de 2009;72(9):829-34.

349. Thal DR, Capetillo-Zarate E, Del Tredici K, Braak H. The development of amyloid beta protein deposits in the aged brain. Sci Aging Knowledge Environ. 8 de marzo de 2006;2006(6):re1.

350. Jellinger KA, Attems J. Incidence of cerebrovascular lesions in Alzheimer's disease: a postmortem study. Acta Neuropathol. enero de 2003;105(1):14-7.

351. Corrada MM, Paganini-Hill A, Berlau DJ, Kawas CH. Apolipoprotein E genotype, dementia, and mortality in the oldest old: the 90+ Study. Alzheimers Dement. enero de 2013;9(1):12-8.

352. Wilson RS, Yu L, Trojanowski JQ, Chen E-Y, Boyle PA, Bennett DA, et al. TDP-43 pathology, cognitive decline, and dementia in old age. JAMA Neurol. noviembre de 2013;70(11):1418-24.

353. Tsien JZ, Chen DF, Gerber D, Tom C, Mercer EH, Anderson DJ, et al. Subregion- and cell type-restricted gene knockout in mouse brain. Cell. 27 de diciembre de 1996;87(7):1317-26.

354. Ruzankina Y, Pinzon-Guzman C, Asare A, Ong T, Pontano L, Cotsarelis G, et al. Deletion of the developmentally essential gene ATR in adult mice leads to age-related phenotypes and stem cell loss. Cell Stem Cell. 7 de junio de 2007;1(1):113-26.

355. Schorpp M, Jäger R, Schellander K, Schenkel J, Wagner EF, Weiher H, et al. The human ubiquitin C promoter directs high ubiquitous expression of transgenes in mice. Nucleic Acids Res. 1 de mayo de 1996;24(9):1787-8.

356. Games D, Adams D, Alessandrini R, Barbour R, Berthelette P, Blackwell C, et al. Alzheimer-type neuropathology in transgenic mice overexpressing V717F beta-amyloid precursor protein. Nature. 9 de febrero de 1995;373(6514):523-7.

357. Masliah E, Sisk A, Mallory M, Games D. Neurofibrillary pathology in transgenic mice overexpressing V717F beta-amyloid precursor protein. J Neuropathol Exp Neurol. abril de 2001;60(4):357-68.

358. Chen G, Chen KS, Knox J, Inglis J, Bernard A, Martin SJ, et al. A learning deficit related to age and beta-amyloid plaques in a mouse model of Alzheimer's disease. Nature. 21 de diciembre de 2000;408(6815):975-9.

359. Dodart JC, Meziane H, Mathis C, Bales KR, Paul SM, Ungerer A. Behavioral disturbances in transgenic mice overexpressing the V717F beta-amyloid precursor protein. Behav Neurosci. octubre de 1999;113(5):982-90.

360. Kobayashi DT, Chen KS. Behavioral phenotypes of amyloid-based genetically modified mouse models of Alzheimer's disease. Genes, Brain and Behavior. 1 de abril de 2005;4(3):173-96.

361. Hurtado DE, Molina-Porcel L, Iba M, Aboagye AK, Paul SM, Trojanowski JQ, et al. A{beta} accelerates the spatiotemporal progression of tau pathology and augments tau amyloidosis in an Alzheimer mouse model. Am J Pathol. octubre de 2010;177(4):1977-88.

362. Lee EB, Leng LZ, Zhang B, Kwong L, Trojanowski JQ, Abel T, et al. Targeting amyloid-beta peptide (Abeta) oligomers by passive immunization with a conformation-selective monoclonal antibody improves learning and memory in Abeta precursor protein (APP) transgenic mice. J Biol Chem. 17 de febrero de 2006;281(7):4292-9.

363. Carroll JC, Iba M, Bangasser DA, Valentino RJ, James MJ, Brunden KR, et al. Chronic stress exacerbates tau pathology, neurodegeneration, and cognitive performance through a corticotropin-releasing factor receptor-dependent mechanism in a transgenic mouse model of tauopathy. J Neurosci. 5 de octubre de 2011;31(40):14436-49.

364. Boyce-Rustay JM, Holmes A. Genetic inactivation of the NMDA receptor NR2A subunit has anxiolytic- and antidepressant-like effects in mice. Neuropsychopharmacology. noviembre de 2006;31(11):2405-14.

365. Carroll JC, Boyce-Rustay JM, Millstein R, Yang R, Wiedholz LM, Murphy DL, et al. Effects of mild early life stress on abnormal emotion-related behaviors in 5-HTT knockout mice. Behav Genet. enero de 2007;37(1):214-22.

366. Brunden KR, Zhang B, Carroll J, Yao Y, Potuzak JS, Hogan A-ML, et al. Epothilone D improves microtubule density, axonal integrity, and cognition in a transgenic mouse model of tauopathy. J Neurosci. 13 de octubre de 2010;30(41):13861-6.

367. O'Leary TP, Savoie V, Brown RE. Learning, memory and search strategies of inbred mouse strains with different visual abilities in the Barnes maze. Behav Brain Res. 20 de enero de 2011;216(2):531-42.

368. Corrada MM, Brookmeyer R, Berlau D, Paganini-Hill A, Kawas CH. Prevalence of dementia after age 90: results from the 90+ study. Neurology. 29 de julio de 2008;71(5):337-43.

369. Hebert LE, Weuve J, Scherr PA, Evans DA. Alzheimer disease in the United States (2010-2050) estimated using the 2010 census. Neurology. 7 de mayo de 2013;80(19):1778-83.

370. Giannakopoulos P, Hof PR, Michel JP, Guimon J, Bouras C. Cerebral cortex pathology in aging and Alzheimer's disease: a quantitative survey of large hospital-based geriatric and psychiatric cohorts. Brain Res Brain Res Rev. octubre de 1997;25(2):217-45.

371. Nelson PT, Head E, Schmitt FA, Davis PR, Neltner JH, Jicha GA, et al. Alzheimer's disease is not «brain aging»: neuropathological, genetic, and epidemiological human studies. Acta Neuropathol. mayo de 2011;121(5):571-87.

372. Mukaetova-Ladinska EB, Garcia-Siera F, Hurt J, Gertz HJ, Xuereb JH, Hills R, et al. Staging of cytoskeletal and beta-amyloid changes in human isocortex reveals biphasic synaptic protein response during progression of Alzheimer's disease. Am J Pathol. agosto de 2000;157(2):623-36.

373. Aisen PS. Pre-dementia Alzheimer's trials: overview. J Nutr Health Aging. abril de 2010;14(4):294.

374. Jack CR, Knopman DS, Jagust WJ, Petersen RC, Weiner MW, Aisen PS, et al. Tracking pathophysiological processes in Alzheimer's disease: an updated hypothetical model of dynamic biomarkers. Lancet Neurol. febrero de 2013;12(2):207-16.

375. Gómez-Isla T, Price JL, McKeel DW, Morris JC, Growdon JH, Hyman BT. Profound loss of layer II entorhinal cortex neurons occurs in very mild Alzheimer's disease. J Neurosci. 15 de julio de 1996;16(14):4491-500.

376. Honer WG. Pathology of presynaptic proteins in Alzheimer's disease: more than simple loss of terminals. Neurobiol Aging. diciembre de 2003;24(8):1047-62.

377. Sokolow S, Luu SH, Nandy K, Miller CA, Vinters HV, Poon WW, et al. Preferential accumulation of amyloid-beta in presynaptic glutamatergic terminals (VGluT1 and VGluT2) in Alzheimer's disease cortex. Neurobiol Dis. enero de 2012;45(1):381-7.

378. Nieweg K, Andreyeva A, van Stegen B, Tanriöver G, Gottmann K. Alzheimer's disease-related amyloid-β induces synaptotoxicity in human iPS cell-derived neurons. Cell Death Dis. 2015;6:e1709.

379. Mitew S, Kirkcaldie MTK, Dickson TC, Vickers JC. Altered synapses and gliotransmission in Alzheimer's disease and AD model mice. Neurobiol Aging. octubre de 2013;34(10):2341-51.

380. Medina M, Avila J. Understanding the relationship between GSK-3 and Alzheimer's disease: a focus on how GSK-3 can modulate synaptic plasticity processes. Expert Rev Neurother. mayo de 2013;13(5):495-503.

381. Lo Monte F, Kramer T, Gu J, Anumala UR, Marinelli L, La Pietra V, et al. Identification of glycogen synthase kinase-3 inhibitors with a selective sting for glycogen synthase kinase-3α. J Med Chem. 10 de mayo de 2012;55(9):4407-24.

382. Lo Monte F, Kramer T, Gu J, Brodrecht M, Pilakowski J, Fuertes A, et al. Structure-based optimization of oxadiazole-based GSK-3 inhibitors. Eur J Med Chem. marzo de 2013;61:26-40.

383. Forlenza OV, Diniz BS, Radanovic M, Santos FS, Talib LL, Gattaz WF. Disease-modifying properties of long-term lithium treatment for amnestic mild

cognitive impairment: randomised controlled trial. Br J Psychiatry. mayo de 2011;198(5):351-6.

384. Hampel H, Ewers M, Bürger K, Annas P, Mörtberg A, Bogstedt A, et al. Lithium trial in Alzheimer's disease: a randomized, single-blind, placebo-controlled, multicenter 10-week study. J Clin Psychiatry. junio de 2009;70(6):922-31.

VIII. ABREVIATIONS

ABBREVIATIONS

80+	80 years old and older
90+	90 years old and older
AAV2/1	recombinant adeno-associated virus 2/1
Aβ	β-amyloid peptides
Aβ40	40 amino acid form of β-amyloid peptides
Aβ42	42 amino acid form of β-amyloid peptides
AD	Alzheimer's disease
ADL	Activities of daily living
AICD	Amyloid precursor protein intracellular domain
ANOVA	Analysis of variance
APOE	A*polipoprotein E*
APP	Amyloid precursor protein
αCTF	α-C-Terminal fragment
βCTF	β-C-Terminal fragment
CA1	Region 1 of the cornus ammonis of hippocampus
CAMKIIα	Calcium/calmodulin-dependent protein kinase IIα
CDK-5	cyclin-dependent kinase 5
CIND	Cognitive impairment but no dementia
CKO	Conditional knockout
CNS	Central nervous system
CRE	Causes recombination protein
CRE-ERT2	Cre protein fused to a triple mutant form of the human estrogen receptor
CVD	Cerebrovascular disease
DNA	Deoxyribonucleic acid
ELISA	Enzyme-linked immunosorbent assay
GAPDH	Glyceraldehydes 3-phosphate dehydrogenase
GSK-3	Glycogen synthase kinase 3
GSK-3α	Glycogen synthase kinase 3 isoform α
GSK-3β	Glycogen synthase kinase 3 isoform β
GSK-3β_2	Splicing variant of glycogen synthase kinase 3 isoform β
HS	Hippocampal sclerosis
KD	Knockdown
KO	Knockout
loxP	locus of cross over in P1
mAb	monoclonal antibody
MAPT	Microtubule-associated protein tau gene
MCI	Mild cognitive impairment
MMSE	Mini-Mental State Examination
MT	Microtubule
NFT	Neurofibrillary tangles
NMDA	*N*-methyl-D-aspartate

PDAPP	APP minigene harboring the V717F mutation, driven by the platelet-derived growth factor promoter
PHF	paired helical filament
p-S21-GSK-3α	Glycogen synthase kinase3 isoform α phophorylated at serine 21
p-S9-GSK-3β	Glycogen synthase kinase3 isoform β phosphorylated at serine 9
p-Y279-GSK-3α	Glycogen synthase kinase3 isoform α phosphorylated at serine 279
p-Y216-GSK-3β	Glycogen synthase kinase3 isoform β phosphorylated at serine 216
PSEN1	Presenilin-1
PSEN2	Presenilin-2
rAAV2/1	Recombinant adeno-associated virus 2/1
RIPA	Radioimmunoprecipitation assay buffer
RIRs	Relative immunointensity ratios
shRNA	Short/small hairpin ribonucleic acid
shRNA-α	shRNA construct that specifically reduces GSK-3α expression
shRNA-β	shRNA construct that specifically reduces GSK-3α expression
SNAP	soluble N-ethylmaleimide sensitive factor attachement protein
SNARE	soluble N-ethylmaleimide sensitive factor attachement receptor
SP	Senile plaques
SV2	synaptic vesicle glycoprotein 2
SV2A	synaptic vesicle glycoprotein 2 isoform A
TDP-43	43-kDa transactive response sequence DNA-binding protein
UBC	Human Ubiquitin C promoter
VGLUT	vesicular glutamate transporter
VGLUT1	vesicular glutamate transporter isoform 1
WB	western blot
WT	wild type

IX. ACKNOWLEDGEMENTS

ACKNOWLEDGEMENTS / AGRADECIMIENTOS

I am very grateful to Virginia Lee and John Trojanowski for giving me the opportunity to join their lab, for their guidance and all the support they gave me, for their inspiring passion for science, and for creating such a wonderful and enriching environment that made me grow more than I anticipated.

Special thanks to David for sharing the GSK-3 project with me and for all the techniques he taught me. Thanks to JR for making the 90+ paper possible despite the distance. Thanks to Awo, Caryn and Kevin for their hard work and technical support. Thanks to Jenna Carroll for sharing her expertise in behavior and for all her edits on the original paper of GSK-3. Thanks to Maria M.Corrada for her statistical analysis and all the edits into the original paper of The 90+ Study, and to Claudia H. Kawas for letting me work with this amazing cohort of The 90+ Study. Thanks to all the students that helped us: Amanda, Brigid, Erin, Stylianos and Nick, it was very refreshing and motivating having them around. Thanks to all the CNDR members: Sue, Terry, Linda, Jen, Dawn, Rob, Amy, Cindy, Kevin, Michiyo, Dave, Scott, Lionel, Paola, Anna, Bin, Vicky, Kelvin, Laura V, Hide, Jing, Selsuk, Johannes, Alex, Kurt, Hiro, Felix, Chi, Jin, Nuria, Charlotte, Adam, Susana and Jon for helping me through all these years, I have learnt so much from all of them. Gracias a “Juno” por su inteligencia emocional y guía. Mi más profundo agradecimiento a María, mi “coach” y editora personal, por ser mi puente y embajadora en Filadelfia, y por todas las cosas positivas que me ha aportado personal y profesionalmente en la última década. Y a mi querida Aitziber, compañera de residencia, tesis, aventuras y desventuras, por pensar “out of the box”, por su coraje y por estar siempre cerca a pesar de la distancia.

Quisiera agradecer a Teresa Gómez Isla y Rafael Blesa por crear la Unidad de Memoria del Hospital de Sant Pau, darme la oportunidad de formarme clínicamente y de iniciarme en la investigación básica. Agradecer a Alberto Lleó y Jordi Clarimón por todo lo que me han enseñado, por su guía y continuo apoyo que tanto ha significado para mí. Gracias a mis primeros “básicos” Cristina, Jose, y Lidia por todo

lo que pacientemente me enseñaron, y especialmente a Cristina por sacar el tiempo de donde no hay y revisar esta tesis. Gracias a la parte clínica de la unidad de memoria Isabel, Estela, Gemma y Belén, por su ayuda y lo mucho que aprendí de ellas. Quisiera agradecer a Toni Escartín todo su apoyo todos estos años y a Joan Martí por enseñarme a explorar, introducirme en el pensamiento crítico y en la investigación clínica. Gracias también al resto de “neuros” (Mercè, Dani, Lola, Roberto, Alex, Sergi, Marta, Jordi y Pago) por su apoyo y por compartir esta pasión por nuestra especialidad que ha hecho mi residencia tan estimulante.

Quiero agradecer al Instituto Carlos III y a la fundación Caja Madrid su apoyo económico durante la realización de esta tesis. Thanks to the Marian S. Ware Program for Drug Discovery and grants from the National Institutes of Health (AG11542, AG17586, T32-GM07229, T32-AG000255, AG10124, AG16573, AG21055, P50-AG16573, MH64045) for funding these projects.

Thanks to the participants of the 90+Study and their families for their generosity. Agradecer a mis pacientes y a sus familiares que a lo largo de los años han depositado su confianza en mí por ser mi principal fuente de motivación.

Y para acabar, quiero agradecer a mi familia su apoyo y por hacerme sentir tan querida y afortunada. Nada de esto tendría sentido sin vosotros.

X. APPENDIX

Appendix 1. “Perforant path synaptic loss correlates with cognitive impairment and Alzheimer´s disease in the oldest-old. Robinson JL, Molina-Porcel L, Corrada MM, Raible K, Lee EB, Lee VM, Kawas CH, Trojanowski JQ. Brain. 2014 Sep;137(Pt 9):2578-87.

doi:10.1093/brain/awu190 Brain 2014: 137; 2578–2587 | 2578

BRAIN
A JOURNAL OF NEUROLOGY

Perforant path synaptic loss correlates with cognitive impairment and Alzheimer's disease in the oldest-old

John L. Robinson,[1] Laura Molina-Porcel,[1] Maria M. Corrada,[2] Kevin Raible,[1] Edward B. Lee,[1] Virginia M.-Y. Lee,[1] Claudia H. Kawas[3] and John Q. Trojanowski[1]

1 Centre for Neurodegenerative Disease Research, Institute on Aging and Department of Pathology and Laboratory Medicine, University of Pennsylvania, Philadelphia, PA, USA
2 Department of Neurology, and Institute for Memory Impairments and Neurological Disorders, University of California at Irvine, Irvine, CA, USA
3 Department of Neurology, Department of Neurobiology and Behaviour, and Institute for Memory Impairments and Neurological Disorders, University of California at Irvine, Irvine, CA, USA

Correspondence to: John Q. Trojanowski, M.D., Ph.D.,
Centre for Neurodegenerative Disease Research and Institute on Aging,
Department of Pathology and Laboratory Medicine,
University of Pennsylvania School of Medicine, HUP,
Maloney 3rd Floor, 36th and Spruce Streets, Philadelphia,
PA 19104-4283, USA
E-mail: trojanow@mail.med.upenn.edu

Alzheimer's disease, which is defined pathologically by abundant amyloid plaques and neurofibrillary tangles concurrent with synaptic and neuronal loss, is the most common underlying cause of dementia in the elderly. Among the oldest-old, those aged 90 and older, other ageing-related brain pathologies are prevalent in addition to Alzheimer's disease, including cerebrovascular disease and hippocampal sclerosis. Although definite Alzheimer's disease pathology can distinguish dementia from normal individuals, the pathologies underlying cognitive impairment, especially in the oldest-old, remain poorly understood. We therefore conducted studies to determine the relative contributions of Alzheimer's disease pathology, cerebrovascular disease, hippocampal sclerosis and the altered expression of three synaptic proteins to cognitive status and global cognitive function. Relative immunohistochemistry intensity measures were obtained for synaptophysin, Synaptic vesicle transporter Sv2 (now known as SV2A) and Vesicular glutamate transporter 1 in the outer molecular layer of the hippocampal dentate gyrus on the first 157 participants of 'The 90+ Study' who came to autopsy, including participants with dementia ($n = 84$), those with cognitive impairment but no dementia ($n = 37$) and those with normal cognition ($n = 36$). Thal phase, Braak stage, cerebrovascular disease, hippocampal sclerosis and Pathological 43-kDa transactive response sequence DNA-binding protein (TDP-43) were also analysed. All measures were obtained blind to cognitive diagnosis. Global cognition was tested by the Mini-Mental State Examinaton. Logistic regression analysis explored the association between the pathological measures and the odds of being in the different cognitive groups whereas multiple regression analyses explored the association between pathological measures and global cognition scores. No measure clearly distinguished the control and cognitive impairment groups. Comparing the cognitive impairment and dementia groups, synaptophysin and SV2 were reduced, whereas Braak stage, TDP-43 and hippocampal sclerosis frequency increased. Thal phase and VGLUT1 did not distinguish the cognitive impairment and dementia groups. All measures distinguished the dementia and control groups and all markers associated with the cognitive test scores. When all markers were analysed simultaneously, a reduction in synaptophysin, a high Braak stage and the presence of TDP-43 and hippocampal sclerosis associated with global cognitive function. These findings suggest that tangle pathology, hippocampal sclerosis, TDP-43 and perforant pathway synaptic loss are the major contributors to dementia in the oldest-old. Although an increase in plaque pathology and glutamatergic synaptic loss may be early events associated

Received March 12, 2014. Revised May 27, 2014. Accepted June 2, 2014. Advance Access publication July 9, 2014

with cognitive impairment, we conclude that those with cognitive impairment, but no dementia, are indistinguishable from cognitively normal subjects based on the measures reported here.

Keywords: Alzheimer's disease; Braak stage; Thal phase; synaptic loss; oldest-old; cognitive impairment

Abbreviations: CIND = cognitively impaired no dementia; MMSE = Mini-Mental State Examination; RIR = relative immunointensity ratio

Introduction

Along with tangles and plaques, Alzheimer's disease is characterized by the loss of neurons and their synapses. Indeed, significant synapse loss has been documented in all brain regions affected by Alzheimer's disease pathology (DeKosky *et al*., 1996) and reductions in the number of presynaptic and synaptic proteins may be the most consistent progression marker of Alzheimer's disease as the burden of plaques and tangles grows and neurons continue to degenerate (Beeri *et al*., 2012). For example, significant reductions in synaptophysin and VGLUT1 were found in both the parietal and occipital cortices of Alzheimer's disease brains in one study (Kirvell *et al*., 2006) and our group previously reported a decrease in synaptophysin in the frontal cortex of dementia patients (Head *et al*., 2009). Nonetheless, the relationship between anatomy, synaptic proteins and Alzheimer's disease pathology is complex (Honer, 2003). In our previous study, individuals with cognitive impairment, but no dementia (CIND) had increases in synaptophysin whereas others have reported a significant decrease in the hippocampal levels of synaptophysin, even in CIND individuals (Sze *et al*., 2000).

Because it has long been known that changes in the perforant pathway are associated with memory impairment (Hyman *et al*., 1986; Senut *et al*., 1991), we hypothesized that perforant pathway synaptic changes may be one of the major correlates of cognitive impairment in Alzheimer's disease. The perforant pathway arises from neurons in layers 2 and 3 of the entorhinal cortex and projects into the outer molecular layer of the hippocampal dentate gyrus. Importantly, neurons and synapses in the inner molecular layer remain unaffected by perforant pathway loss in the outer molecular layer. There are several markers of synaptic health that are reliably detected by immunohistochemistry in sections of CNS tissues including synaptophysin, SV2 and VGLUT1.

Synaptophysin is involved in multiple, important aspects of synaptic vesicle exo- and endocytosis (Valtorta *et al*., 2004). SV2, besides being a ubiquitous presynaptic protein, is the binding site for the antiepileptic drug levetiracetam, a drug shown to improve cognition in CIND individuals (Bakker *et al*., 2012). VGLUT1 mediates the accumulation of glutamate—the major excitatory neurotransmitter—into secretory vesicles in the neocortex and hippocampus (El Mestikawy *et al*., 2011).

Individuals in the 'The 90+ Study', a population-based cohort of nonagenarians, have a high prevalence of cognitive impairment (Peltz *et al*., 2012) allowing for the assessment at autopsy of a significant number of CIND individuals. This investigation is a cross-sectional clinical-pathological correlation study involving the first 157 individuals to come to autopsy. For our analysis, we compared measures of perforant pathway synaptic health across each cognitive group. Since the prevalence of severe Alzheimer's disease pathology is reduced in nonagenarians, whereas the proportion with hippocampal sclerosis and cerebrovascular disease pathology increases (Nelson *et al*., 2011*b*), we also measured the underlying pathologies affecting these individuals, specifically their Braak stage, Thal phase, and the presence of hippocampal sclerosis and cerebrovascular disease. Our aim was to understand both the synaptic and pathological changes underlying cognitive impairment and dementia.

Materials and methods

Study participants were the first 157 individuals to come to autopsy from the 90+ Study, a longitudinal population-based study of ageing and dementia in people aged 90 and older who are survivors of the Leisure World Cohort Study (Corrada *et al*., 2012). Briefly, individuals live at home as well as in institutions, and represent the full spectrum of health and cognitive abilities. All 90+ Study participants had evaluations every 6 months including a neurological examination by a trained physician or nurse practitioner and a full neuropsychological battery that included the Mini-Mental State Examination (MMSE). Relevant medical history, medication use, and demographic information were obtained from the participants or their informants. Medical records, including brain imaging evaluations were obtained from the participant's physicians. Information about cognitive (Clark and Ewbank, 1996) and functional abilities (Pfeffer *et al*., 1982) were obtained from informants in frequent contact with the participants. To inquire about the onset of cognitive problems, the Dementia Questionnaire (Silverman *et al*., 1986; Kawas *et al*., 1994) interview was conducted over the phone with informants of participants with evidence of cognitive impairment. Shortly after death, the Dementia Questionnaire was done with the decedent's informant to inquire about the participant's condition since the last evaluation. The Institutional Review Board of the University of California, Irvine, approved all procedures and all participants or their surrogates gave written informed consent.

Determination of cognitive status

After a participant's death, all available information was reviewed and discussed during a multidisciplinary consensus diagnostic conference led by 'The 90+ Study' principal investigator (C.K.). Participants were classified as normal, CIND, or as having dementia. Dementia diagnosis was established using Diagnostic and Statistical Manual of Mental Disorders 4th Edition criteria (American Psychiatric Association *et al*., 1994). CIND is defined by initial cognitive impairments such as deficits in episodic memory (Albert *et al*., 2001), executive dysfunction (Chen *et al*., 2001), naming difficulties or other aphasias (Saxton *et al*., 2004). Participants were classified as CIND if they showed cognitive or functional deficits that were not severe enough to meet criteria for dementia. All cognitive diagnoses were made blinded to pathological evaluations.

Neuropathology

All autopsies were performed at the University of California, Irvine. After weighing the whole brain and gross inspection, one hemisphere was dissected as previously described (Berlau *et al*., 2009). Six-micrometre thick, coronal sections of mid-frontal cortex superior temporal cortex, anterior hippocampus, amygdala, substantia nigra and medulla oblongata were cut. All histological staining, immunohistochemistry and microscopic analyses were performed in the Centre for Neurodegenerative Disease Research (CNDR) at the University of Pennsylvania as described (Robinson *et al*., 2011). Briefly, sections were subjected to immunohistochemistry using the avidin-biotin complex detection method (VECTASTAIN® ABC kit; Vector Laboratories) with ImmPACT™ diaminobenzidine peroxidase substrate (Vector Laboratories) as the chromogen using monoclonal antibodies to phosphorylated tau (mouse PHF1; 1:1K, gift of Dr Peter Davies, Manhasset, NY), β-amyloid (mouse NAB228; 1:15K; generated in CNDR), TARDBP (rat 409/410; 1:500; gift of Dr Manuela Neumann, Zurich, Switzerland), SV2 (mouse SV2; 1:20K; DSH Iowa), synaptophysin (mouse MAB368; 1:1K; Millipore) and VGLUT1 (Guinea pig VGLUT1; 1:7.5K; SYSY).

Topographical Braak staging (stages I–VI) was assigned from PHF1 stained slides ($n = 157$) (Braak *et al*., 2006). Thal phases were determined from NAB228 stained hippocampal slides: phase 0–1, 2, 3 and 4 ($n = 150$) (Thal *et al*., 2006). TARDBP inclusions and neurites were determined from 409/410 stained hippocampal slides: presence/absence.

The assessment of cerebrovascular disease pathology ($n = 108$) and hippocampal sclerosis ($n = 155$) was determined from Harris haematoxylin and eosin stained mid-frontal cortex, superior temporal cortex, hippocampus, amygdala, substantia nigra and medulla sections. Hippocampal sclerosis was assessed as follows: 0 for no gliosis or neuronal loss; 1+ for mild gliosis or neuronal loss in the CA1 or subiculum; 2+ for moderate or severe gliosis and neuronal loss consistent with definite hippocampal sclerosis. Cerebrovascular lesions such as infarcts, micro-infarcts or micro-bleeds along with cerebral amyloid angiopathy and hippocampal sclerosis were used to generate cerebrovascular disease pathology scores following a simplified staging of Jellinger and Attems as follows: 0 for cases without major infarcts, hippocampal sclerosis, cerebral amyloid angiopathy or other lesions; 1+ for minimal vascular pathology cases with mild to moderate cerebral amyloid angiopathy and/or 1–2 small lacunes; 2+ for moderate vascular pathology cases with severe cerebral amyloid angiopathy and/or hippocampal sclerosis and/or major infarcts (Jellinger and Attems, 2003).

Synaptic relative immunointensity ratios (RIRs) were obtained by the following process. A preliminary study of synaptic and presynaptic proteins was done including antibodies to synaptophysin, SV2, VGLUT1, synataxin 1, VAMP2, synapsin 1, synaptotagmin 1, dynamin, VGAT, PSD95 and GLUR1; obvious outer molecular layer synaptic loss was observed on slides obtained from patients with Alzheimer's disease when stained with antibodies to synaptophysin, SV2 and VGLUT1. For this study, hippocampal slides were stained for synaptophysin ($n = 149$), SV2 ($n = 151$) or VGLUT1 ($n = 152$). Sections were scanned (Nikon DS-Fi2 camera, gain 1.2, exposure 15 ms) at $\times 10$ on a Nikon Eclipse TE2000 microscope using NIS Elements software (Nikon Instruments, Inc.). ImageJ 1.47t (National Institutes of Health) was used for analysis. Mean pixel intensities of the inner- and outer molecular layer of the dentate gyrus just under CA1 were captured (Fig. 1). Raw values on an 8-bit scale (range of 45–185) were normalized to a blank area for each slide (median value 41). Synaptic RIRs of the outer/inner molecular layer were calculated from (outer molecular layer − blank) / (inner molecular layer − blank) for each case. To verify the repeatability of our measurements, 10 random cases were stained twice by the synaptic antibodies and synaptic RIRs were obtained independently by two researchers (L.M.P., J.L.R.). A K of 0.987 was obtained (Type C intraclass correlation coefficient).

All pathological diagnoses were done blinded to clinical diagnosis.

Statistical analysis

We compared characteristics of the three cognitive groups: normal, CIND and dementia using χ^2 tests for categorical variables and ANOVA for continuous variables. We used multinomial logistic regression models to determine the association between each individual neuropathological or synaptic protein measure and cognitive diagnosis. We report the odds of being in the CIND group compared to the normal group, the odds of being in the dementia group compared to the CIND group, and the odds of being in the dementia group compared to the normal group. Neuropathological and synaptic protein measures were analysed as continuous variables in the logistic regression analyses. Separate regression models were used for each neuropathological and synaptic protein measure. We also explored the association between the individual neuropathological or synaptic measures and the MMSE, a measure of global cognition, using multiple linear regression analyses. Finally, we analysed the relative contribution of the different pathological measures to global cognitive scores, by including all synaptic and pathological measures in a multiple regression model. All regression models were adjusted for age at death and gender and all analyses were performed using SAS version 9.3 (SAS Institute Inc.).

Results

Subject characteristics

Of the 157 participants of this study, 36 had normal cognition, 37 were diagnosed with CIND and the majority ($n = 84$) had dementia (Table 1). The most frequent clinical diagnosis of the participants with dementia was Alzheimer's disease alone (65%) or in combination with other dementias (21%) followed by vascular dementia (7%) and dementia with Lewy bodies (6%).

Participants had an average age at death of 98 years (range: 94–101 years), were mostly female (71%), and highly educated (71% had at least a college education). MMSE scores were available for the majority of individuals within 1 year before death (Table 1). The overall frequency of the *APOE* alleles were 14% for the e2 allele and 22% for the e4 allele. While there was an increase in the frequency of the e4 allele in the dementia group (27%) compared to the normal group (21%), this non-significant increase is consistent with previous work where we found that the e4 allele no longer plays a role in dementia and mortality at very old ages (Corrada *et al*., 2013). Brain weight was non-significantly lower in the dementia group.

Alzheimer's disease pathology

In the normal group, Braak stage (median III; mean 3.3) and Thal phase (median 1; mean 1.9) scores indicate that Alzheimer's disease pathology was present in at least mild to moderate amounts (Fig. 2D and E). The CIND group presented with similar Braak

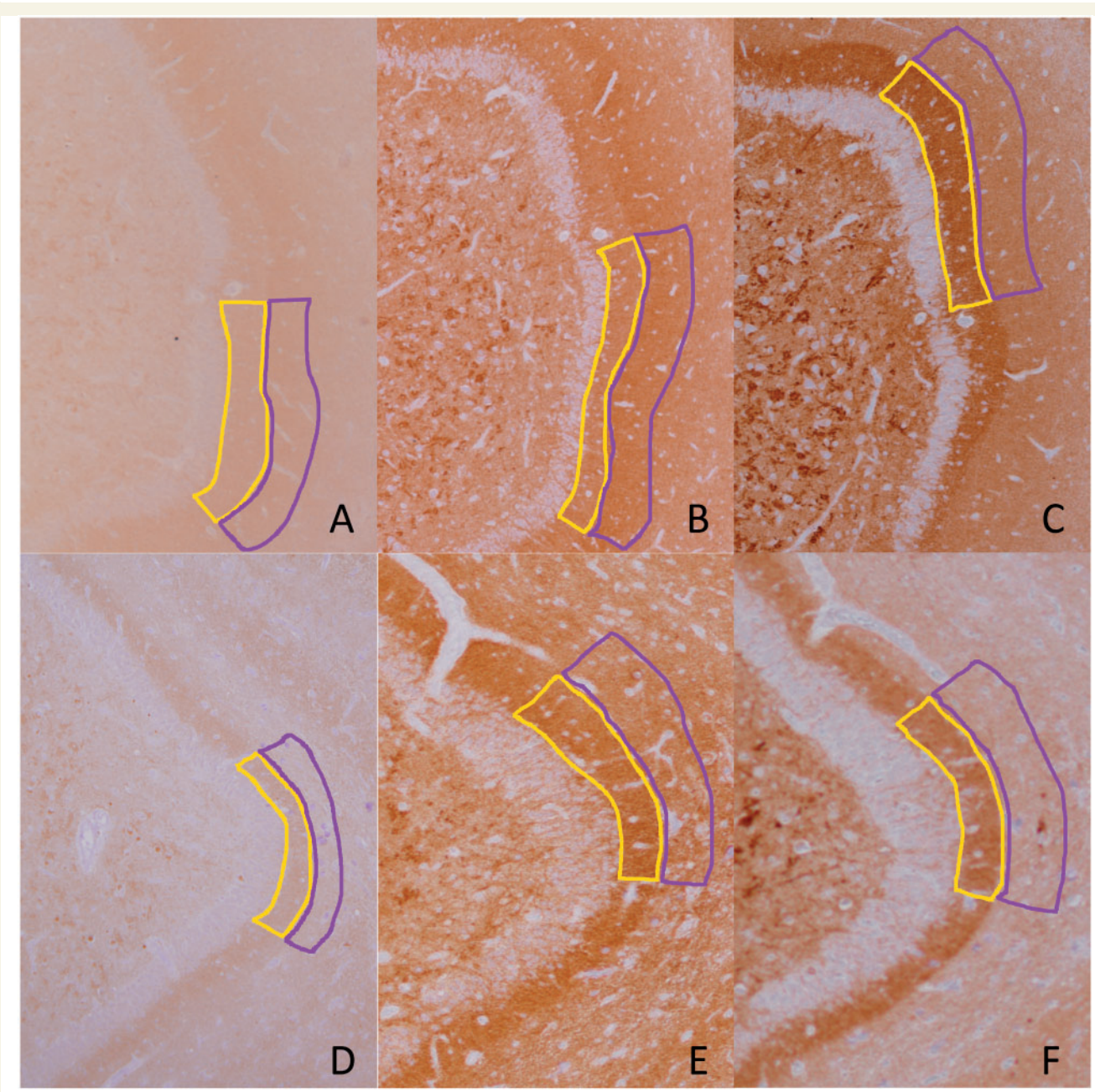

Figure 1 Representative images of synaptic protein immunoreactivity. Synaptic marker immunohistochemistry from two cases shows distinct staining of the inner molecular layer (highlighted in yellow) and the outer molecular (highlighted in purple) of the hippocampus. (**A–C**) The relatively healthy outer molecular layer: (**A**) synaptophysin, (**B**) SV2 and (**C**) VGLUT1 with synaptic ratios 1.19, 1.13 and 0.78, respectively (note that VGLUT1 is consistently lower than the other two). In contrast, (**D–F**) represents an individual with severely reduced outer molecular layer, whose inner molecular layer is preserved: (**D**) synaptophysin, (**E**) SV2 and (**F**) VGLUT1 with synaptic ratios 0.53, 0.74 and 0.56, respectively.

stage (median III; mean 3.4) and Thal phase (median 3; mean 2.3) scores, while Braak stage (median V; mean 4.3) and Thal phase (median 3; mean 2.6) were more moderate to severe in the dementia group. Higher Braak stages were significantly associated with higher odds of being in the dementia versus normal group [odds ratio (OR) = 1.68, $P = 0.001$] and of being in the dementia versus CIND group (OR = 1.52, $P = 0.02$) (Table 2). Higher Thal phases were associated with higher odds of being in the dementia versus the normal group (OR = 1.64, $P = 0.011$) but did not distinguish between the dementia and CIND groups ($P > 0.15$). Neither Alzheimer's disease marker distinguished between the normal and CIND groups.

Higher levels of Alzheimer's disease plaque and tangle burdens were significantly associated with lower MMSE scores (Thal phase,

Table 1 Characteristics of The 90+ Study participants

Characteristic	All subjects (*n* = 157)	Normal (*n* = 36)	CIND (*n* = 37)	Dementia (*n* = 84)
	Mean (SD)			
Age at death	98.0 (3.6)	97.8 (2.5)	98.4 (4.0)	97.7 (3.7)
Last MMSE score[a]	18.1 (10.1)	27.8 (1.6)	23.7 (5.4)	11.2 (8.6)
MMSE interval to death (months)	7.5 (7.7)	5.9 (3.3)	6.5 (4.5)	8.6 (9.8)
Brain weight (g)	1127 (121)	1179 (104)	1123 (125)	1104 (121)
	n (%)			
APOE E4[b]				
0 alleles	119 (78)	27 (79)	33 (89)	59 (73)
⩾ 1 alleles	33 (22)	7 (21)	4 (11)	22 (27)
APOE E2				
0 alleles	131 (86)	29 (85)	31 (84)	71 (88)
⩾ 1 alleles	21 (14)	5 (15)	6 (16)	10 (12)
Gender				
Male	45 (29)	15 (42)	10 (27)	20 (24)
Female	112 (71)	21 (58)	27 (73)	64 (76)
Education[c]				
⩽ High school	45 (29)	7 (19)	8 (22)	30 (36)
Any college	73 (47)	16 (44)	20 (54)	37 (45)
Any graduate school	38 (24)	13 (36)	9 (24)	16 (19)
Normal cognition	36 (23)	36 (100)		
CIND	37 (24)			
Memory impairment			13 (35)	
Executive impairment			12 (32)	
Other impairment[d]			12 (32)	
Dementia	84 (54)			
Alzheimer's disease only				55 (65)
Alzheimer's disease plus[e]				18 (21)
Vascular dementia				6 (7)
Other dementia				5 (6)

[a]Excludes four participants with missing MMSE score.
[b]Excludes five participants with unknown ApoE allele status.
[c]Excludes one participant with unknown degree of education.
[d]Includes impairment in domains other than memory or executive function.
[e]Includes mixed Alzheimer's disease/vascular dementia, Alzheimer's disease/other and Alzheimer's disease with dementia with Lewy bodies.

$P = 0.02$; Braak stage, $P < 0.001$). The greatest decreases on the cognitive tests occurred with the highest plaque and tangle burdens. The mean MMSE score was significantly lower in Thal phase 4 compared to Thal phases 2 and earlier ($P < 0.01$) and even to Thal phase 3 ($P < 0.05$). For Braak stage, the mean MMSE score was significantly lower in stage VI compared to all the other Braak stages ($P < 0.001$), and in stage V compared to stages III and IV ($P < 0.05$).

Hippocampal sclerosis and cerebrovascular disease

As the prevalence of hippocampal sclerosis and cerebrovascular disease pathology increases with age, we investigated what proportion of individuals had these lesions in our cohort. Hippocampal sclerosis was found in 15% of all individuals, but in only one individual without dementia. The presence of hippocampal sclerosis in 28% of those with dementia (23/82) allowed the measure to significantly distinguish the dementia group from both the normal ($P = 0.003$) and CIND ($P = 0.002$) groups (Table 2).

Cerebrovascular lesions and cerebral amyloid angiopathy were present in modest amounts in The 90+ Study. Cerebral amyloid angiopathy was found in 52% (56/108) of the cases whereas cerebrovascular disease lesions such as infarcts, micro-infarcts or micro-bleeds were rarer (10%; 11/108). Althogether, 63% of all individuals had some level of cerebrovascular disease pathology, including 45% of both the normal and CIND groups and 74% of the dementia group. Although the prevalence of cerebrovascular disease was not different between the normal and CIND groups (Fig. 2F), people with higher levels were more likely to be in the dementia group compared to both the normal and CIND groups (both $P = 0.009$) (Table 2).

TDP-43

TDP-43 is a common co-morbidity and may associate with a more rapid cognitive decline in the ageing brain (Wilson *et al.*, 2013). In

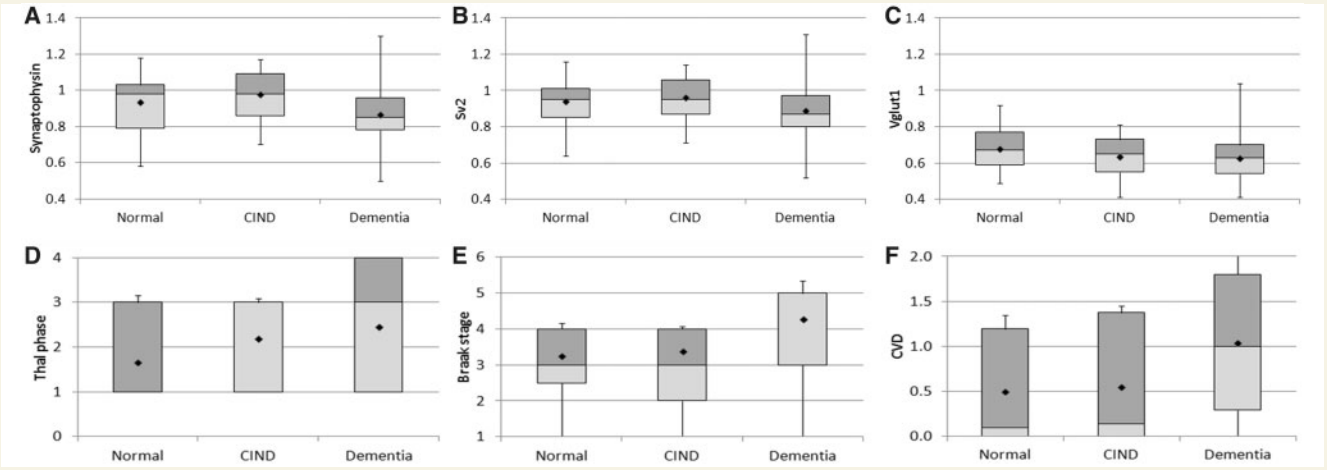

Figure 2 Synaptic intensity and neuropathology measures by cognitive group. Synaptic ratios (**A–C**) and neuropathology measures (**D–F**) in the oldest-old. All three synaptic RIRs were reduced in dementia compared to normal with (**A**) synaptophysin and (**B**) SV2 and significantly different between the three cognitive groups, however, (**C**) VGLUT1 did not distinguish between CIND and dementia. No synaptic RIR distinguished normal from CIND. (**D**) Thal phase and scores were all increased in dementia compared to normal with (**D**) similar Thal phases reported for CIND and dementia, whereas (**E**) Braak stage and (**F**) cerebrovascular disease (CVD) pathologies, including hippocampal sclerosis, were significantly different between the three cognitive groups. Each measure is graphed with the first and third quartiles boxed with the median band dividing the box into darker upper and lighter lower ranges; a whisker line extends to the minimums and maximums; shaded diamonds represent the means.

Table 2 Association between markers and cognitive groups

Measure	Wald test *P*-value	CIND versus Normal OR (95% CI) *P*-value	Dementia versus CIND OR (95% CI) *P*-value	Dementia versus Normal OR (95% CI) *P*-value
Synaptophysin	0.002	5.59 (0.20–159.45) 0.314	0.01 (<0.01–0.11) **0.001**	0.03 (<0.01–0.59) **0.021**
SV2	0.017	2.85 (0.10–84.75) 0.546	0.02 (<0.01–0.35) **0.008**	0.05 (<0.01–0.93) **0.045**
VGLUT1	0.099	0.04 (<0.01–2.41) 0.124	0.56 (0.02–18.84) 0.747	0.02 (<0.01–0.76) **0.034**
Braak stage	0.001	1.06 (0.75–1.50) 0.740	1.52 (1.07–2.16) **0.020**	1.68 (1.24–2.30) **0.001**
Thal phase	0.037	1.37 (0.89–2.11) 0.158	1.20 (0.84–1.71) 0.318	1.64 (1.12–2.38) **0.011**
Hippocampal sclerosis	<0.001	0.94 (0.36–2.49) 0.906	3.32 (1.56–7.05) **0.002**	3.13 (1.48–6.64) **0.003**
Cerebrovascular disease	0.004	0.94 (0.35–2.55) 0.900	2.99 (1.31–6.83) **0.009**	2.81 (1.29–6.13) **0.009**
TDP-43	0.008	0.90 (0.20–4.05) 0.893	4.32 (1.34–13.95) **0.014**	3.89 (1.23–12.36) **0.021**

Odds ratios and 95% CIs were generated from multinomial logistic regression models where the dependent (outcome) variable was cognitive group (normal, CIND, or dementia) and the independent variables were the neuropathological markers as continuous variables, except TARDBP which was a binary variable. *P*-values <0.05 are in bold. Age at death and gender were included as covariates and each neuropathological measure was analysed in a separate model. The overall *P*-value corresponds to the type 3 analyses and tests whether the neuropathological marker (independent variable) is significantly associated with the cognitive group (outcome variable). Odds ratios are per unit. *n* for each group = 149 (synaptophysin), 151 (SV2), 152 (VGLUT1), 157 (Braak stage), 150 (Thal phase), 155 (hippocampal sclerosis, 108 (cerebrovascular disease) and 146 (TARDBP).

our cohort, TDP-43 pathology was present in the hippocampus of 24% (35/146) of the cases. While a small number of both normal (11%, 4/35) and CIND (12%, 4/33) individuals had pathology, TARDBP inclusions affected a more substantial portion of the dementia group (35%, 27/78). As in our earlier study (Robinson *et al*., 2011), TARDBP was almost exclusively in individuals with hippocampal sclerosis. 77% (17/22) of the cases with hippocampal sclerosis also had TARDBP inclusions. While 15% (18/124) of

individuals without hippocampal sclerosis also had TARDBP pathology, the numbers were too low to analyse the significance of the TARDBP pathology after controlling for hippocampal sclerosis (data not shown).

Synaptic health

As described above, to measure the synaptic levels of the perforant pathway, synaptic RIRs were generated by measuring the intensity of synaptophysin, SV2, and VGLUT1 by immunohistochemistry in the outer molecular layer of the hippocampus relative to the inner molecular layer (Fig. 1). Higher RIRs represent a relatively healthy outer layer in relation to the inner layer, whereas lower RIRs correspond to synaptic loss in the outer layer (Fig, 2A–C). In the normal group, synaptophysin (mean 0.94) and SV2 (mean 0.94) had RIRs close to 1.00, whereas the glutamate-specific VGLUT1 RIR was lower (mean 0.67). Similar values were obtained in the CIND group: synaptophysin (mean 0.98), SV2 (mean 0.96) and VGLUT1 (mean 0.64). In the dementia group, these values were mildly lower: synaptophysin (mean 0.87), SV2 (mean 0.89) and VGLUT1 (mean 0.63).

All three synaptic RIRs distinguished between the dementia and normal groups with higher RIRs associated with lower odds of being in the dementia group ($P < 0.05$) (Table 2). The synaptophysin and SV2 RIRs also distinguished between the dementia and CIND groups (synaptophysin, $P < 0.001$; SV2, $P = 0.008$), whereas the VGLUT1 RIR did not ($P = 0.747$). No RIR distinguished between the CIND and normal groups (all $P > 0.12$). We also examined the association between synaptic RIRs and global cognitive scores and found that for all three synaptic markers, higher RIR values were significantly associated with higher MMSE scores (synaptophysin, $P < 0.001$; SV2, $P < 0.001$, VGLUT1, $P < 0.05$).

Multiple pathologies

Pearson correlation coefficients showed significant correlations between the three synaptic RIRs (VGLUT1 and SV2, corr = 0.37, $P < 0.001$; VGLUT1 and synaptophysin, corr = 0.45, $P < 0.001$; SV2 and synaptophysin, corr = 0.50, $P < 0.001$). Given the correlation between synaptic markers, we wanted to explore the independent contribution of each with respect to global cognitive scores. In a multiple regression model that included all three synaptic markers, we found that higher RIRs for both synaptophysin (beta = 20.3, $P = 0.002$) and SV2 (beta = 13.4, $P = 0.03$) remained significantly associated with better MMSE scores.

Post hoc analysis revealed that the SV2 RIR was significantly lower at Braak stage VI ($P < 0.001$) and the VGLUT1 RIR was significantly lower in individuals with hippocampal sclerosis ($P = 0.024$). To estimate the independent contribution of all the different measures to global cognitive scores, we included all three synaptic RIRs, the Alzheimer's disease pathology scores, and hippocampal sclerosis in a multiple regression analysis. In this model, the synaptophysin ratio, Braak stage, TARDBP and hippocampal sclerosis all remained significantly associated with MMSE scores (*P*-values: < 0.05, 0.001, < 0.01 and 0.001, respectively).

Memory impairment only subjects

The primary impairment in 13 of the CIND individuals was memory (Table 1). As those with executive impairment may have dysfunction related more to a frontotemporal lobar degeneration rather than Alzheimer's disease and those with 'other' impairment cannot be well defined, it's possible that the 13 with memory impairment are more likely to be on the continuum between normal cognition and Alzheimer's disease. To test this hypothesis, we compared the RIRs and our pathological markers in the 'memory impairment only' CIND subjects to the normal and dementia subjects to see if our results had more significance. No new associations were found (data not shown), suggesting that the memory impairment subjects weren't more likely to lead to the intermediate level of Alzheimer's disease apparent in the dementia group than the other CIND individuals. Similar subgroup analysis with the executive impairment and 'other' impairment CIND individuals also did not reveal any new associations that the comparisons with the group as a whole hadn't already shown (data not shown).

Discussion

We hypothesized that perforant pathway synaptic loss may be one of the early correlates of cognitive impairment in The 90+ Study, but this was not the case. None of the measures distinguished the normal and CIND groups and almost all the measures distinguished the CIND and dementia groups from the cognitively normal individuals. This implies that synaptic loss is tightly linked to pathology associated with dementia in the oldest-old.

This is not the case in younger age groups where it is hypothesized that plaques and neurofibrillary tangles accumulate years, even decades, before cognitive impairment and where pathology accumulates progressively (Sperling *et al*., 2011). Perhaps nonagenarians represent individuals with significant cognitive reserve? Although their brains may be exposed to the same pathological insults during progressive cognitive impairment as younger cohorts, they are able to minimize any synaptic loss and accumulations of pathology. At the very least, our data are consistent with an acceleration of the pathological cascade implied by other studies.

In this autopsy study of a large cohort of CIND individuals, we sought to elucidate which pathologies among those examined here associate with normal ageing, which associate with dementia and which, if any, associate with cognitive impairment. We review all of our findings below.

First, cognitively normal nonagenarians in The 90+ Study have a median Braak stage of III and a Thal phase of 1 consistent with predictable, age-dependent deposition of Alzheimer's disease pathology (Braak *et al*., 2011). Of course, many pathologies besides Alzheimer's disease affect the ageing brain including other neurodegenerative diseases, cerebrovascular disease and hippocampal sclerosis among others. In this study, we did not examine the role of multiple neurodegenerative diseases, but we previously reported that α-synuclein and TARDBP pathology affect $<20\%$ of cognitively normal individuals in this age category and then

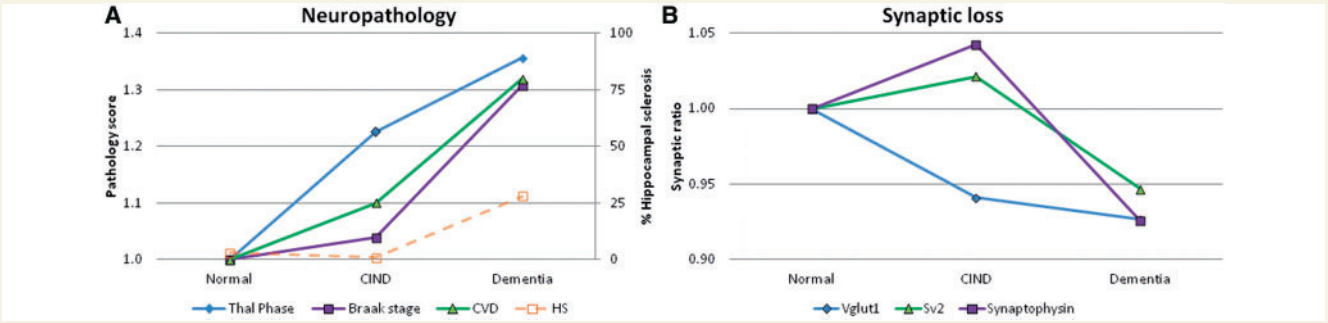

Figure 3 A model of changes associated with cognitive impairment and dementia in the oldest-old. Neuropathology and synaptic measures are associated with cognitive impairment in 'The 90+ Study'. (**A**) Mild to moderate Alzheimer's disease pathology already exists in the oldest-old for cognitively normal individuals and the Thal phase may increase with cognitive impairment. With dementia, all markers increase significantly, especially Braak stage, cerebrovascular disease (CVD) pathology and hippocampal sclerosis (HS). (**B**) Glutamatergic specific synaptic loss (VGLUT1) in the perforant pathology may occur during cognitive impairment, while significant synaptic loss occurs with dementia. All values are relative to the normal group's means normalized to 1.0 (see Fig. 1), except cerebrovascular disease which factors out the contribution of hippocampal sclerosis before normalizing; the hippocampal sclerosis percentages are graphed separately on the right axis.

primarily as co-morbidities (Robinson *et al*., 2011). Cerebrovascular disease, on the other hand, was common, affecting 45% of the group while hippocampal sclerosis was almost non-existent ($n = 1$).

Against this background level of multiple age-related pathologies in cognitively normal individuals, we can analyse the increases in Alzheimer's disease burden, cerebrovascular disease and hippocampal sclerosis associated with dementia (Fig. 3A). As 90+ individuals have a moderate burden of age-related tangles and plaques and a particularly high prevalence of dementia (Corrada *et al*., 2008), it is not surprising that Alzheimer's disease pathology is the most common underlying contributor to dementia in this group (Hebert *et al*., 2013). For individuals with dementia, the median Braak stage is V and the Thal phase of 3. Compared with the normal group, these are substantial increases consistent with an intermediate burden of Alzheimer's disease neuropathological change (Montine *et al*., 2012). Along with Alzheimer's disease, the prevalence of cerebrovascular disease—not including hippocampal sclerosis—increased to 74% of individuals in the dementia group. Additionally, dementia was associated with the appearance of hippocampal sclerosis in a substantial minority (28%). Similarly, and primarily comorbidly, TARDBP also affected a large minority (35%). Both the cerebrovascular disease and hippocampal sclerosis percentages are consistent with reported frequencies of these pathologies in this age-group (Giannakopoulos *et al*., 1997; Nelson *et al*., 2011*a*).

The changes in all three of the synaptic markers studied here are consistent with the interpretation that significant perforant pathway loss occurs with dementia in the 90+ subjects (Fig. 3B). This is consistent with our previous work involving 32 individuals in The 90+ Study where neocortical synaptophysin protein levels were significantly decreased with dementia (Head *et al*., 2009). In our multiple logistic regression analysis, both the synaptophysin RIR and Braak stage tightly associated with cognitive scores. Concurrently, *post hoc* analysis revealed that the SV2 RIR was significantly lower at Braak stage VI, raising the possibility that synaptic protein loss is tightly correlated with tau burden. This is supported by studies in tau transgenic mice (Yoshiyama *et al*., 2007) and in human cohorts where synaptic protein loss only occurs at the highest Braak stages (Mukaetova-Ladinska *et al*., 2000). On the other hand, as the synaptophysin RIR, Braak stage, hippocampal sclerosis and the TDP-43 pathology measures all remained significantly associated with MMSE scores in our multiple logistic regression analysis, perhaps something more than pathological Alzheimer's disease is taking place and that synaptic protein loss in the perforant pathway and hippocampal sclerosis are independent factors that contribute to dementia in the oldest-old.

If cognitively normal individuals have age-related tangles and plaques, and these pathologies increase along with synaptic loss in dementia, what changes occur during CIND? CIND in the oldest-old may be associated with a greater substantial distribution of plaques as measured by Thal phase (Fig. 3A). Cognitively normal nonagenarians at Thal phase 2 have plaque deposition that has spread into layers 2/3 of the entorhinal cortex (Thal *et al*., 2006), suggesting that plaques are already present in the perforant pathway. In the CIND group, the median Thal phase was 3 indicating a greater plaque burden affecting the perforant pathway. As there is no concurrent increase in the Braak stage (median III), this may signify that plaques are having an earlier effect than tangles, which is consistent with numerous biomarker studies that show amyloid-β becomes abnormal before tau in cognitively normal individuals (Aisen, 2010; Jack *et al*., 2013).

CIND may also be associated with a decrease in glutamatergic synapses in the perforant pathway as measured by the VGLUT1 RIR (Fig. 3B). Although the VGLUT1 RIR can clearly distinguish the normal and dementia groups ($P = 0.034$), this measure does not distinguish the CIND from the dementia groups ($P = 0.747$), whereas the synaptophysin ($P < 0.001$) and SV2 RIRs ($P = 0.008$) still do (Table 2). The most parsimonious explanation is that non-glutamatergic neurons remain relatively unaffected during CIND whereas glutamatergic neurons experience synaptic loss. If true,

this is consistent with previous work showing that observed presynaptic proteins, such as synaptophysin, remain constant or increase in earlier phases of illness before decreasing with dementia onset (Honer, 2003; Head *et al*., 2009). That the decrease in the VGLUT1 RIR is coincident with the increase in Thal phase may imply that plaques damage glutermatergic synapses. Of course, there are many possibilities including that the reduction in VGLUT1 may simply signify a loss of transporters, rather than the loss of glutamatergic afferents (Tannenberg *et al*., 2004).

Importantly, our study suggests that individuals with CIND are for the most part pathologically and synaptically indistinguishable from individuals with normal cognition. This being the case, pharmaceutical interventions that target tau and amyloid-β or protect synapses are all viable therapeutic strategies for a population at risk of dementia due to Alzheimer's disease. In addition, interventions designed to maintain a healthy synaptic system and a strict control of vascular risk factors may be good strategies to preserve cognitive function in nonagenarians and centenarians.

Acknowledgements

We wish to thank the assistance of Terry Schuck, Felix Geser and Laura Volpicelli-Daley.

Funding

This work was supported in part by grants from the National Institutes of Health (AG10124, AG16573, AG17586, AG21055, P50AG16573 and MH64045).

References

Aisen PS. Pre-dementia Alzheimer's trials: overview. J Nutr Health Aging 2010; 14: 294.

Albert MS, Moss MB, Tanzi R, Jones K. Preclinical prediction of AD using neuropsychological tests. J Int Neuropsychol Soc 2001; 7: 631–639.

American Psychiatric Association, American Psychiatric Association, and Task Force on DSM-IV. Diagnostic and statistical manual of mental disorders: DSM-IV. Washington, DC: American Psychiatric Association; 1994.

Bakker A, Krauss GL, Albert MS, Speck CL, Jones LR, Stark CE, et al. Reduction of hippocampal hyperactivity improves cognition in amnestic mild cognitive impairment. Neuron 2012; 74: 467–474.

Beeri MS, Haroutunian V, Schmeidler J, Sano M, Fam P, Kavanaugh A, et al. Synaptic protein deficits are associated with dementia irrespective of extreme old age. Neurobiol Aging 2012; 33: 1125.e1–8.

Berlau DJ, Corrada MM, Head E, Kawas CH. APOE epsilon2 is associated with intact cognition but increased Alzheimer pathology in the oldest old. Neurology 2009; 72: 829–834.

Braak H, Alafuzoff I, Arzberger T, Kretzschmar H, Del Tredici K. Staging of Alzheimer disease-associated neurofibrillary pathology using paraffin sections and immunocytochemistry. Acta Neuropathol 2006; 112: 389–404.

Braak H, Thal DR, Ghebremedhin E, Del Tredici K. Stages of the pathologic process in Alzheimer disease: age categories from 1 to 100 years. J Neuropathol Exp Neurol 2011; 70: 960–969.

Chen P, Ratcliff G, Belle SH, Cauley JA, DeKosky ST, Ganguli M. Patterns of cognitive decline in presymptomatic Alzheimer disease: a prospective community study. Arch Gen Psychiatry 2001; 58: 853–858.

Clark CM, Ewbank DC. Performance of the dementia severity rating scale: a caregiver questionnaire for rating severity in Alzheimer disease. Alzheimer Dis Assoc Disord 1996; 10: 31–39.

Corrada MM, Berlau DJ, Kawas CH. A population-based clinicopathological study in the oldest-old: the 90+ study. Curr Alzheimer Res 2012; 9: 709–717.

Corrada MM, Brookmeyer R, Berlau D, Paganini-Hill A, Kawas CH. Prevalence of dementia after age 90: results from the 90+ study. Neurology 2008; 71: 337–343.

Corrada MM, Paganini-Hill A, Berlau DJ, Kawas CH. Apolipoprotein E genotype, dementia, and mortality in the oldest old: the 90+ Study. Alzheimers Dement 2013; 9: 12–18.

DeKosky ST, Scheff SW, Styren SD. Structural correlates of cognition in dementia: quantification and assessment of synapse change. Neurodegener J Neurodegener Disord Neuroprotection Neuroregeneration 1996; 5: 417–421.

El Mestikawy S, Wallén-Mackenzie A, Fortin GM, Descarries L, Trudeau LE. From glutamate co-release to vesicular synergy: vesicular glutamate transporters. Nat Rev Neurosci 2011; 12: 204–216.

Giannakopoulos P, Hof PR, Michel JP, Guimon J, Bouras C. Cerebral cortex pathology in aging and Alzheimer's disease: a quantitative survey of large hospital-based geriatric and psychiatric cohorts. Brain Res Brain Res Rev 1997; 25: 217–245.

Head E, Corrada MM, Kahle-Wrobleski K, Kim RC, Sarsoza F, Goodus M, et al. Synaptic proteins, neuropathology and cognitive status in the oldest-old. Neurobiol Aging 2009; 30: 1125–1134.

Hebert LE, Weuve J, Scherr PA, Evans DA. Alzheimer disease in the United States (2010–2050) estimated using the 2010 census. Neurology 2013; 80: 1778–1783.

Honer WG. Pathology of presynaptic proteins in Alzheimer's disease: more than simple loss of terminals. Neurobiol Aging 2003; 24: 1047–1062.

Hyman BT, Van Hoesen GW, Kromer LJ, Damasio AR. Perforant pathway changes and the memory impairment of Alzheimer's disease. Ann Neurol 1986; 20: 472–481.

Jack CR Jr, Knopman DS, Jagust WJ, Petersen RC, Weiner MW, Aisen PS, et al. Tracking pathophysiological processes in Alzheimer's disease: an updated hypothetical model of dynamic biomarkers. Lancet Neurol 2013; 12: 207–216.

Jellinger KA, Attems J. Incidence of cerebrovascular lesions in Alzheimer's disease: a postmortem study. Acta Neuropathol 2003; 105: 14–17.

Kawas C, Segal J, Stewart WF, Corrada M, Thal LJ. A validation study of the Dementia Questionnaire. Arch Neurol 1994; 51: 901–906.

Kirvell SL, Esiri M, Francis PT. Down-regulation of vesicular glutamate transporters precedes cell loss and pathology in Alzheimer's disease. J Neurochem 2006; 98: 939–950.

Montine TJ, Phelps CH, Beach TG, Bigio EH, Cairns NJ, Dickson DW, et al. National Institute on Aging-Alzheimer's Association guidelines for the neuropathologic assessment of Alzheimer's disease: a practical approach. Acta Neuropathol 2012; 123: 1–11.

Mukaetova-Ladinska EB, Garcia-Siera F, Hurt J, Gertz HJ, Xuereb JH, Hills R, et al. Staging of cytoskeletal and beta-amyloid changes in human isocortex reveals biphasic synaptic protein response during progression of Alzheimer's disease. Am J Pathol 2000; 157: 623–636.

Nelson PT, Head E, Schmitt FA, Davis PR, Neltner JH, Jicha GA, et al. Alzheimer's disease is not "brain aging": neuropathological, genetic, and epidemiological human studies. Acta Neuropathol 2011a; 121: 571–587.

Nelson PT, Schmitt FA, Lin Y, Abner EL, Jicha GA, Patel E, et al. Hippocampal sclerosis in advanced age: clinical and pathological features. Brain J Neurol 2011b; 134: 1506–1518.

Peltz CB, Corrada MM, Berlau DJ, Kawas CH. Cognitive impairment in nondemented oldest-old: prevalence and relationship to cardiovascular risk factors. Alzheimers Dement 2012; 8: 87–94.

Pfeffer RI, Kurosaki TT, Harrah CH Jr, Chance JM, Filos S. Measurement of functional activities in older adults in the community. J Gerontol 1982; 37: 323–329.

Robinson JL, Geser F, Corrada MM, Berlau DJ, Arnold SE, Lee VMY, et al. Neocortical and hippocampal amyloid-β and tau measures associate with dementia in the oldest-old. Brain J Neurol 2011; 134: 3708–3715.

Saxton J, Lopez OL, Ratcliff G, Dulberg C, Fried LP, Carlson MC, et al. Preclinical Alzheimer disease: neuropsychological test performance 1.5 to 8 years prior to onset. Neurology 2004; 63: 2341–2347.

Senut MC, Roudier M, Davous P, Fallet-Bianco C, Lamour Y. Senile dementia of the Alzheimer type: is there a correlation between entorhinal cortex and dentate gyrus lesions? Acta Neuropathol 1991; 82: 306–315.

Silverman JM, Breitner JC, Mohs RC, Davis KL. Reliability of the family history method in genetic studies of Alzheimer's disease and related dementias. Am J Psychiatry 1986; 143: 1279–1282.

Sperling RA, Aisen PS, Beckett LA, Bennett DA, Craft S, Fagan AM, et al. Toward defining the preclinical stages of Alzheimer's disease: recommendations from the National Institute on Aging-Alzheimer's Association workgroups on diagnostic guidelines for Alzheimer's disease. Alzheimers Dement 2011; 7: 280–292.

Sze CI, Bi H, Kleinschmidt-DeMasters BK, Filley CM, Martin LJ. Selective regional loss of exocytotic presynaptic vesicle proteins in Alzheimer's disease brains. J. Neurol Sci 2000; 175: 81–90.

Tannenberg RK, Scott HL, Westphalen RI, Dodd PR. The identification and characterization of excitotoxic nerve-endings in Alzheimer disease. Curr Alzheimer Res 2004; 1: 11–25.

Thal DR, Capetillo-Zarate E, Del Tredici K, Braak H. The development of amyloid beta protein deposits in the aged brain. Sci. Aging Knowl Environ 2006; 2006: re1.

Valtorta F, Pennuto M, Bonanomi D, Benfenati F. Synaptophysin: leading actor or walk-on role in synaptic vesicle exocytosis? BioEssays News Rev Mol Cell Dev Biol 2004; 26: 445–453.

Wilson RS, Yu L, Trojanowski JQ, Chen EY, Boyle PA, Bennett DA, et al. TDP-43 Pathology, cognitive decline, and dementia in old age. JAMA Neurol 2013; 70: 1418–1424.

Yoshiyama Y, Higuchi M, Zhang B, Huang SM, Iwata N, Saido TC, et al. Synapse loss and microglial activation precede tangles in a P301S tauopathy mouse model. Neuron 2007; 53: 337–351.

Appendix 2 “Selectively silencing GSK-3 isoforms reduces plaques and tangles in mouse models of Alzheimer´s disease” Hurtado DE, Molina-Porcel L, Carroll JC, Macdonald C, Aboagye AK, Trojanowski JQ, Lee VM. J Neurosci. 2012 May 23;32(21):7392-402.

Behavioral/Systems/Cognitive

Selectively Silencing GSK-3 Isoforms Reduces Plaques and Tangles in Mouse Models of Alzheimer's Disease

David E. Hurtado,[1]* Laura Molina-Porcel,[1,2]* Jenna C. Carroll,[1] Caryn MacDonald,[1] Awo K. Aboagye,[1] John Q. Trojanowski,[1] and Virginia M.-Y. Lee[1]

[1]Center for Neurodegenerative Disease Research, Department of Pathology and Laboratory Medicine, and Institute on Aging, University of Pennsylvania School of Medicine, Philadelphia, Pennsylvania 19104-4283 and [2]Universitat Autònoma de Barcelona, Barcelona, Spain 08193

Glycogen synthase kinase-3 (GSK-3) is linked to the pathogenesis of Alzheimer's disease (AD), senile plaques (SPs), and neurofibrillary tangles (NFTs), but the specific contributions of each of the GSK-3 α and β isoforms to mechanisms of AD have not been clarified. In this study, we sought to elucidate the role of each GSK-3α and GSK-3β using novel viral and genetic approaches. First, we developed recombinant adeno-associated virus 2/1 short hairpin RNA constructs which specifically reduced expression and activity of GSK-3α or GSK-3β. These constructs were injected intraventricularly in newborn AD transgenic (tg) mouse models of SPs (PDAPP $^{+/-}$), both SPs and NFTs (PDAPP $^{+/-}$;PS19 $^{+/-}$), or wild-type controls. We found that knockdown (KD) of GSK-3α, but not GSK-3β, reduced SP formation in PDAPP $^{+/-}$ and PS19 $^{+/-}$;PDAPP $^{+/-}$ tg mice. Moreover, both GSK-3α and GSK-3β KD reduced tau phosphorylation and tau misfolding in PS19 $^{+/-}$;PDAPP $^{+/-}$ mice. Next, we generated triple tg mice using the CaMKIIα-Cre (α-calcium/calmodulin-dependent protein kinase II-Cre) system to KD *GSK-3*α in PDAPP $^{+/-}$ mice for further study of the effects of GSK-3α reduction on SP formation. GSK-3α KD showed a significant effect on reducing SPs and ameliorating memory deficits in PDAPP $^{+/-}$ mice. Together, the data from both approaches suggest that GSK-3α contributes to both SP and NFT pathogenesis while GSK-3β only modulates NFT formation, suggesting common but also different targets for both isoforms. These findings highlight the potential importance of GSK-3α as a possible therapeutic target for ameliorating behavioral impairments linked to AD SPs and NFTs.

Introduction

Alzheimer's disease (AD) is the most common form of dementia and presents clinically with progressive memory loss and cognitive impairments. AD is characterized pathologically by extracellular senile plaques (SPs), composed of amyloid-β (Aβ) peptides derived from the proteolysis of the amyloid precursor protein (APP), and by intracellular neurofibrillary tangles (NFTs), composed of hyperphosphorylated tau protein. Glycogen synthase kinase-3 (GSK-3) is a serine/threonine kinase that has been implicated in the formation of both SPs and NFTs (Jope and Johnson, 2004; Giese, 2009). For example, GSK-3 activation modulates Aβ production (Phiel et al., 2003; Ryder et al., 2003), while Aβ activates GSK-3 (Kim et al., 2003; Akiyama et al., 2005; Ryan and Pimplikar, 2005). Additionally, GSK-3 is a principal kinase that phosphorylates tau at key residues found in AD NFT (Hanger et al., 2009). Thus, GSK-3 modulates pathways related to SP and NFT formation and it has been suggested that GSK-3 reduction may represent an attractive therapeutic target for AD (Phiel et al., 2003; Ryder et al., 2003).

There are two mammalian GSK-3 isoforms, i.e., GSK-3α and GSK-3β, each of which is encoded by a separate gene. Both are highly conserved and widely expressed serine/threonine kinases that share a high degree of homology (Woodgett, 1990). Historically, the most widely used strategy to study the effects of GSK-3 reduction *in vivo* has been to use pharmacological GSK-3 inhibitors. When administered to various AD transgenic (tg) mice, these inhibitors reduce hyperphosphorylated tau accumulation, Aβ production, and/or SP burden (Pérez et al., 2003; Phiel et al., 2003; Su et al., 2004; Noble et al., 2005; Serenó et al., 2009). However, available inhibitors lack specificity for GSK-3 isoforms and may also have off-target effects, which may confound experimental results. Although a few recent studies have used genetic approaches *in vivo* (Gómez-Sintes et al., 2007; Alon et al., 2011; Jaworski et al., 2011), they have been unable to fully distinguish which GSK-3 isoform is responsible for hyperphosphorylated tau accumulation and/or SP formation.

In this study, we used two distinct approaches to evaluate the effect of GSK-3α or GSK-3β knockdown (KD) *in vivo* on AD-related neuropathology: a viral short hairpin RNA (shRNA) approach and a genetic approach. First, we intraventricularly delivered adeno-associated virus (AAV) encoding shRNAs directed toward GSK-3α or GSK-3β into newborn tg mice display-

Received Feb. 23, 2012; revised April 6, 2012; accepted April 13, 2012.

Author contributions: D.E.H., L.M.-P., J.Q.T., and V.M.-Y.L. designed research; D.E.H., L.M.-P., J.C.C., C.M., and A.K.A. performed research; D.E.H., L.M.-P., J.C.C., and V.M.-Y.L. analyzed data; D.E.H., L.M.-P., J.C.C., J.Q.T., and V.M.-Y.L. wrote the paper.

This study is supported by National Institutes of Health grants AG11542, AG17586, T32-GM07229, and T32-AG000255, the Marian S. Ware Alzheimer Program, the Fundación Caja Madrid, and Instituto de Salud Carlos III. We thank Jon Toledo, Amanda Piarulli, Brigid Jensen, Erin Coffey, and Stylianos Monos for technical and statistical assistance.

*D.E.H. and L.M.-P. contributed equally to this work.

The author(s) declare(s) no competing financial interests.

Correspondence should be addressed to Virginia M.-Y. Lee, Department of Pathology and Laboratory Medicine, University of Pennsylvania School of Medicine, Maloney Building 3rd Floor, HUP, 3600 Spruce Street, Philadelphia, PA 19104-4283. E-mail: vmylee@upenn.edu.

DOI:10.1523/JNEUROSCI.0889-12.2012

 0270-6474/12/327392-11$15.00/0

ing SP pathology (PDAPP $^{+/-}$), both SPs and NFTs (PDAPP $^{+/-}$; PS19 $^{+/-}$), or wild-type (wt) control mice. Second, we generated a triple tg mouse model using CaMKIIα-cre (α-calcium/calmodulin-dependent protein kinase II-Cre) system to KD *GSK-3α* alleles in PDAPP $^{+/-}$ mice. Using these two models, we demonstrated that knocking down GSK-3α or GSK-3β reduces the accumulation of phosphorylated tau; however, a single GSK-3α KD was sufficient to decrease plaque formation and improve cognition in the triple tg mouse model.

Materials and Methods

Screening shRNA

Neuro 2a (N2a) cells were transfected with shRNA plasmids directed toward murine GSK-3α or GSK-3β. shRNA plasmids containing the puromycin selection marker were purchased from Origene. Forty-eight hours post-transfection, cells were treated with 5 μg/ml puromycin for 7 d. Immunoblot analysis of cell lysates led to the identification of specific GSK-3 shRNAs used in this study with the following sequences: GSK-3α shRNA: AAGGACGAGCTGTATTTGAATCTGGTGCT and GSK-3β shRNA: GGCGACCGAGAACCACCTCCTTTGCGGAG along with a scramble control shRNA: TGACCACCCTGACCTACGGCGTGCAGTGC, designated as shRNA-α, shRNA-β, and shRNA-scr, respectively.

To measure eukaryotic translation initiation factor 2α (eIF2α) response, N2a cells were transfected with shRNA-α, shRNA-β, and shRNA-scr as described above and compared with untreated N2a cells. As a positive control, N2a cells were treated with thapsigargin (300 nM; Sigma) for 1 h and cell lysates were used for immunoblotting.

AAV construction, packaging, and intraventricular injection

Recombinant AAV 2/1 (rAAV2/1) expressing shRNA used in this study was produced at the University of Pennsylvania Vector Core as described previously (Gao et al., 2006). These AAV vectors were purified by two rounds of cesium chloride–gradient centrifugation, buffer-exchanged with PBS, and concentrated using Amicon Ultra 15 centrifugal filter devices-100K (Millipore). Genome titer (genome copies per milliliter) of AAV vectors were determined by real-time PCR. Viral vector titers were as follows: 4.7×10^{12} GC/ml for shRNA-α, 3.2×10^{12} GC/ml for shRNA-β, and 2.1×10^{12} GC/ml for shRNA-scr. The recombinant genome contained AAV 2 (AAV2) inverted terminal repeats that flanked five cassettes: the U6 promoter; a 29 bp palindromic DNA sequence with a 7 bp loop and a termination (TTTTTT) sequence, the CMV promoter, cDNA ZsGreen (Clontech), and an SV-40 poly(A) sequence. Recombinant AAV2 genome was cross-packaged with AAV-1 cap proteins generating pseudotype rAAV2/1.

Mouse intraventricular injection procedure was adapted from previously described studies (Passini and Wolfe, 2001; Li and Daly, 2002). Briefly, on the day of birth (designated as P 0.5), neonatal females were cryo-anesthetized on ice for 5 min. Once anesthetized, neonates were transilluminated over a cold fiber-optic illuminator to highlight cranial landmarks and 2 μl rAAV2/1 (containing shRNA-α, shRNA-β, or shRNA-scr) was injected into each lateral ventricle using a 10 μl Hamilton syringe with a 33 gauge needle. Pups were subsequently placed on a heating pad for recovery and then returned to their home cage. Of the ~230 total mice injected, ~218 pups survived surgery and were tattooed 10 d later, yielding a "success rate" of ~95%.

Generation of tg mice

Using the abovementioned approach, three mouse lines were generated: (1) heterozygous PDAPP (PDAPP $^{+/-}$), (2) heterozygous PS19;PDAPP (PS19 $^{+/-}$;PDAPP $^{+/-}$), and (3) control wt (B6C3 background strain). The PDAPP mouse model is well described, and was engineered to encode a human APP minigene carrying the V717F mutation driven by the PDGF promoter (Games et al., 1995). The PS19 model harbors the T34 isoform of tau with one N-terminal insert and four microtubule binding repeats (1N4R) encoding the P301S mutation driven by the mouse prion promoter (Yoshiyama et al., 2007). F1 hybrid PS19 $^{+/-}$;PDAPP $^{+/-}$ and PDAPP $^{+/-}$ were generated by crossing parental strains PS19 $^{+/-}$ and homozygous PDAPP. F1 hybrids wt were generated by mating parental strains heterozygous PS19 $^{+/-}$ and WT mice. Only female F1 hybrids were used in experimental groups.

Using the abovementioned lines, five cohorts of mice were generated for this study: (1) 4-month-old wt mice, (2) 11-month-old wt mice, (3) 11-month-old PDAPP $^{+/-}$ mice, (4) 11-month-old PDAPP $^{+/-}$; PS19 $^{+/-}$ mice, and (5) wt survival group. In each cohort, a separate group of mice received one of four injection paradigms: rAAV containing shRNA-α, shRNA-β, shRNA-scr, or noninjected control. Each group consisted of 15 mice except for the survival cohort ($n = 10$/group).Together, a grand total of 20 experimental groups and 280 mice were used.

Conditional knock-out generation

GSK-3α conditional knock-out (cko) mice were generated using the Cre-loxP system through a contract with Taconic. To produce heterozygous GSK-3α floxed (GSK-3$\alpha^{flox/-}$) mice, the targeting vector based on a 9.9 kb genomic fragment from the GSK-3α gene encompassing exons 1–11 and surrounding sequences was obtained from the C57BL/6J RP23 Bacterial Artificial Chromosomes Library and was modified by inserting a loxP site and an FRT-flanked neomycin resistance gene in intron 1 and a loxP site in intron 4, as well as a ZsGreen cassette at its 3′ end (see Fig. 5*A*). Thirty micrograms of linearized DNA vector were electroporated using a Bio-Rad Gene Pulser at 240 V and 500 μF into 1×10^7 cells of the C57BL/6N embryonic stem (ES) cell lines. Only nonfluorescent clones suggesting the absence of the ZsGreen region were selected on day 8. After expansion and freezing clones in nitrogen, 176 clones were analyzed by using 5′, 3′, and neomycin probes after digestion by KpnI, EcoRI, AflIII, PflFI, and BglII restriction enzymes in standard Southern blotting techniques (Fig. 5*A–D*). Proper homologous recombination was identified in four of the clones, and clone B-C9 was used for blastocyst injection.

Ten to fifteen targeted C57BL/6N.tac ES cells were microinjected into each blastocyst obtained after superovulation of BALB/c females and 8 injected blastocysts were transferred to each uterine horn of a 2.5 days postcoitum, pseudopregnant Naval Medical Research Institute female mouse. Highly chimeric mice were bred to female C57BL/6 mice with Flp-Deleter recombinase gene to remove the Neo selection marker. Germline transmission was identified by the presence of black C57BL/6 offspring.

Triple tg mice were generated by crossing the GSK-3$\alpha^{flox/-}$ mice with CaMKIIα-cre (C57BL/6 background) (Tsien et al., 1996) and PDAPP lines. Four crosses resulted in triple tg mice GSK-3$\alpha^{flox/flox}$;CaMKIIα-cre $^{+/-}$; PDAPP $^{+/-}$ that were subsequently mated with GSK-3$\alpha^{flox/flox}$ mice, generating four genotypes: GSK-3$\alpha^{flox/flox}$;CaMKIIα-cre $^{-/-}$;PDAPP $^{-/-}$ (GSK-3α wt), GSK-3$\alpha^{flox/flox}$;CaMKIIα-cre $^{+/-}$ PDAPP $^{-/-}$ (GSK-3α cko), GSK-3$\alpha^{flox/flox}$; CaMKIIα-cre $^{-/-}$;PDAPP $^{+/-}$ (GSK-3α wt;PDAPP), and GSK-3$\alpha^{flox/flox}$; CaMKIIα-cre $^{+/-}$;PDAPP $^{+/-}$ (GSK-3α cko;PDAPP). Each of the four groups consisted of $n = 10$–15 mice that were analyzed at 17 months of age.

Histology and brain preparation

Mice were anesthetized and transcardially perfused with PBS, pH 7.0, in accordance with protocols approved by the Institutional Animal Care and Use Committee of the University of Pennsylvania. Brains were surgically removed and the right hemisphere was fixed in 4% neutral buffered formalin (NBF), while the left hemisphere was dissected into various brain regions and frozen at −80°C for biochemical analysis. To maintain consistency of dissection and to facilitate analysis brains were coronally sliced starting with an initial cut parallel to the olfactory tract as it bends toward the median eminence. Bisection at this point generated anterior and posterior cortical regions which were fixed in NBF and paraffin embedded. Paraffin blocks were sectioned at 6 μm exhaustively. Tissue sections were stained using a Polymer horseradish peroxidase detection system (Biogenex) and automatically stained using the i6000 Automated Staining System (Biogenex) as previously described (Hurtado et al., 2010).

Antibodies used in histology

Viral distribution was assessed using rabbit polyclonal antibody (pAb) ZsGreen (Clontech). ShRNA off-target effects were identified by activated microglia using ionized calcium binding adaptor molecule 1 (iba1) rabbit pAb (019-19741; Wako Chemicals), and activated astrocytes using

glial fibrillary acidic protein (GFAP) rabbit pAb (Dako). GSK-3 expression was monitored through the use of a GSK-3α rabbit pAb (9338) and GSK-3β rabbit mouse monoclonal antibody (mAb) (27C10; Cell Signaling Technology). To track the distribution of Aβ plaques, we used mouse mAb Nab228 which binds to 1–11 in Aβ peptides (Lee et al., 2006). Anti-tau antibodies used in this study include: AT8 mouse mAb specific for phosphorylated Ser202/Thr205 (Innogenetics), 12E8 mouse mAb specific for phosphorylated S262 (gift from P. Seubert, Elan Pharma), AT180 mouse mAb specific for phosphorylated Thr231 (Innogenetics), and anti-tau mouse mAb T14, which is specific for human tau (Yoshiyama et al., 2007). Additionally we used Alz50 and MC1 mouse mAb (a gift from Peter Davies) to monitor conformational tau. Fibrillary tau lesions were detected using Thioflavine-S/Lipofuscin (ThS) autofluorescence quenching protocols as described by Yoshiyama et al. (2007).

Immunohistochemical quantification

Aβ deposits, phospho-tau, Iba1, and GFAP immunoreactive (IR) burden were quantified by a researcher blinded to experimental conditions as previously described (Carroll et al., 2011). Images from immunolabeled sections were captured and digitized using a video capture system (Nikon camera coupled to an Olympus DP71 upright microscope). Using NIH ImageJ software, the areas of interest were drawn freehand (i.e., entire hippocampus). Afterward, digital grayscale images were converted into binary positive/negative data using a constant threshold limit. The percentage of positive pixels (i.e., IR area) was quantified for each image to generate IR "load" values (i.e., percentage area occupied by the IR product). For phospho-tau burden, images of AT180- or 12E8-stained sections of CA3 regions close to bregma −3.28 mm were measured. For Aβ deposit quantification; images of Nab228-stained sections of hippocampus were more anterior (bregma −1.95).

Sandwich ELISA analysis

Aβ 40 and Aβ 42 levels were detected using Aβ sandwich ELISA protocols as previously described (Lee et al., 2003). Briefly, brain regions were sonicated in radioimmunoprecipitation assay (RIPA) buffer (0.5% sodium deoxycholate, 0.1% SDS, 1% NP-40, 5 mM EDTA in TBS, pH 8.0) containing protease inhibitors (1 μg/ml pepstatin A, leupeptin, L-1-tosylamido-2-phenylethyl chloromethyl ketone, 1-chloro-3-tosylamido-7-amino-2-heptanone, soybean trypsin inhibitor, and 0.5 mM phenylmethanesulfonyl fluoride) at 6 μl/mg of tissue followed by centrifugation at 100,000 *g* for 20 min at 4°C. The resulting pellet was further extracted by sonication with 70% formic acid (FA) at 1 μl/mg tissue followed by a second identical centrifugation. Both RIPA and FA lysates were assayed by sandwich ELISA using Ban50 (anti-Aβ_{1-10}) as a capturing antibody and end-specific BC05 and BA27 antibodies to distinguish Aβ 40 and Aβ 42, respectively.

Western blots

To measure soluble proteins, hippocampi and N2a cells were homogenized in RIPA buffer in the presence of protease inhibitors and briefly sonicated. Samples were centrifuged at 100,000 *g* for 30 min at 4°C, and protein concentration was measured by bicinchoninic acid assay. Samples were electrophoresed on 10% Tris-glycine acrylamide gels and transferred to a nitrocellulose or polyvinylidene fluoride membrane. Immunoblots were probed with the following antibodies: GSK-3$\alpha\beta$ mouse mAb (Calbiochem), eIF2α (9722) rabbit pAb, phospho-eIF2α (Ser51) (119A11) rabbit mAb (Cell Signaling Technology), C terminus of APP (5685) rabbit pAb (Lee et al., 2005), PhAT, a phospho rabbit pAb raised to residues 665–673 containing phospho-Thr668 at the C terminus of APP (Lee et al., 2005), and GAPDH mouse mAb (Advanced Immunochemical) as a loading control. Immunoblots were then exposed to species-specific horseradish peroxidase-conjugated anti-IgG antibodies (Santa Cruz Biotechnology) and visualized by enhanced chemiluminescence (PerkinElmer) using a Fuji Imager. Images were quantified using Multi Gauge version 3.2 FujiFilm software.

GSK-3 kinase activity assay

Frozen hippocampal sections were sonicated 20 times at 1 s pulses, on ice at 6 μl/mg of tissue in homogenization buffer (D-PBS w/ Ca^{2+}, Mg^{2+}), pH 7.3 (Invitrogen), containing protease and phosphates inhibitors (complete, Mini, EDTA-free Protease Inhibitor Cocktail, and PhosSTOP) (Roche Applied Science). Samples were centrifuged at 100,000 × *g* for 30 min at 4°C and supernatant protein concentrations were determined using a Bradford assay (Bio-Rad). Fifty micrograms of lysate was used for immunoprecipitation (IP) for GSK-3α or GSK-3β. IP was performed using 35 μl of Protein A/G PLUS-Agarose slurry (Santa Cruz Biotechnology), 50 μg of lysate, and 2 μl of GSK-3α- or GSK-3β-specific antibodies (Cell Signaling Technology). IP was incubated overnight at 4°C on a rotator and subsequently washed and resuspended in homogenization buffer. Resuspended bead slurry was used for GSK-3 kinase activity assay. The activity assay was performed in kinase buffer (25 mM Tris-HCl, pH 7.5, 0.5 mM EGTA, 75 mM NaCl, 0.015%, Brij-35, 0.05% β-mercaptoethanol, pH 7.4, and 1 μM cAMP-dependent protein kinase inhibitor tide) and ATP buffer (10 mM $MgCl_2$, 0.1 mM adenosine 5′-triphosphate, 3MBq/ml adenosine 5′-triphosphate [γ^{-32}P]), with the GSK-3 substrate, phospho-glycogen synthase peptide-2 (Millipore). Reactions were performed at 37°C for 15 min. ^{32}P-labeled peptide was absorbed on P81 phosphocellulose paper (GE Healthcare) and washed several times in 75 mM phosphoric acid followed by an acetone wash and briefly dried. Quantitation was performed in a β-scintillation counter, 1450 MicroBeta TriLux (PerkinElmer).

Behavioral analysis

Open field. To assess general activity, locomotion, and anxiety, mice were tested in the open field as adapted as previously described (Boyce-Rustay and Holmes, 2006; Carroll et al., 2007). The apparatus was a square arena (40 × 40 × 35 cm) with black Plexiglas walls and white floor that was evenly illuminated to ~95 lux. Mice were individually placed in the center and allowed to freely explore for 13 min while the trial was videotaped. Subsequent video scoring was completed by an observer blind to treatment groups using the SMARTv25 video-tracking software (Panlab, S.LU.). Total distance moved was automatically calculated by the tracking software as a direct measure of locomotion and activity.

Barnes maze. Mice were tested for hippocampal-dependent spatial memory on the Barnes maze (San Diego Instruments) using a previously described protocol from our laboratory (Brunden et al., 2010). Briefly, mice were tested over >6 d. On training days 1–3, mice were exposed to the Barnes maze for three 2.5 min trials, 15 min apart. On testing days 4–6, they were exposed to two 2.5 min trials. On all 6 d, only the two last trials were scored. Mice were tested on their ability to learn and remember a fixed position of an escape compartment, and their performance was scored for strategy and latency to find the escape compartment. Strategies were defined as (1) spatial (mouse navigates directly to the escape hole with both first intent deviation and total errors < or = 3), (2) serial (mouse systematically searches of consecutive holes with no center crosses), and (3) random (no strategy at all) as previously described (O'Leary et al., 2011).

Statistical analysis

The majority of data analysis was completed using one-way ANOVA followed by Bonferroni's *post hoc* test. ELISA was assessed using the Kruskal–Wallis analysis and Dunn's *post hoc* test. Barnes maze search strategy was analyzed using a χ^2 and latency with a two-way ANOVA. Life-span studies were analyzed using the Kaplan–Meier survival curve.

Results

Identification, development, and implementation of rAAV2/1 shRNA targeting GSK-3α and GSK-3β

Four hairpin shRNA constructs were designed using a proprietary Origene algorithm to target GSK-3α or GSK-3β and they were evaluated by transfection into N2a cells along with a scrambled hairpin control to determine which shRNA yielded the highest expression (Fig. 1*A*,*B*). Due to high sequence homology of GSK-3 isoforms, each hairpin was assessed for both GSK-3α and GSK-3β expression. In the case of GSK-3α, since shRNA GSK-3α #1 showed no target reduction and #4 displayed cellular toxicity ($t_{(4)} = 1.459$, $p = 0.2182$ and >50%, respectively), both were eliminated from the study (Fig. 1*A*). The GSK-3α #2 and #3 of

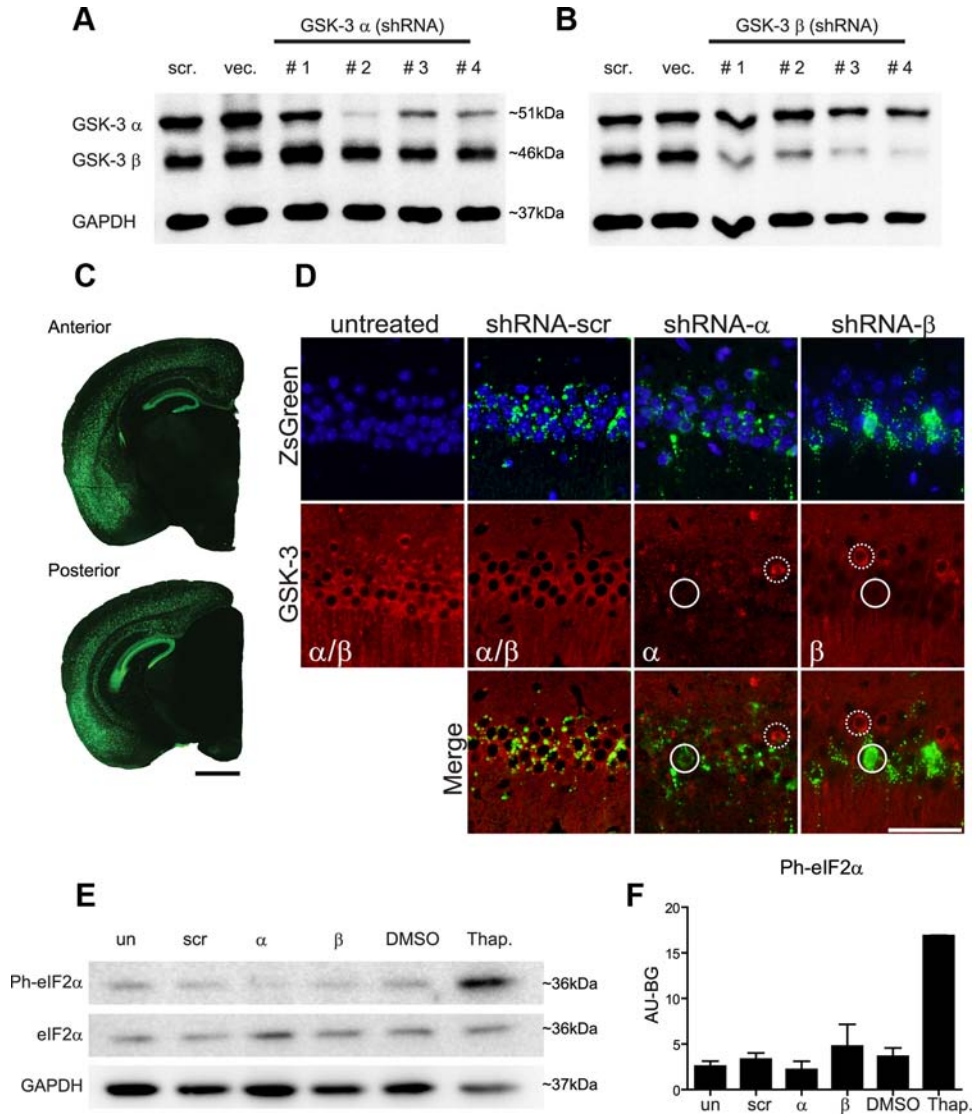

Figure 1. shRNA selection, rAAV distribution and expression, and lack of evidence of off-target effects. N2a cells were transfected with hairpin constructs and selected with puromycin for 7d. As controls, N2a cells were transfected with an empty vector (VEC) or a scrambled hairpin control (scr). ***A***, Representative Western blot of GSK-3α shRNA #1–4 and (***B***) GSK-3β shRNA #1–4 demonstrates that shRNA GSK-3α #2 showed the highest KD level ($F_{(2,6)} = 54.82, p < 0.0001$), and GSK-3$\beta$ #2 showed a GSK-3β reduction without affecting GSK-3α levels ($F_{(2,5)} = 298.5, p < 0.0004$). Wt neonates ($n = 15$/group) were uninjected or injected with shRNA-scr, shRNA-α, or shRNA-β and evaluated at 4 months of age to confirm rAAV distribution and targeted-gene KD. ***C***, Representative images of both anterior and posterior brain after shRNA-scr treatment shows rAAV distribution stained for ZsGreen (green) within hippocampal regions and deeper cortical layers in a rostrocaudal pattern. Scale bar, 1 mm. ***D***, Representative immunofluorescence images of the CA1 region of hippocampus from each of the three shRNA treatment groups and uninjected controls are shown immunostained for ZsGreen or for both GSK-3$\alpha\beta$ isoforms (red) and counterstained with DAPI (blue). Merging GSK-3 and ZsGreen expression reveals that expression of rAAV2/1 directly leads to reduction of targeted GSK-3 isoforms (highlighted by white circles), whereas neurons lacking rAAV2/1 show no loss of GSK-3 expression (highlighted by dashed white circles). Scale bar, 50 μm. To analyze possible off-target effects, N2a cells were treated with shRNA-scr, shRNA-α, and shRNA-β. DMSO and thapsigargin (Thap) treatment were used as negative and positive controls, respectively (***E***). Representative Western blot and (***F***) densitometric analysis of phosphorylated eIF2α (Ph-eIF2α) normalized to GAPDH reveals no significant alterations ($F_{(4,5)} = 0.6255, p = 0.6650$). Untreated, un; shRNA-scr-treated cells, scr; shRNA-α-treated cells, α; and shRNA-β-treated cells, β.

both shRNAs showed a significant GSK-3α reduction (82 and 74%, respectively, $p < 0.001$) compared with untreated cells ($F_{(2,6)} = 54.82$, $p < 0.0001$) without affecting GSK-3β expression. Since shRNA GSK-3α #2 showed higher KD levels, it was chosen for further development (Fig. 1*B*). In the case of GSK-3β, shRNAs GSK-3β #3 and #4 displayed cellular toxicity (>50%) and were therefore eliminated from consideration. ShRNA GSK-3β #1 and #2 showed similar levels of GSK-3β reduction (65 and 57%, respectively, $p < 0.001$) and little toxicity compared with untreated cells ($F_{(2,5)} = 298.5$, $p < 0.0004$). However, in shRNA GSK-3β #1, we observed a nonsignificant trend toward GSK-3α reduction (17%, $p = 0.34$), therefore shRNA GSK-3β #2 was selected for further development. No alterations in GSK-3 expression were observed with scramble shRNA control ($F_{(3,4)} = 1.125$, $p = 0.4386$).

Pseudotype rAAV2/1 viruses containing hairpin sequences for GSK-3α #2, GSK-3β #2, and a scrambled shRNA (designated as shRNA-α, shRNA-β, and shRNA-scr, respectively) were produced and injected into newborn wt mice (see Material and Methods). To evaluate AAV distribution, wt mice were examined at 4 months postinjection by monitoring ZsGreen expression which was found predominately in hippocampal regions CA1–CA3, the granular cell layer of the dentate gyrus, and with more variability in deeper cortical layers four through six along with cortical amygdala regions (Fig. 1*C*). Overall, cortical regions in close proximity to the lateral ventricles showed higher transduction than

regions further away. Minor or no ZsGreen expression was detected in basal ganglia, thalamus, brainstem, or cerebellum.

To confirm that rAAV2/1 vectors expressing shRNA silenced the target genes, we double-labeled mouse sections with ZsGreen and GSK-3α or GSK-3β antibodies (Fig. 1*D*). We observed that in shRNA-α-injected and shRNA-β-injected wt mice, cells with ZsGreen staining showed a concomitant reduction in GSK-3α or GSK-β protein expression, respectively, whereas neurons lacking ZsGreen did not. In shRNA-scr-injected mice, ZsGreen was not associated with a reduction in either GSK-3 isoform. Together, these results validate that rAAV2/1 vectors expressing shRNA lead to direct silencing of the target genes in mouse brain.

To determine potential off-target effects of rAAV2/1 infection, we assessed whether our double-stranded RNA (dsRNA) would evoke an interferon response. dsRNA is a common intermediate produced during virus infection in mammalian cells. Its binding motifs activate protein kinase R (PKR) which phosphorylates eIF2α, leading to global inhibition of cellular protein synthesis and viral replication (Sledz et al., 2003; Sledz and Williams, 2005). To test if hairpins would elicit an antiviral defense, we examined phosphorylation of elF2α in N2a cells transfected with shRNA-α, shRNA-β, or shRNA-scr plasmids. Cells treated with dimethylsulfoxide (DMSO) and thapsigargin were used as a negative and positive control, respectively. No significant change in eIF2α phosphorylation state was observed in shRNA-treated versus shRNA-untreated cells, suggesting that shRNA presence did not prompt an off-target PKR-eIF2α response (Fig. 1*E*,*F*). Second, to investigate whether the injection or the presence of the different shRNAs in the CNS produced an immune response or brain injury in mice, we analyzed the activation of astrocytes and microglia in the hippocampus of wt mice at 4 months of age (n = 9 per group). No statistical differences in astrocytosis ($F_{(3,32)}$ = 1.934, p = 0.144) or activated microglia ($F_{(3,32)}$ = 0.7316, p = 0.5408) in the shRNA-treated mice were observed, suggesting that shRNA presence did not abnormally activate the immune system (data not shown).

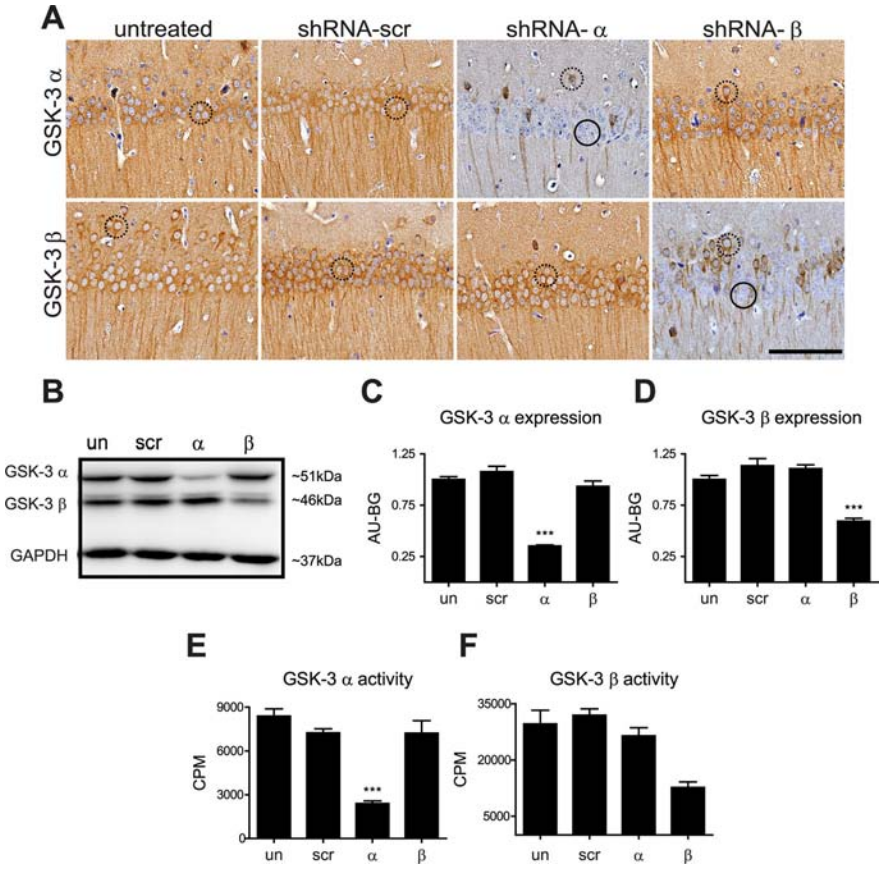

Figure 2. Confirmation of GSK-3 KD. ShRNA-treated and noninjected wt mice were evaluated at 4 months of age to confirm targeted-gene KD. ***A***, Representative IHC images of the CA1 region of hippocampus counterstained with hematoxylin reveal normal, baseline GSK-3$\alpha\beta$ expression levels in untreated and shRNA-scr-treated mice. ShRNA-α treatment significantly reduced GSK-3α expression without altering GSK-3β expression and vice versa for shRNA-β-treated mice. Neurons with reduced GSK-3 expression are highlighted by black circles and neurons expressing normal GSK-3 levels are highlighted by dashed black circles. Scale bar, 100 μm. ***B***, Immunoblot analyses of hippocampal lysates probed with GSK-3 isoform-specific antibodies. ***C***, Corresponding quantification showing that shRNA-α treatment significantly reduced GSK-3α expression without altering GSK-3β expression ($F_{(3,12)}$ = 68.47, $p < 0.0001$) and (***D***) vice versa for shRNA-β-treated mice ($F_{(3,12)}$ = 29.05, $p < 0.0001$). Wt injected and uninjected mice were evaluated at 11 months of age to confirm targeted-gene KD by analyzing GSK-3 activity using a ^{32}P-labeled assay (n = 4–6/group). ***E***, ShRNA-α significantly decreased GSK-3α activity levels ($F_{(3,14)}$ = 38.64, $p < 0.0001$) and (***F***) shRNA-β significantly decreased GSK-3β activity ($F_{(3,12)}$ = 12.87, $p < 0.0005$). Data show mean ± SEM; ***$p < 0.001$ and **$p < 0.01$ compared with all other groups. Uninjected, un; shRNA-scr-injected mice, scr; shRNA-α-injected mice, α; and shRNA-β-injected mice, β.

GSK-3 expression and survival analysis in shRNA-α-injected and shRNA-β-injected wt mice

To further define the extent of GSK-3α versus GSK-3β KD by specific shRNAs, we examined the distribution, protein levels, and kinase activity of both GSK-3 isoforms. First, immunohistochemistry (IHC) confirmed that silencing GSK-3α significantly reduced GSK-3α immunoreactivity but had no effect on GSK-3β levels and vice versa in the hippocampus of 4-month-old wt mice (Fig. 2*A*). Moreover, we did not detect any alterations in GSK-3α or GSK-3β staining in untreated or scramble-treated mice (Fig. 2*A*).

Second, immunoblot analyses showed that GSK-3α protein levels were reduced by ~58–72% in shRNA-α-injected mice compared with noninjected, shRNA-scr-injected, and shRNA-β-injected mice whereas GSK-3β protein levels were reduced by ~40–54% in shRNA-β-injected mice (Fig. 2*B–D*). No statistically significant difference in GSK-3 protein expression levels was observed between noninjected and shRNA-scr-injected mice (t = 1.365, $p > 0.05$ for GSK-3α and t = 2.055, $p > 0.05$ for GSK-3β) and no change in the total levels of the nontargeted isoform was observed when compared with uninjected control (t = 1.625, $p >$ 0.05 for GSK-3α levels in shRNA-β mice, and $t_{(6)}$ = 1.180, $p >$ 0.05 for GSK-3β levels in shRNA-α mice) (Fig. 2*B–D*). These results validate the specificity of the shRNA-α and shRNA-β used in this study, and suggest that silencing one isoform does not induce a compensatory response in the other.

Third, since total protein levels may not necessarily correlate with enzyme activity, GSK-3α and GSK-3β activity levels in

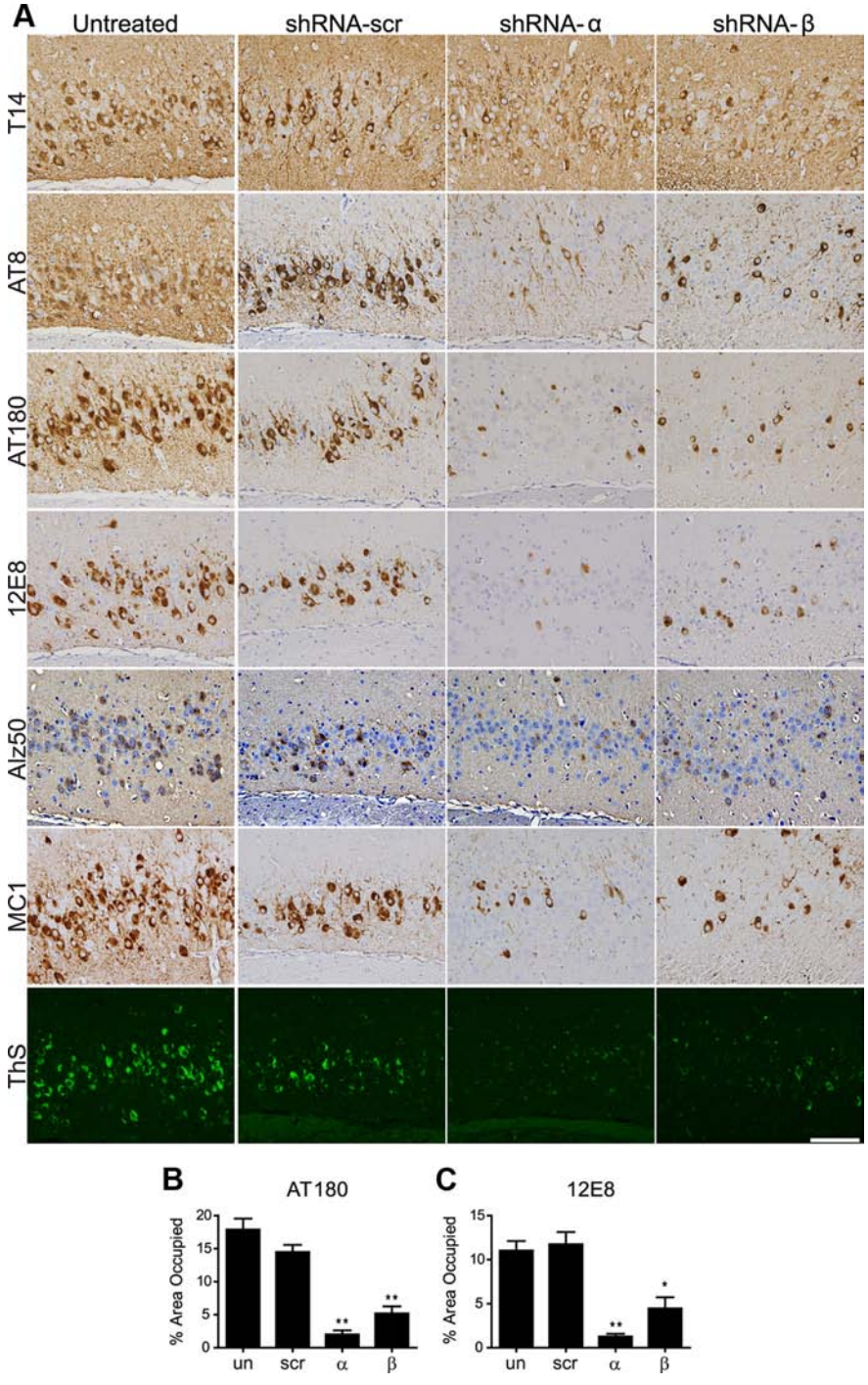

Figure 3. GSK-3α or GSK-3β KD reduces tau phosphorylation and conformational changes in PS19 $^{+/-}$;PDAPP $^{+/-}$ mice. PS19 $^{+/-}$;PDAPP $^{+/-}$ neonates were uninjected (un) or injected with shRNA-α, shRNA-β, or shRNA-scr and evaluated at 11 months of age ($n = 15$ per group). ***A***, Representative IHC images counterstained with hematoxylin show CA3 regions of posterior hippocampus stained with antibodies to total tau (T14), phospho-tau Ser202/Thr205 (AT8), phospho-tau Thr231 (AT180), phospho-tau Ser262 (12E8), or conformational specific antibodies Alz50, MC1, or ThS as indicated. Scale bar, 100 μm. PS19 $^{+/-}$; PDAPP $^{+/-}$ mice treated with shRNA-α or shRNA-β showed a significant reduction in phospho-tau, Alz50, MC1, and ThS staining, but not in total tau load compared with shRNA-scr and noninjected controls. The phospho-tau burden in the CA3 region was quantified using ImageJ for mAb AT180 (***B***) and 12E8 (***C***) in $n = 3$–4 mice/group, to demonstrate the quantification of >50% reduction with shRNA-α and shRNA-β treatment compared with controls ($F_{(3,8)} = 8.283$, $p = 0.0078$ and $F_{(3,9)} = 15.28$, $p = 0.0007$, respectively). Data show mean ± SEM; $^{**}p < 0.01$, $^{*}p < 0.05$ compared with shRNA-scr controls.

hippocampal lysates of shRNA-α-injected, shRNA-β-injected, and shRNA-scr-injected 11-month-old wt mice were compared with noninjected controls for GSK-3 enzyme activity. Importantly, a significant 71% decrease in GSK-3α activity in shRNA-α-injected mice (Fig. 2*E*), and a comparable 67% reduction in GSK-3β activity in shRNA-β-injected mice (Fig. 2*F*) were observed. Significantly, GSK-3α KD did not affect GSK-3β activity levels ($t = 0.9417$, $p > 0.05$), and GSK-3β KD did not affect GSK-3α activity ($t = 1.673$, $p > 0.05$), suggesting that a single isoform KD did not trigger a compensatory effect in the alternate isoform. Further, shRNA-scr had no effect on GSK-3α or GSK-3β activity levels ($t = 1.641$ and $t = 0.6733$, respectively, $p > 0.05$). Last, these results suggest that KD of the targeted genes was persistent over 11 months.

Finally, we sought to confirm whether GSK-3 KD would have deleterious effects on life span. Survival analysis of wt mice injected with shRNA-α, shRNA-β, or -scr rAAV2/1 monitored up to 12 months showed no difference in life span between injected and uninjected controls ($\chi^2 = 2.210$, $p = 0.53$, $n = 10$ per group) suggesting that GSK-3 KD does not alter survival in wt mice.

GSK-3α or GSK-3β KD reduces NFTs and tau phosphorylation as well as mitigates conformational changes in PDAPP $^{+/-}$;PS19 $^{+/-}$ bigenic mice

To evaluate the effect of GSK-3α and GSK-3β KD on tau phosphorylation and NFT formation, newborn PDAPP $^{+/-}$; PS19 $^{+/-}$ bigenic mice were injected with shRNA-α, shRNA-β, or shRNA-scr rAAV2/1 and were examined at 11 months of age ($n = 15$ per group). Although shRNA-α-injected and shRNA-β PDAPP $^{+/-}$;PS19 $^{+/-}$-injected mice had lower reduction of GSK-3α and GSK-β protein expression than previous experiments with wt or PDAPP $^{+/-}$ mice, they were, nonetheless, statistically significant (30%, $F_{(2,57)} = 6.271$, $p = 0.0035$, and 29%, $F_{(2,57)} = 32.38$, $p < 0.0001$, respectively).

To determine whether specific phosphorylation sites of tau were affected by GSK-3α or GSK-3β KD, we conducted IHC using antibodies on a number of different phosphorylation-dependent epitopes, as well as on abnormal conformation epitopes of tau and total tau in the CA3 hippocampus region. Quantification of the IR load showed that total human tau levels measured by T14 were not altered by silencing GSK-3α or GSK-3β (Fig. 3*A*). In contrast, NFTs and tau hyperphosphorylation associated with pathological tau on Ser202/Thr205 (detected by mAb AT8), Thr231 (mAb AT180), and Ser262 (mAb 12E8) were markedly decreased (Fig. 3*A*) and quantitation of IHC with both AT180 (Fig. 3*B*) and 12E8 (Fig. 3*C*) showed significant reductions after GSK-3α or GSK-3β KD. Interestingly, reduction in tau hyperphosphorylation was accompanied

by a decrease in the accumulation of abnormal tau conformers as detected by conformation-specific antibodies Alz50, MC1, and a dramatic reduction in NFTs as monitored by ThS, which recognizes β-pleated conformations in tau amyloid inclusions. Together, these results suggest that both GSK-3α and GSK-3β KD were effective in reducing tau hyperphosphorylation, pathological tau conformational changes, and NFT formation.

GSK-3α but not GSK-3β KD decreases Aβ levels and SPs in PDAPP $^{+/-}$ and PDAPP $^{+/-}$;PS19 $^{+/-}$ brains

The effects of GSK-3 KD on Aβ amyloid deposition in SPs and Aβ levels in brain were also evaluated in PDAPP $^{+/-}$ and PDAPP $^{+/-}$; PS19 $^{+/-}$ mice injected with rAAV2/1 containing shRNA-α, shRNA-β, or shRNA-scr and examined at 11 months of age. ShRNA-α and shRNA-β KD resulted in a reduction of GSK-3α (~70%) and GSK-3β (~50%) protein expression, respectively, in PDAPP $^{+/-}$ mice (Fig. 4*E*,*G*). Aβ levels were measured using IHC and Aβ sandwich ELISA. IHC to monitor Aβ SP burden in hippocampal regions of PDAPP $^{+/-}$ and PDAPP $^{+/-}$; PS19 $^{+/-}$ mice showed a statistically significant reduction in Aβ load after GSK-3α but not GSK-3β KD in PDAPP $^{+/-}$ and PDAPP $^{+/-}$;PS19 $^{+/-}$ mice (Fig. 4*A*,*B*). In general, the reduction in Aβ deposition was more pronounced in PDAPP $^{+/-}$; PS19 $^{+/-}$ mice and a modest increase in Aβ accumulation was detected in shRNA-β-treated PDAPP $^{+/-}$ and PDAPP $^{+/-}$; PS19 $^{+/-}$ mice when compared with shRNA-scr-treated and shRNA-scr-untreated mice (Fig. 4*B*). Moreover, measurements of brain Aβ levels by ELISA corroborated IHC studies of Aβ load by demonstrating a similar reduction in soluble and insoluble Aβ 40/42 levels in hippocampus from both RIPA (Fig. 4*C*) and FA extracted fractions (Fig. 4*D*). Overall, Aβ 40 and Aβ 42 levels were statistically different between treatment groups in both fractions and genotypes. Moreover, we observed that GSK-3α KD significantly decreased both soluble and insoluble Aβ 40 and Aβ 42 levels compared with noninjected controls, whereas mice treated with shRNA-scr or shRNA-β had little to no change in Aβ 40/42 levels (Fig. 4*C*,*D*). Thus GSK-3α KD but not GSK-3β KD reduces Aβ levels in PDAPP $^{+/-}$ and PDAPP $^{+/-}$; PS19 $^{+/-}$ mice.

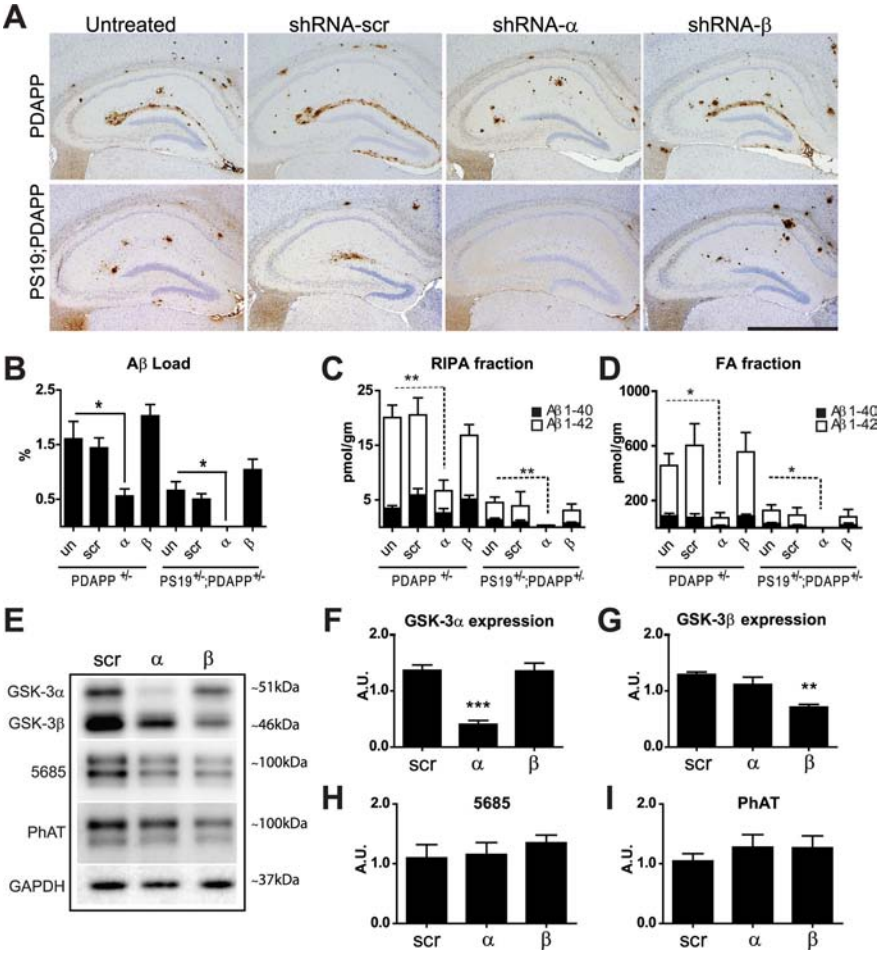

Figure 4. GSK-3α KD decreases Aβ levels and plaque deposition in PDAPP $^{+/-}$ and PDAPP $^{+/-}$;PS19 $^{+/-}$ brains. PDAPP $^{+/-}$ or PDAPP $^{+/-}$;PS19 $^{+/-}$ neonates were uninjected (un) or injected with shRNA-α, shRNA-β, or shRNA-scr and evaluated at 11 months of age. ***A***, Representative images of sections immunostained for Aβ (Nab228) and counterstained with hematoxylin demonstrated a significant reduction in plaque load after GSK-3α KD ($n = 15$ per group). Scale bar, 1 mm. ***B***, Hippocampal Aβ load was quantified using ImageJ software ($n = 7$–12 per group). In both PDAPP $^{+/-}$ and PDAPP $^{+/-}$; PS19 $^{+/-}$ models, shRNA-α treatment decreased Aβ burden compared with untreated mice ($F_{(3,124)} = 5.269$, $p = 0.0019$ and $F_{(3,91)} = 7.701$, $p = 0.0001$, respectively). ***C***, ***D***, In PDAPP $^{+/-}$ and PDAPP $^{+/-}$;PS19 $^{+/-}$ mice, hippocampal regions were analyzed for soluble and insoluble Aβ levels using Aβ sandwich ELISA ($n = 5$–8/group). In PDAPP $^{+/-}$ mice, shRNA-α decreased soluble Aβ 40 and Aβ 42 levels in the RIPA fraction (***C***) (Aβ40 $H_4 = 16.84$, $p = 0.0008$ and Aβ42 $H_4 = 13.39$, $p = 0.0039$); and FA fraction (***D***) (Aβ 40 $H_4 = 14.67$, $p = 0.0021$ and Aβ 42 $H_4 = 13.07$, $p = 0.0045$). Likewise, shRNA-α decreased soluble Aβ 40 and Aβ 42 levels in PS19 $^{+/-}$;PDAPP $^{+/-}$ mice in the RIPA fraction (***C***) (Aβ 40 $H_4 = 10.55$, $p = 0.0144$ and Aβ 42 $H_4 = 10.74$, $p = 0.0132$), and FA fraction (***D***) (Aβ 40 $H_4 = 10.44$, $p = 0.0152$ and Aβ 42 $H_4 = 9.178$, $p = 0.0270$). Data are shown as mean ± SEM. $^*p < 0.05$, $^{**}p < 0.01$. ***E***, Western blot and densitometric analysis were performed in triplicate with $n = 4$–5 mice/group. Representative blots show GSK-3$\alpha\beta$, total APP (5685), phosphorylated APP (PhAT), and a loading control (GAPDH). GSK-3α levels (***F***) were significantly reduced in mice treated with shRNA-α ($F_{(2,15)} = 26.96$, $p < 0.001$), and GSK-3β levels (***G***) were significantly reduced in mice treated with shRNA-β ($F_{(2,15)} = 12.40$, $p = 0.0007$) compared with shRNA-scr controls. However, neither the total APP (***H***) nor phospho-APP levels (***I***) were altered across treatment groups ($F_{(2,21)} = 0.3396$, $p = 0.7159$, and $F_{(2,21)} = 0.4014$, $p = 0.6744$, respectively). Data show mean ± SEM; $^{***}p < 0.001$ compared with untreated controls.

To investigate potential mechanisms by which GSK-3α KD reduces Aβ levels and plaque load, we evaluated APP levels in the hippocampus of treated PDAPP $^{+/-}$ mice by immunoblots (Fig. 4*E*) and showed no group differences in APP expression (Fig. 4*E*,*H*, 5685) or phosphorylation at Thr668 (Fig. 4*E*,*I*, PhAT) of APP. Together, these results suggest that the reduction in Aβ plaque load by lowering GSK-3α expression is not mediated by alterations in total APP levels or APP phosphorylation.

Conditional knockout of GSK-3α decreases Aβ amyloid deposition and prevents memory deficits in PDAPP $^{+/-}$ mice

To further confirm the effects of GSK-3α on Aβ deposition, we used a genetic approach and the cre-loxP system to generate tg cko mice overexpressing mutant APP in four genotypes: *GSK-3α wt*, *GSK-3α cko*, *GSK-3α wt;PDAPP*$^{+/-}$, and *GSK-3α cko; PDAPP*$^{+/-}$, all of which were analyzed at 17 months of age. IHC studies showed a dramatic reduction in GSK-3α immunostaining in brains *of GSK-3α cko* mice without altering GSK-3β im-

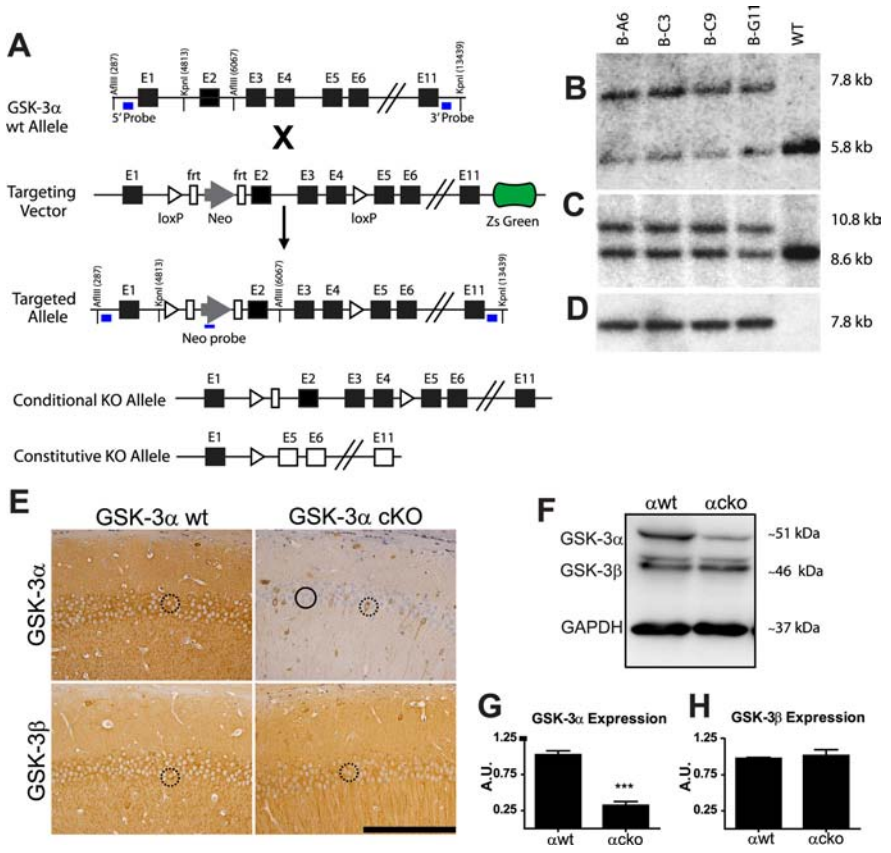

Figure 5. Generation of GSK-3α fx mice, confirmation and characterization of GSK-3α cko mice. cko GSK-3α mice generation. ***A***, Restriction maps (from top to bottom) of the genomic locus, targeting vector, homologous alleles, cko allele, and a constitutive KO allele. After proper homologous recombination, exons 2–4 of targeted allele were flanked by loxP sites with the addition of a neomycin (neo) resistant marker flanked by FRT sites and in the absence of ZsGreen. Nonfluorescent selected clones were analyzed by Southern blot. Probes (blue rectangles) were located at the 5′ and 3′ ends and in the neo fragment. Genomic DNA was digested with AflIII for the 5′ (***B***) and Neo probe (***D***) or KpnI for the 3′ probe (***C***). All four clones were positive for proper homologous recombination and ES clone BC-09 was selected. After Flp-mediated deletion, a conditional KO allele was generated without Neo through mating with a Cre-deleter mouse line. Using this Cre-loxP system, wt or cko genotypes ($n = 10–15$ mice/group) were generated (GSK-3α wt, GSK-3α cko, GSK-3α wt;PDAPP, and GSK-3α cko;PDAPP) and analyzed at 17 months of age. GSK-3α cko was confirmed by IHC using GSK-3$\alpha\beta$-specific antibodies. ***E***, Representative images counterstained with hematoxylin show that in the CA1 region of hippocampus, GSK-3α cko produced a mosaic pattern of neuronal GSK-3α expression and significantly reduced GSK-3α but not GSK-3β immunoreactivity. Scale bar, 100 μm. Neurons with reduced GSK-3 expression are highlighted by black circles and neurons expressing normal GSK-3 levels are highlighted by dashed black circles. ***F***, GSK-3α cko was also confirmed by Western blot from hippocampal lysates ($n = 4$ mice/group) and densitometric analysis showing a significant reduction in GSK-3α (***G***) (67%, $t_{(5)} = 9$, $p = 0.0003$) but not in GSK-3β levels (***H***) ($t_{(3)} = 0.4912$, $p = 0.6570$). Data show mean ± SEM; ***$p < 0.001$ compared with αwt. GSK-3α wt, αwt; GSK-3α cko, αcko.

munostaining (Fig. 5*A*). Although complete knockout (KO) of GSK-3α was not achieved, only a small number of GSK-3α-positive neurons were detected in clearly defined regions, and this was consistent throughout our cohort. Specifically, consistent with a previous report (Tsien et al., 1996), the most robust reduction overall was observed in the cortex, limbic system, and thalamus. To a lesser extent, we observed a reduction in the CA2 and CA3 of hippocampus, layers 4–5 of cortex, lateral amygdale nuclei, caudate, putamen, and reticular part of substantia nigra, and there were no changes in the hypothalamus, fornix, septal nuclei, brainstem, and cerebellum (data not shown). Moreover, ~70% reduction in hippocampal GSK-3α levels was detected by immunoblot analyses (Fig. 5*B*,*C*), without any evident compensatory increase in GSK-3β expression (Fig. 5*D*).

To evaluate the effect of GSK-3α KO on Aβ SP burden in our genetic models, hippocampi from age-matched GSK-3α wt; PDAPP$^{+/-}$ and GSK-3α cko;PDAPP$^{+/-}$ mice were interrogated by IHC with anti-Aβ mAb Nab228 (Fig. 6*A*), and Aβ IR load was quantified using ImageJ (Fig. 6*B*). In the CA1, we observed a significant reduction in Aβ IR SP load in GSK-3α cko; PDAPP$^{+/-}$ compared with GSK-3α wt; PDAPP$^{+/-}$ mice.

Last, to determine whether the above-mentioned changes in Aβ IR load corresponded to alterations in motor activity or spatial memory, GSK-3α wt, GSK-3α cko, GSK-3α wt;PDAPP$^{+/-}$, and GSK-3α cko; PDAPP$^{+/-}$ mice were tested in the open field and Barnes maze. GSK-3α wt; PDAPP$^{+/-}$ mice manifested an increased level of locomotor activity in the open field compared with control groups (Fig. 6*C*), displayed significant deficits in latency to find the target on the Barnes maze (Fig. 6*D*), and used a poor maze strategy compared with all three other groups (Fig. 6*E*). However, GSK-3α cko;PDAPP$^{+/-}$ performed at a level indistinguishable from GSK-3α wt on all three behavioral measures (Fig. 6*C–E*), suggesting that GSK-3α KO can prevent the locomotor hyperactivity and memory deficits demonstrated in PDAPP mice. Importantly, these results are not confounded by GSK-3α KO as we did not detect any differences between GSK-3α wt and GSK-3α cko mice on locomotor activity or spatial memory. Together, these data suggest that GSK-3α KO can prevent behavioral deficits and reduce Aβ plaque burden in PDAPP$^{+/-}$ mice.

Discussion

To identify the respective roles of both GSK-3α and GSK-3β in modulating formation of AD SPs and NFTs *in vivo*, we used a novel viral approach and a genetic approach to manipulate the levels of these two GSK-3 isoforms. Importantly, both GSK-3α and GSK-3β underwent successful KD using isoform-specific shRNA rAAV2/1. Moreover, we successfully generated cko of GSK-3α in GSK-3α cko and GSK-3α cko;PDAPP$^{+/-}$ mice as a second approach to further confirm our findings using the viral approach. Based on both approaches, we report that GSK-3α, but not GSK-3β, KD reduced Aβ levels and formation of SPs and that both GSK-3α and GSK-3β KD reduced tau phosphorylation, tau misfolding, and NFT numbers in these tg mice. These results suggest that GSK-3α contributes to both SP and NFT pathogenesis while GSK-3β only modulates NFT formation.

Our study corroborates previous reports demonstrating that GSK-3 may regulate APP metabolism (Sun et al., 2002; Li et al., 2003; Phiel et al., 2003; Ryder et al., 2003; Su et al., 2004; Serenó et al., 2009). However, this is the first study to analyze the impact of manipulating individual GSK-3 isoforms on the formation of SPs and NFTs in aged tg mouse models of these two signature lesions of AD. In accordance with a previous cell-based study (Phiel et al., 2003), our data suggest that inhibition of GSK-3α but not

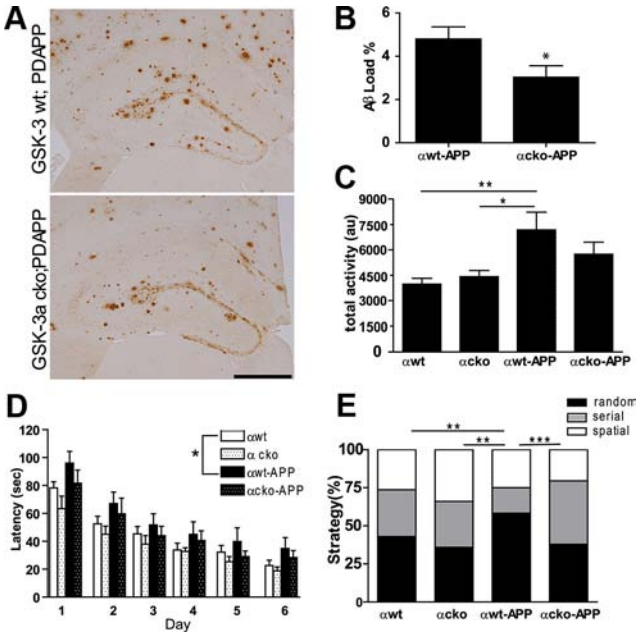

Figure 6. GSK-3α cko decreases amyloid deposition and prevents memory deficits in PDAPP $^{+/-}$ mice. At 17 months of age, GSK-3α wt, GSK-3α cko, GSK-3α wt;PDAPP, and GSK-3α cko;PDAPP mice were evaluated for Aβ levels and behavioral phenotype ($n = 10–15$/group). ***A***, Representative images show hippocampal Aβ using mAb Nab228 in GSK-3α wt; PDAPP and GSK-3α cko;PDAPP mice. Scale bar, 500 μm. GSK-3α cko showed significantly reduced Aβ immunoreactivity ($t_{(12)} = 2.253$, $p = 0.0438$) which was quantified as Aβ load using ImageJ (***B***). Mice were also assessed for locomotor activity on the open field test (***C***) and spatial memory (***D***) and search strategy (***E***) on the Barnes maze. Compared with GSK-3α wt and GSK-3α cko mice, GSK-3α wt;PDAPP displayed hyperactivity on the open field test ($F_{(3,25)} = 5.234$, $p = 0.0061$) (***C***). Compared with GSK-3α wt mice, GSK-3α wt;PDAPP mice performed significantly worse (longer latency to find the target) in the Barnes maze ($F_{(3,43)} = 3.589$, $p = 0.021$) while GSK-3α cko;PDAPP mice were statistically indistinguishable from both groups (***D***). Last, GSK-3α wt;PDAPP mice were more likely to use a poor search strategy (random) on the Barnes maze compared with the other three genotype groups ($\chi^2_{(6)} = 26.198$, $p < 0.0001$), while GSK-3α cko;PDAPP were more likely to use beneficial search strategies (serial and spatial) (***E***). Search strategy data are shown as the percentage of mice using each strategy per genotype column. *$p < 0.05$, **$p < 0.01$, ***$p < 0.001$. GSK-3α wt, αwt; GSK-3α cko, αcko; GSK-3α wt;PDAPP, αwt-APP; and GSK-3α cko;PDAPP, αcko-APP.

GSK-3β is sufficient to reduce Aβ levels and plaque load, suggesting differential roles of GSK-3α and GSK-3β in Aβ production, accumulation, and SP formation. In contrast, a recent study failed to report any changes in Aβ 40 and Aβ 42 levels after 3 weeks of AAV-APP injection in GSK-3α cko mouse brains (Jaworski et al., 2011). However, this difference is most likely due to technical issues such as the different levels of APP expression or the drastically shorter treatment term (3 weeks) compared with 11 months in our study. Further studies are necessary to elucidate the mechanism of GSK-3α in Aβ and APP metabolism.

Currently, it is unclear if inhibition of GSK-3 directly regulates APP proteolysis or indirectly through interaction with an unidentified protein. Our results are consistent with previous reports demonstrating no change in APP (Ryder et al., 2003; Jaworski et al., 2011) or phospho-APP levels (Plattner et al., 2006; Jaworski et al., 2011) after GSK-3 reduction. Furthermore, GSK-3 inhibition could lead to the accumulation and increased activity of various GSK-3 phosphorylation substrates including β-catenin, CREB, c-Myc, NFAT, and Notch (Jope and Johnson, 2004; Rayasam et al., 2009), that may activate an array of genes and modulate APP metabolism. Importantly, this effect may have the greatest impact in brain regions specifically relevant to AD such as the hippocampus where GSK-3 is highly expressed and active in resting neuronal and glia cells (Yao et al., 2002). Our study and others highlight the importance of further effort aimed at uncovering the mechanism behind GSK-3 regulation of APP and Aβ processing.

Our data on tau phosphorylation by GSK-3α and GSK-3β corroborate previous findings that both isoforms contribute to normal and pathological tau phosphorylation (Ishiguro et al., 1988, 1993; Pérez et al., 2003; Noble et al., 2005; Serenó et al., 2009). Other isoform-specific studies *in vivo* have shown that overexpression of GSK-3β increases phosphorylation of tau (Spittaels et al., 2000; Lucas et al., 2001) while overexpression of a dominant-negative form of GSK-3β (Gómez-Sintes et al., 2007) or KO of GSK-3α (Alon et al., 2011) decreases endogenous tau phosphorylation. Our results strengthen these conclusions by revealing that targeting either GSK-3 isoform is sufficient to reduce levels of pathological phospho-tau species linked to NFT formation and conformational changes associated with formation of NFTs in a double tg mice model of AD. While our results are largely consistent with previous studies, it is important to note that this study is the first to separately assess the impact of individual GSK-3α and GSK-3β isoforms in NFT pathology.

The use of a viral injection model and a conditional KO approach in AD tg mice in the present study offers significant strengths and advantages over previous studies. For example, we avoided the use of GSK-3 inhibitors which act indiscriminately on both GSK-3 isoforms and other kinases or cellular processes and therefore may confound data interpretation. By individually targeting GSK-3α and GSK-β isoforms, we circumvented the broad and poorly understood targets of kinase inhibitors and instead focused on one kinase and one isoform at a time. This allowed us to confirm and extend our previous conclusion that selectively silencing GSK-3α reduces Aβ plaque load as well as the tau tangle burden. Moreover, in addition to demonstrating that silencing GSK-3α with shRNA reduced soluble and insoluble levels of both Aβ 40 and Aβ 42 and plaque load in multiple AD tg lines, we were able to further demonstrate a significant amelioration of cognitive deficits in our *GSK-3α cko;PDAPP*$^{+/-}$ mice. Thus, the utilization of two distinct experimental approaches strengthens our conclusion that selectively silencing GSK-3α reduces the Aβ plaque load.

However, one significant limitation of this study was the variability of KD efficiency between GSK-3 α and GSK-3β isoforms. Specifically, GSK-3β protein levels were only reduced by ~50% compared with~70% for GSK-3α. In an attempt to achieve higher GSK-3β KD, we attempted to generate a triple tg mouse (*GSK-3$\beta^{flox/flox}$;α CaMKII-Cre*$^{+/-}$*;PDAPP*$^{+/-}$). However, this cross failed to generate viable offspring that survived beyond 6 months of age (9 of 11 mice died by 6 months) similar to a previous report (Jaworski et al., 2011). Therefore, we were limited to achieving 50% GSK-3β KD using our shRNA approach. Although this GSK-3β KD efficiency was sufficient to confirm the effects of this in the behavioral bioassay (forced swim test, data not shown) and to quantify changes in tau phosphorylation, it was not sufficient to observe any effects on Aβ. Therefore, we cannot rule out the possibility that full GSK-3β KD could influence APP proteolysis *in vivo* and future studies using conditional, inducible, brain-specific KO mice is required to address this issue.

Similarly, this study was complicated by the variability of GSK-3 KD efficiency between tg mouse genotypes. Using the viral approach, GSK-3 was sufficiently silenced in wt and PDAPP $^{+/-}$ mice; however, the KD in PS19 $^{+/-}$;PDAPP $^{+/-}$ mice was ~40% lower. All genotypes were injected at the same time and under the

same conditions by one of two researchers. However, reducing protein levels by injection of rAAV2 containing shRNA is fraught with several technical problems such as the reproducibility of the injections and virus stability. Alternatively, this difference may have been caused by differential tolerability of the virus and mortality as PS19$^{+/-}$;PDAPP$^{+/-}$ mice displayed a higher mortality rate compared with other lines ($\chi^2_{(3)} = 34.24, p < 0.0001$) regardless of the shRNA injection. Therefore it is possible that mice with lower GSK-3 KD preferentially survived. Despite this issue, bigenic PS19$^{+/-}$;PDAPP$^{+/-}$ mice displayed a more profound reduction in Aβ plaques after GSK-3 KD compared with monogenic PDAPP$^{+/-}$ with greater KD efficiency, suggesting that other factors contribute to reducing Aβ pathology in these mice.

In terms of mortality, we did observe an unexpected shortened life span of PS19$^{+/-}$;PDAPP$^{+/-}$ and PDAPP$^{+/-}$ mice treated with shRNA-α (data not shown). This effect has not been observed in other GSK-3α KD models (MacAulay et al., 2007; Jaworski et al., 2011), our GSK-3α cko mice ($\chi^2_{(31,26)} = 0.8387$, $p = 0.3598$), or our GSK-3α cko;PDAPP mice ($\chi^2_{(20,31)} = 2.317$, $p = 0.1279$), suggesting that it might be an artifact or technical issue of our viral injection paradigm. We speculate that abruptly reducing GSK-3α levels at the 12 h postnatal developmental stage when critical neocortical regions are still under development (Rice et al., 1985) may contribute to additional deleterious brain abnormalities separate from transgene expression of APP and tau, as supported by recent studies (Kaidanovich-Beilin et al., 2009; Kim et al., 2009).

In conclusion, our study highlights the importance of GSK-3α in the formation of Aβ plaques as well as the role both GSK-3α and GSK-3β play in the pathological development of NFTs formed by pathological tau. Our observations demonstrate that reducing GSK-3α expression ameliorates the key pathological signatures of AD, i.e., SPs and NFTs, and improves AD-like cognitive impairment in our mouse models. These results have important implications for future design of therapeutics that may preferentially target GSK-3α over GSK-3β. However, before therapeutic development can proceed in a fully informed manner, the differential roles of GSK-3 isoforms in various cellular mechanisms need to be delineated to fully appreciate such specific targeting. The broad functions of both GSK-3 isoforms allow them to be potential drug targets in a number of diseases including cancer, bipolar mood disorder, diabetes, and AD (Jope and Johnson, 2004). Through the use of cko models and RNAi techniques, we may begin to understand the critical functions of both isoforms in the pathogenesis of a variety of diseases.

References

Akiyama H, Shin RW, Uchida C, Kitamoto T, Uchida T (2005) Pin1 promotes production of Alzheimer's amyloid beta from beta-cleaved amyloid precursor protein. Biochem Biophys Res Commun 336:521–529.

Alon LT, Pietrokovski S, Barkan S, Avrahami L, Kaidanovich-Beilin O, Woodgett JR, Barnea A, Eldar-Finkelman H (2011) Selective loss of glycogen synthase kinase-3alpha in birds reveals distinct roles for GSK-3 isozymes in tau phosphorylation. FEBS Lett 585:1158–1162.

Boyce-Rustay JM, Holmes A (2006) Genetic inactivation of the NMDA receptor NR2A subunit has anxiolytic- and antidepressant-like effects in mice. Neuropsychopharmacology 31:2405–2414.

Brunden KR, Zhang B, Carroll J, Yao Y, Potuzak JS, Hogan AM, Iba M, James MJ, Xie SX, Ballatore C, Smith AB 3rd, Lee VM, Trojanowski JQ (2010) Epothilone D improves microtubule density, axonal integrity, and cognition in a transgenic mouse model of tauopathy. J Neurosci 30:13861–13866.

Carroll JC, Boyce-Rustay JM, Millstein R, Yang R, Wiedholz LM, Murphy DL, Holmes A (2007) Effects of mild early life stress on abnormal emotion-related behaviors in 5-HTT knockout mice. Behav Genet 37:214–222.

Carroll JC, Iba M, Bangasser DA, Valentino RJ, James MJ, Brunden KR, Lee VM, Trojanowski JQ (2011) Chronic stress exacerbates tau pathology, neurodegeneration, and cognitive performance through a corticotropin-releasing factor receptor-dependent mechanism in a transgenic mouse model of tauopathy. J Neurosci 31:14436–14449.

Games D, Adams D, Alessandrini R, Barbour R, Berthelette P, Blackwell C, Carr T, Clemens J, Donaldson T, Gillespie F (1995) Alzheimer-type neuropathology in transgenic mice overexpressing V717F beta-amyloid precursor protein. Nature 373:523–527.

Gao G, Lu Y, Calcedo R, Grant RL, Bell P, Wang L, Figueredo J, Lock M, Wilson JM (2006) Biology of AAV serotype vectors in liver-directed gene transfer to nonhuman primates. Mol Ther 13:77–87.

Giese KP (2009) GSK-3: a key player in neurodegeneration and memory. IUBMB Life 61:516–521.

Gómez-Sintes R, Hernández F, Bortolozzi A, Artigas F, Avila J, Zaratin P, Gotteland JP, Lucas JJ (2007) Neuronal apoptosis and reversible motor deficit in dominant-negative GSK-3 conditional transgenic mice. EMBO J 26:2743–2754.

Hanger DP, Anderton BH, Noble W (2009) Tau phosphorylation: the therapeutic challenge for neurodegenerative disease. Trends Mol Med 15:112–119.

Hurtado DE, Molina-Porcel L, Iba M, Aboagye AK, Paul SM, Trojanowski JQ, Lee VM (2010) A{beta} accelerates the spatiotemporal progression of tau pathology and augments tau amyloidosis in an Alzheimer mouse model. Am J Pathol 177:1977–1988.

Ishiguro K, Ihara Y, Uchida T, Imahori K (1988) A novel tubulin-dependent protein kinase forming a paired helical filament epitope on tau. J Biochem 104:319–321.

Ishiguro K, Shiratsuchi A, Sato S, Omori A, Arioka M, Kobayashi S, Uchida T, Imahori K (1993) Glycogen synthase kinase 3 beta is identical to tau protein kinase I generating several epitopes of paired helical filaments. FEBS Lett 325:167–172.

Jaworski T, Dewachter I, Lechat B, Gees M, Kremer A, Demedts D, Borghgraef P, Devijver H, Kügler S, Patel S, Woodgett JR, Van Leuven F (2011) GSK-3alpha/beta kinases and amyloid production in vivo. Nature 480:E4–E5; discussion E6.

Jope RS, Johnson GV (2004) The glamour and gloom of glycogen synthase kinase-3. Trends Biochem Sci 29:95–102.

Kaidanovich-Beilin O, Lipina TV, Takao K, van Eede M, Hattori S, Laliberté C, Khan M, Okamoto K, Chambers JW, Fletcher PJ, MacAulay K, Doble BW, Henkelman M, Miyakawa T, Roder J, Woodgett JR (2009) Abnormalities in brain structure and behavior in GSK-3alpha mutant mice. Mol Brain 2:35.

Kim JW, Lee JE, Kim MJ, Cho EG, Cho SG, Choi EJ (2003) Glycogen synthase kinase 3 beta is a natural activator of mitogen-activated protein kinase/extracellular signal-regulated kinase kinase kinase 1 (MEKK1). J Biol Chem 278:13995–14001.

Kim WY, Wang X, Wu Y, Doble BW, Patel S, Woodgett JR, Snider WD (2009) GSK-3 is a master regulator of neural progenitor homeostasis. Nat Neurosci 12:1390–1397.

Lee EB, Skovronsky DM, Abtahian F, Doms RW, Lee VM (2003) Secretion and intracellular generation of truncated Abeta in beta-site amyloid-beta precursor protein-cleaving enzyme expressing human neurons. J Biol Chem 278:4458–4466.

Lee EB, Leng LZ, Zhang B, Kwong L, Trojanowski JQ, Abel T, Lee VM (2006) Targeting amyloid-beta peptide (Abeta) oligomers by passive immunization with a conformation-selective monoclonal antibody improves learning and memory in Abeta precursor protein (APP) transgenic mice. J Biol Chem 281:4292–4299.

Lee EB, Zhang B, Liu K, Greenbaum EA, Doms RW, Trojanowski JQ, Lee VM (2005) BACE overexpression alters the subcellular processing of APP and inhibits Abeta deposition in vivo. J Cell Biol 168:291–302.

Li B, Ryder J, Su Y, Zhou Y, Liu F, Ni B (2003) FRAT1 peptide decreases Abeta production in swAPP(751) cells. FEBS Lett 553:347–350.

Li J, Daly TM (2002) Adeno-associated virus-mediated gene transfer to the neonatal brain. Methods 28:203–207.

Lucas JJ, Hernández F, Gómez-Ramos P, Morán MA, Hen R, Avila J (2001) Decreased nuclear beta-catenin, tau hyperphosphorylation and neurodegeneration in GSK-3beta conditional transgenic mice. EMBO J 20:27–39.

MacAulay K, Doble BW, Patel S, Hansotia T, Sinclair EM, Drucker DJ, Nagy

A, Woodgett JR (2007) Glycogen synthase kinase 3alpha-specific regulation of murine hepatic glycogen metabolism. Cell Metab 6:329–337.

Noble W, Planel E, Zehr C, Olm V, Meyerson J, Suleman F, Gaynor K, Wang L, LaFrancois J, Feinstein B, Burns M, Krishnamurthy P, Wen Y, Bhat R, Lewis J, Dickson D, Duff K (2005) Inhibition of glycogen synthase kinase-3 by lithium correlates with reduced tauopathy and degeneration in vivo. Proc Natl Acad Sci U S A 102:6990–6995.

O'Leary TP, Savoie V, Brown RE (2011) Learning, memory and search strategies of inbred mouse strains with different visual abilities in the Barnes maze. Behav Brain Res 216:531–542.

Passini MA, Wolfe JH (2001) Widespread gene delivery and structure-specific patterns of expression in the brain after intraventricular injections of neonatal mice with an adeno-associated virus vector. J Virol 75:12382–12392.

Pérez M, Hernández F, Lim F, Díaz-Nido J, Avila J (2003) Chronic lithium treatment decreases mutant tau protein aggregation in a transgenic mouse model. J Alzheimers Dis 5:301–308.

Phiel CJ, Wilson CA, Lee VM, Klein PS (2003) GSK-3alpha regulates production of Alzheimer's disease amyloid-beta peptides. Nature 423:435–439.

Plattner F, Angelo M, Giese KP (2006) The roles of cyclin-dependent kinase 5 and glycogen synthase kinase 3 in tau hyperphosphorylation. J Biol Chem 281:25457–25465.

Rayasam GV, Tulasi VK, Sodhi R, Davis JA, Ray A (2009) Glycogen synthase kinase 3: more than a namesake. Br J Pharmacol 156:885–898.

Rice FL, Gomez C, Barstow C, Burnet A, Sands P (1985) A comparative analysis of the development of the primary somatosensory cortex: interspecies similarities during barrel and laminar development. J Comp Neurol 236:477–495.

Ryan KA, Pimplikar SW (2005) Activation of GSK-3 and phosphorylation of CRMP2 in transgenic mice expressing APP intracellular domain. J Cell Biol 171:327–335.

Ryder J, Su Y, Liu F, Li B, Zhou Y, Ni B (2003) Divergent roles of GSK3 and CDK5 in APP processing. Biochem Biophys Res Commun 312:922–929.

Serenó L, Coma M, Rodríguez M, Sánchez-Ferrer P, Sánchez MB, Gich I, Agulló JM, Pérez M, Avila J, Guardia-Laguarta C, Clarimón J, Lleó A, Gómez-Isla T (2009) A novel GSK-3beta inhibitor reduces Alzheimer's pathology and rescues neuronal loss in vivo. Neurobiol Dis 35:359–367.

Sledz CA, Williams BR (2005) RNA interference in biology and disease. Blood 106:787–794.

Sledz CA, Holko M, de Veer MJ, Silverman RH, Williams BR (2003) Activation of the interferon system by short-interfering RNAs. Nat Cell Biol 5:834–839.

Spittaels K, Van den Haute C, Van Dorpe J, Geerts H, Mercken M, Bruynseels K, Lasrado R, Vandezande K, Laenen I, Boon T, Van Lint J, Vandenheede J, Moechars D, Loos R, Van Leuven F (2000) Glycogen synthase kinase-3beta phosphorylates protein tau and rescues the axonopathy in the central nervous system of human four-repeat tau transgenic mice. J Biol Chem 275:41340–41349.

Su Y, Ryder J, Li B, Wu X, Fox N, Solenberg P, Brune K, Paul S, Zhou Y, Liu F, Ni B (2004) Lithium, a common drug for bipolar disorder treatment, regulates amyloid-beta precursor protein processing. Biochemistry 43:6899–6908.

Sun X, Sato S, Murayama O, Murayama M, Park JM, Yamaguchi H, Takashima A (2002) Lithium inhibits amyloid secretion in COS7 cells transfected with amyloid precursor protein C100. Neurosci Lett 321:61–64.

Tsien JZ, Chen DF, Gerber D, Tom C, Mercer EH, Anderson DJ, Mayford M, Kandel ER, Tonegawa S (1996) Subregion- and cell type-restricted gene knockout in mouse brain. Cell 87:1317–1326.

Woodgett JR (1990) Molecular cloning and expression of glycogen synthase kinase-3/factor A. EMBO J 9:2431–2438.

Yao HB, Shaw PC, Wong CC, Wan DC (2002) Expression of glycogen synthase kinase-3 isoforms in mouse tissues and their transcription in the brain. J Chem Neuroanat 23:291–297.

Yoshiyama Y, Higuchi M, Zhang B, Huang SM, Iwata N, Saido TC, Maeda J, Suhara T, Trojanowski JQ, Lee VM (2007) Synapse loss and microglial activation precede tangles in a P301S tauopathy mouse model. Neuron 53:337–351.